Environmental Chemistry of Perfluoroalkyl and Polyfluoroalkyl Substances in Aqueous Film Forming Foams

by

Lisa A. D'Agostino

A thesis submitted in conformity with the requirements
for the degree of Doctor of Philosophy

Department of Chemistry
University of Toronto

Environmental Chemistry of Perfluoroalkyl and Polyfluoroalkyl Substances in Aqueous Film Forming Foams

Lisa A. D'Agostino

Doctor of Philosophy

Department of Chemistry
University of Toronto

2017

Abstract

While aqueous film forming foam (AFFF) release has been known to result in environmental contamination with perfluoroalkyl and polyfluoroalkyl substances (PFASs) for over fifteen years, identities of individual PFASs in AFFFs have been largely unknown, proprietary information. Using mixed-mode ion exchange solid phase extraction (SPE), high resolution mass spectrometry (HR-MS), quadrupole time-of-flight (qTOF) tandem mass spectrometry (MS/MS), and liquid chromatography (LC)-MS/MS, 103 individual PFASs were identified in AFFFs and surfactant concentrates, including multiple chain-length congeners. Aerobic wastewater treatment plant sludge biodegradation of two AFFF components, 6:2 fluorotelomer sulfonamide alkylbetaine (FTAB) and alkylamine (FTAA), was investigated revealing biodegradation to short-chain perfluoroalkyl carboxylates (PFCAs) and known PFCA precursors. Additional degradation products were also identified, including 6:2 fluorotelomer sulfonamide (FTSAm) as a degradation product of both 6:2 FTAB and 6:2 FTAA, and six additional degradation products of 6:2 FTAA. A survey of selected Canadian surface waters for AFFF-related PFASs using SPE and LC-MS/MS revealed that several AFFF-related

PFASs could be detected in urban and AFFF-impacted surface waters. These included FTABs and fluorotelomer betaines (FTBs), which were the fluorotelomer PFASs with the highest maximum concentrations. Other PFASs, such as perfluorohexane sulfonamide (FHxSA), 6:2 FTSAm, and 6:2 fluorotelomer mercaptoalkylamido sulfonate sulfone (FTSAS-SO_2) were identified in some samples. Extraction and analysis of sediment from an AFFF-impacted river and batch sorption experiments with 6:2 FTAA and 6:2 FTAB in an agricultural soil provide preliminary insights into sorption behaviour of AFFF components, where longer chain-length FTBs were apparently more sorptive than shorter chain-lengths and 6:2 FTAA was more sorptive than 6:2 FTAB. This work is significant in identifying numerous PFASs found in AFFF that require further research in regards to their environmental fate and toxicology, demonstrating the presence of AFFF-related PFASs in Canadian environmental samples, and investigating biodegradation forming PFCAs and sorption of selected PFASs found in AFFFs.

Acknowledgments

I would not have been able to complete the research in this thesis without the assistance and support of the current and past members of the Mabury group and our supervisor Scott Mabury. Leo was a very important mentor and shared so much of his extensive knowledge about perfluoroalkyl and polyfluoroalkyl substances, instrumentation, and analytical techniques. Holly, Keegan, Derek, Amy, Anne, Angela, Rob and Jessica provided so much useful advice on how to work in our lab and how to work with our instruments. Lennart and Shira rescued the lab from shrinking to nothing and brought energy and new perspectives, which I really appreciate.

I appreciate the assistance of Derek Muir, Eric Reiner, Patrick Crozier, Paul Helm, Amila De Silva, and Shane de Solla with providing samples of aqueous film forming foams (AFFFs), surface water, and sediments that were instrumental in the preparation of this thesis. I also appreciate the advice of Karl Jobst on the interpretation of mass spectra and his contribution of running AFFF samples on the Fourier transform ion cyclotron resonance mass spectrometer (FTICR-MS).

Personally, the support of so many people in the broader Environmental Chemistry division has been so important in getting me through to this point, including but not limited to Tev, Sarah, Emma, Alyson, Nicole, Laura, Megan, Ran, Rachel, Ramina, Dorea, and Greg. All those lunches, coffees, and beer o'clocks made this a supportive environment.

I really appreciate all of the emotional and practical support I have received from my loving husband Alan, which has been key in getting to this point. Mom and Leslie, I thank you so much for your support and coming to me when my body failed me. Dad, thank you for all your support and showing me science when I was little. Grandma, thank you for helping me to become such a lover of words and books. I also appreciate all the support I've received from my aunts and uncles, although you're going to miss bugging me about being a grad student. Nonna, I will always remember you, your love of learning, and your support of my interests. The warmth and support I've received from my in-laws, Peter, Olive, Eva, Stephanie, Jared, Matt, Jacqueline, and Ted, has been really wonderful.

Table of Contents

List of Tables

List of Figures

List of Appendices

Table of Acronyms

Acronym	Meaning
3M	Minnesota Mining and Manufacturing Company
AFB	air force base
AFFF	aqueous film forming foam
BAF	bioaccumulation factor
BCF	bioconcentration factor
CID	collision induced dissociation
CTMA	cetyltrimethylammonium chloride
diPAP	fluorotelomer phosphate diester
DMAPFNAE	N-(3-(dimethylamino)propyl)perfluorononanamide
ECF	electrochemical fluorination
EOF	extractable organic fluorine
EPA	Environmental Protection Agency
ESI	electrospray ionization
ESI-	negative ion mode electrospray ionization
ESI+	positive ion mode electrospray ionization
EtFOSA	N-ethyl perfluorooctane sulfonamide
EtFOSAA	N-ethyl perfluorooctane sulfonamido acetic acid
F-35B	chloro-perfluoroalkyl ether sulfonate
FASAAA	perfluoroalkane sulfonamide alkylamine acid
FASAAm	perfluoroalkane sulfonamide alkylamine
FASAB	perfluoroalkane sulfonamide alkylbetaine
FASADA	perfluoroalkane sulfonamide alkylamine diacids
FBSAAA	perfluorobutane sulfonamide alkylamine acid
FBSAAm	perfluorobutane sulfonamide alkylamine
FBSADA	perfluorobutane sulfonamide alkylamine diacid
FHxSA	perfluorohexane sulfonamide
FHxSAAA	perfluorohexane sulfonamide alkylamine acid
FHxSAAm	perfluorohexane sulfonamide alkylamine
FHxSAAm	perfluorohexane sulfonamide alkylamine
FHxSAB	perfluorohexane sulfonamide alkylbetaine
FHxSADA	perfluorohexane sulfonamide alkylamine diacid
FOSA	perfluorooctane sulfonamide

Acronym	Meaning
FOSAA	perfluorooctane sulfonamido acetic acid
FPeSAAA	perfluoropentane sulfonamide alkylamine acid
FPeSAAm	perfluoropentane sulfonamide alkylamine
FPeSAB	perfluoropentane sulfonamide alkylbetaine
FPeSADA	perfluoropentane sulfonamide alkylamine diacid
FPrSAAA	perfluoropropane sulfonamide alkylamine acid
FPrSADA	perfluoropropane sulfonamide alkylamine diacid
FS-1520	Mason Chemicals fluorinated surfactant concentrate
FS-330	Mason Chemicals fluorinated surfactant concentrate
FTAA	fluorotelomer sulfonamide alkylamine
FTAB	fluorotelomer sulfonamide alkylbetaine
FTAC	fluorotelomer acrylate
FTAL	fluorotelomer aldehyde
FTB	fluorotelomer betaine
FTCA	fluorotelomer carboxylic acid
FTI	fluorotelomer iodide
FTICR-MS	Fourier transform ion cyclotron resonance mass spectrometry
FTMAC	fluorotelomer methacrylate
FTOH	fluorotelomer alcohol
FTSA	fluorotelomer sulfonic acid
FTSAB	fluorotelomerthioalkylamido betaine
FTSAm	fluorotelomer sulfonamide
FTSAS	fluorotelomer mercaptoalkylamido sulfonate
FTSAS-SO	fluorotelomer mercaptoalkylamido sulfonate sulfoxide
FTSAS-SO_2	fluorotelomer mercaptoalkylamido sulfonate sulfone
FTSH	fluorotelomer thiol
FTSHA	fluorotelomerthiohydroxyl ammonium
FTSHA-SO	fluorotelomerthiohydroxyl ammonium sulfoxide
$FTSO_2Cl$	fluorotelomer sulfonyl chloride
FTUAL	fluorotelomer unsaturated aldehyde
FTUCA	fluorotelomer unsaturated carboxylic acid
GC-MS	gas chromatography-mass spectrometry
GCxGC	comprehensive two dimensional gas chromatography
HR-MS	high resolution mass spectrometry

Acronym	Meaning
ICR	ion cyclotron resonance
K_d	soil/sediment-water distribution coefficient
K_{oc}	organic carbon normalized soil/sediment-water distribution coefficient
LC-MS/MS	liquid chromatography-tandem mass spectrometry
LC-TOF-MS	liquid chromatography-time-of-flight mass spectrometry
LOD	limit of detection
LOQ	limit of quantification
MeFBSE	N-methyl perfluorobutane sulfonamido ethanol
MeFOSA	N-methyl perfluorooctane sulfonamide
MeFOSAA	N-methyl perfluorooctane sulfonamido acetic acid
mol	molar
monoPAP	fluorotelomer phosphate monoester
MS	mass spectrometry
MS/MS	tandem mass spectrometry
MSDS	material safety data sheet
MTBE	methyl *tert*-butyl ether
NAS	naval air station
NMR	nuclear magnetic resonance
PAP	fluorotelomer phosphate ester
PFAA	perfluoroalkyl acid
PFAAB	perfluoroalkylamido betaine
PFAI	perfluoroalkyl iodide
PFAS	perfluoroalkyl and polyfluoroalkyl substance
PFASAC	perfluoroalkylsulfonamido amino carboxylate
PFASNO	perfluoroalkylsulfonamido amine oxide
PFBA	perfluorobutanoate
PFBS	perfluorobutane sulfonate
PFCA	perfluoroalkyl carboxylate
PFDA	perfluorodecanoate
PFHpA	perfluoroheptanoate
PFHpS	perfluoroheptane sulfonate
PFHxA	perfluorohexanoate
PFHxS	perfluorohexane sulfonate

Acronym	Meaning
PFNA	perfluorononanoate
PFOA	perfluorooctanoate
PFOS	perfluorooctane sulfonate
PFOSAmS	perfluorooctane sulfonamido quaternary ammonium salt
PFOSI	perfluorooctane sulfinic acid
PFPA	perfluoroalkyl phosphonate
PFPeA	perfluoropentanoate
PFPeS	perfluoropentane sulfonate
PFPiA	perfluoroalkyl phosphinate
PFSA	perfluoroalkane sulfonate
PFTeDA	perfluorotetradecanoate
PFUnDA	perfluoroundecanoate
PHxSF	perfluorohexane sulfonyl fluoride
POSF	perfluorooctane sulfonyl fluoride
qTOF-MS	quadrupole-time-of-flight mass spectrometry
S/N	signal-to-noise
SAmPAP diester	N-ethyl perfluorooctane sulfonamido ethanol-based phosphate diester
SI	supporting information
SPE	solid phase extraction
TFA	trifluoroacetic acid
TOF-CIC	total organofluorine combustion ion chromatography
TOF-MS	time-of-flight mass spectrometry
U.S. EPA	United State Environmental Protection Agency
UL	Underwriters Laboratories
UPLC	ultra performance liquid chromatography
WAX	weak anion exchange
WCX	weak cation exchange
WWTP	wastewater treatment plant
XAD	styrene-divinylbenzene resin sorbent

Chapter One

Introduction to Perfluoroalkyl and Polyfluoroalkyl Substances in Aqueous Film Forming Foams

1 Introduction to Perfluoroalkyl and Polyfluoroalkyl Substances in Aqueous Film Forming Foams

1.1 Introduction to AFFFs and synthesis of PFASs for AFFF

1.1.1 Function and composition of AFFF

Aqueous film forming foam (AFFF) is a firefighting tool used in extinguishing fires fuelled by flammable liquids, which are also known as Class B fires. AFFFs typically contain a mixture of ingredients, including fluorinated surfactants, hydrocarbon surfactants or hydrolyzed protein, solvents, and other components.[1,2] Deployment of AFFF involves mixing AFFF concentrate with water and spraying it from a specialized nozzle as a foam containing more than eighty percent air, which spreads over the surface of a burning liquid.[1] The percentage of AFFF concentrate in the AFFF concentrate-water mixture is usually between one and six percent, depending on the specific AFFF formulation. Fires are extinguished by AFFF through cooling of the fire by evaporation of water from the foam and by the formation of an aqueous layer on top of the flammable liquid inhibiting the evaporation and re-ignition of vapours.[1]

Fluorinated surfactants, which are typically perfluoroalkyl and polyfluoroalkyl substances (PFASs), contribute to the ability of AFFFs to spread over a burning liquid. Fluorinated surfactants in AFFF lower the air-aqueous phase surface tension by partitioning to the water-air interface where their hydrophobic-lipophobic tails can stick out into the air.[1,2] Hydrocarbon surfactants lower the surface tension at the water-hydrocarbon interface by occupying sites primarily at the water-hydrocarbon interface with their hydrophobic tails facing into the hydrocarbon phase.[1,2] In combination, fluorinated and hydrocarbon surfactants generate a foam that spreads readily over flammable liquids as it possesses a positive spreading coefficient.[1,2] Hydrocarbon surfactants alone do not generate a foam with a positive spreading coefficient, as required to meet United States military AFFF specifications.[2]

Table 1.1: Structures of PFASs discussed in Chapter 1

Name	Structure	Acronym
perfluoroalkane sulfonate (PFSA)	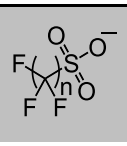	PFBS n = 4 PFHxS n = 6 PFOS n = 8
perfluoroalkyl carboxylate (PFCA)	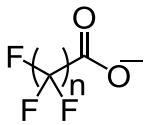	PFBA n = 3; PFPeA n = 4; PFHxA n = 5; PFHpA n = 6; PFOA n = 7; PFNA n = 8; PFDA n = 9; PFUnDA n = 10, PFTeDA n =13
perfluoroalkane sulfonyl fluoride	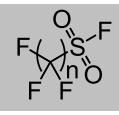	PHxSF n = 6 POSF n = 8
fluorotelomer iodide	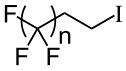	n:2 FTI
fluorotelomer alcohol	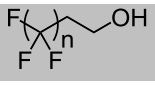	n:2 FTOH
fluorotelomer thiol	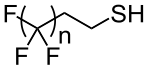	n:2 FTSH
fluorotelomer sulfonyl chloride	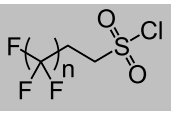	n:2 FTSO$_2$Cl
fluorotelomer sulfonic acid	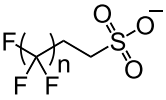	n:2 FTSA
fluorotelomer mercaptoalkylamido sulfonate	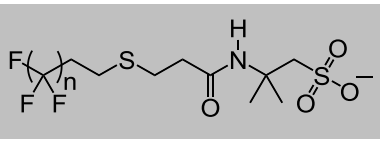	n:2 FTSAS
fluorotelomer mercaptoalkylamido sulfonate sulfoxide	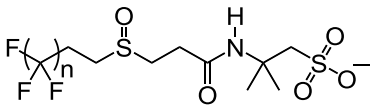	n:2 FTSAS-SO
fluorotelomer mercaptoalkylamido sulfonate sulfone	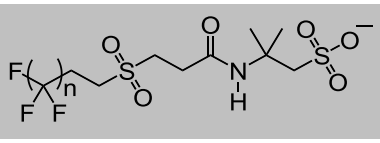	n:2 FTSAS-SO$_2$
perfluoroalkane sulfonamide	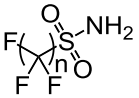	FHxSA n = 6 FOSA n = 8
perfluoroalkane sulfonamide alkylamine (FASAAm)	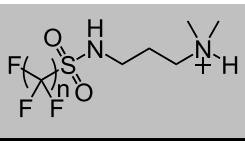	FHxSAAm (n = 6)

Name	Structure	Acronym
perfluorooctane sulfonamido acetic acids	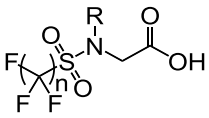	MeFOSAA R = CH_3-, n = 8 EtFOSAA R = CH_3CH_2-, n = 8 FOSAA R = H-, n = 8
N-ethyl and N-methyl perfluorooctane sulfonamide	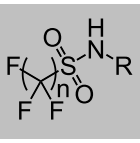	EtFOSA R = CH_3CH_2- n = 8 MeFOSA R = CH3- n = 8
perfluoroalkane sulfonamido ethanols	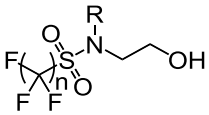	MeFBSE R = CH_3-, n = 4 EtFOSE R = CH_3CH_2-, n = 8 FOSE R = H-, n = 8
perfluorooctane sulfinic acid	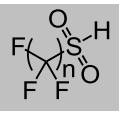	PFOSI n = 8
EtFOSE-based phosphate diester	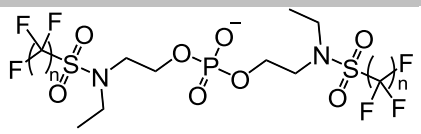	SAmPAP diester n = 8
perfluorooctane sulfonamido quaternary ammonium salt	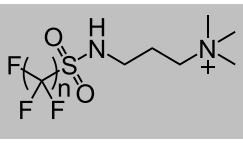	PFOSAmS n =8
n:2 fluorotelomer aldehyde	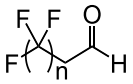	n:2 FTAL
n:2 fluorotelomer unsaturated aldehyde	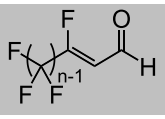	n:2 FTUAL
n:2 fluorotelomer carboxylic acid	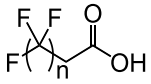	n:2 FTCA
n:2 fluorotelomer unsaturated carboxylic acid	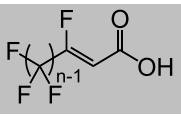	n:2 FTUCA
n:3 fluorotelomer carboxylic acid	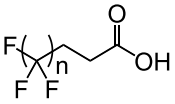	n:3 FTCA
n:3 fluorotelomer unsaturated carboxylic acid	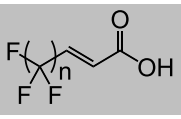	n:3 FTUCA
n:2 fluorotelomer sulfonamide alkylbetaine	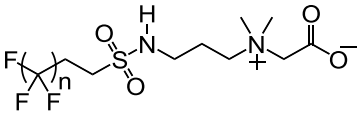	n:2 FTAB
n:2 fluorotelomer sulfonamide alkylamine	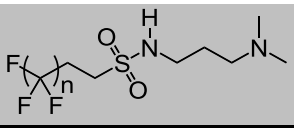	n:2 FTAA

Name	Structure	Acronym
n:2 fluorotelomer sulfonamide	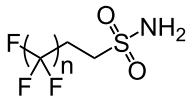	n:2 FTSAm
fluorotelomer acrylate and fluorotelomer methacrylate	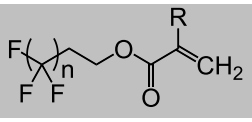	n:2 FTAC R = H- n:2 FTMAC R = CH_3-
fluorotelomer phosphate monoester	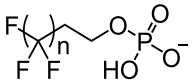	n:2 monoPAP
fluorotelomer phosphate diester	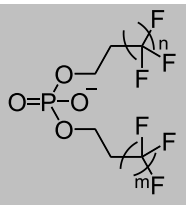	n:2/m:2 diPAP
chloro perfluoroalkyl ether sulfonate	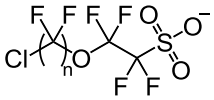	F-35B n = 6
perfluoroalkyl phosphonate	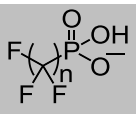	Cn PFPA
perfluoroalkyl phosphinate	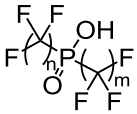	Cn/Cm PFPiA

1.1.2 Manufacture of PFASs for AFFF by electrochemical fluorination

The first manufacturer of AFFF was the Minnesota Mining and Manufacturing Company (3M), which developed the technology with the United States Navy.[2] 3M used a synthetic technique known as electrochemical fluorination (ECF) in its manufacturing of PFASs for use in AFFFs.

The ECF process involves applying a low voltage (5 to 7 V) to a solution of a hydrocarbon starting material dissolved in anhydrous hydrogen fluoride in an electrochemical cell with a nickel anode and an iron or nickel cathode.[3] The reaction proceeds with reduction of all hydrogen atoms on the staring material to H_2 and oxidation of carbon atoms on the starting material through binding of fluorine atoms in place of hydrogen atoms.[3] Typical starting materials for industrial ECF include linear aliphatic acyl fluorides (RC(O)F) and linear aliphatic sulfonyl fluorides ($RS(O_2)F$) for the

production perfluoroalkyl acid fluorides and perfluoroalkyl sulfonyl fluorides, respectively. The ECF reaction is a harsh process that produces only moderate yields of the corresponding linear perfluoroalkyl acid or sulfonyl fluoride from 10–80% depending on the chain-length of the starting material and an extensive suite of side products.[2] These side products include a mixture of perfluoroalkyl chain lengths, branched isomers of the perfluoroalkyl chain, cyclic perfluoroalkyl chains, and other side products and are a result of radical reactions in the ECF mixture.[3,4] In technical perfluorooctane sulfonate (PFOS), this results in a mixture containing 62–70% linear PFOS and 37–29% branched isomers.[5]

The key products of ECF used to manufacture fluorinated surfactants for AFFF are perfluorooctane sulfonyl fluoride (POSF) and perfluorohexane sulfonyl fluoride (PHxSF). POSF is base hydrolyzed to produce PFOS or reacted in an amidation with a primary or secondary amine as a first step in producing higher order fluorinated surfactants.[3] PHxSF yields perfluorohexane sulfonate (PFHxS) through hydrolysis or may be amidated with primary or secondary amines to facilitate functionalization.[3,6,7] Figure 1.1 is a simple schematic for the production of PFOS, PFHxS, or higher ordered fluorinated surfactants starting with ECF.

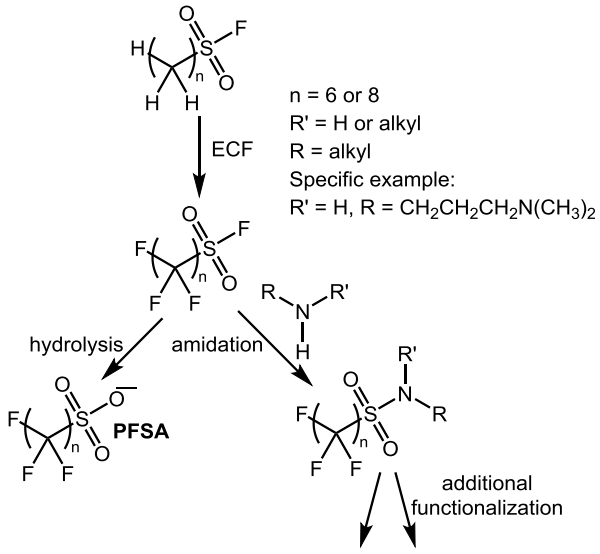

Figure 1.1: Schematic for industrial production of perfluoroalkane sulfonates (PFSAs) and perfluoroalkane sulfonamide-based surfactants for AFFFs by ECF. Specific example based on Great Britain Patent GB1302612A[8] and United States Patent 5144069A.[6]

1.1.3 Manufacture of PFASs for AFFF by telomerization

Another industrially relevant strategy for the synthesis of PFASs that are used in AFFFs is telomerization, which was developed for the production of perfluoroalkyl iodides (PFAIs) by the DuPont Company in 1962.[9] Telomerization builds up perfluoroalkyl chains in two carbon increments starting with a short PFAI called the telogen, most often pentafluoroethyl iodide (CF_3CF_2I), and adding length with a taxogen that is typically tetrafluoroethene ($CF_2=CF_2$).[3] The telomerization reaction is essentially a radical polymerization with initiation and propagation steps as shown in Figure 1.2 and termination by reaction of two radicals.

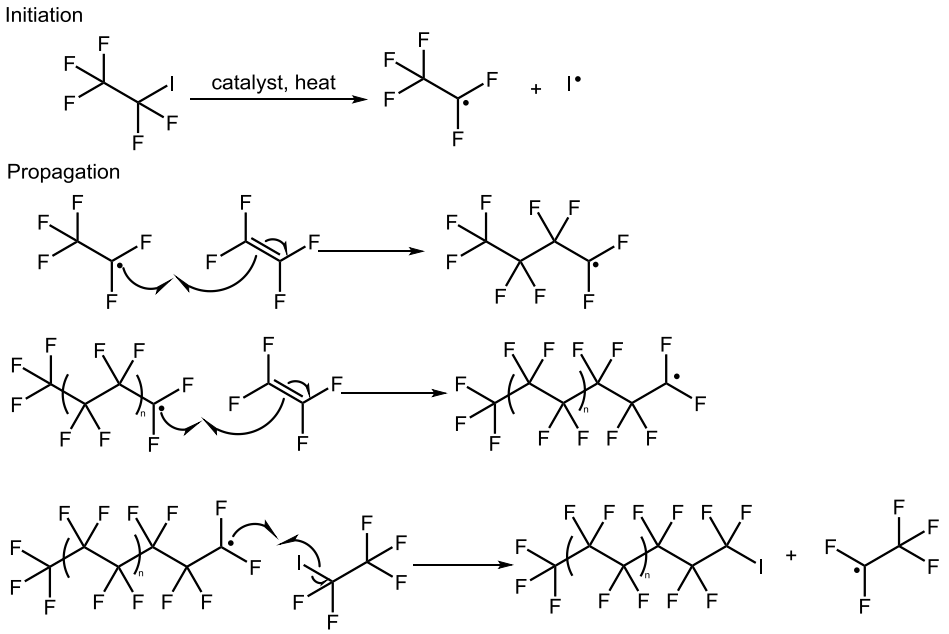

Figure 1.2: Reaction scheme for the telomerization of pentafluoroethyl iodide and tetrafluoroethane.

By controlling the proportions of reagents and therefore the number of tetrafluoroethylene units that are added, different chain lengths of PFAIs can be prepared.[3] Control of the number of tetrafluoroethane units incorporated tends to be imperfect, resulting in a mix of PFAIs each with an even number of carbons, if pentafluoroethyl iodide and tetrafluoroethane are used.[2]

To manufacture fluorinated surfactants for AFFFs and other PFASs, subsequent functionalization is necessary. Due to the lack of reactivity of PFAIs with nucleophiles they are usually reacted with ethene, which produces a fluorotelomer iodide (FTI, $F(CF_2CF_2)_nCH_2CH_2I$).[3,10] The chain length of the FTI is denoted as an *x*:2 FTI, where *x* is the number of perfluoroalkyl carbons and 2 is the number of hydrogenated carbons.[10] Hydrolysis of the FTI yields a fluorotelomer alcohol (FTOH, $F(CF_2CF_2)_nCH_2CH_2OH$) that may be used to incorporate the fluorotelomer group in fluorinated surfactants or other PFASs by an ester linkage.[3,10] Alternatively, the FTI can be reacted with thiourea and then hydrolyzed to produce a fluorotelomer thiol (FTSH). The FTSH may be utilized to form a thioether linkage in the preparation of fluorinated surfactants or may be converted to a fluorotelomer sulfonyl chloride ($FTSO_2Cl$). Industrially, $FTSO_2Cl$s are synthesized

by the reaction of a FTSH with chlorine gas and water.[3,11] The $FTSO_2Cl$ facilitates the formation of a sulfonamide through reaction with a primary or secondary amine, which may be further reacted to incorporate additional functionalities.

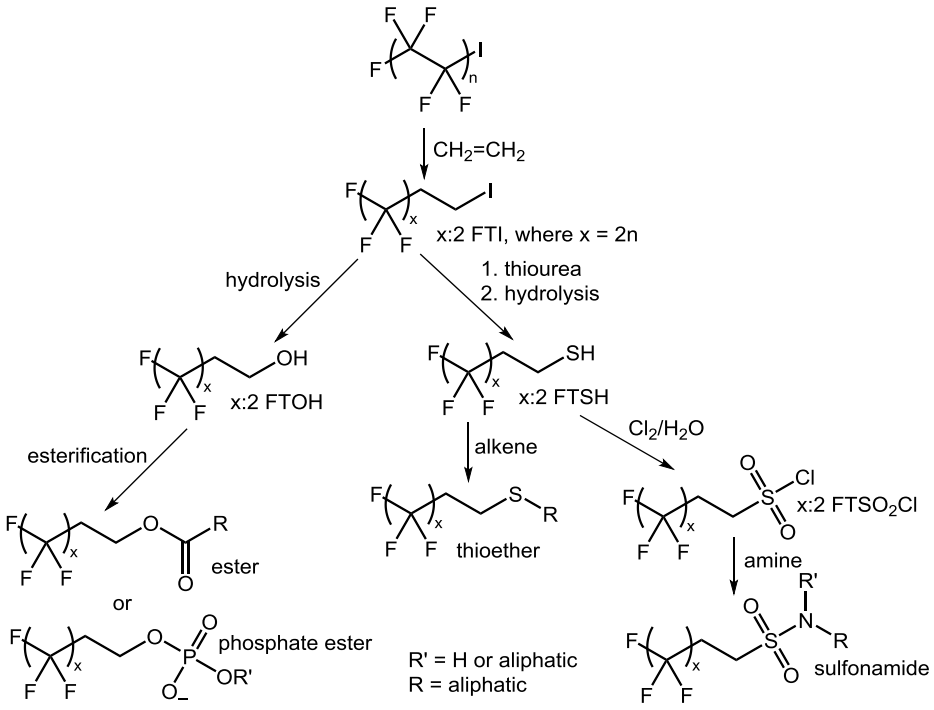

Figure 1.3: Synthetic options for building fluorinated surfactants and other PFASs from FTIs

1.1.4 "Trade Secrets": Structures of PFASs in AFFFs were generally unknown

Prior to commencement of this research, the knowledge of the environmental science community about the chemical identity of the fluorinated surfactants used in AFFFs was severely limited because the industry does not disclose the contents of its proprietary AFFF mixtures.[2,12] Material safety data sheets (MSDSs) for AFFFs often contain cryptic entries such as: "proprietary mixture of fluorosurfactants,"[13] "proprietary mixture consisting of hydrocarbon surfactants, fluorosurfactants, inorganic salts, high molecular weight polysaccharide, and water,"[14] or "amphoteric fluoroalkyl amide."[15]

In 2004, Schultz *et al.* were able to identify three chain length congeners of one fluorotelomer surfactant in an AFFF sample as 4:2, 6:2, and 8:2 fluorotelomer mercaptoalkylamido sulfonates (FTSASs).[12] Until 2012, this was the only reported identification of a novel PFAS in an AFFF.[7,16] Weiner *et al.* revealed the substantial gap in knowledge about PFASs in AFFF by comparing the total organofluorine in twelve AFFFs by total organofluorine combustion ion chromatography (TOF-CIC) to their content of perfluoroalkane sulfonates (PFSAs), perfluoroalkyl carboxylates (PFCAs), fluorotelomer sulfonic acids (FTSAs), and FTSASs by liquid chromatography-tandem mass spectrometry (LC-MS/MS). This revealed that these known PFASs accounted for between 1 and 52% of the total organofluorine, which means that a substantial amount of the organofluorine was in the form of unknown PFASs.[17] The properties of unknown PFASs cannot be known including their environmental partitioning, bioavailability, degradation mechanisms, and toxicology.

1.2 AFFF as a source of environmental PFAS contamination

1.2.1 Reports of PFAS contamination due to AFFF

The initial indication that AFFF was associated with contamination with PFASs due to the fluorinated surfactants used in AFFF was a 1997 study looking for metabolites of jet fuel at a former military firefighting training site on Tyndall Air Force Base (AFB) in Florida. In that study, diazomethane derivatization and gas chromatography-mass spectrometry (GC-MS) analysis of groundwater extracts revealed the presence of unspecified fluorinated surfactants both up-gradient and down-gradient of the known jet fuel plume.[18] This result lead to further investigation of Tyndall AFB and other former military fire training areas. Initially, Moody and Field used GC-MS analysis of derivatized ground water extracts to quantify four PFCAs at Tyndall AFB and Naval Air Station (NAS) Fallon in Nevada. The profile of perfluorohexanoate (PFHxA), perfluoroheptanoate (PFHpA), and perfluorooctanoate (PFOA) at NAS Fallon was dominated by PFOA at concentrations up to 6,570,000 ng/L of PFOA. At Tyndall AFB, concentrations of PFCAs were lower with similar concentrations of PFHxA and PFOA and a maximum of 298,000 ng/L of total PFCAs.[19] The derivatization and GC-MS

method used to measure PFCAs in this early study was limited to measurement of PFCAs and not PFSAs, which cannot be readily derivatized.

Using the newer analytical technique of liquid chromatography tandem mass spectrometry (LC-MS/MS), Moody *et al.* were able to measure the PFSA and PFCA concentrations in surface water and fish associated with an accidental release of AFFF into Etobicoke Creek in Ontario, Canada.[20,21] These results showed that PFOS was the most abundant PFAS measured in areas impacted by the spill at concentrations of up to 2,210,000 ng/L in water and 72,900 ng/g in fish liver. Elevated PFOS, PFOA, and PFHxS concentrations downstream of the spill and analysis of an AFFF product showed that AFFF was a source of these perfluoroalkyl acids (PFAAs).[20,21] Long-chain PFCAs were detected in similar concentrations in fish livers upstream and downstream of the release, indicating sources other than AFFF were important[21] and these were found to include atmospheric inputs based on results including analysis of snow from isolated areas of the arctic.[22]

Investigation of military fire training areas also continued using newer analytical approaches enabling the measurement of PFSAs. Direct infusion electrospray ionization (ESI) mass spectrometry was used to measure PFSAs in groundwater around a fire training area at Wurtsmith AFB in Michigan.[23,24] Concentrations of PFOS, PFHxS, and PFOA in groundwater were similar to each other at Wurtsmith AFB with maximum concentrations of 110,000 ng/L of PFOS, 120,000 ng/L of PFHxS, and 105,000 ng/L of PFOA found in the two wells nearest the fire training area.[24]

In attempting to use 6:2 fluorotelomer sulfonate (FTSA) as an internal standard in LC-MS/MS analysis of PFSAs, Schultz *et al.* found that it was present in un-spiked groundwater, which lead to a study of FTSAs in groundwater around former military fire training areas.[12,25] Extremely high concentrations of 6:2 FTSA were found at Tyndall AFB with up to 14,600,000 ng/L measured in groundwater, while FTSAs were not detected at NAS Fallon and lower concentrations up to 173,000 ng/L of 6:2 FTSA in groundwater were measured at Wurtsmith AFB.[12] Interestingly, the distribution of PFCAs, PFSAs, and FTSAs differed greatly between the three sites with FTSAs ranging

from not detected at NAS Fallon to 82% of the total measured PFASs at Tyndall AFB. In addition, it was determined that FTSAs were not major components of AFFFs and that their presence may be due to degradation of other AFFF components, including FTSASs, which were identified in an AFFF concentrate by fast atom bombardment mass spectrometry and ESI-tandem mass spectrometry (MS/MS).[12]

In 2005, 48,000 L of AFFF were deployed in a ravine of Etobicoke Creek in Ontario, Canada to fight an aircraft fire. Unlike the accidental release in 2000, elevated PFOS could not be detected in downstream fish relative to upstream fish. Although a relatively broad suite of PFCAs, PFSAs, fluorotelomer unsaturated carboxylic acids (FTUCAs), perfluorooctane sulfonamido substances, and FTSAs were measured in upstream and downstream blacknose dace livers, only 8:2 FTSA was elevated in the downstream fish (1.1–2.0 ng/g) relative to upstream fish (0.45–0.77 ng/g) indicating that a substantially different AFFF formulation was used to fight this fire than was accidentally released in 2000.[26] Further monitoring of Etobicoke Creek for PFOS in the nine years following the release of AFFF in 2000 showed that PFOS remained elevated 0.1 km from the release site with concentrations of PFOS in water of 290 ng/L in 2009 and that PFOS concentrations in water and fish further downstream of the release were still 2 to 10 times higher than those found upstream in 2009.[27] This indicates that AFFF impacts may still be detected in affected surface waters after nearly a decade.

Other locations where PFAS contamination attributed to AFFF have been reported include, around the fire drill area at Flesland Airport near Bergen, Norway;[28] downstream of Hamilton International Airport in Ontario, Canada;[29,30] in Meretta Lake and Resolute Lake downstream of Resolute Bay Airport in Nunavut, Canada;[31,32] in the Ringvaart canal surrounding Schiphol Amsterdam Airport in The Netherlands;[33] around an air force base in Sweden;[34] downstream of Stockholm Arlanda Airport in Sweden;[35] military fire training areas in Australia's Northern Territory;[36] and additional United States military bases with historic AFFF releases.[37–40] Highlights of the PFASs measured at these sites and those examined in earlier studies in various matrices are summarized in Table 1.2, Table 1.3, Table 1.4, and Table 1.5. Additional PFASs were measured in some studies but PFOS, PFHxS, PFOA, PFHxA, and 6:2 FTSA are recorded in these tables

because they are frequently measured and provide an indication of both ECF AFFF used (PFOS, PFHxS, some by-product $PFOA^3$) and fluorotelomer AFFF use (6:2 FTSA, PFHxA and PFOA from degradation-see Sections 1.4.1.2 and 1.4.2.2).

Table 1.2: Maximum and minimum concentrations of selected PFASs reported in surface waters at suspected AFFF-impacted sites

Location	PFOS		PFHxS		PFOA		PFHxA		6:2 FTSA	
	Max. (ng/L)	Min. (ng/L)	Max. (ng/L)	Min. (ng/L)	Max. (ng/L)	Min. (ng/L)	Max. (ng/L)	Min. (ng/L)	Max. (ng/L)	Min. (ng/L)
Etobicoke Creek downstream of Toronto Pearson Airport, Ontario, Canada (June 2000, spill)[21]	2210000	nd	134000	nd	11300	nd	na	na	na	na
Etobicoke Creek downstream of Toronto Pearson Airport, Ontario, Canada (2003)[27]	690	44	190	9	58	28	na	na	na	na
Etobicoke Creek downstream of Toronto Pearson Airport, Ontario, Canada (2009)[27]	290	32	92	9.4	34	14	na	na	na	na
Resolute and Meretta Lakes near Resolute Bay Airport, Nunavut, Canada (2003-05)[31]	90	23	24	1.5	16	5	na	na	na	na
Resolute and Meretta Lakes near Resolute Bay Airport, Nunavut, Canada (2010-11)[32]	41 ± 9	26 ± 5	30 ± 4	20 ± 4	17 ± 1	9.4 ± 2.0	30 ± 5	22 ± 3	1.4 ± 1.7	0.20 ± 0.21
Welland River downstream of Hamilton Airport, Ontario, Canada (2010)[29]	458	30.2	na	na	62.4	7.4	176.6	13.3	na	na
Ringvaart near Amsterdam Airport, The Netherlands (July 2008, spill)[33]	1600000	480000	na	na	na	na	na	na	na	na
Ringvaart near Amsterdam Airport, The Netherlands (October 2008, after spill)[33]	490	340	106	43	na	na	na	na	na	na
Ringvaart near Amsterdam Airport, The Netherlands (2011, after spill)[33]	34		na	na	na	na	na	na	na	na
AFB F18 outside Stockholm, Sweden[34]	45	<1	25	<0.5	8.8	<1	4.4	<0.5	na	na
Lake Halmsjön near Stockholm Arlanda Airport, Sweden[35]	137	59	104	54	80	13	34	8.2	<LOD	<LOD
Drainage ditch at Stockholm Arlanda Airport, Sweden[35]	2340		980		210		290		176	
Ten active United States AFBs[37]	8970000 (Median: 2170)	<13	815000 (Median: 710)	<7	210000 (Median: 382)	<10	292000 (Median: 320)	<3	na	na

Table 1.3: Maximum and minimum concentrations of selected PFASs reported in groundwater at suspected AFFF-impacted sites

Location	PFOS		PFHxS		PFOA		PFHxA		6:2 FTSA	
	Max. (ng/L)	Min. (ng/L)	Max. (ng/L)	Min. (ng/L)	Max. (ng/L)	Min. (ng/L)	Max. (ng/L)	Min. (ng/L)	Max. (ng/L)	Min. (ng/L)
NAS Fallon, Nevada, United States[12,19]	380000	<620	876000	<470	6570000	<18000	372000	nd	<330	<330
Tyndall AFB, Florida, United States[12,19]	2300000	147000	920000	107000	116000	<18000	144000	nd	14600000	1080000
Wurtsmith AFB, Michigan, United States[12,24]	110000	4000	120000	5000	105000	<3000	8000	nd	173000	<13000
Flesland Airport near Bergen, Norway[28]	2078	1371	540	319	191	130	561	385	6693	3878
United States Military Base Site A[40]	78000	15000	360000	36000	220000	12000	350000	19000	220000	8900
United States Military Base Site B[40]	65000	88	170000	81	57000	8.6	99000	<4.7	37000	<LOD
Ellsworth AFB, South Dakota, United States[38]	100000 (Median: 19000)	nd (<100)	530000 (Median: 71000)	nd (<100)	190000 (Median: 26000)	nd (<100)	320000 (Median: 36000)	nd (<100)	270000 (Median: 25000)	nd (<60)
Ellsworth AFB, South Dakota, United States[39]	54200	<LOQ (<100)	338000	<LOQ (<100)	152000	<LOQ (<3)	247000	<LOQ (<6)	na	na
AFB F18 outside Stockholm, Sweden[34]	42200	<1	3470	<0.5	4470	<1	900	<0.5	na	na
Ten active United States AFBs[37]	4300000 (Median: 4220)	<14	290000 (Median: 870)	<7	250000 (Median: 405)	<10	120000 (Median: 820)	<3	na	na

Table 1.4: Maximum and minimum concentrations of selected PFASs reported in sediment/soil at suspected AFFF-impacted sites

Location	Max. (ng/g)	Min. (ng/g)	Max. (ng/g)	Min. (ng/g)	Max. (ng/g)	Min. (ng/g)	Max. (ng/g)	Min. (ng/g)	Max. (ng/g)	Min. (ng/g)
Sediment										
Etobicoke Creek downstream of Toronto Pearson Airport, Ontario, Canada (2003)[27]	13	0.2	0.3	<0.1	0.5	<0.05	na	na	na	na
Etobicoke Creek downstream of Toronto Pearson Airport, Ontario, Canada (2009)[27]	13	0.5	0.3	<0.2	0.2	0.1	na	na	na	na
Resolute Lake near Resolute Bay Airport, Nunavut, Canada (1983-2003, sediment core)[31]	85	24	3.5	1.2	7.5	<1.8	na	na	na	na
Resolute and Meretta Lakes near Resolute Bay Airport, Nunavut, Canada (2010-11)[32]	49 ± 29	28 ± 43	0.67 ± 0.17	0.45 ±0.04	1.8 ± 2.4	1.8 ± 0.3	0.23 ± 0.21	0.065 ± 0.057	~17	~11
Ringvaart near Amsterdam Airport, The Netherlands (October 2008, after spill)[33]	16	14	0.6	nd	na	na	na	na	na	na
Ringvaart near Amsterdam Airport, The Netherlands (October 2011, after spill)[33]	13	0.9	nd	nd	na	na	na	na	na	na
Ten active United States AFBs[37]	190000 (Mdn.: 31)	<0.24	2700 (Mdn.: 9.1)	<0.48	950 (Mdn.: 2.45)	<0.40	710 (Mdn.: 1.7)	<0.26	na	na
Soil										
Flesland Airport near Bergen, Norway[28]	1905	1.6	21	0.12	12.2	0.23	18.5	0.18	2101	0.84
AFB F18 outside Stockholm, Sweden[34]	8520	<0.5	21.3	<0.02	287	<0.1	13.3	<1.5	na	na
Ellsworth AFB, South Dakota, United States[38]	20000 (Mdn.: 2400)	11	13000 (Mdn.: 66)	3	5200 (Mdn.: 21)	nd (<0.8)	2000 (Mdn.: 11)	nd (<0.8)	6200	nd (<0.4)
Ellsworth AFB, South Dakota, United States[39]	36534	0.953	23875	<LOQ (0.02)	11484	<LOQ (<0.05)	2761	<LOQ (<0.05)	na	na
Ten active United States AFBs[37]	9700 (Mdn.: 11.5)	<0.15	1300 (Mdn.: 4.4)	<0.29	140 (Mdn.: 1.45)	<0.24	140 (Mdn.: 1.04)	<0.16	na	na
Tindal and Darwin fire training areas, Northern Territory, Australia[36]	16170	1830	na	na	na	na	na	na	na	na

NOTE: Mdn. = median

Table 1.5: Maximum and minimum concentrations of selected PFASs reported in biota at suspected AFFF-impacted sites

Location	PFOS		PFHxS		PFOA		PFHxA		6:2 FTSA	
	Max. (ng/g)	Min. (ng/g)	Max. (ng/g)	Min. (ng/g)	Max. (ng/g)	Min. (ng/g)	Max. (ng/g)	Min. (ng/g)	Max. (ng/g)	Min. (ng/g)
Fish Liver										
Etobicoke Creek downstream of Toronto Pearson Airport, Ontario, Canada (2000, fish liver)[21]	72900	2000	62	<2.3	40	6	40	3.3	na	na
Etobicoke Creek downstream of Toronto Pearson Airport, Ontario, Canada (2005, blacknose dace liver)[26]	350	219	<LOQ	<LOQ	<LOQ	<LOQ	<LOQ	<LOQ	0.21	0.1
Etobicoke Creek downstream of Toronto Pearson Airport, Ontario, Canada (2003, fish liver)[27]	1100	460	3.7	<LOD	1.6	<LOD	na	na	na	na
Etobicoke Creek downstream of Toronto Pearson Airport, Ontario, Canada (2009, fish liver)[27]	1756	168	1.3	0.4	1.3	0.1	na	na	na	na
Lake Langavatnet near Flesland Airport, Norway (trout liver)[28]	2532	2082	268	118	0.49	<0.2	0.24	<0.05	>LOD	>LOD
Fish Muscle/fillet										
Binbrook Reservoir downstream of Hamilton Airport, Ontario, Canada (2009-12, fish dorsal muscle)[30]	2400	14	na	na	<1	<0.1	na	na	na	na
Ringvaart near Amsterdam Airport, The Netherlands (October 2008, eel fillet, after spill)[33]	400	100	4.5	3.5	na	na	na	na	na	na
AFB F18 outside Stockholm, Sweden (fish muscle)[34]	370	0.7	0.85	<0.02	<0.1	<0.05	<1	<0.07	na	na
Fish-Whole Body										
Ringvaart near Amsterdam Airport, The Netherlands (October 2008, perch, after spill)[33]	1500	630	3.3	1	na	na	na	na	na	na
Lake Halmsjön near Stockholm Arlanda Airport, Sweden (perch)[35]	254									
Resolute and Meretta Lakes near Resolute Bay Airport, Nunavut, Canada (2010-11, juvenile char)[32]	224 ± 491	181 ± 50	0.18 ± 0.06	<0.036	51 ± 151	1.31 ± 0.65	<0.036	<0.036	1.0 ± 1.5	<0.19
Amphibian Plasma										
Welland River downstream of Hamilton Airport, Ontario, Canada (2010, snapping turtle plasma)[29]	2065		3.2		<0.1		<0.1		na	
Invertebrates										
Welland River downstream of Hamilton Airport, Ontario, Canada (2010, amphipods)[29]	1126	49.2	40.2	0.7	60.4	17.2	5.4	0.1	na	na
Resolute and Meretta Lakes near Resolute Bay Airport, Nunavut, Canada (2010-11, benthic invertebrates)[32]	445 ± 545	287 ± 273	<0.069	<0.069	<0.1	<0.1	0.38 ± 0.42	0.34 ± 0.50	<1.3	<1.3

1.2.2 Unknown organofluorine in AFFF-impacted environments

As discussed in the previous section, the initial reports about PFAS contamination at AFFF-impacted sites involved analysis of PFASs and PFCAs that were receiving attention due to the recent discovery of their ubiquity in human blood[41] and biota samples.[42] It first became apparent that these analytes do not provide full coverage of the PFASs at AFFF-impacted sites through the work of Moody *et al.* surrounding the accidental release of PFOS-containing AFFF into Etobicoke Creek in Ontario, Canada.[20,21] Two independent analytical methods were used to analyze water samples from the creek with PFOS, PFHxS, and PFOA quantified by LC-MS/MS, while ^{19}F-NMR was used to measure the total PFAS concentration. There was a substantial discrepancy between the results of the two methods with the total PFASs by ^{19}F-NMR three to eleven times greater than the sum of PFOS, PFHxS, and PFOA measured by LC-MS/MS in the water. This suggested that other PFASs in the AFFF with similar ^{19}F-NMR spectra to PFOS were likely present and targeted LC-MS/MS analysis was missing a significant portion of PFASs in the water after the spill.[20,21] In fish liver downstream of the release, BCFs approximately five times higher than expected were calculated for PFOS, which may have been due to bioconcentration and biotransformation of PFOS precursors in the AFFF.[21]

Schultz *et al.* identified another significant component of the PFAS contamination at some AFFF-impacted sites in finding that 6:2 FTSA was more abundant that PFCAs or PFSAs in groundwater at the former military fire training site at Tyndall AFB in Florida.[12] Unexpectedly, they also found that 6:2 FTSA was present in relatively low concentrations in AFFF concentrate that would lead to a concentration of around 50,000 ng/L in the applied foam, while 6:2 FTSA was present at over 1,000,000 ng/L in all groundwater samples from Tyndall AFB.[12] This indicates that 6:2 FTSA is probably a degradation product of other PFASs in AFFF, including the 6:2 FTSAS identified in the AFFF concentrate using mass spectrometry techniques.[12,25]

A method to quantify all PFASs that may be PFAA precursors was developed by Houtz and Sedlak and is called the total oxidizable precursor assay.[43] This method uses

thermolysis of persulfate to generate hydroxyl radicals that oxidize all PFAA precursors, including perfluoroalkane sulfonamido substances and fluorotelomer compounds, to PFCAs then measures the resulting PFCAs by LC-MS/MS.[43] Application of the method to samples from Ellsworth AFB, South Dakota, provides insight into the contribution of known and unknown PFAA precursors to PFAS contamination at that site. In groundwater, 23% of the PFASs were PFAA precursors and approximately 40% of those were unknown PFAA precursors, while the known precursors detected were perfluorohexane sulfonamide (FHxSA), 6:2 FTSA, and 8:2 FTSA. In soil and aquifer solids from the site, PFAA precursors were approximately 35% of total PFASs and of those approximately half were unknown PFAA precursors. The known PFAA precursors measured in soil and aquifer solids were FHxSA, perfluorooctane sulfonamide (FOSA), 6:2 FTSA, 8:2 FTSA, and the AFFF component perfluorohexane sulfonamide alkylamine (FHxSAAm). Houtz *et al.* also attempted to measure other AFFF components that had recently been identified,[7] but did not detect any other than FHxSAAm.[38] The relatively high proportion of unknown PFAA precursors at this site suggests that other unknown AFFF components and/or degradation products of PFASs in AFFFs were present in significant quantitites.[38]

Another strategy to quantify the total PFAS content of samples is total organofluorine combustion ion chromatography (TOF-CIC), which involves combusting a sample or extract at high temperatures to convert organofluorine to HF, collecting the combustion products in an aqueous absorption solution to convert HF to fluoride ions, and quantifying the fluoride ions by ion chromatography.[44] This strategy has been applied to AFFF concentrates[17] and rainbow trout extracts from a bioconcentration study using an ECF AFFF and a fluorotelomer-based AFFF.[45] For AFFF concentrates, between 48% and 99% of the total organofluorine was unknown PFASs, which were not accounted for by measuring PFSAs, PFCAs, FTSAs, and FTSASs with LC-MS/MS.[17] In fish exposed to ECF AFFF, approximately 40% of the organofluorine in an extract was attributable to unknown PFASs after measuring PFCAs, PFSAs, FTSAs, 6:2 and 8:2 FTSASs, N-methyl perfluorooctane sulfonamido acetic acid (MeFOSAA), N-ethyl perfluorooctane sulfonamido acetic acid (EtFOSAA), perfluorooctane sulfonamide acetic acid (FOSAA), 6:2 and 8:2 FTUCAs, and 5:3 and 7:3 fluorotelomer carboxylic acids

(FTCAs).[45] With the fluorotelomer AFFF, more than 93% of the organofluorine in fish liver and carcass extracts could not be attributed to the measured PFASs.[45] This indicates that AFFF components and/or degradation products thereof that were not measured were bioconcentrated into rainbow trout to a significant extent.

The unattributed organofluorine and unknown PFAA precursors in AFFF impacted sites and in the rainbow trout exposed to AFFF indicates that there remain significant unknown AFFF components and/or degradation products thereof.

1.2.3 Regulatory actions and industrial trends regarding AFFFs

Manufacturing of AFFF containing PFOS as a major ingredient decreased drastically with the phase out of POSF and PHxSF chemistry by 3M between 2000 and 2001.[46] Since then, production of POSF has continued in China, perhaps for the production of AFFF, with release of PFOS equivalents in China estimated at 70 tonnes in 2010.[47] In 2009, PFOS and POSF were added to Annex B of the Stockholm Convention as a persistent organic pollutant with limited acceptable uses and ongoing efforts towards the elimination of their production and use.[48] Use of PFOS-containing AFFF has been increasingly regulated and is currently banned in Canada[49] and the European Union,[50] although existing stocks may be used in the United States and other countries without these regulations.

After 3M removed its ECF AFFFs containing PFOS from the market, fluorotelomer AFFFs were and continue to be the remaining fluorinated alternative on the market. The industrial and regulatory trends regarding fluorotelomer AFFFs and other fluorotelomer products have been away from 8:2 fluorotelomer and longer long-chain PFASs and toward 6:2 fluorotelomer and shorter short-chain PFASs. Concerns about the persistence, toxicity, and bioaccumulation potential of PFOA led to a partnership between American, European, and Japanese fluorochemical companies and the United States Environmental Protection Agency (U.S. EPA) on the 2010/2015 PFOA Stewardship Program toward the reduction and then elimination of PFOA, longer chain PFCAs, and their precursors. The goals of the program are a 95% reduction from a year 2000 baseline of emissions and product content of PFOA, longer chain PFCAs, and their precursors by

2010 with elimination of these emissions and product contents by 2015.[51,52] This has led the fluorotelomer surfactant suppliers to produce 6:2 fluorotelomer surfactants with increasingly lower content of longer chain fluorotelomer congeners. An example of this effort to limit long chain fluorotelomers is the DuPont product Forafac 1157 used in AFFFs, which was examined in a toxicology study in turbot, where the formulation Forafac 1157 contained primarily 6:2 fluorotelomer sulfonamide alkylbetaine (FTAB) with traces of 8:2 FTAB and the formulation Forafac 1157N contained mainly 6:2 FTAB with some 8:2, 10:2, and 12:2 FTAB.[53] Hagenaars *et al.* concluded that the short chain Forafac 1157 was less toxic than Forafac 1157N with more long chain fluorotelomer surfactants.[53] PFOA is also currently under consideration for addition to the Stockholm Convention as a persistent organic pollutant to be eliminated after being nominated by the European Union.[54]

In addition the transition to short-chain fluorotelomer-based AFFFs, efforts have also been undertaken by industry to develop new firefighting foams for liquid fuelled fires without fluorinated surfactants and some AFFF users have adopted these products for their firefighting needs. In 2014, an EPA Presidential Green Chemistry Challenge Award for Designing Green Chemicals went to Solberg Foams for their organohalogen-free Re-Healing foams, which incorporate a mixture of complex carbohydrates and non-fluorinated surfactants and meet Underwriters Laboratories (UL) standard 162 for firefighting foam performance.[55] International airports in Stockholm and Gothenburg, Sweden switched to another fluorine free foam called Moussol FF, which is alcohol resistant and utilizes surfactants, polymer film formers, and other ingredients in a pseudoplastic product, in 2008.[56,57] Other manufacturers also advertise fluorine-free firefighting foams,[58–60] although these may be less effective than AFFF containing fluorinated surfactants.[61] Manufacturer claims that products are fluorine-free may not be entirely reliable as at least one firefighting foam has been promoted as "fluorosurfactant-free" while containing a high molecular weight side-chain fluorinated polymer.[62] A recent development in research into alternative firefighting technologies is a fluorine-free, silica sol gel-forming firefighting foam, although it has not been demonstrated on a liquid-fueled fire.[63]

1.3 Approaches to the identification of unknown PFASs

Identification of previously unknown PFASs, whether in environmental samples or product samples typically relies on mass spectrometry techniques. Although ^{19}F-NMR enables the detection of fluorinated compounds to the exclusion of other chemicals, it has major limitations in terms of identifying specific chemicals in samples. With ^{19}F-NMR it is possible to detect resonances corresponding to perfluoroalkyl groups at approximately -70 to -80 *ppm* and between -110 and -130 *ppm* and a higher number of resonances in this region can be indicative of structural isomers from ECF.[17] Resonances outside these ranges may also be indicative of variations on a perfluoroalkyl group, such as a -CHF- or the substitution of a fluorine with a chlorine. However, there is no clear relationship between the chemical shifts of a perfluoroalkyl group and the nature of the hydrocarbon portion of a PFAS.

Mass spectrometry allows the detection of individual PFASs and determination of their exact mass allowing the determination of a molecular formula, while the masses of fragment ions from their dissociation provide information about their molecular structures. Use of mass spectrometry has enabled the identification of previously unknown PFAS structures.[25,12,7,64–67]

1.3.1 High resolution mass spectrometry

In order to determine the molecular formula of a compound by mass spectrometry, high resolution mass spectrometry (HR-MS) is required to determine the mass to charge ratio (*m/z*) with a high degree of accuracy and precision. This enables differentiation between molecular formulas with equivalent nominal *m/z* (i.e.: rounded to the nearest whole number) but different exact masses. For example, ethene and carbon monoxide both have a nominal mass of 28 Da. To differentiate between these two gasses an electron ionization (EI) mass spectrometer must differentiate between ethane at *m/z* 28.0308 and carbon monoxide at *m/z* 27.9944. High resolution refers to a resolving power greater than approximately 10,000, where resolving power is defined as $m/\Delta m_{50\%}$ and m is the ion mass and $\Delta m_{50\%}$ is the width of the mass spectral peak at half height.[68] The major types of high resolution mass analyzer are double focusing electromagnetic

sectors, time-of-flight mass spectrometers, Fourier transform ion cyclotron resonance mass spectrometers, and Orbitraps.

1.3.1.1 Double focusing electromagnetic sector mass spectrometry

The earliest high resolution mass spectrometers were sector instruments. The mass analyzer in these instruments uses a magnetic field to bend the path of ions, which are accelerated into the sector by an electric potential. The equation governing a magnetic sector is derived from the equations for kinetic energy of an ion accelerated by an electric potential, magnetic force, and centripetal force and is given below as Equation 1-1, where *m/z* is the mass to charge ratio of the ion, *B* is the magnetic field strength, *r* is the radius of the curve in the sector, *e* is the charge of an electron, and *V* is the electric potential the ions are accelerated by:

$$\frac{m}{z} = \frac{B^2 r^2 e}{2v} \quad \text{Equation 1-1}$$

However, using only a magnetic sector as described in Equation 1-1 does not result in a high resolution mass spectrometer. The resolution is limited due to the existence of a range of kinetic energies among the ions being analyzed. In order to achieve high resolution, a double focusing instrument that incorporates one or two electrostatic analyzers to isolate ions over a very narrow range of kinetic energies is needed.[69] These instruments are very expensive, take up a lot of space, and let through only one *m/z* at a time resulting in the loss of ions of interest at all other times in scanning mode, which reduces sensitivity.[70] However, double focusing sector instruments can achieve resolving powers up to 75,000 to 150,000.[71]

1.3.1.2 Time-of-flight mass spectrometry

Time-of-flight mass spectrometry (TOF-MS) operates on the simplest physical principle of all mass spectrometers based entirely on the kinetic energy of ions accelerated across an electric potential. The equation governing TOF-MS is given as Equation 1-2, where *m* is the mass of the ion, *q* is its charge, *V* is the electric potential that accelerates the ion, *t* is flight time of the ion, and *L* is the length of the flight tube.

$$\frac{m}{z} = \frac{2Vt^2}{L^2}$$ Equation 1-2

Several technological developments were necessary to enable modern high resolution TOF-MS instruments. Exceptionally fast electronics are needed in detectors to differentiate flight times for ions of similar *m/z* given that the collection of an entire spectrum may take less than 100 μs and small differences in flight times of around 100 ns must be measured.[70] High resolution TOF-MS like high resolution sector mass spectrometry requires compensation for the kinetic energy distribution of the ions, which will cause them to have a range of flight times and consequently wider mass spectral peaks and lower resolution. In modern TOF-MS instruments, resolution is improved using a reflectron, which functions as an electrostatic ion mirror. This compensates for the kinetic energy distribution of ions because faster ions penetrate more deeply than slow moving ions, which increases the flight time of faster ions more than slower ions and narrows the distribution of flight times for each *m/z*.[68,70] While a single reflectron can reach a resolving power of approximately 10,000, use of multiple reflectrons further narrows the flight time distribution and increases the flight path resulting in resolving powers of 40,000 to 50,000 or more.[68] Another approach to narrowing the distribution of flight times in TOF-MS is to use multiple electric sectors to generate a multipass flight path that focuses ions in time.[68,70]

A key advantage of TOF-MS instruments is that sensitivity is not compromised in collecting full scan spectra since they intrinsically analyze a broad range of *m/z* at all times rather than relatively slowly scanning through each *m/z* one at a time with a sector or quadrupole.[72] With orthogonal acceleration, where ions are accelerated into the flight tube perpendicular to the initial ion beam, ions can be accumulated continuously between spectral acquisitions further improving sensitivity.[68] TOF-MS has the fastest acquisition speed among high resolution mass spectrometers enabling its use as a detector for applications requiring this speed, such as fast separations by comprehensive two dimensional gas chromatography (GC×GC) and aerosol mass spectrometry.[68]

1.3.1.3 Fourier transform ion cyclotron resonance mass spectrometry

The highest resolving powers in mass spectrometry, which can be over 1,000,000, are achieved on Fourier transform ion cyclotron resonance mass spectrometers (FTICR-MS). FTICR-MS operates based on the characteristic frequency of the circular motion of an ion in a magnetic field, which is called the cyclotron frequency.[69] The cyclotron frequency, ω_c, is inversely proportional to the *m/z* of the ion as shown in Equation 1-3, where *v* is the velocity of the ion, *r* is the radius of the ion orbit, *z* is the charge of the ion, *e* is the charge of an electron, *B* is the magnetic field strength, and *m* is the mass of the ion.[69]

$$\omega_c = \frac{v}{r} = \frac{zeB}{m} \quad \text{Equation 1-3}$$

In an FTICR-MS, ions are trapped in an ion cyclotron resonance (ICR) cell in a strong magnetic field. The ions are then excited by a radiofrequency pulse that sweeps through all their cyclotron frequencies, which brings the orbits of the ions in the cell into phase and increases the amplitude of their orbits. The cyclotron frequencies of the ion orbits are observed by measuring the oscillating image current generated between two parallel receiver plates on the walls of the cell. The time domain image current is then Fourier transformed to determine the frequencies giving rise to the image current, which are the cyclotron frequencies of the ions and are inversely proportional to *m/z*.[68,69] Resolving power in FTICR-MS is improved by collecting the image current for a longer period of time, but the length of time that it can be collected for is limited by repulsions between like charged ions, collisions between ions and neutral species, and imperfections in the electric and magnetic fields in the ICR cell.[68] The resolving power, dynamic range, maximum measurable *m/z*, and mass accuracy of FTICR-MS are all increased on instruments with higher magnetic field strength.[68]

FTICR-MS instruments are very large, very expensive, and require cryogens to maintain their superconducting magnets.[69] Some advantages of FTICR-MS are the ability to attain extremely high resolving power, the capacity to perform tandem mass

spectrometry experiments in the ICR cell, and the generation of full scan mass spectra without scanning.[68]

1.3.1.4 Orbitrap mass spectrometry

Orbitrap mass spectrometry is another form of Fourier transform mass spectrometry. In an Orbitrap, ions oscillate axially in an electric field with a characteristic frequency that is dependent on their *m/z*, an image current arising from this oscillation is recorded using detector electrodes, and that current is Fourier transformed to obtain the oscillation frequencies corresponding to the *m/z* of ions in the trap. The oscillation frequency, ω, of ions in an Orbitrap is described by Equation 1-4, where e is the charge of an electron, U_r is the electric potential on the central electrode, R_1 is the central electrode radius, R_2 is the outer electrode radius, and R_m is the characteristic radius.[68]

$$\omega = \sqrt{\frac{e}{m/z} \times \frac{2U_r}{{R_m}^2 \ln\left(\frac{R_2}{R_1}\right) - \frac{1}{2}\left({R_2}^2 - {R_1}^2\right)}} \quad \text{Equation 1-4}$$

The resolving power in an Orbitrap is also dependent on the length of time the image current is observed for, which is limited by imperfections in the electric field, ion-ion repulsions, and collisions of ions with neutrals.[68] Orbitraps with higher resolving power can also be built by increasing the electric potential applied (U_r) and decreasing the ratio of the electrode radii (R_2/R_1).[68]

Orbitraps have the second highest resolving power with resolving powers of over 600,000 possible without the need for cryogens for a superconducting magnet.[68] As with FTICR-MS, an Orbitrap generates inherently full scan mass spectra. However, tandem mass spectrometry cannot be done inside the orbitrap.[68]

1.3.2 Mass defects and PFASs

Identification of chlorinated and brominated organic compounds in mass spectra can be assisted by examining their isotope distributions.[73] Fluorine on the other hand has only one naturally occurring isotope.[73] Fortunately, the identification of PFASs in mass spectra can be assisted by the impact of the negative mass defect of fluorine on the mass

defect of PFAS ions. Mass defect is the difference between exact mass and nominal mass for a species and a negative mass defect is when the exact mass is less than the nominal mass. In the case of a fluorine atom, the nominal mass is 19 Da and the exact mass is 18.9984 Da.[74] Because of the substitution of fluorine for protons (1.00794 Da) in PFASs, they tend to have low mass defects, often between -0.10 and +0.15 Da.[7] Therefore, mass spectra can be screened for likely PFAS ions by calculating mass defects and looking for those ions with low mass defects, which is a strategy that numerous studies have applied in untargeted efforts to identify PFASs.[7,64,65,67,75,76]

Mass defects can also aid in the visualization and interpretation of HR-MS data through mass defect plots. A mass defect plot is constructed by plotting the *m/z* of the ions detected on the x-axis and their mass defects, which are exact masses minus nominal masses, on the y-axis.[77] In order to show patterns in the data, the basis of the mass defects can be modified from the IUPAC scale, where the mass of ^{12}C is exactly 12 Da, to alternate mass scales that highlight patterns in the spectrum.[78] This method was first used by Kendrick to convert from the IUPAC scale to a scale where CH_2 is exactly 14 Da, which is called the Kendrick mass scale and is useful for analyzing petroleum hydrocarbons.[79] With PFASs, a useful mass scale to use is a CF_2-based scale where CF_2 is exactly 50 Da.[75] Using this scale, PFAS congeners differing in fluorinated chain length appear in horizontal rows on a mass defect plot.[75] The CF_2 scale can be implemented by applying the following two equations to all the peaks in a mass spectrum:

$$m/z\,(CF_2\ scale) = m/z(IUPAC\ scale)\ \times \left(\frac{50}{49.99681}\right) \quad \text{Equation 1-5}$$

$$mass\ defect\ (CF_2\ scale) = m/z\,(CF_2\ scale) - nominal\ \ m/z\,(rounded) \quad \text{Equation 1-6}$$

An example section of a mass defect plot on the CF_2 scale showing PFSAs and related impurities in a 3M AFFF is shown below in
Figure 1.4.

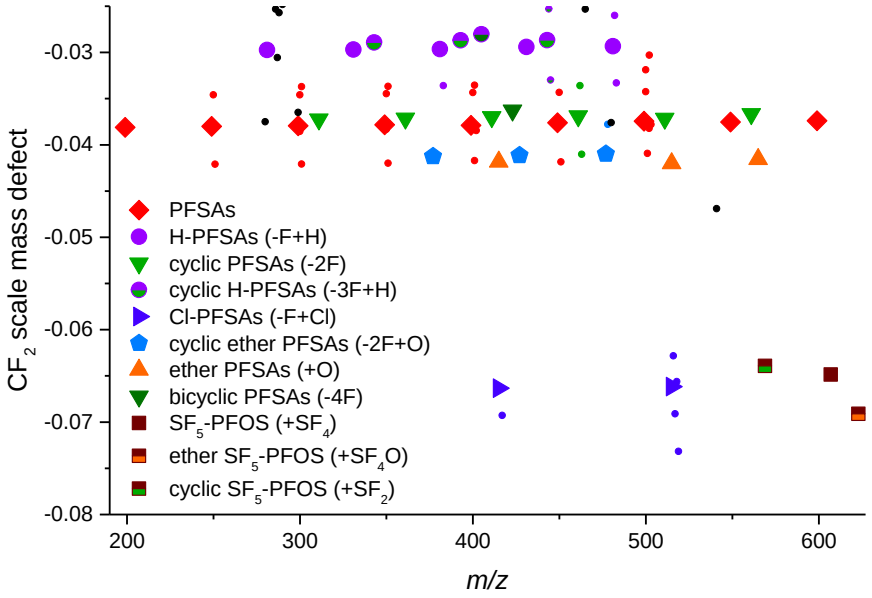

Figure 1.4: Part of the CF_2 scale mass defect plot made with the FTICR-MS spectrum of a 3M AFFF showing PFSA-related compounds. Series' of fluorinated chain length congeners can be found along horizontal lines. PFOS was selectively ejected prior to collecting this spectrum in order to focus on other AFFF components. Data presented were collected as part of Chapter 2 and interpreted based in part on the results presented in Rotander e*t al.* [67] and Baren-Hanson *et al.*[80]

1.3.3 Collision induced dissociation

Fluorinated surfactants, including those used in AFFFs, are generally not volatile and not amenable to gas chromatography mass spectrometry (GC-MS) with electron ionization (EI), which is a hard ionization source and generally results in fragmentation of the molecular ion. The fragmentation in EI mass spectra is highly reproducible and its interpretation for structural information is well established.[73] Fluorinated surfactants are usually ionized by electrospray ionization (ESI), which is a soft ionization technique. ESI primarily results in intact pseudomolecular ions, which are either the protonated or deprotonated molecule, or adducts with ions in the solution undergoing ESI.[81] This property is very useful for determining the molecular formula of unknown components using accurate mass and mass defects. However, mass spectra with intact pseudomolecular ions do not provide structural information about the connectivity of

atoms in unknown components. For this, collision induced dissociation (CID), is used to generate product ions from a precursor ions of interest.[82] CID occurs when gas phase ions collide with neutral gas molecules in their path and may occur with variable amounts of kinetic energy imparted to the ions.[82–84]

CID mass spectra may be generated with tandem-in-time mass spectrometry, which can be done at low resolution with ion trap mass spectrometers or at high resolution inside an FTICR-MS cell.[68] Alternatively, CID spectra may be generated with tandem-in-space mass spectrometry using instruments with a collision cell between two mass analyzers, such that the first mass analyzer can select the precursor ion while the second mass analyzer collects a full scan mass spectrum of the product ions.[82,83] To generate a mass spectrum of the product ions at high resolution various tandem mass spectrometers with at least one high resolution analyzer can be used, such as a quadrupole-time-of-flight (qTOF) MS, a time-of-flight–time-of-flight (TOF-TOF) MS, linear ion trap coupled to Orbitrap MS, or a tandem double focusing electromagnetic sector MS.

Interpretation of CID mass spectra is more complicated than for EI mass spectra because the CID conditions vary depending on the instrument settings used and from instrument to instrument, whereas the conditions of EI with 70 eV electrons are standard and reproducible. Because of this, extensive databases of EI mass spectra exist and can be searched to identify unknowns that are in the database.[73] A more involved approach is needed to interpret CID mass spectra keeping in mind their key properties. To interpret CID mass spectra generated using ESI, it is important to understand that the ions formed in ESI are usually even electron, although there are some exceptions.[81] With even electron ions, it is important to consider the "nitrogen rule" for both precursor and fragment ions where ions of even nominal *m/z* have an odd number of nitrogen atoms and ions of odd nominal *m/z* have an even number of nitrogen atoms, which could be zero.[73] In CID of even electron ions, each fragmentation generally results in an ionic fragment that retains the initial charge and a neutral loss. The fragmentations that occur should involve a chemically plausible fragmentation mechanism that results in fragments that are chemically plausible for gas phase ions. Referring to the literature for CID mass spectra

of compounds of the same class being analyzed,[85] CID mass spectra for compounds containing the functional groups you suspect to be present, or general guides to the fragmentation behaviour of common functional groups can be helpful in interpreting structural information from CID mass spectra.[81] Obtaining a high resolution product ion spectrum improves confidence in the assignment molecular formulae to the product ions, which reduces uncertainty in the interpretation.

1.4 Transformations of PFASs in the environment

1.4.1 Biological transformations of PFASs

PFSAs and PFCAs do not undergo biological transformations due to the exceptional strength of the carbon-fluorine bond, which is the strongest single bond in organic chemistry.[86] This is why the release of fluoride ions from mineralization of PFSAs and PFCAs cannot be detected in aerobic or anaerobic biodegradation.[87–90] Therefore, the discussion of biological transformations of PFASs applies to partially fluorinated PFASs here specifically, perfluoroalkane sulfonamido substances and fluorotelomer PFASs.

1.4.1.1 Biological transformations of perfluoroalkane sulfonamido substances

Perfluoroalkane sulfonamide-based surfactants are major fluorinated ingredients in ECF AFFFs in addition to PFOS.[7,38] Experiments to elucidate the biological transformations of these AFFF components have not been published in the literature but looking at the biological transformations of other perfluoroalkane sulfonamido substances provide insight into what is likely. The most studied perfluorooctane sulfonamido substances in terms of their biotransformation are N-ethyl perfluorooctane sulfonamide (EtFOSA),[91–98] which is the insecticide Sulfluramid, and N-ethyl perfluorooctane sulfonamidoethanol (EtFOSE),[99–104,98,105] which is used in the synthesis of surfactants.

The biological transformations of EtFOSA have been studied in rats;[91–93] sheep;[94] cytochrome P450 isozymes;[96] soil;[98] and rainbow trout,[95] human,[96] polar bear,[97] beluga whale,[97] ringed seal,[97] and rat liver microsomes.[95] The initial studies in rats and sheep

used gas chromatography with an electron capture detector (GC-ECD) for analysis and so were unable to detect non-volatile PFOS, but they did identify perfluorooctane sulfonamide (FOSA) as a metabolite of EtFOSA[91–94] with a longer half-life than EtFOSA.[92,94] With LC-MS/MS it became possible to identify PFOS as the terminal degradation product of EtFOSA in rainbow trout liver microsomes with FOSA as an intermediate.[95] Rat, polar bear, and ringed seal liver microsomes were able to convert EtFOSA to FOSA *in vitro*, while formation of PFOS and transformation of EtFOSA by beluga whale liver microsomes were not observed.[97] With human liver microsomes and cytochrome P450 isozymes, differences in the transformation rates of linear and branched EtFOSA isomers into FOSA were observed, but formation of PFOS was not.[96] The investigation of EtFOSA biodegradation in soil incorporated HR-MS to identify additional intermediates between EtFOSA and FOSA, which were perfluorooctane sulfonamido ethanol (FOSE) and perfluorooctane sulfonamido acetic acid (FOSAA), and illustrate the oxidative nature of aerobic EtFOSA biodegradation.[98]

Biological transformations of EtFOSE have been studied in wastewater treatment plant (WWTP) sludge[99,101–103] rat liver microsomes, cytosol, and slices;[100] rat and human cytochrome P450 enzymes;[100] marine sediments;[104] soil;[98] and earthworms in soil[105] These studies have shown that EtFOSE is a precursor to PFOS in WWTP sludge,[99,102]rat liver slices,[100] marine sediments,[104] soil,[98] and earthworms in soil.[105] Intermediates in the biological transformation include EtFOSAA,[99–102,104,98] EtFOSA,[98,102,104] FOSE,[98,100] FOSAA,[100,102,104,98,105] FOSA,[100,102,104,98,105] and perfluorooctane sulfinic acid (PFOSI).[101,102] The longest lived intermediate in the WWTP sludge biodegradation of EtFOSE is FOSA.[102] In rat liver microsomes, O- and N-glucuronides of EtFOSE, FOSE, and FOSA have also been observed. A general biological transformation scheme for the perfluoroalkane sulfonamido substances is provided as Figure 1.5. Attempts to study the biodegradation of an EtFOSE-based phosphate diester (SAmPAP diester) in marine sediments resulted in negligible degradation over 120 days, probably due to limited bioavailability resulting from the size of the SAmPAP diester with two perfluorooctane chains.[104]

Biodegradation of a perfluorooctane sulfonamido quaternary ammonium salt (PFOSAmS) and an analogous perfluorooctane amido quaternary ammonium salt in soil were found to result in PFOS and PFOA, respectively through hydrolysis of the sulfonamide and amide bonds with amide hydrolysis occurring on much shorter time scales than sulfonamide hydrolysis.[106] Intermediates were identified by HR-MS in both biodegradation pathways consisting of N-demethylation products, the carboxylic acid resulting from loss of the ammonium moiety by N-dealkylation and oxidation, and in the case of the PFOSAmS, FOSA.[106]

From these biodegradation and biotransformation experiments with perfluoroalkane sulfonamido substances, it would be predicted that for sufficiently bioavailable perfluoroalkane sulfonamido substances, biodegradation will occur through oxidation of non-perfluoroalkyl moieties eventually forming corresponding perfluoroalkane sulfonamides that degrade to the corresponding PFSA.

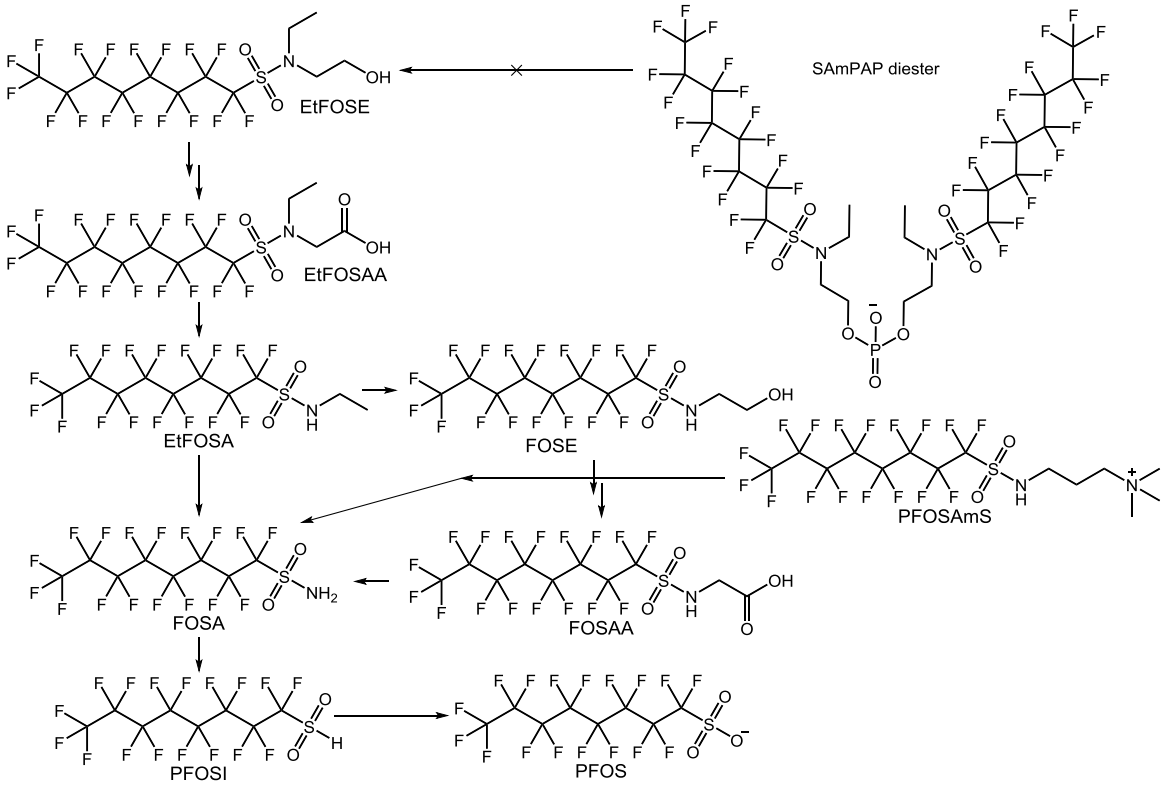

Figure 1.5: Biological transformation scheme for perfluorooctane sulfonamido substances.

1.4.1.2 Biological transformations of fluorotelomer-based substances

Biological transformations of a broader variety of fluorotelomer-based substances have been investigated, including fluorotelomer alcohols (FTOHs),[107–119] fluorotelomer acrylate (FTAC) and fluorotelomer methacrylate (FTMAC) monomers,[120–122] fluorotelomer phosphate esters (PAPs),[123–126] FTSAs,[127–129] fluorotelomer urethane monomers,[130] FTSASs,[17,131] fluorotelomer iodides (FTIs),[132] fluorotelomer stearate and citrate esters,[133,134] and fluorotelomer side-chain fluorinated polymers.[135–140]

The 8:2 FTOH was the starting point in investigating the biological transformations of fluorotelomer-based substances, and has been assessed in a variety of systems, including aerobic WWTP sludge,[108,109,111] rat hepatocytes,[110] anaerobic digester WWTP sludge,[115] soil,[140] rats,[107,117] and human liver cytochrome P450s, microsomes, and cytosol.[119] The biological transformation of 8:2 FTOH begins with oxidation of the alcohol to 8:2 fluorotelomer aldehyde (FTAL).[108,111] The 8:2 FTAL may undergo either oxidation to 8:2 fluorotelomer carboxylic acid (FTCA)[107–111] or loss of HF forming the 8:2 fluorotelomer unsaturated aldehyde (FTUAL),[110] which can bind to nucleophilic sites on proteins[141] or glutathione.[110] Protein binding was observed in rats dosed with 8:2 FTOH, particularly in the liver.[117] The 8:2 FTCA may undergo an α-oxidation-like reaction forming perfluorononanoate (PFNA) as one possible terminal product, which was observed with rat hepatocytes[110] and rats.[117] Loss of HF can also occur with 8:2 FTCA forming 8:2 fluorotelomer unsaturated carboxylic acid (FTUCA).[108–111] The 8:2 FTUCA may undergo a multistep transformation into PFOA, another terminal degradation product, observed in aerobic WWTP sludge,[108,109] rat hepatocyte,[110] rat,[107,117] and soil systems.[140] Alternatively, 8:2 FTUCA may undergo dehydrohalogenation forming 7:3 FTUCA,[111] which may be reversibly hydrogenated to 7:3 FTCA,[111,142] in a pathway with multiple intermediates that leads to PFHpA and possibly PFHxA as terminal products.[117,140] The additional intermediates that have been identified in the biological transformation of 8:2 FTOH to PFCAs are numerous and include fluorotelomer ketones, secondary fluorotelomer alcohols, and unsaturated PFCAs.[111,140] While PFCA production from 8:2 FTOHs was observed in most biological systems, the terminal product observed in anaerobic WWTP digester sludge was 7:3 FTCA,[115]

indicating that final degradation to PFCAs may not be possible in all biological systems. Phase II conjugation of 8:2 FTOH through sulfation and glucuronidation can also occur to a significant extent.[110,119] Biological transformations of 6:2 FTOH have also been investigated, revealing equivalent intermediates and products to 8:2 FTOH with shorter perfluoroalkyl groups although the product distribution may differ.[112–116,118]

Other fluorotelomer PFASs whose biological transformations have been investigated tend to ultimately yield PFCAs through many of the intermediates in the FTOH to PFCA degradation pathway. Several fluorotelomer substances consisting of esters of 8:2 FTOH, including 8:2 FTAC,[120–122] 8:2 FTMAC,[122] 8:2 fluorotelomer stearate,[133,134] and 8:2 fluorotelomer citrate[134] have been shown to undergo enzymatic hydrolysis of the ester followed by degradation of resulting 8:2 FTOH following the known degradation pathway in rainbow trout[120,121] and aerobic soil.[122,133,134] Two 8:2 fluorotelomer urethane monomers were also found to undergo hydrolysis of the carbamate group forming 8:2 FTOH and eventually PFOA in one soil but not in another.[130] Both PAP monoesters (monoPAPs) and PAP diesters (diPAPs), which have been detected in human blood,[143,144] of various chain-lengths have been found to undergo hydrolysis of the phosphate ester forming FTOHs that then degrade to FTCAs, FTUCAs, and finally PFCAs in aerobic WWTP sludge,[124] rats,[123] and soil-plant sytems.[125] In a soil system, 6:2 FTI, the intermediate in 6:2 FTOH production, was found to undergo hydrolysis forming 6:2 FTOH with subsequent biodegradation to FTCAs and finally PFCAs.[132]

The sulfur-containing fluorotelomer substances 6:2 FTSA and FTSASs were found to ultimately degrade to PFCAs under aerobic conditions.[17,127–129,131] In aerobic WWTP sludge[127,128] and aerobic sediments,[129] 6:2 FTSA was found to biodegrade to PFCAs, including perfluoropentanoate (PFPeA),[128,129] PFHxA,[127–129] and PFHpA,[127,129] through intermediates, including 6:2 FTOH and PFASs in the FTOH to PFCA biodegradation pathway. However, biodegradation of 6:2 FTSA was not observed in anaerobic sediment.[129] Biodegradation of 6:2 FTSAS in aerobic WWTP sludge and a commercial mixture containing 4:2, 6:2, and 8:2 FTSASs in aerobic soil was found to occur through oxidation of the thioether to the sulfoxide and sulfone, hydrolysis of the

carbon-sulfur bonds leading to corresponding FTSAs and FTOHs, and ultimately biodegradation to PFCAs through FTCA intermediates.[17,131] The biological transformation of the AFFF component 6:2 fluorotelomer sulfonamide alkylbetaine (FTAB) was studied in turbot and blue mussels with no findings of 6:2 FTSA or PFCA formation above background levels, while 6:2 fluorotelomer sulfonamide (FTSAm) and N-dealkylation products, including 6:2 fluorotelomer sulfonamide alkylamine (FTAA) were observed.[16]

Assessing the biodegradation of side-chain fluorinated fluorotelomer-based polymers is substantially more complex than for discrete small molecules due to the inability to measure the starting material with conventional LC-MS/MS or GC-MS methods, difficulties in selecting a starting material representative of commercial polymers, and the presence of residual monomers or FTOHs in the polymers.[138,139,145] In part due to the analytical challenges, there have been considerable discrepancies in different assessments of the degradability of side-chain fluorinated polymers with estimates of the half-life of an acrylate side-chain fluorinated polymer at 1200–1700 years and an urethane side-chain fluorinated polymer at 28–241 years in soil microcosms by DuPont researchers,[135,137] while EPA researchers determined a half-life in soil of 870–1400 years for a coarse-grained polymer that may be as short as 10-17 years for fine-grained polymers.[136] Rankin *et al.* were the first to show that side-chain fluorinated polymer degradation occurred in soil-plant microcosms by matrix assisted laser desorption ionization (MALDI) TOF-MS of the polymer itself and estimated the half-life of an in-house synthesized polymer at between 8 and 111 years.[138] Most recently, Washington *et al.* reported half-lives of 33–112 years for two commercial side-chain fluorinated acrylate polymers in four aerobic soils.[139] Taken together most of these investigations of biodegradation of side-chain fluorinated polymers in soil show that the side-chains are hydrolyzed releasing FTOHs that biodegrade to PFCAs with the polymers having half-lives on the order of decades.[136–139]

A simplified biological degradation scheme for 6:2 fluorotelomer substances is shown in Figure 1.6, with the 6:2 fluorotelomer chain-length chosen because it was found to be most abundant in AFFF components, including FTSASs.[12,17]

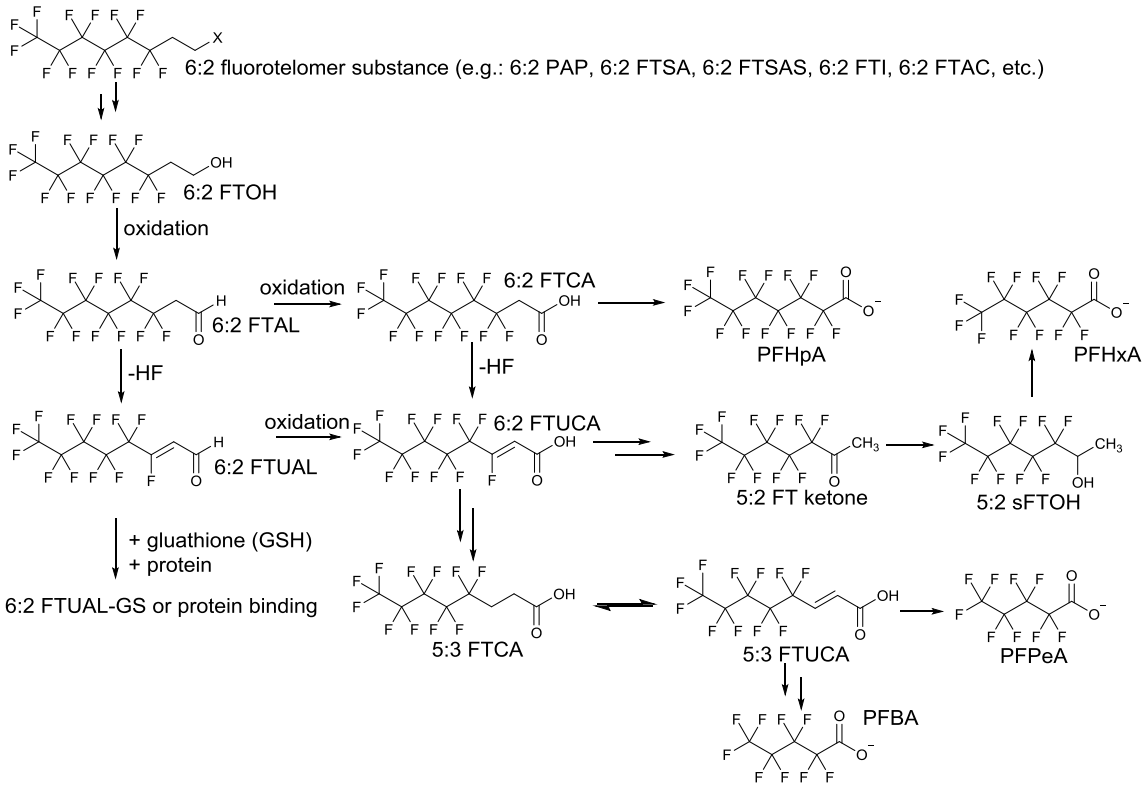

Figure 1.6: Simplified scheme for biological transformation of 6:2 fluorotelomer substances to PFCAs.

1.4.2 Abiotic transformations of PFASs in the environment

Degradation of PFASs other than PFCAs and PFSAs in the environment can also occur by abiotic mechanisms. These include atmospheric oxidation of volatile PFASs by gas phase oxidants and direct or indirect aqueous photolysis in sunlit surface waters.

1.4.2.1 Atmospheric oxidation of volatile PFASs

In the atmosphere, certain volatile PFASs, including FTOHs, FTIs, FTACs, perfluoroalkane sulfonamido substances, and perfluoroalkyl amides, can be oxidized by atmospheric oxidants producing PFCAs and/or PFSAs depending on the starting PFAS[146–152] as has been reviewed by Young and Mabury.[153] For FTOHs,[146,147] FTIs,[150] FTACs,[151] and perfluoroalkyl amides,[152] the only PFAAs produced are PFCAs, although the mechanism includes a cyclical perfluoroalkyl chain-shortening step yielding a range of PFCAs with shorter perfluoroalkyl chains than the starting material and CF_2O.[146] With volatile perfluoroalkane sulfonamido substances, production of PFCAs in a mechanism

including the chain-shortening cycle occurs,[148,149] but with N-methyl perfluorobutane sulfonamido ethanol (MeFBSE) D'Eon *et al.* also observed production of perfluorobutane sulfonate (PFBS) in smog chamber atmospheric oxidation experiments, indicating the potential for atmospheric PFSA production from volatile perfluoroalkane sulfonamido substances.[149]

Atmospheric oxidation of these PFASs would generally be initiated by the abstraction of a hydrogen atom by a gas phase hydroxyl radical ($^{\bullet}OH$),[146–149,151–153] although with FTIs photolysis of the carbon-iodine bond can also occur.[150] Atmospheric oxidation generally continues through multiple rounds of oxygen addition, reactions with nitrogen monoxide or peroxy radicals, and losses of alkoxy radicals or NO_2, resulting in oxidation of the PFAS and shortening of the molecule through losses of carbon dioxide.[146–152,154] When a perfluoroalkyl radical is produced, either a perfluoroalkyl chain-shortening cycle with loss of COF_2 or production of a PFCA through reaction with a alkyl peroxy radical, loss of an aldehyde, loss of HF, and hydrolysis may occur.[154] In the case of perfluoroalkane sulfonamido substances, an alternative pathway involving cleavage of the sulfur-nitrogen bond may occur resulting in a PFSA.[149] To illustrate the production of PFCAs from volatile precursors, a simplified scheme for atmospheric oxidation of an FTOH is shown in Figure 1.7.

When considering PFASs found in AFFFs, atmospheric degradation mechanisms should be kept in mind because they may be relevant for any volatile degradation products, such as FTOHs, uncharged perfluoroalkane sulfonamido substances, or uncharged fluorotelomer sulfonamides. Volatile PFAA precursors, particularly FTOHs, FTACs, and perfluoroalkane sulfonamido substances have been measured in air samples from around the world at concentrations that vary with location due to the short atmospheric half lives (under 1 month) of these PFASs.[153] The concentrations of FTOHs in the atmosphere range from sub pg/m^3 to over 1000 pg/m^3 and tend to decrease when moving from urban to remote locations,[153,155–157] while concentrations of FTACs tend to be lower and are typically less than 100 pg/m^3 with some exceptions,[153] and perfluorooctane sulfonamido substances and perfluorobutane sulfonamido substances are associated with atmospheric particles more than FTOHs and are usually found at sub

pg/m^3 to hundreds of pg/m^3 concentrations.[153,155,156] WWTPs can be sources of volatile PFASs to the atmosphere[158] and may enable release of volatile products of AFFF-related PFAS degradation.

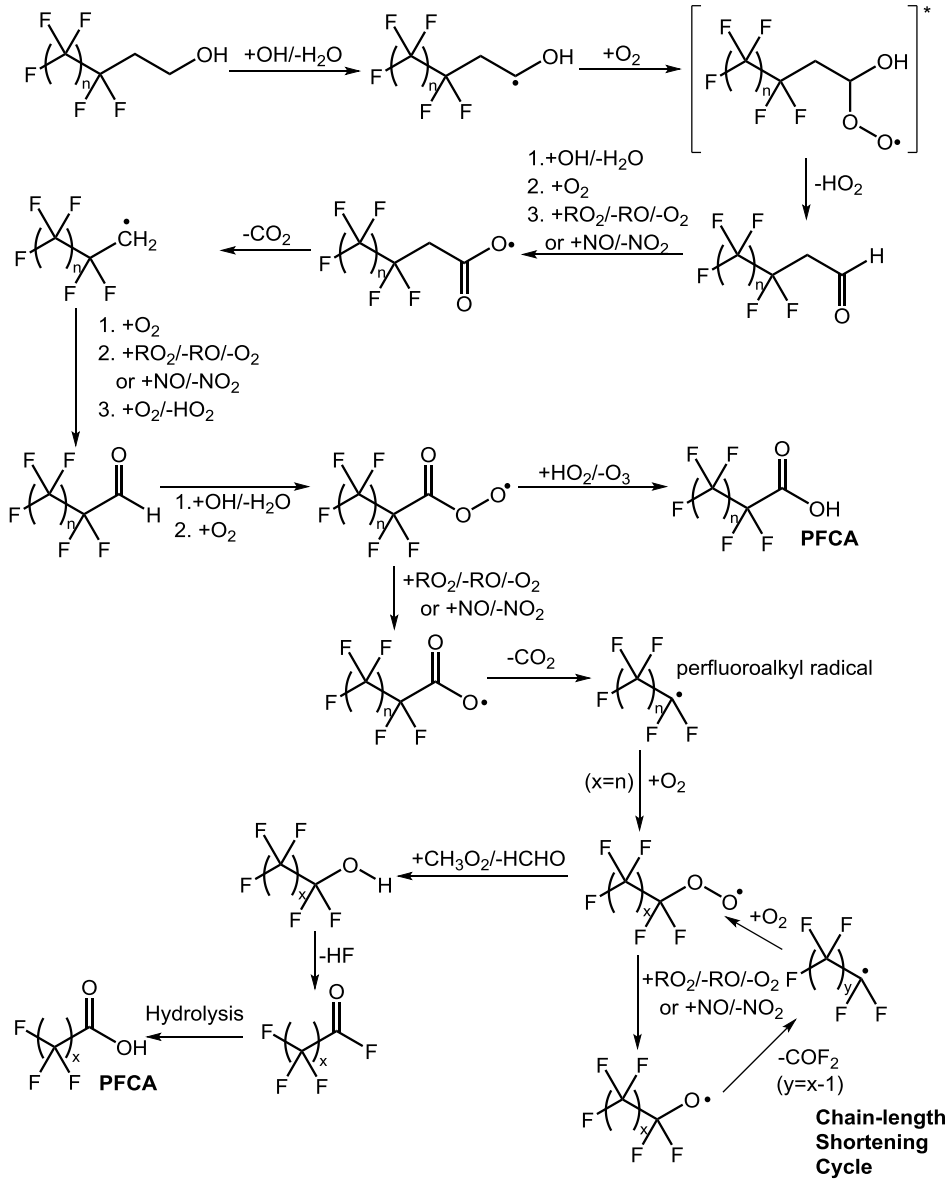

Figure 1.7: Simplified scheme for atmospheric oxidation of an FTOH producing PFCAs and undergoing chain-length shortening.

1.4.2.2 Aqueous photolysis of PFASs

In sunlit surface waters, PFASs may be degraded by either direct photolysis or indirect photolysis. Direct photolysis occurs when the molecule in question absorbs a

photon and the energy imparted by that photon causes the molecule to chemically react.[159] When photons are absorbed by other molecules in the water leading to production of aqueous phase oxidants, such as hydroxyl radicals ($^{\bullet}OH$), ozone, carbonate radicals ($CO_3^{\bullet-}$), and nitrate radicals ($NO_3^{\bullet-}$), which react with the molecule in question that is indirect photolysis.[159] The aqueous photolysis of a few PFASs has been investigated.

Aqueous photolysis of 8:2 FTOH has been investigated in deionized water, deionized water with hydrogen peroxide (H_2O_2), synthetic field water, and Lake Ontario surface water in a sunlight simulator.[160] It was found that 8:2 FTOH undergoes only indirect photolysis, primarily by hydroxyl radical, with products including 8:2 FTAL, 8:2 FTCA, 8:2 FTUCA, PFOA, and PFNA.[160] The indirect photolysis of EtFOSAA, EtFOSE, EtFOSA, and FOSA by $^{\bullet}OH$ was investigated using solutions of H_2O_2 in deionized water in a sunlight simlulator.[161,162] Except for FOSA, which did not degrade, these perfluorooctane sulfonamido substances degraded by oxidation of alkyl substituents on the sulfonamide nitrogen, N-dealkylation of the sulfonamide, and cleavage of the sulfur-carbon bond followed by oxidation and hydrolysis of the perfluoroalkyl chain forming PFOA.[161,162] Production of PFOS by indirect photolysis was not observed.[161,162]

The aqueous photolysis of the AFFF component 6:2 FTAB has been investigated in sunlit surface waters using commercial material in seawater[16] and in deionized water and synthetic field water using purified 6:2 FTAB synthesized as part of this thesis.[163] It was found that 6:2 FTAB underwent both direct and indirect photolysis.[163] Both studies detected 6:2 fluorotelomer sulfonamide (FTSAm) as a major photodegradation product of 6:2 FTAB and 6:2 FTAA as an additional product.[16,163] Only using the purified 6:2 FTAB was it possible to measure further aqueous photolysis products, including 6:2 FTSA, 6:2 FTOH, 6:2 FTUCA, PFHpA, PFHxA, and PFPeA, indicating that 6:2 FTAB is a PFCA precursor by aqueous photolysis likely involving $^{\bullet}OH$ and $CO_3^{\bullet-}$ radicals.[163]

Although investigations of the aqueous photolysis of PFASs are quite limited, the literature that is available suggests that aqueous photolysis of perfluoroalkane

sulfonamido substances and fluorotelomer PFASs tends to lead to PFCAs and involves some of the same intermediates as biodegradation of PFASs.

1.5 Non-transformative processes affecting the fate of PFASs in the environment

1.5.1 Sorption of PFASs to soils and sediments

In the environment, PFASs may be present in the dissolved phase in environmental waters, both surface water and groundwater, or they may undergo sorption to the solid phase in soils and sediments. Research into the factors influencing the sorption of PFASs to soils and sediments has focused primarily on PFCAs and PFSAs, especially PFOA and PFOS, although perfluorooctane sulfonamido substances are sometimes included.

Laboratory studies of the sorption of PFASs are performed using either batch sorption[164–166] or flow through column techniques[167,168] and allow control of variables affecting both the aqueous phase and the soil, sediment, or component thereof being examined. These experiments allow the determination of soil/sediment-water distributions coefficients (K_d), which are ratios between concentrations in soil or sediment and water at equilibrium. These equilibrium coefficients can also be expressed as the ratio of concentration in the organic carbon component of the soil or sediment to the concentration in water for an organic carbon normalized distribution coefficient (K_{oc}). While field-based determinations of distribution coefficients lack the control of variables available in the laboratory, they can help to confirm the relevance of trends observed in the laboratory to the real environment.

Investigations of the sorption of PFASs to soils and sediments have found that the properties of the PFAS that impact sorption include the perfluoroalkyl chain-length and the nature of additional functional groups. Beyond a minimum chain-length that may depend on the particular soil or sediment,[165] increasing perfluoroalkyl chain-length has been found to increase sorption of homologous series' of PFASs, including PFCAs and PFSAs.[165,169] In Table 1.6, a selection of distribution coefficients determined for PFCAs in the laboratory and the field illustrate the influence of perfluoroalkyl chain-length on

sorption. The influence of other functional groups on the sorption of PFASs is demonstrated by the $\log K_{oc}$ values determined by Higgins and Luthy for PFNA (2.50 ±0.12), PFOS (2.68 ±0.09), and EtFOSAA (3.49 ±0.07) all of which have eight perfluoroalkyl carbons, where the PFCA is less sorptive than the PFSA, which is less sorptive than the N-ethyl sulfonamido acetic acid.[164] This trend of PFCAs being less sorptive than PFSAs with the same number of perfluoroalkyl carbons was found to extend to PFBS and PFHxS in laboratory studies by Guelfo and Higgins in soil[165] and by Zhao *et al.* in sediments.[170] The greater sorption of EtFOSAA compared to PFOS has also been observed in the field.[171,172] Enhanced sorption of uncharged FOSA compared to anionic PFOS was determined in the laboratory[166] and observed in sediments in the field by Ahrens *et al.*[171] While perfluoroalkyl chain-length and additional functional groups influence sorption, laboratory and field data on the sorption of PFASs other than PFCAs and PFSAs is limited and more study is required to understand the fate of these other PFASs in aqueous environments.

Table 1.6: Selected laboratory and field PFCA distribution coefficients ($logk_d$) and organic carbon normalized distribution coefficients ($logK_{oc}$)

Sorbent	PFBA		PFPeA		PFHxA		PFHpA		PFOA		PFNA		PFDA		PFUnDA		Reference
	$logK_d$	$logK_{oc}$	$logK_d$	$logK_{oc}$	$logK_d$	$logK_{oc}$	$logK_d$	$logK_{oc}$	$logK_d$	$logK_{oc}$	$logK_d$	$logK_{oc}$	$logK_d$	$logK_{oc}$	$logK_d$	$logK_{oc}$	
Laboratory																	
freshwater sediments	--	--	--	--	--	--	--	--	--	2.11	--	2.50 ±0.12	--	2.92 ±0.04	--	3.47 ±0.04	Higgins & Luthy[164]
sandy soil	--	--	--	--	--	--	-0.20 ±0.01	-0.20	0.18 ±0.03	0.18	0.72 ±0.03	0.72	1.48 ±0.02	1.48	--	--	Enevoldsen & Juhler[173]
clay soil	--	--	--	--	--	--	-0.20 ±0.05	0.18	0.26 ±0.06	0.63	0.89 ±0.02	1.26	1.52 ±0.02	1.90	--	--	Enevoldsen & Juhler[173]
kaolinite	--	--	--	--	--	--	--	--	0.36 ±0.08	--	0.74 ±0.06	--	1.30 ±0.04	--	1.70 ±0.05	--	Xiao *et al*[174].
river sediment	--	--	--	1.70 ±0.02	--	--	--	1.72 ±0.01	--	2.09 ±0.01	--	2.50 ±0.01	--	3.23 ±0.07	--	--	Zhao *et al.*[170]
wetland sediment	--	--	--	2.11 ±0.05	--	--	--	2.05 ±0.02	--	2.17 ±0.01	--	2.35 ±0.01	--	2.78 ±0.06	--	--	Zhao *et al.*[170]
sediment column	-2.4	0.8	-1.4	1.8	-0.18	3.0	--	--	0.82	4.0	0.65	3.8	--	--	--	--	Vierke *et al.*[167]
3 soils	--	1.88 ±0.11	--	1.37 ±0.46	--	1.31 ±0.29	--	1.63 ±0.15	--	1.89 ±0.02	--	2.36 ±0.04	--	2.96 ± 0.15	--	3.56	Guelfo & Higgins[165]
loamy sand soil	-0.22	--	-0.63	--	-0.73	--	-0.35	--	-0.13	--	0.31	--	0.94	--	1.56	--	Guelfo & Higgins[165]
loam soil	0.50	--	-0.44	--	-0.31	--	0.13	--	0.54	--	1.04	--	1.77	--	--	--	Guelfo & Higgins[165]
sandy clay loam	-0.10	--	-0.28	--	-0.49	--	-0.33	--	-0.19	--	0.28	--	0.73	--	--	--	Guelfo & Higgins[165]
Field																	
Tokyo Bay sediment	--	--	--	--	--	--	--	--	0.04 ±0.03	1.9 ±0.1	0.6 ±0.1	2.4 ±0.1	1.8 ±0.1	3.6 ±0.1	3.0 ±0.1	4.8 ±0.2	Ahrens *et al.*[171]
Netherlands canal sed.	--	--	--	--	--	--	--	--	1.85 ±0.41	--	2.89 ±0.53	--	2.87 ±0.23	--	--	--	Kwadijk *et al.*[175]
Orge River sediment	--	--	--	--	0.8 ±0.0	2.1 ±0.2	0.8 ±0.1	2.1 ±0.2	--	--	1.5 ±0.1	2.9 ±0.1	2.4 ±0.2	3.8 ±0.2	3.4 ±0.1	4.7 ±0.1	Labadie & Chevreuil[169]
Dianchi Lake sediment	1.18 ±0.10	2.62 ±0.10	1.14 ±0.38	2.54 ±0.51	1.33 ±0.37	2.72 ±0.40	1.24 ±0.15	2.62 ±0.21	1.27 ±0.40	2.63 ±0.45	1.18 ±0.21	2.75 ±0.22	1.64 ±0.28	3.05 ±0.30	1.89 ±0.11	3.28 ±0.21	Zhang *et al*[176].
Singapore river sed.	--	--	--	--	--	--	--	--	--	3.4 ±0.2	--	4.0 ±0.3	--	4.6 ±0.3	--	4.9 ±0.4	Nguyen *et al.*[172]

Properties of the aqueous phase and sorbent also have been found to influence the sorption of PFASs. In their laboratory study of the sorption long-chain PFCAs, PFSAs, and FOSAAs, Higgins and Luthy found that sorption was positively correlated with organic carbon percentage in sediment and calcium ion concentration in the aqueous phase, negatively correlated with pH, and not influenced by sodium ion concentrations.[164] Lower pH likely increases protonation of the sediment reducing repulsions between the anionic PFASs and sediment.[164] The correlation between PFAA sorption and organic carbon content of sorbents has not been found consistently for all PFAAs, however.[165,166] The influence of dissolved ions on PFAA sorption has been observed by several authors in the laboratory[164,174,177] and in the field.[178–180] Dissolved ions have a salting out effect, whereby sorption is greater in more saline waters, particularly those with higher concentrations of Ca^{2+},[164] perhaps due to formation of ion pairs with PFAAs[179] or increased presence of cations at the surface of the sorbent reducing electrostatic repulsion of PFAAs.[164,179]

The sorption of PFAAs may also involve competition for sorption sites, since sorption coefficients of short-chain PFAAs on kaolinite were found to decrease in the presence long-chain PFAAs.[174] But, in another study competitive effects on PFOS and PFOA sorption were only observed in one out of three soils.[165] The reversibility of sorption of PFAAs is another aspect of their sorption that has been investigated and it has been found that while sorption is highly reversible for weakly sorptive, short-chain PFAAs,[70] it is increasingly irreversible as perfluoroalkyl chains get longer.[170,181]

1.5.2 Biological uptake of PFASs

The most studied PFASs in terms of their uptake to animals and plants are PFCAs and PFSAs. The initial studies of the uptake and PFCAs and PFSAs to living things were conducted with animals, especially various species of fish. The bioconcentration of PFCAs and PFSAs from water into fish generally increases with increasing chain-length and is greater for PFSAs than PFCAs of the same perfluoroalkyl chain-length.[182–185] These patterns are also seen in wild fish, such as in an AFFF-impacted lake near Stockholm Airport in European perch[35] and in carp and sharpbelly from a highly

contaminated lake in China,[186] where patterns of field bioaccumulation factors (BAFs) were consistent with the laboratory observations. The accumulation of PFCAs and PFSAs into aquatic organisms from water may be concentration dependent with greater bioconcentration factors (BCFs) for lower concentrations of PFAAs in water.[184] Dietary accumulation of PFCAs and PFSAs to rainbow trout was also found to depend on perfluoroalkyl chain-length and head group with greater BAFs and slower depuration rates associated with longer perfluoroalkyl chains and with PFSAs versus PFCAs.[187,188] Bioconcentration of some alternatives to PFOS and PFOA has been investigated with mixed findings where a perfluoroalkyl ether carboxylate polymerization aid (2,3,3,3-tetrafluoro-2-(heptafluoropropoxy)-propanoate) had low bioconcentration in common carp,[189] while a chloro-perfluoroalkyl ether sulfonic acid (F-35B) PFOS alternative was found to bioaccumulate to a greater extent than PFOS in wild crucian carp in a contaminated environment.[190] This highlights the importance of evaluating replacement chemistries to determine if they are actually less bioaccumulative and less persistent.

Investigations of the uptake of fluorotelomer substances have demonstrated the importance of biological transformations for PFASs that can be rapidly biotransformed. When rainbow trout were dosed with 8:2 FTAC in their food, it was rapidly transformed with very little detected in tissues or feces, while transformation products were detected in the fish at much higher concentrations.[120] When rats were dosed with monoPAPs or diPAPs by oral gavage, monoPAPs were not absorbed but transformation products were measured in the rats' blood, while diPAPs were absorbed with higher bioavailability for shorter chain-lengths and also underwent biotransformation.[191] Bioconcentration and bioaccumulation of 6:2 FTSA in rainbow trout were found to be low with a BCF less than 40 and a dietary biomagnification factor of 0.295, but biotransformation was assumed to be insignificant and not investigated *in vivo*.[192] In a bioconcentration study on rainbow trout with AFFF concentrates, uptake of substantial quantities of unknown organofluorine from the AFFFs was found with approximately 50% of organofluorine unknown in fish dosed with an ECF AFFF and 95% of organofluorine unknown in fish dosed with the fluorotelomer AFFF.[45] This indicates that bioconcentration of poorly characterized AFFF components and their biotransformation products can be significant.

An experiment to determine the dietary bioaccumulation of perfluoroalkyl phosphinates (PFPiAs) and perfluoroalkyl phosphonates (PFPAs) provided further evidence of the influence of polar head groups on PFAA bioaccumulation with lower bioaccumulation observed than for PFCAs or PFSAs of equivalent chain-length.[193] Unexpectedly for a PFAA, the trout appeared to eliminate PFPiAs by metabolizing them to PFPAs, which is the first observed transformation of a PFAA.[193]

In animals, PFAAs tend to accumulate in protein rich compartments, especially liver, blood, and kidneys, unlike conventional persistent organic pollutants, which tend to accumulate in lipids.[182,188,193,194] This is probably due to different mechanisms for the bioconcentration and distribution of anionic PFAAs versus neutral, hydrophobic contaminants, which appear to involve binding with functional proteins, including serum albumin[195] and liver fatty acid binding protein[196,197] as well as interactions with phospholipids.[198]

Recently, the uptake of PFCAs and PFSAs by plants has been investigated for plants grown both hydroponically and in soil.[199–205] In plants grown in soil, bioaccumulation generally decreases with increasing perfluoroalkyl chain-length and PFCAs accumulate more than PFSAs, at least for plant compartments beyond the roots.[199–204] This result is opposite to what is found in animals, particularly fish, due to the importance of water solubility in transport of PFAA s through plants.[206] In the field, it has been determined that leaves of deciduous and coniferous trees in Dalian, China contain higher concentrations of short-chain PFCAs than other PFAAs, which is consistent with these studies.[207] Increased accumulation in plants of more hydrophilic degradation products of 6:2 diPAP[125] and 8:2 diPAP,[208] including short-chain PFCAs has been found in plants grown in diPAP spiked soils and in plants grown in soil amended with biosolids, paper fiber, and/or compost containing diPAPs.[125] In hydroponically grown plants, greater accumulation of PFAAs with increasing chain-length in the roots occurs for long-chain PFAAs, probably due to sorption to roots without soil sorption sites available.[209–211,205,206] This can lead to greater accumulation factors for long-chain PFAAs than short-chain PFAAs in plant stems and even leaves, for hydroponically grown plants,[210,211,206] despite more efficient transport of short-chain PFAAs from roots to stems

and beyond.[209,212] Since plants grown in soil are more relevant to agriculture and to natural vegetation, the increased accumulation of short-chain PFAAs, especially PFCAs, in most plant compartments is most relevant to the exposure of people and grazing animals through eating plants. With the switch to short-chain fluorotelomer-based AFFFs, degradation of these PFASs may contribute to contamination with short-chain PFCAs that can accumulate in plants with BAFs greater than 1.[200]

1.6 Presence of PFASs in surface water

PFASs are ubiquitous in surface water environments, but are found at highly variable concentrations and profiles of different PFAS congeners. In general, the highest PFAS concentrations area associated with close proximity to a point source of PFASs, while the lowest concentrations are found in remote environments such as in the ocean far from PFAS sources.[213] Point sources of PFASs include sites of AFFF release,[19,21,29] fluorochemical industries,[186,214] WWTP effluents,[215–217] landfills,[218,219] and runoff from contaminated areas.[220,221] Some selected examples of the range of PFAS concentrations that have been found in surface waters are shown in Figure 1.8a. These concentrations range over seven orders of magnitude from millions of ng/L at highly contaminated sites, such as downstream of a Chinese fluorochemical industrial site[214] and in Etobicoke Creek immediately following an AFFF spill,[21] to under 0.1 ng/L in remote ocean sites, such as in the Atlantic Ocean near the southern tip of South America,[222] or in the depths of meromictic, remote arctic lakes.[223] In between these concentrations are more typical urban surface waters[224,217,225] and surface waters in relatively remote terrestrial locations.[223,226,32,227]

The PFAS profiles in surface waters also vary depending on the source of the PFASs and what is measured. A selection of example PFAS profiles are shown in Figure 1.8b and serve to highlight the variability in PFAS profiles across different locations. These profiles can vary tremendously from mostly PFOS after a PFOS-containing AFFF was released,[21] to predominantly PFOA downstream of a fluoropolymer plant,[214] to primarily short-chain PFCAs in remote terrestrial sites,[32,226,227] to largely PFBS and perfluorobutanoate (PFBA) in Lake Tangxun near a Chinese fluorochemical industry.[186]

However, it is often difficult to compare conclusions about PFAS profiles between studies that measure different suites of PFCAs and PFSAs, that may include or exclude various long- and short-chain PFAAs. For example, Lescord *et al.* analyzed PFCAs from PFHxA to perfluorotetradecanoic acid (PFTeDA) in water from remote Canadian arctic lakes,[32] so one cannot know if these waters also have a predominance of PFBA and PFPeA as seen in remote sites in Tibet and Svalbard.[226,227] Nevertheless, differences in PFAS profiles can provide clues about the locations and identities of sources of contamination.[217,228,29] For example, equal concentrations of even and odd chain PFCA pairs, such as PFOA/PFNA and PFDA/PFUnDA , may indicate an atmospheric source due to atmospheric oxidation of precursors.[22,31,229]

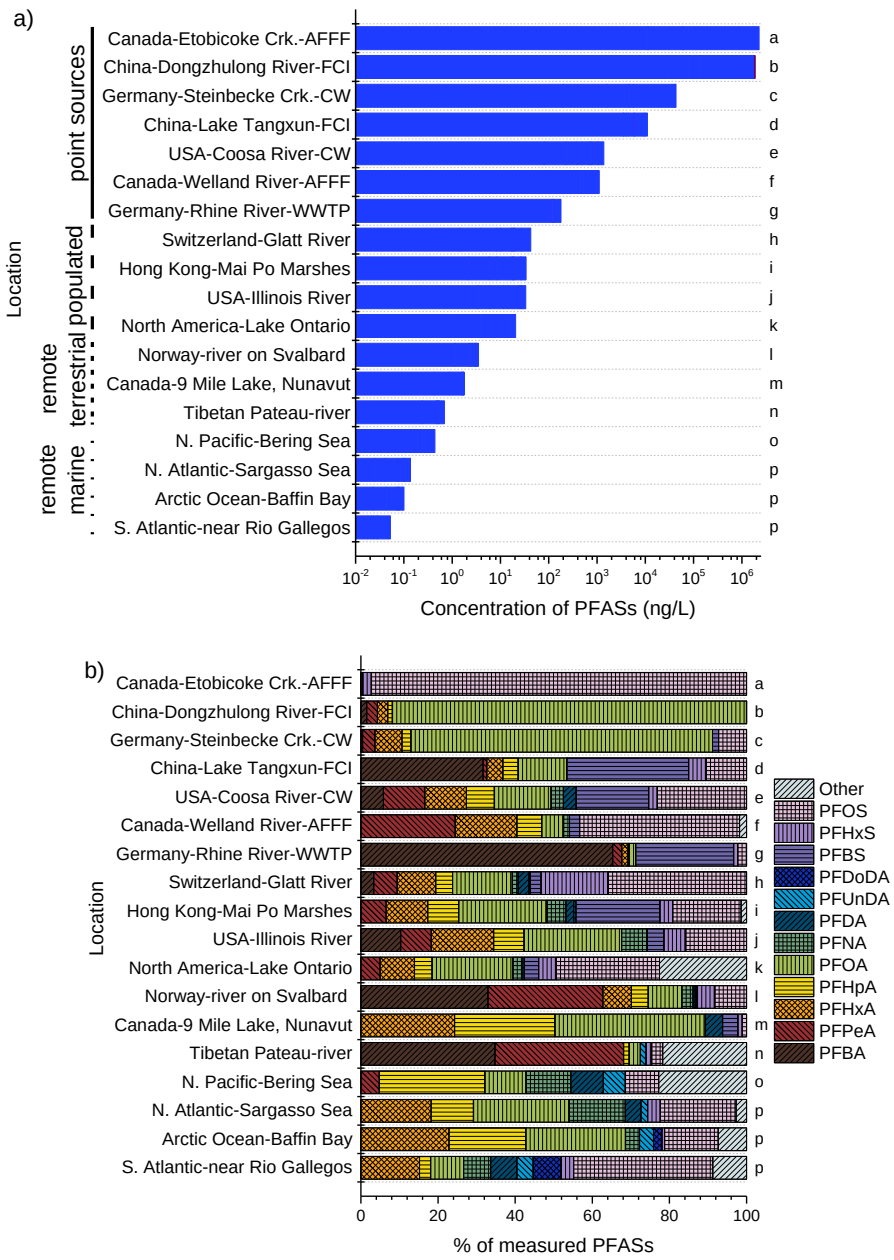

Figure 1.8: Illustrative examples of PFASs measured in surface waters showing variability in PFAS a) concentrations and b) congener profiles. Examples are from references a-Moody *et al.*[21], b-Liu *et al.*[214], c-Skutlarek *et al.*[220], d-Zhou *et al.*[186], e-Lasier *et al.*[221], f-de Solla *et al.*[29], g-Möller *et al.*[217], h-Müller et al.[228], i- Loi *et al.*[225], j-Nakayama *et al.*[224], k-De Silva *et al*[230]., l-Kwok *et al.*[226], m-Lescord *et al.*[32], n-Yamazaki *et al.*[227], o-Cai *et al.*[231], and p-Benskin *et al.*[222] For the most contaminated sites sources of PFASs are identified including AFFF release, fluorochemical industries (FCI), land application of contaminated wastes (CW), and WWTP effluent.

The FTSAs have long been associated with AFFF-impacted sites with very high concentrations of up to 14,600,000 ng/L of 6:2 FTSA in groundwater found near United States military fire training areas.[12] In surface water, lower concentrations of FTSAs have been measured with a maximum concentration of 176 ng/L of 6:2 FTSA found adjacent to a fire training area at Stockholm Airport in Sweden.[35] In other studies , even lower concentrations of FTSAs have been detected in some surface water samples with up to 1.46 ng/L of 6:2 FTSA and 0.32 ng/L of 8:2 FTSA detected in a lake in Albany, New York,[232] up to 1.1 ng/L of 6:2 FTSA in water from River Elbe in Germany,[216] up to 36 ng/L of 6:2 FTSA in rivers and canals in Singapore,[233] up to 1.4 ng/L of 6:2 FTSA and lower levels of 4:2 and 8:2 FTSA in AFFF-impacted Meretta and Resolute Lakes in Nunavut, Canada,[32] and a maximum of 0.4 ng/L of 6:2 FTSA in thirteen Chinese rivers.[234] In looking at the sources of FTSAs, 6:2 FTSA has been measured in WWTP influents and effluents in the United States where concentrations of 6:2 FTSA in effluent compared to effluent increased in 4 of 10 WWTPs and decreased in 5 of 10 WWTPs with a maximum concentration of 370 ng/L in one effluent.[215] These mixed results likely result from a combination of 6:2 FTSA precursors, such as 6:2 FTSAS, biodegrading to 6:2 FTSA and sorption and biodegradation of 6:2 FTSA itself.[17,131,215] Effluents from WWTPs in Germany have also been found to contain 6:2 FTSA in some cases at concentrations up to 38 ng/L.[216] Based on these results, WWTP effluents may be a source of 6:2 FTSA to surface waters in addition to AFFFs.

Precursors to PFOS, such as EtFOSA, N-methyl perfluorooctane sulfonamide (MeFOSA), FOSA, FOSAA, and EtFOSAA, have also been measured in surface water samples although these are relatively sorptive PFASs compared to PFSAs and PFCAs.[164,166] Measurements of low levels of FOSA (<0.1 ng/L) in ocean water have been made in a number of surveys[222,231,235,236] and MeFOSA has also been measured in ocean water.[231,235] Relatively high levels of FOSA between 75 and 283 ng/L were measured in water from the Conasauga River in Georgia, USA, which drains land where treated wastewater from the carpet industry was applied.[237] In Bahia state, Brazil, where EtFOSA (Sulfluramid) is used as a pesticide, FOSA was the most abundant PFAS measured in four of eight surface water samples with concentrations in the low ng/L.[238]

Perfluorooctane sulfonamido substances, such as FOSA, have also been measured in surface waters at numerous other locations, including Lake Ontario,[239] Tokyo Bay,[171] rivers and canals in Singapore,[172,233] and rivers in Switzerland[228] and Germany.[216]

New classes of PFASs have also been identified in surface water samples. D'Eon *et al.* first reported perfluoroalkyl phosphonates (PFPAs) in Canadian surface waters at concentrations between 0.088 and 3.4 ng/L for C8-PFPA with the PFPAs less abundant than PFCAs and PFSAs.[240] Wang *et al.* discovered F-35B, a chloro-perfluoroalkyl ether sulfonic acid, in surface water downstream of Chinese chrome plating facilities at concentrations of approximately 10 to 50 ng/L, which were similar to PFOS concentrations in the area.[241] Strynar *et al.* made use of high resolution TOF-MS to identify twelve perfluoroalkyl ether carboxylic acids and sulfonic acids in surface water from the Cape Fear River in North Carolina.[65] Presumably further classes of PFASs remain to be found in surface waters.

1.7 Goals and Hypotheses

This thesis is focused on exploring the identities and environmental chemistry of PFASs that are components of AFFFs. To begin, Chapter 2 addresses what specific PFASs are present in AFFFs. Chapter 3 is a study of the biodegradation of 6:2 FTAB and 6:2 FTAA, which are two recently identified AFFF components[7,16] found in four out of ten AFFF concentrates in Chapter 2. Finally, Chapter 4 is a survey of AFFF-related PFASs in rural, urban, and AFFF-impacted surface waters in Canada.

The objective of Chapter 2 is to identify as many PFASs in a set of ten AFFFs and two commercial fluorinated surfactant concentrates as possible using solid phase extraction (SPE), HR-MS, CID, and LC-MS/MS approaches. A variety of PFASs were expected in the AFFFs, including anionic, cationic, and amphoteric fluorinated surfactants based on the patent literature.[3] A mixed mode ion exchange SPE approach was developed in order to simplify the mixture of PFASs and provide confidence in the assignment of structures with different charge properties. Both PFASs produced by ECF and fluorotelomer PFASs were expected[2,3] and LC-MS/MS chromatograms were used to provide separation of linear and branched isomers of ECF PFASs as a line of evidence of

their nature. A variety of perfluoroalkyl chain-length congeners were predicted for the AFFF components[2,3] that the sensitivity of LC-MS/MS would detect. Accurate masses from HR-MS combined with CID mass spectra were applied to identifying PFASs with the hypothesis that these techniques would have the sensitivity and resolving power to identify individual PFASs in the complex AFFF mixtures.

In Chapter 3, the hypothesis was that 6:2 FTAB and 6:2 FTAA are precursors to PFCAs through aerobic biodegradation with WWTP sludge. Despite the lack of detection of PFCAs in the biotransformation of 6:2 FTAB in blue mussels and turbot,[16] synthesized and purified 6:2 FTAB and 6:2 FTAA standards were expected to facilitate sensitive detection of biodegradation products that may not have been possible with industrial material, which Chapter 2 demonstrates can contain mixtures of side-products, synthetic intermediates, and degradation products. This hypothesis is based on what is known about the biodegradation of other fluorotelomer PFASs, including PAPs,[124] 6:2 FTSA,[127,128] and FTSASs.[17,131] In addition, qTOF-MS and CID mass spectra were collected to enable the identification of additional degradation products of 6:2 FTAB and FTAA providing insight into degradation products that may be present in the environment.

In Chapter 4, a survey of Canadian surface waters for AFFF-related PFASs using SPE and LC-MS/MS was developed to have the sensitivity to detect a number of relatively novel PFASs in urban and AFFF-impacted surface waters. The PFASs present in surface waters were expected to vary between different sites and provide insights into the types PFAS inputs different sites receive and AFFF-related PFASs that should be priorities for future research based on their presence in a high proportion of surface waters and/or at high concentrations in surface waters. Additional analysis of sediments from the Welland River, an AFFF-impacted site, was combined with analysis of surface waters, to provide insight into which PFASs are relatively more sorptive. Finally, batch equilibration soil sorption tests with 6:2 FTAB and 6:2 FTAA were conducted to provide initial indications whether betaine PFASs or amine PFASs are more sorptive. It was hypothesized that 6:2 FTAA would be more sorptive due to electrostatic interactions of the protonated amine with soil cation exchange sites.

Chapter 5 summarizes key findings from Chapters 2, 3, and 4 and suggests directions for future research based on the findings of this thesis.

1.8 References

(1) Pabon, M.; Corpart, J. Fluorinated surfactants: synthesis, properties, effluent treatment. *J. Fluor. Chem.* **2002**, *114* (2), 149–156.

(2) Moody, C.; Field, J. Perfluorinated surfactants and the environmental implications of their use in fire-fighting foams. *Environ. Sci. Technol.* **2000**, *34* (18), 3864–3870.

(3) Kissa, E. *Fluorinated surfactants and repellents*; Marcel Dekker: New York, 2001; Vol. 2nd ed., rev. and expanded.

(4) Ignat'ev, N. V.; Welz-Biermann, U.; Heider, U.; Kucheryna, A.; von Ahsen, S.; Habel, W.; Sartori, P.; Willner, H. Carbon-chain isomerization during the electrochemical fluorination in anhydrous hydrogen fluoride—a mechanistic study. *J. Fluor. Chem.* **2003**, *124* (1), 21–37.

(5) Arsenault, G.; Chittim, B.; Gu, J.; McAlees, A.; McCrindle, R.; Robertson, V. Separation and fluorine nuclear magnetic resonance spectroscopic (19F NMR) analysis of individual branched isomers present in technical perfluorooctanesulfonic acid (PFOS). *Chemosphere* **2008**, *73* (1, Supplement), S53–S59.

(6) Stern, R. M.; Guenthner, R. a; Alm, R. R.; Wilkinson, T. K. Process for the Preparation of Fluoroaliphatic Aminocarboxylate Surfactants. U.S. 5,144,069, September 1, 1992.

(7) Place, B. J.; Field, J. A. Identification of Novel Fluorochemicals in Aqueous Film-Forming Foams Used by the US Military. *Environ. Sci. Technol.* **2012**, *46* (13), 7120–7127.

(8) Fluorinated Amine Oxides. GB1302612 (A), January 10, 1973.

(9) Blanchard, W. A.; Rhode, J. C. Process for preparing perfluoroalkyl iodides. US3226449 (A), December 28, 1965.

(10) Buck, R. C.; Franklin, J.; Berger, U.; Conder, J. M.; Cousins, I. T.; de Voogt, P.; Jensen, A. A.; Kannan, K.; Mabury, S. A.; van Leeuwen, S. Perfluoroalkyl and polyfluoroalkyl substances in the environment: Terminology, classification, and origins. *Integr. Environ. Assess. Manag.* **2011**, *7* (4), 513–541.

(11) Hoffmann, D.; Stach, H. Perfluoro-Alkyl-Alkylene-Sulfonamidoalkylene-Dialkylamines and Their Quaternary Ammonium Salts. US3721706 (A), March 20, 1973.

(12) Schultz, M. M.; Barofsky, D. F.; Field, J. A. Quantitative Determination of Fluorotelomer Sulfonates in Groundwater by LC MS/MS. *Environ. Sci. Technol.* **2004**, *38* (6), 1828–1835.

(13) Ansul Incorporated. Ansulite 3% AFFF (Formula DC-3) Material Safety Data Sheet. September 2003.

(14) Ansul Incorporated. Ansulite ARC Material Safety Data Sheet. September 2006.

(15) 3M Company. Material Safety Data Sheet for FC-203FC Light Water (TM) AFFF; Document ID 07-1198-6. September 30, 1999.

(16) Moe, M. K.; Huber, S.; Svenson, J.; Hagenaars, A.; Pabon, M.; Trümper, M.; Berger, U.; Knapen, D.; Herzke, D. The structure of the fire fighting foam surfactant Forafac®1157 and its biological and photolytic transformation products. *Chemosphere* **2012**, *89* (7), 869–875.

(17) Weiner, B.; Yeung, L. W. Y.; Marchington, E. B.; D'Agostino, L. A.; Mabury, S. A. Organic fluorine content in aqueous film forming foams (AFFFs) and biodegradation of the foam component 6 : 2 fluorotelomermercaptoalkylamido sulfonate (6 : 2 FTSAS). *Environ. Chem.* **2013**, *10* (6), 486–493.

(18) Levine, A.; Libelo, E.; Bugna, G.; Shelley, T.; Mayfield, H.; Stauffer, T. Biogeochemical assessment of natural attenuation of JP-4-contaminated ground water in the presence of fluorinated surfactants. *Sci. Total Environ.* **1997**, *208* (3), 179–195.

(19) Moody, C.; Field, J. Determination of perfluorocarboxylates in groundwater impacted by fire-fighting activity. *Environ. Sci. Technol.* **1999**, *33* (16), 2800–2806.

(20) Moody, C.; Kwan, W.; Martin, J.; Muir, D.; Mabury, S. Determination of perfluorinated surfactants in surface water samples by two independent analytical techniques: Liquid chromatography/tandem mass spectrometry and F-19 NMR. *Anal. Chem.* **2001**, *73* (10), 2200–2206.

(21) Moody, C. A.; Martin, J. W.; Kwan, W. C.; Muir, D. C. G.; Mabury, S. A. Monitoring Perfluorinated Surfactants in Biota and Surface Water Samples Following an Accidental Release of Fire-Fighting Foam into Etobicoke Creek. *Environ. Sci. Technol.* **2002**, *36* (4), 545–551.

(22) Young, C. J.; Furdui, V. I.; Franklin, J.; Koerner, R. M.; Muir, D. C. G.; Mabury, S. A. Perfluorinated Acids in Arctic Snow: New Evidence for Atmospheric Formation. *Environ. Sci. Technol.* **2007**, *41* (10), 3455–3461.

(23) Hebert, G.; Odom, M.; Craig, P.; Dick, D.; Strauss, S. Method for the determination of sub-ppm concentrations of perfluoroalkylsulfonate anions in water. *J. Environ. Monit.* **2002**, *4* (1), 90–95.

(24) Moody, C.; Hebert, G.; Strauss, S.; Field, J. Occurrence and persistence of perfluorooctanesulfonate and other perfluorinated surfactants in groundwater at a fire-training area at Wurtsmith Air Force Base, Michigan, USA. *J. Environ. Monit.* **2003**, *5* (2), 341–345.

(25) Field, J.; Schultz, M.; Barofsky, D. Identifying hydrocarbon and fluorocarbon surfactants in specialty chemical formulations of environmental interest by fast atom bombardment/mass spectrometry. *Chimia* **2003**, *57* (9), 556–560.

(26) Oakes, K. D.; Benskin, J. P.; Martin, J. W.; Ings, J. S.; Heinrichs, J. Y.; Dixon, D. G.; Servos, M. R. Biomonitoring of perfluorochemicals and toxicity to the downstream fish community of Etobicoke Creek following deployment of aqueous film-forming foam. *Aquat. Toxicol.* **2010**, *98* (2), 120–129.

(27) Awad, E.; Zhang, X.; Bhavsar, S. P.; Petro, S.; Crozier, P. W.; Reiner, E. J.; Fletcher, R.; Tittlemier, S. A.; Braekevelt, E. Long-Term Environmental Fate of Perfluorinated Compounds after Accidental Release at Toronto Airport. *Environ. Sci. Technol.* **2011**, *45* (19), 8081–8089.

(28) Karrman, A.; Elgh-Dalgren, K.; Lafossas, C.; Moskeland, T. Environmental levels and distribution of structural isomers of perfluoroalkyl acids after aqueous fire-fighting foam (AFFF) contamination. *Environ. Chem.* **2011**, *8* (4), 372–380.

(29) de Solla, S. R.; De Silva, A. O.; Letcher, R. J. Highly elevated levels of perfluorooctane sulfonate and other perfluorinated acids found in biota and surface water downstream of an international airport, Hamilton, Ontario, Canada. *Environ. Int.* **2012**, *39* (1), 19–26.

(30) Gewurtz, S. B.; Bhavsar, S. P.; Petro, S.; Mahon, C. G.; Zhao, X.; Morse, D.; Reiner, E. J.; Tittlemier, S. A.; Braekevelt, E.; Drouillard, K. High levels of perfluoroalkyl acids in sport fish species downstream of a firefighting training facility at Hamilton International Airport, Ontario, Canada. *Environ. Int.* **2014**, *67*, 1–11.

(31) Stock, N. L.; Furdui, V. I.; Muir, D. C. G.; Mabury, S. A. Perfluoroalkyl Contaminants in the Canadian Arctic: Evidence of Atmospheric Transport and Local Contamination. *Environ. Sci. Technol.* **2007**, *41* (10), 3529–3536.

(32) Lescord, G. L.; Kidd, K. A.; De Silva, A. O.; Williamson, M.; Spencer, C.; Wang, X.; Muir, D. C. G. Perfluorinated and Polyfluorinated Compounds in Lake Food Webs from the Canadian High Arctic. *Environ. Sci. Technol.* **2015**, *49* (5), 2694–2702.

(33) Kwadijk, C. J. A. F.; Kotterman, M.; Koelmans, A. A. Partitioning of Perfluorooctanesulfonate and Perfluorohexanesulfonate in the Aquatic Environment After an Accidental Release of Aqueous Film Forming Foam at Schiphol Amsterdam Airport. *Environ. Toxicol. Chem.* **2014**, *33* (8), 1761–1765.

(34) Filipovic, M.; Woldegiorgis, A.; Norström, K.; Bibi, M.; Lindberg, M.; Österås, A.-H. Historical usage of aqueous film forming foam: A case study of the widespread distribution of perfluoroalkyl acids from a military airport to groundwater, lakes, soils and fish. *Chemosphere* **2015**, *129*, 39–45.

(35) Ahrens, L.; Norström, K.; Viktor, T.; Cousins, A. P.; Josefsson, S. Stockholm Arlanda Airport as a source of per- and polyfluoroalkyl substances to water, sediment and fish. *Chemosphere* **2015**, *129*, 33–38.

(36) Das, P.; Megharaj, M.; Naidu, R. Perfluorooctane sulfonate release pattern from soils of fire training areas in Australia and its bioaccumulation potential in the earthworm Eisenia fetida. *Environ. Sci. Pollut. Res.* **2013**, *22* (12), 8902–8910.

(37) Anderson, R. H.; Long, G. C.; Porter, R. C.; Anderson, J. K. Occurrence of select perfluoroalkyl substances at U.S. Air Force aqueous film-forming foam release sites other than fire-training areas: Field-validation of critical fate and transport properties. *Chemosphere* **2016**, *150*, 678–685.

(38) Houtz, E. F.; Higgins, C. P.; Field, J. A.; Sedlak, D. L. Persistence of Perfluoroalkyl Acid Precursors in AFFF-Impacted Groundwater and Soil. *Environ. Sci. Technol.* **2013**, *47* (15), 8187–8195.

(39) McGuire, M. E.; Schaefer, C.; Richards, T.; Backe, W. J.; Field, J. A.; Houtz, E.; Sedlak, D. L.; Guelfo, J. L.; Wunsch, A.; Higgins, C. P. Evidence of Remediation-Induced Alteration of Subsurface Poly- and Perfluoroalkyl Substance Distribution at a Former Firefighter Training Area. *Environ. Sci. Technol.* **2014**, *48* (12), 6644–6652.

(40) Backe, W. J.; Day, T. C.; Field, J. A. Zwitterionic, Cationic, and Anionic Fluorinated Chemicals in Aqueous Film Forming Foam Formulations and Groundwater from U.S. Military Bases by Nonaqueous Large-Volume Injection HPLC-MS/MS. *Environ. Sci. Technol.* **2013**, *47* (10), 5226–5234.

(41) Hansen, K. J.; Clemen, L. A.; Ellefson, M. E.; Johnson, H. O. Compound-Specific, Quantitative Characterization of Organic Fluorochemicals in Biological Matrices. *Environ. Sci. Technol.* **2001**, *35* (4), 766–770.

(42) Giesy, J. P.; Kannan, K. Global distribution of perfluorooctane sulfonate in wildlife. *Environ. Sci. Technol.* **2001**, *35* (7), 1339–1342.

(43) Houtz, E. F.; Sedlak, D. L. Oxidative Conversion as a Means of Detecting Precursors to Perfluoroalkyl Acids in Urban Runoff. *Environ. Sci. Technol.* **2012**, *46* (17), 9342–9349.

(44) Miyake, Y.; Yamashita, N.; Rostkowski, P.; So, M. K.; Taniyasu, S.; Lam, P. K. S.; Kannan, K. Determination of trace levels of total fluorine in water using combustion ion chromatography for fluorine: A mass balance approach to determine individual perfluorinated chemicals in water. *J. Chromatogr. A* **2007**, *1143* (1–2), 98–104.

(45) Yeung, L. W. Y.; Mabury, S. A. Bioconcentration of Aqueous Film-Forming Foam (AFFF) in Juvenile Rainbow Trout (Oncorhyncus mykiss). *Environ. Sci. Technol.* **2013**, *47* (21), 12505–12513.

(46) Weppner, W. *Letter by William Weppner, 3M, to Charles Auer, EPA OPPT, regarding the Phase-out Plan for POSF-Based Products*; US EPA Public Docket EPA-HQ-OPPT-2002-0043-0009; 3M General Offices: St. Paul, MN, 2000.

(47) Xie, S.; Wang, T.; Liu, S.; Jones, K. C.; Sweetman, A. J.; Lu, Y. Industrial source identification and emission estimation of perfluorooctane sulfonate in China. *Environ. Int.* **2013**, *52*, 1–8.

(48) Stockholm Convention. *SC-4/17: Listing of perfluorooctane sulfonic acid, its salts and perflurooctane sulfonyl fluoride*; 2009; Vol. SC-4/17.

(49) *SOR/2008-178 Perfluorooctane Sulfonate and its Salts and Certain Other Compounds Regulations*; 2008.

(50) *Directive 2006/122/EC of the European Parliament and of the Council; European Union*; 2006.

(51) Stephen L. Johnson. PFOA Stewardship Program Invitation Letter, 2006.

(52) US EPA, O. 2010/2015 PFOA Stewardship Program https://www.epa.gov/assessing-and-managing-chemicals-under-tsca/20102015-pfoa-stewardship-program (accessed Apr 14, 2016).

(53) Hagenaars, A.; Meyer, I. J.; Herzke, D.; Pardo, B. G.; Martinez, P.; Pabon, M.; De Coen, W.; Knapen, D. The search for alternative aqueous film forming foams (AFFF) with a low environmental impact: Physiological and transcriptomic effects of two Forafac (R) fluorosurfactants in turbot. *Aquat. Toxicol.* **2011**, *104* (3-4), 168–176.

(54) European Union. Proposal to list pentadecafluorooctanoic acid (CAS No: 335-67-1, PFOA, perfluorooctanoic acid), its salts and PFOA-related compounds in Annexes A, B and/or C to the Stockholm Convention on Persistent Organic Pollutants. United Nations Environmental Program June 9, 2015.

(55) United States Environmental Protection Agency. The Presidential Green Chemistry Challenge Award Recipients 1996-2015.

(56) Karin Norstrom; Tomas Viktor; Anna Palm Cousins; Magnus Rahmberg; IVL. *Risks and Effects of the dispersion of PFAS on Aquatic, Terrestrial and Human populations in the vicinity of International Airports: Rinal report of the RE-PATH project 2009-2014*; IVL Report B 2232; IVL Swedish Environmental Research Institute, 2015.

(57) Dr. Sthamer - Moussol-FF: Alcohol resistant fluorine free fire extinguishing foam concentrate http://sthamer.com/englisch/c24_moussol.html (accessed Apr 15, 2016).

(58) Ecopol 100% Fluorine free foam - ZERO Fire Systems - <keywords> http://www.zerofiresystems.nl/en/products-and-services/repression/ecopol-100-fluorine-free-foam.html (accessed Apr 19, 2016).

(59) Fluorine-Free Foam Concentrate - Ecoguard Ecoguard http://www.chemguard.com/fire-suppression/catalog/foam-concentrates/fluorine-free-foam/cf3.aspx (accessed Apr 19, 2016).

(60) Fluorine free foam http://www.fomtec.com/fluorine-free/category38.html (accessed Apr 19, 2016).

(61) Schaefer, T. H.; Dlugogorski, B. Z.; Kennedy, E. M. Sealability Properties of Fluorine-Free Fire-Fighting Foams (FfreeF). *Fire Technol. 44* (3), 297–309.

(62) Riecher, A. Is fluorine finished? Chemguard introduces no-fluorine fire foam. *Ind. Fire World* **2003**.

(63) Vinogradov, A. V.; Kuprin, D. S.; Abduragimov, I. M.; Kuprin, G. N.; Serebriyakov, E.; Vinogradov, V. V. Silica Foams for Fire Prevention and Firefighting. *ACS Appl. Mater. Interfaces* **2016**, *8* (1), 294–301.

(64) Liu, Y.; Pereira, A. D. S.; Martin, J. W. Discovery of C5–C17 Poly- and Perfluoroalkyl Substances in Water by In-Line SPE-HPLC-Orbitrap with In-Source Fragmentation Flagging. *Anal. Chem.* **2015**, *87* (8), 4260–4268.

(65) Strynar, M.; Dagnino, S.; McMahen, R.; Liang, S.; Lindstrom, A.; Andersen, E.; McMillan, L.; Thurman, M.; Ferrer, I.; Ball, C. Identification of Novel Perfluoroalkyl Ether Carboxylic Acids (PFECAs) and Sulfonic Acids (PFESAs) in Natural Waters Using Accurate Mass Time-of-Flight Mass Spectrometry (TOFMS). *Environ. Sci. Technol.* **2015**, *49* (19), 11622–11630.

(66) Ruan, T.; Lin, Y.; Wang, T.; Liu, R.; Jiang, G. Identification of Novel Polyfluorinated Ether Sulfonates as PFOS Alternatives in Municipal Sewage Sludge in China. *Environ. Sci. Technol.* **2015**, *49* (11), 6519–6527.

(67) Rotander, A.; Kärrman, A.; Toms, L.-M. L.; Kay, M.; Mueller, J. F.; Gómez Ramos, M. J. Novel Fluorinated Surfactants Tentatively Identified in Firefighters Using Liquid Chromatography Quadrupole Time-of-Flight Tandem Mass Spectrometry and a Case-Control Approach. *Environ. Sci. Technol.* **2015**, *49* (4), 2434–2442.

(68) Xian, F. High Resolution Mass Spectrometry. *Anal. Chem.* **2012**, *84* (2), 708–719.

(69) Skoog, D. A.; Holler, F. J.; Crouch, S. R. *Principles of Instrumental Analysis 6th Edition*; Brooks/Cole: Cengage Learning: Belmont, CA, 2007.

(70) Guilhaus, M. Special feature: Tutorial. Principles and instrumentation in time-of-flight mass spectrometry. Physical and instrumental concepts. *J. Mass Spectrom.* **1995**, *30* (11), 1519–1532.

(71) Russell, D. H.; Edmondson, R. D. High-resolution Mass Spectrometry and Accurate Mass Measurements with Emphasis on the Characterization of Peptides and Proteins by Matrix-assisted Laser Desorption/Ionization Time-of-flight Mass Spectrometry. *J. Mass Spectrom.* **1997**, *32* (3), 263–276.

(72) Aceña, J.; Stampachiacchiere, S.; Pérez, S.; Barceló, D. Advances in liquid chromatography–high-resolution mass spectrometry for quantitative and qualitative environmental analysis. *Anal. Bioanal. Chem.* **2015**, *407* (21), 6289–6299.

(73) McLafferty, F. W. *Interpretation of mass spectra*; Tureček, F., Series Ed.; University Science Books: Sausalito, Calif., 1993.

(74) Kadar, H.; Veyrand, B.; Antignac, J.-P.; Durand, S.; Monteau, F.; Bizec, B. L. Comparative study of low- versus high-resolution liquid chromatography-mass spectrometric strategies for measuring perfluorinated contaminants in fish. *Food Addit. Contam. Part A* **2011**, *28* (9), 1261–1273.

(75) Myers, A. L.; Jobst, K. J.; Mabury, S. A.; Reiner, E. J. Using mass defect plots as a discovery tool to identify novel fluoropolymer thermal decomposition products. *J. Mass Spectrom.* **2014**, *49* (4), 291–296.

(76) Crimmins, B. S.; Xia, X.; Hopke, P. K.; Holsen, T. M. A targeted/non-targeted screening method for perfluoroalkyl carboxylic acids and sulfonates in whole fish using quadrupole time-of-flight mass spectrometry and MSe. *Anal. Bioanal. Chem.* **2013**, *406* (5), 1471–1480.

(77) Sleno, L. The use of mass defect in modern mass spectrometry. *J. Mass Spectrom.* **2012**, *47* (2), 226–236.

(78) Taguchi, V. Y.; Nieckarz, R. J.; Clement, R. E.; Krolik, S.; Williams, R. Dioxin analysis by gas chromatography-Fourier transform ion cyclotron resonance mass spectrometry (GC-FTICRMS). *J. Am. Soc. Mass Spectrom.* **2010**, *21* (11), 1918–1921.

(79) Kendrick, E. A Mass Scale Based on CH_2 = 14.0000 for High Resolution Mass Spectrometry of Organic Compounds. *Anal. Chem.* **1963**, *35* (13), 2146–2154.

(80) Barzen-Hanson, K. A.; Roberts, S. C.; Choyke, S. J.; Oetjen, K.; McAlees, A.; Riddell, N.; McCrindle, R.; Ferguson, P. L.; Higgins, C. P.; Field, J. A. Discovery of 40 classes of per- and polyfluoroalkyl substances in historical aqueous film-forming foams (AFFFs) and AFFF-impacted groundwater. *Environ. Sci. Technol.* **2017**. DOI: 10.1021/acs.est.6b05843

(81) Holčapek, M.; Jirásko, R.; Lísa, M. Basic rules for the interpretation of atmospheric pressure ionization mass spectra of small molecules. *J. Chromatogr. A* **2010**, *1217* (25), 3908–3921.

(82) Kondrat, R. W.; Cooks, R. G. Direct analysis of mixtures by mass spectrometry. *Anal. Chem.* **1978**, *50* (1), 81A – 92A.

(83) Yost, R. A.; Enke, C. G. Selected ion fragmentation with a tandem quadrupole mass spectrometer. *J. Am. Chem. Soc.* **1978**, *100* (7), 2274–2275.

(84) Cooks, R. G. Special feature: Historical. Collision-induced dissociation: Readings and commentary. *J. Mass Spectrom.* **1995**, *30* (9), 1215–1221.

(85) Trier, X.; Granby, K.; Christensen, J. H. Tools to discover anionic and nonionic polyfluorinated alkyl surfactants by liquid chromatography electrospray ionisation mass spectrometry. *J. Chromatogr. A* **2011**, *1218* (40), 7094–7104.

(86) O'Hagan, D. Understanding organofluorine chemistry. An introduction to the C–F bond. *Chem. Soc. Rev.* **2008**, *37* (2), 308–319.

(87) Quinete, N.; Orata, F.; Maes, A.; Gehron, M.; Bauer, K.-H.; Moreira, I.; Wilken, R.-D. Degradation Studies of New Substitutes for Perfluorinated Surfactants. *Arch. Environ. Contam. Toxicol.* **2010**, *59* (1), 20–30.

(88) Remde, A.; Debus, R. Biodegradability of fluorinated surfactants under aerobic and anaerobic conditions. *Chemosphere* **1996**, *32* (8), 1563–1574.

(89) R.J.W. Meesters; H.Fr. Schoder. Perfluorooctane sulfonate - a quite mobile anionic anthropogenic surfactant, ubiquitously found in the environment. *Water Sci. Technol.* **2004**, *50* (5), 235–242.

(90) Schröder, H. F. Determination of fluorinated surfactants and their metabolites in sewage sludge samples by liquid chromatography with mass spectrometry and tandem mass spectrometry after pressurised liquid extraction and separation on fluorine-modified reversed-phase sorbents. *J. Chromatogr. A* **2003**, *1020* (1), 131–151.

(91) Arrendale, R. F.; Stewart, J. T.; Manning, R.; Vitayavirasuk, B. Determination of GX 071 and its major metabolite in rat blood by cold on-column injection capillary GC/ECD. *J. Agric. Food Chem.* **1989**, *37* (4), 1130–1135.

(92) Manning, R. O.; Bruckner, J. V.; Mispagel, M. E.; Bowen, J. M. Metabolism and disposition of sulfluramid, a unique polyfluorinated insecticide, in the rat. *Drug Metab. Dispos.* **1991**, *19* (1), 205–211.

(93) Grossman, M. R.; Mispagel, M. E.; Bowen, J. M. Distribution and tissue elimination in rats during and after prolonged dietary exposure to a highly fluorinated sulfonamide pesticide. *J. Agric. Food Chem.* **1992**, *40* (12), 2505–2509.

(94) Vitayavirasuk, B.; Bowen, J. M. Pharmacokinetics of sulfluramid and its metabolite desethylsulfluramid after intravenous and intraruminal administration of sulfluramid to sheep. *Pestic. Sci.* **1999**, *55* (7), 719–725.

(95) Tomy, G. T.; Tittlemier, S. A.; Palace, V. P.; Budakowski, W. R.; Braekevelt, E.; Brinkworth, L.; Friesen, K. Biotransformation of N-Ethyl Perfluorooctanesulfonamide by Rainbow Trout (Onchorhynchus mykiss) Liver Microsomes. *Environ. Sci. Technol.* **2004**, *38* (3), 758–762.

(96) Benskin, J. P.; Holt, A.; Martin, J. W. Isomer-Specific Biotransformation Rates of a Perfluorooctane Sulfonate (PFOS)-Precursor by Cytochrome P450 Isozymes and Human Liver Microsomes. *Environ. Sci. Technol.* **2009**, *43* (22), 8566–8572.

(97) Letcher, R. J.; Chu, S.; McKinney, M. A.; Tomy, G. T.; Sonne, C.; Dietz, R. Comparative hepatic in vitro depletion and metabolite formation of major perfluorooctane sulfonate precursors in arctic polar bear, beluga whale, and ringed seal. *Chemosphere* **2014**, *112*, 225–231.

(98) Mejia Avendaño, S.; Liu, J. Production of PFOS from aerobic soil biotransformation of two perfluoroalkyl sulfonamide derivatives. *Chemosphere* **2015**, *119*, 1084–1090.

(99) Cleston C. Lange. *The aerobic biodegradation of N-EtFOSE alcohol by the microbial activity present in municipal wastewater treatment sludge.*; 3M Project ID: LIMS E00-2252; Pace Analytical Services, Science Solutions Division, 2000; p 55.

(100) Xu, L.; Krenitsky, D. M.; Seacat, A. M.; Butenhoff, J. L.; Anders, M. W. Biotransformation of N-Ethyl-N-(2-hydroxyethyl)perfluorooctanesulfonamide by Rat Liver Microsomes, Cytosol, and Slices and by Expressed Rat and Human Cytochromes P450. *Chem. Res. Toxicol.* **2004**, *17* (6), 767–775.

(101) Boulanger, B.; Vargo, J. D.; Schnoor, J. L.; Hornbuckle, K. C. Evaluation of Perfluorooctane Surfactants in a Wastewater Treatment System and in a Commercial Surface Protection Product. *Environ. Sci. Technol.* **2005**, *39* (15), 5524–5530.

(102) Rhoads, K. R.; Janssen, E. M.-L.; Luthy, R. G.; Criddle, C. S. Aerobic Biotransformation and Fate of N-Ethyl Perfluorooctane Sulfonamidoethanol (N-EtFOSE) in Activated Sludge. *Environ. Sci. Technol.* **2008**, *42* (8), 2873–2878.

(103) Rhoads, K. R.; Rostkowski, K. H.; Kitanidis, P. K.; Criddle, C. S. Use of on-site bioreactors to estimate the biotransformation rate of N-ethyl perfluorooctane sulfonamidoethanol (N-EtFOSE) during activated sludge treatment. *Chemosphere* **2013**, *92* (6), 702–707.

(104) Benskin, J. P.; Ikonomou, M. G.; Gobas, F. A. P. C.; Begley, T. H.; Woudneh, M. B.; Cosgrove, J. R. Biodegradation of N-Ethyl Perfluorooctane Sulfonamido Ethanol (EtFOSE) and EtFOSE-Based Phosphate Diester (SAmPAP Diester) in Marine Sediments. *Environ. Sci. Technol.* **2013**, *47* (3), 1381–1389.

(105) Zhao, S.; Ma, X.; Fang, S.; Zhu, L. Behaviors of N-ethyl perfluorooctane sulfonamide ethanol (N-EtFOSE) in a soil-earthworm system: Transformation and bioaccumulation. *Sci. Total Environ.* **2016**, *554–555*, 186–191.

(106) Mejia-Avendaño, S.; Vo Duy, S.; Sauvé, S.; Liu, J. Generation of Perfluoroalkyl Acids from Aerobic Biotransformation of Quaternary Ammonium Polyfluoroalkyl Surfactants. *Environ. Sci. Technol.* **2016**, *50* (18), 9923–9932.

(107) Hagen, D. F.; Belisle, J.; Johnson, J. D.; Venkateswarlu, P. Characterization of fluorinated metabolites by a gas chromatographic-helium microwave plasma detector—The biotransformation of 1H,1H,2H,2H-perfluorodecanol to perfluorooctanoate. *Anal. Biochem.* **1981**, *118* (2), 336–343.

(108) Dinglasan, M. J. A.; Ye, Y.; Edwards, E. A.; Mabury, S. A. Fluorotelomer Alcohol Biodegradation Yields Poly- and Perfluorinated Acids. *Environ. Sci. Technol.* **2004**, *38* (10), 2857–2864.

(109) Wang, N.; Szostek, B.; Folsom, P. W.; Sulecki, L. M.; Capka, V.; Buck, R. C.; Berti, W. R.; Gannon, J. T. Aerobic Biotransformation of 14C-Labeled 8-2 Telomer B Alcohol by Activated Sludge from a Domestic Sewage Treatment Plant. *Environ. Sci. Technol.* **2005**, *39* (2), 531–538.

(110) Martin, J. W.; Mabury, S. A.; O'Brien, P. J. Metabolic products and pathways of fluorotelomer alcohols in isolated rat hepatocytes. *Chem. Biol. Interact.* **2005**, *155* (3), 165–180.

(111) Wang, N.; Szostek, B.; Buck, R. C.; Folsom, P. W.; Sulecki, L. M.; Capka, V.; Berti, W. R.; Gannon, J. T. Fluorotelomer Alcohol BiodegradationDirect Evidence that Perfluorinated Carbon Chains Breakdown. *Environ. Sci. Technol.* **2005**, *39* (19), 7516–7528.

(112) Liu, J.; Wang, N.; Szostek, B.; Buck, R. C.; Panciroli, P. K.; Folsom, P. W.; Sulecki, L. M.; Bellin, C. A. 6-2 Fluorotelomer alcohol aerobic biodegradation in soil and mixed bacterial culture. *Chemosphere* **2010**, *78* (4), 437–444.

(113) Liu, J.; Wang, N.; Buck, R. C.; Wolstenholme, B. W.; Folsom, P. W.; Sulecki, L. M.; Bellin, C. A. Aerobic biodegradation of [14C] 6:2 fluorotelomer alcohol in a flow-through soil incubation system. *Chemosphere* **2010**, *80* (7), 716–723.

(114) Zhao, L.; McCausland, P. K.; Folsom, P. W.; Wolstenholme, B. W.; Sun, H.; Wang, N.; Buck, R. C. 6:2 Fluorotelomer alcohol aerobic biotransformation in activated sludge from two domestic wastewater treatment plants. *Chemosphere* **2013**, *92* (4), 464–470.

(115) Zhang, S.; Szostek, B.; McCausland, P. K.; Wolstenholme, B. W.; Lu, X.; Wang, N.; Buck, R. C. 6:2 and 8:2 Fluorotelomer Alcohol Anaerobic Biotransformation in Digester Sludge from a WWTP under Methanogenic Conditions. *Environ. Sci. Technol.* **2013**, *47* (9), 4227–4235.

(116) Kim, M. H.; Wang, N.; Chu, K. H. 6:2 Fluorotelomer alcohol (6:2 FTOH) biodegradation by multiple microbial species under different physiological conditions. *Appl. Microbiol. Biotechnol.* **2013**, *98* (4), 1831–1840.

(117) Rand, A. A.; Mabury, S. A. Protein Binding Associated with Exposure to Fluorotelomer Alcohols (FTOHs) and Polyfluoroalkyl Phosphate Esters (PAPs) in Rats. *Environ. Sci. Technol.* **2014**, *48* (4), 2421–2429.

(118) Tseng, N.; Wang, N.; Szostek, B.; Mahendra, S. Biotransformation of 6:2 Fluorotelomer Alcohol (6:2 FTOH) by a Wood-Rotting Fungus. *Environ. Sci. Technol.* **2014**, *48* (7), 4012–4020.

(119) Li, Z.-M.; Guo, L.-H.; Ren, X.-M. Biotransformation of 8:2 fluorotelomer alcohol by recombinant human cytochrome P450s, human liver microsomes and human liver cytosol. *Environ. Sci. Process. Impacts* **2016**, *18* (5), 538–546.

(120) Butt, C. M.; Muir, D. C. G.; Mabury, S. A. Biotransformation of the 8:2 fluorotelomer acrylate in rainbow trout. 1. In vivo dietary exposure. *Environ. Toxicol. Chem.* **2010**, *29* (12), 2726–2735.

(121) Butt, C. M.; Muir, D. C. G.; Mabury, S. A. Biotransformation of the 8:2 fluorotelomer acrylate in rainbow trout. 2. In vitro incubations with liver and stomach S9 fractions. *Environ. Toxicol. Chem.* **2010**, *29* (12), 2736–2741.

(122) Royer, L. A.; Lee, L. S.; Russell, M. H.; Nies, L. F.; Turco, R. F. Microbial transformation of 8:2 fluorotelomer acrylate and methacrylate in aerobic soils. *Chemosphere* **2015**, *129*, 54–61.

(123) D'Eon, J. C.; Mabury, S. A. Production of perfluorinated carboxylic acids (PFCAs) from the biotransformation of polyfluoroalkyl phosphate surfictants (PAPS): Exploring routes of human contamination. *Environ. Sci. Technol.* **2007**, *41* (13), 4799–4805.

(124) Lee, H.; D'eon, J.; Mabury, S. A. Biodegradation of Polyfluoroalkyl Phosphates as a Source of Perfluorinated Acids to the Environment. *Environ. Sci. Technol.* **2010**, *44* (9), 3305–3310.

(125) Lee, H.; Tevlin, A. G.; Mabury, S. A.; Mabury, S. A. Fate of Polyfluoroalkyl Phosphate Diesters and Their Metabolites in Biosolids-Applied Soil: Biodegradation and Plant Uptake in Greenhouse and Field Experiments. *Environ. Sci. Technol.* **2014**, *48* (1), 340–349.

(126) Liu, C.; Liu, J. Aerobic biotransformation of polyfluoroalkyl phosphate esters (PAPs) in soil. *Environ. Pollut.* **2016**, *212*, 230–237.

(127) Marchington, E. B. Identification of Known and Novel Fluorinated Compounds in AFFF via 19F-NMR, LC-MS/MS, and LC-QUAD-TOFMS, and the Aerobic Biodegredation of 6:2 FTS. MSc. Thesis, University of Toronto: Toronto, ON, 2008.

(128) Wang, N.; Liu, J.; Buck, R. C.; Korzeniowski, S. H.; Wolstenholme, B. W.; Folsom, P. W.; Sulecki, L. M. 6:2 Fluorotelomer sulfonate aerobic biotransformation in activated sludge of waste water treatment plants. *Chemosphere* **2011**, *82* (6), 853–858.

(129) Zhang, S.; Lu, X.; Wang, N.; Buck, R. C. Biotransformation potential of 6:2 fluorotelomer sulfonate (6:2 FTSA) in aerobic and anaerobic sediment. *Chemosphere* **2016**, *154*, 224–230.

(130) Dasu, K.; Lee, L. S. Aerobic biodegradation of toluene-2,4-di(8:2 fluorotelomer urethane) and hexamethylene-1,6-di(8:2 fluorotelomer urethane) monomers in soils. *Chemosphere* **2016**, *144*, 2482–2488.

(131) Harding-Marjanovic, K. C.; Houtz, E. F.; Yi, S.; Field, J. A.; Sedlak, D. L.; Alvarez-Cohen, L. Aerobic Biotransformation of Fluorotelomer Thioether Amido Sulfonate (Lodyne) in AFFF-Amended Microcosms. *Environ. Sci. Technol.* **2015**, *49* (13), 7666–7674.

(132) Ruan, T.; Szostek, B.; Folsom, P. W.; Wolstenholme, B. W.; Liu, R.; Liu, J.; Jiang, G.; Wang, N.; Buck, R. C. Aerobic Soil Biotransformation of 6:2 Fluorotelomer Iodide. *Environ. Sci. Technol.* **2013**, *47* (20), 11504–11511.

(133) Dasu, K.; Liu, J.; Lee, L. S. Aerobic Soil Biodegradation of 8:2 Fluorotelomer Stearate Monoester. *Environ. Sci. Technol.* **2012**, *46* (7), 3831–3836.

(134) Dasu, K.; Lee, L. S.; Turco, R. F.; Nies, L. F. Aerobic biodegradation of 8:2 fluorotelomer stearate monoester and 8:2 fluorotelomer citrate triester in forest soil. *Chemosphere* **2013**, *91* (3), 399–405.

(135) Russell, M. H.; Berti, W. R.; Szostek, B.; Buck, R. C. Investigation of the Biodegradation Potential of a Fluoroacrylate Polymer Product in Aerobic Soils. *Environ. Sci. Technol.* **2008**, *42* (3), 800–807.

(136) Washington, J. W.; Ellington, J. J.; Jenkins, T. M.; Evans, J. J.; Yoo, H.; Hafner, S. C. Degradability of an Acrylate-Linked, Fluorotelomer Polymer in Soil. *Environ. Sci. Technol.* **2009**, *43* (17), 6617–6623.

(137) Russell, M. H.; Berti, W. R.; Szostek, B.; Wang, N.; Buck, R. C. Evaluation of PFO formation from the biodegradation of a fluorotelomer-based urethane polymer product in aerobic soils. *Polym. Degrad. Stab.* **2010**, *95* (1), 79–85.

(138) Rankin, K.; Lee, H.; Tseng, P. J.; Mabury, S. A. Investigating the Biodegradability of a Fluorotelomer-Based Acrylate Polymer in a Soil–Plant Microcosm by Indirect and Direct Analysis. *Environ. Sci. Technol.* **2014**, *48* (21), 12783–12790.

(139) Washington, J. W.; Jenkins, T. M.; Rankin, K.; Naile, J. E. Decades-Scale Degradation of Commercial, Side-Chain, Fluorotelomer-Based Polymers in Soils and Water. *Environ. Sci. Technol.* **2015**, *49* (2), 915–923.

(140) Washington, J. W.; Jenkins, T. M.; Weber, E. J. Identification of Unsaturated and 2H Polyfluorocarboxylate Homologous Series and Their Detection in Environmental Samples and as Polymer Degradation Products. *Environ. Sci. Technol.* **2015**, *49* (22), 13256–13263.

(141) Rand, A. A.; Mabury, S. A. Covalent Binding of Fluorotelomer Unsaturated Aldehydes (FTUALs) and Carboxylic Acids (FTUCAs) to Proteins. *Environ. Sci. Technol.* **2013**, *47* (3), 1655–1663.

(142) Butt, C. M.; Muir, D. C. G.; Mabury, S. A. Elucidating the Pathways of Poly- and Perfluorinated Acid Formation in Rainbow Trout. *Environ. Sci. Technol.* **2010**, *44* (13), 4973–4980.

(143) Lee, H.; Mabury, S. A. A Pilot Survey of Legacy and Current Commercial Fluorinated Chemicals in Human Sera from United States Donors in 2009. *Environ. Sci. Technol.* **2011**, *45* (19), 8067–8074.

(144) Yeung, L. W. Y.; Robinson, S. J.; Koschorreck, J.; Mabury, S. A. Part I. A Temporal Study of PFCAs and Their Precursors in Human Plasma from Two German Cities 1982–2009. *Environ. Sci. Technol.* **2013**, *47* (8), 3865–3874.

(145) Washington, J. W.; Naile, J. E.; Jenkins, T. M.; Lynch, D. G. Characterizing Fluorotelomer and Polyfluoroalkyl Substances in New and Aged Fluorotelomer-Based Polymers for Degradation Studies with GC/MS and LC/MS/MS. *Environ. Sci. Technol.* **2014**, *48* (10), 5762–5769.

(146) Ellis, D. A.; Martin, J. W.; De Silva, A. O.; Mabury, S. A.; Hurley, M. D.; Sulbaek Andersen, M. P.; Wallington, T. J. Degradation of Fluorotelomer Alcohols: A Likely Atmospheric Source of Perfluorinated Carboxylic Acids. *Environ. Sci. Technol.* **2004**, *38* (12), 3316–3321.

(147) Wallington, T. J.; Hurley, M. D.; Xia, J.; Wuebbles, D. J.; Sillman, S.; Ito, A.; Penner, J. E.; Ellis, D. A.; Martin, J.; Mabury, S. A.; et al. Formation of C7F15COOH (PFOA) and Other Perfluorocarboxylic Acids during the Atmospheric Oxidation of 8:2 Fluorotelomer Alcohol. *Environ. Sci. Technol.* **2006**, *40* (3), 924–930.

(148) Martin, J. W.; Ellis, D. A.; Mabury, S. A.; Hurley, M. D.; Wallington, T. J. Atmospheric Chemistry of Perfluoroalkanesulfonamides: Kinetic and Product Studies of the OH Radical and Cl Atom Initiated Oxidation of N-Ethyl Perfluorobutanesulfonamide. *Environ. Sci. Technol.* **2006**, *40* (3), 864–872.

(149) D'eon, J. C.; Hurley, M. D.; Wallington, T. J.; Mabury, S. A. Atmospheric Chemistry of N-methyl Perfluorobutane Sulfonamidoethanol, C4F9SO2N(CH3)CH2CH2OH: Kinetics and Mechanism of Reaction with OH. *Environ. Sci. Technol.* **2006**, *40* (6), 1862–1868.

(150) Young, C. J.; Hurley, M. D.; Wallington, T. J.; Mabury, S. A. Atmospheric Chemistry of 4:2 Fluorotelomer Iodide (n-C4F9CH2CH2I): Kinetics and Products

of Photolysis and Reaction with OH Radicals and Cl Atoms. *J. Phys. Chem. A* **2008**, *112* (51), 13542–13548.

(151) Butt, C. M.; Young, C. J.; Mabury, S. A.; Hurley, M. D.; Wallington, T. J. Atmospheric Chemistry of 4:2 Fluorotelomer Acrylate [C4F9CH2CH2OC(O)CH═CH2]: Kinetics, Mechanisms, and Products of Chlorine-Atom- and OH-Radical-Initiated Oxidation. *J. Phys. Chem. A* **2009**, *113* (13), 3155–3161.

(152) Jackson, D. A.; Wallington, T. J.; Mabury, S. A. Atmospheric Oxidation of Polyfluorinated Amides: Historical Source of Perfluorinated Carboxylic Acids to the Environment. *Environ. Sci. Technol.* **2013**, *47* (9), 4317–4324.

(153) Young, C. J.; Mabury, S. A. Atmospheric Perfluorinated Acid Precursors: Chemistry, Occurrence, and Impacts. In *Reviews of Environmental Contamination and Toxicology Volume 208*; Voogt, P. D., Ed.; Reviews of Environmental Contamination and Toxicology; Springer New York, 2010; pp 1–109.

(154) Hurley, M. D.; Ball, J. C.; Wallington, T. J.; Sulbaek Andersen, M. P.; Ellis, D. A.; Martin, J. W.; Mabury, S. A. Atmospheric Chemistry of 4:2 Fluorotelomer Alcohol (CF3(CF2)3CH2CH2OH): Products and Mechanism of Cl Atom Initiated Oxidation. *J. Phys. Chem. A* **2004**, *108* (26), 5635–5642.

(155) Xie, Z.; Wang, Z.; Mi, W.; Möller, A.; Wolschke, H.; Ebinghaus, R. Neutral Poly-/perfluoroalkyl Substances in Air and Snow from the Arctic. *Sci. Rep.* **2015**, *5*, 8912.

(156) Wang, Z.; Xie, Z.; Mi, W.; Möller, A.; Wolschke, H.; Ebinghaus, R. Neutral Poly/Per-Fluoroalkyl Substances in Air from the Atlantic to the Southern Ocean and in Antarctic Snow. *Environ. Sci. Technol.* **2015**, *49* (13), 7770–7775.

(157) Lai, S.; Song, J.; Song, T.; Huang, Z.; Zhang, Y.; Zhao, Y.; Liu, G.; Zheng, J.; Mi, W.; Tang, J.; et al. Neutral polyfluoroalkyl substances in the atmosphere over the northern South China Sea. *Environ. Pollut.* **2016**, *214*, 449–455.

(158) Ahrens, L.; Shoeib, M.; Harner, T.; Lee, S. C.; Guo, R.; Reiner, E. J. Wastewater Treatment Plant and Landfills as Sources of Polyfluoroalkyl Compounds to the Atmosphere. *Environ. Sci. Technol.* **2011**, *45* (19), 8098–8105.

(159) Rene P. Schwarzenbach; Gschwend, P. M.; Imboden, D. M. *Environmental Organic Chemistry*, 2nd Edition.; John Wiley & Sons: Hoboken, NJ, 2003.

(160) Gauthier, S. A.; Mabury, S. A. Aqueous photolysis of 8:2 fluorotelomer alcohol. *Environ. Toxicol. Chem.* **2005**, *24* (8), 1837–1846.

(161) Plumlee, M. H.; McNeill, K.; Reinhard, M. Indirect Photolysis of Perfluorochemicals: Hydroxyl Radical-Initiated Oxidation of N-Ethyl Perfluorooctane Sulfonamido Acetate (N-EtFOSAA) and Other Perfluoroalkanesulfonamides. *Environ. Sci. Technol.* **2009**, *43* (10), 3662–3668.

(162) Nguyen, T. V. Rate laws and kinetic modeling of N-ethyl perfluorooctane sulfonamidoethanol (N-EtFOSE) transformation by hydroxyl radical in aqueous solution. **2013**, *47* (7), 2241–2250.

(163) Trouborst, L.; Mabury, S. A. Aqueous photolysis of 6:2 fluorotelomer sulfonamide alkylbetaine. *J Env Sci Prep*.

(164) Higgins, C. P.; Luthy, R. G. Sorption of Perfluorinated Surfactants on Sediments†. *Environ. Sci. Technol.* **2006**, *40* (23), 7251–7256.

(165) Guelfo, J. L.; Higgins, C. P. Subsurface Transport Potential of Perfluoroalkyl Acids at Aqueous Film-Forming Foam (AFFF)-Impacted Sites. *Environ. Sci. Technol.* **2013**, *47* (9), 4164–4171.

(166) Ahrens, L. Partitioning of perfluorooctanoate (PFOA), perfluorooctane sulfonate (PFOS) and perfluorooctane sulfonamide (PFOSA) between water and sediment. *Chemosphere* **2011**, *85* (5), 731–737.

(167) Vierke, L.; Möller, A.; Klitzke, S. Transport of perfluoroalkyl acids in a water-saturated sediment column investigated under near-natural conditions. *Environ. Pollut.* **2014**, *186*, 7–13.

(168) McKenzie, E. R.; Siegrist, R. L.; McCray, J. E.; Higgins, C. P. Effects of Chemical Oxidants on Perfluoroalkyl Acid Transport in One-Dimensional Porous Media Columns. *Environ. Sci. Technol.* **2015**, *49* (3), 1681–1689.

(169) Labadie, P.; Chevreuil, M. Partitioning behaviour of perfluorinated alkyl contaminants between water, sediment and fish in the Orge River (nearby Paris, France). *Environ. Pollut.* **2011**, *159* (2), 391–397.

(170) Zhao, L.; Zhu, L.; Yang, L.; Liu, Z.; Zhang, Y. Distribution and desorption of perfluorinated compounds in fractionated sediments. *Chemosphere* **2012**, *88* (11), 1390–1397.

(171) Ahrens, L.; Taniyasu, S.; Yeung, L. W. Y.; Yamashita, N.; Lam, P. K. S.; Ebinghaus, R. Distribution of polyfluoroalkyl compounds in water, suspended particulate matter and sediment from Tokyo Bay, Japan. *Chemosphere* **2010**, *79* (3), 266–272.

(172) Nguyen, T. V.; Reinhard, M.; Chen, H.; Gin, K. Y.-H. Fate and transport of perfluoro- and polyfluoroalkyl substances including perfluorooctane sulfonamides in a managed urban water body. *Environ. Sci. Pollut. Res.* **2016**, *23* (11), 10382–10392.

(173) Enevoldsen, R.; Juhler, R. K. Perfluorinated compounds (PFCs) in groundwater and aqueous soil extracts: using inline SPE-LC-MS/MS for screening and sorption characterisation of perfluorooctane sulphonate and related compounds. *Anal. Bioanal. Chem.* **2010**, *398* (3), 1161–1172.

(174) Xiao, F.; Zhang, X.; Penn, L.; Gulliver, J. S.; Simcik, M. F. Effects of Monovalent Cations on the Competitive Adsorption of Perfluoroalkyl Acids by Kaolinite: Experimental Studies and Modeling. *Environ. Sci. Technol.* **2011**, *45* (23), 10028–10035.

(175) Kwadijk, C. J. A. F.; Korytár, P.; Koelmans, A. A. Distribution of Perfluorinated Compounds in Aquatic Systems in The Netherlands. *Environ. Sci. Technol.* **2010**, *44* (10), 3746–3751.

(176) Zhang, Y.; Meng, W.; Guo, C.; Xu, J.; Yu, T.; Fan, W.; Li, L. Determination and partitioning behavior of perfluoroalkyl carboxylic acids and perfluorooctanesulfonate in water and sediment from Dianchi Lake, China. *Chemosphere* **2012**, *88* (11), 1292–1299.

(177) Jeon, J.; Kannan, K.; Lim, B. J.; An, K. G.; Kim, S. D. Effects of salinity and organic matter on the partitioning of perfluoroalkyl acid (PFAs) to clay particles. *J. Environ. Monit.* **2011**, *13* (6), 1803–1810.

(178) Pan, G.; You, C. Sediment–water distribution of perfluorooctane sulfonate (PFOS) in Yangtze River Estuary. *Environ. Pollut.* **2010**, *158* (5), 1363–1367.

(179) Hong, S.; Khim, J. S.; Park, J.; Kim, M.; Kim, W.-K.; Jung, J.; Hyun, S.; Kim, J.-G.; Lee, H.; Choi, H. J.; et al. In situ fate and partitioning of waterborne perfluoroalkyl acids (PFAAs) in the Youngsan and Nakdong River Estuaries of South Korea. *Sci. Total Environ.* **2013**, *445–446*, 136–145.

(180) Wang, S.; Wang, H.; Deng, W. Perfluorooctane sulfonate (PFOS) distribution and effect factors in the water and sediment of the Yellow River Estuary, China. *Environ. Monit. Assess.* **2013**, *185* (10), 8517–8524.

(181) Chen, H.; Reinhard, M.; Nguyen, V. T.; Gin, K. Y.-H. Reversible and irreversible sorption of perfluorinated compounds (PFCs) by sediments of an urban reservoir. *Chemosphere* **2016**, *144*, 1747–1753.

(182) Martin, J. W.; Mabury, S. A.; Solomon, K. R.; Muir, D. C. G. Bioconcentration and tissue distribution of perfluorinated acids in rainbow trout (Oncorhynchus mykiss). *Environ. Toxicol. Chem.* **2003**, *22* (1), 196–204.

(183) Jeon, J.; Kannan, K.; Lim, H. K.; Moon, H. B.; Kim, S. D. Bioconcentration of perfluorinated compounds in blackrock fish, Sebastes schlegeli, at different salinity levels. *Environ. Toxicol. Chem.* **2010**, *29* (11), 2529–2535.

(184) Liu, C.; Gin, K. Y. H.; Chang, V. W. C.; Goh, B. P. L.; Reinhard, M. Novel Perspectives on the Bioaccumulation of PFCs – the Concentration Dependency. *Environ. Sci. Technol.* **2011**, *45* (22), 9758–9764.

(185) Inoue, Y.; Hashizume, N.; Yakata, N.; Murakami, H.; Suzuki, Y.; Kikushima, E.; Otsuka, M. Unique Physicochemical Properties of Perfluorinated Compounds and

Their Bioconcentration in Common Carp Cyprinus carpio L. *Arch. Environ. Contam. Toxicol.* **2011**, *62* (4), 672–680.

(186) Zhou, Z.; Liang, Y.; Shi, Y.; Xu, L.; Cai, Y. Occurrence and Transport of Perfluoroalkyl Acids (PFAAs), Including Short-Chain PFAAs in Tangxun Lake, China. *Environ. Sci. Technol.* **2013**, *47* (16), 9249–9257.

(187) Martin, J. W.; Mabury, S. A.; Solomon, K. R.; Muir, D. C. G. Dietary accumulation of perfluorinated acids in juvenile rainbow trout (Oncorhynchus mykiss). *Environ. Toxicol. Chem.* **2003**, *22* (1), 189–195.

(188) Falk, S.; Failing, K.; Georgii, S.; Brunn, H.; Stahl, T. Tissue specific uptake and elimination of perfluoroalkyl acids (PFAAs) in adult rainbow trout (Oncorhynchus mykiss) after dietary exposure. *Chemosphere* **2015**, *129*, 150–156.

(189) Hoke, R. A.; Ferrell, B. D.; Sloman, T. L.; Buck, R. C.; Buxton, L. W. Aquatic hazard, bioaccumulation and screening risk assessment for ammonium 2,3,3,3-tetrafluoro-2-(heptafluoropropoxy)-propanoate. *Chemosphere* **2016**, *149*, 336–342.

(190) Shi, Y.; Vestergren, R.; Zhou, Z.; Song, X.; Xu, L.; Liang, Y.; Cai, Y. Tissue Distribution and Whole Body Burden of the Chlorinated Polyfluoroalkyl Ether Sulfonic Acid F-53B in Crucian Carp (Carassius carassius): Evidence for a Highly Bioaccumulative Contaminant of Emerging Concern. *Environ. Sci. Technol.* **2015**, *49* (24), 14156–14165.

(191) D'eon, J. C.; Mabury, S. A. Exploring indirect sources of human exposure to perfluoroalkyl carboxylates (PFCAs): evaluating uptake, elimination, and biotransformation of polyfluoroalkyl phosphate esters (PAPs) in the rat. *Environ. Health Perspect.* **2011**, *119* (3), 344+.

(192) Hoke, R. A.; Ferrell, B. D.; Ryan, T.; Sloman, T. L.; Green, J. W.; Nabb, D. L.; Mingoia, R.; Buck, R. C.; Korzeniowski, S. H. Aquatic hazard, bioaccumulation and screening risk assessment for 6:2 fluorotelomer sulfonate. *Chemosphere* **2015**, *128*, 258–265.

(193) Lee, H.; De Silva, A. O.; Mabury, S. A. Dietary Bioaccumulation of Perfluorophosphonates and Perfluorophosphinates in Juvenile Rainbow Trout: Evidence of Metabolism of Perfluorophosphinates. *Environ. Sci. Technol.* **2012**, *46* (6), 3489–3497.

(194) Ulhaq, M.; Sundström, M.; Larsson, P.; Gabrielsson, J.; Bergman, Å.; Norrgren, L.; Örn, S. Tissue uptake, distribution and elimination of 14C-PFOA in zebrafish (Danio rerio). *Aquat. Toxicol.* **2015**, *163*, 148–157.

(195) D'eon, J. C.; Simpson, A. J.; Kumar, R.; Baer, A. J.; Mabury, S. A. Determining the molecular interactions of perfluorinated carboxylic acids with human sera and isolated human serum albumin using nuclear magnetic resonance spectroscopy. *Environ. Toxicol. Chem.* **2010**, *29* (8), 1678–1688.

(196) Woodcroft, M. W.; Ellis, D. A.; Rafferty, S. P.; Burns, D. C.; March, R. E.; Stock, N. L.; Trumpour, K. S.; Yee, J.; Munro, K. Experimental characterization of the mechanism of perfluorocarboxylic acids' liver protein bioaccumulation: The key role of the neutral species. *Environ. Toxicol. Chem.* **2010**, *29* (8), 1669–1677.

(197) Ng, C. A.; Hungerbühler, K. Bioconcentration of Perfluorinated Alkyl Acids: How Important Is Specific Binding? *Environ. Sci. Technol.* **2013**, *47* (13), 7214–7223.

(198) Armitage, J. M.; Arnot, J. A.; Wania, F.; Mackay, D. Development and evaluation of a mechanistic bioconcentration model for ionogenic organic chemicals in fish. *Environ. Toxicol. Chem.* **2013**, *32* (1), 115–128.

(199) Stahl, T.; Heyn, J.; Thiele, H.; Hüther, J.; Failing, K.; Georgii, S.; Brunn, H. Carryover of Perfluorooctanoic Acid (PFOA) and Perfluorooctane Sulfonate (PFOS) from Soil to Plants. *Arch. Environ. Contam. Toxicol.* **2008**, *57* (2), 289–298.

(200) Blaine, A. C.; Rich, C. D.; Hundal, L. S.; Lau, C.; Mills, M. A.; Harris, K. M.; Higgins, C. P. Uptake of Perfluoroalkyl Acids into Edible Crops via Land Applied Biosolids: Field and Greenhouse Studies. *Environ. Sci. Technol.* **2013**, *47* (24), 14062–14069.

(201) Blaine, A. C.; Rich, C. D.; Sedlacko, E. M.; Hyland, K. C.; Stushnoff, C.; Dickenson, E. R. V.; Higgins, C. P. Perfluoroalkyl Acid Uptake in Lettuce (Lactuca sativa) and Strawberry (Fragaria ananassa) Irrigated with Reclaimed Water. *Environ. Sci. Technol.* **2014**, *48* (24), 14361–14368.

(202) Blaine, A. C.; Rich, C. D.; Sedlacko, E. M.; Hundal, L. S.; Kumar, K.; Lau, C.; Mills, M. A.; Harris, K. M.; Higgins, C. P. Perfluoroalkyl Acid Distribution in Various Plant Compartments of Edible Crops Grown in Biosolids-Amended soils. *Environ. Sci. Technol.* **2014**, *48* (14), 7858–7865.

(203) Wen, B.; Li, L.; Zhang, H.; Ma, Y.; Shan, X.-Q.; Zhang, S. Field study on the uptake and translocation of perfluoroalkyl acids (PFAAs) by wheat (Triticum aestivum L.) grown in biosolids-amended soils. *Environ. Pollut.* **2014**, *184*, 547–554.

(204) Zhao, S.; Fang, S.; Zhu, L.; Liu, L.; Liu, Z.; Zhang, Y. Mutual impacts of wheat (Triticum aestivum L.) and earthworms (Eisenia fetida) on the bioavailability of perfluoroalkyl substances (PFASs) in soil. *Environ. Pollut.* **2014**, *184*, 495–501.

(205) Krippner, J.; Falk, S.; Brunn, H.; Georgii, S.; Schubert, S.; Stahl, T. Accumulation Potentials of Perfluoroalkyl Carboxylic Acids (PFCAs) and Perfluoroalkyl Sulfonic Acids (PFSAs) in Maize (Zea mays). *J. Agric. Food Chem.* **2015**, *63* (14), 3646–3653.

(206) Müller, C. E.; LeFevre, G. H.; Timofte, A. E.; Hussain, F. A.; Sattely, E. S.; Luthy, R. G. Competing mechanisms for perfluoroalkyl acid accumulation in plants

revealed using an Arabidopsis model system. *Environ. Toxicol. Chem.* **2016**, *35* (5), 1138–1147.

(207) Zhang, H.; Liu, W.; He, X.; Wang, Y.; Zhang, Q. Uptake of perfluoroalkyl acids in the leaves of coniferous and deciduous broad-leaved trees. *Environ. Toxicol. Chem.* **2015**, *34* (7), 1499–1504.

(208) Bizkarguenaga, E.; Zabaleta, I.; Prieto, A.; Fernández, L. A.; Zuloaga, O. Uptake of 8:2 perfluoroalkyl phosphate diester and its degradation products by carrot and lettuce from compost-amended soil. *Chemosphere* **2016**, *152*, 309–317.

(209) Felizeter, S.; McLachlan, M. S.; de Voogt, P. Uptake of Perfluorinated Alkyl Acids by Hydroponically Grown Lettuce (Lactuca sativa). *Environ. Sci. Technol.* **2012**, *46* (21), 11735–11743.

(210) Felizeter, S.; McLachlan, M. S.; De Voogt, P. Root Uptake and Translocation of Perfluorinated Alkyl Acids by Three Hydroponically Grown Crops. *J. Agric. Food Chem.* **2014**, *62* (15), 3334–3342.

(211) García-Valcárcel, A. I.; Molero, E.; Escorial, M. C.; Chueca, M. C.; Tadeo, J. L. Uptake of perfluorinated compounds by plants grown in nutrient solution. *Sci. Total Environ.* **2014**, *472*, 20–26.

(212) Krippner, J.; Brunn, H.; Falk, S.; Georgii, S.; Schubert, S.; Stahl, T. Effects of chain length and pH on the uptake and distribution of perfluoroalkyl substances in maize (Zea mays). *Chemosphere* **2014**, *94*, 85–90.

(213) Ahrens, L. Polyfluoroalkyl compounds in the aquatic environment: a review of their occurrence and fate. *J. Environ. Monit.* **2011**, *13* (1), 20–31.

(214) Liu, Z.; Lu, Y.; Wang, T.; Wang, P.; Li, Q.; Johnson, A. C.; Sarvajayakesavalu, S.; Sweetman, A. J. Risk assessment and source identification of perfluoroalkyl acids in surface and ground water: Spatial distribution around a mega-fluorochemical industrial park, China. *Environ. Int.* **2016**, *91*, 69–77.

(215) Schultz, M. M.; Barofsky, D. F.; Field, J. A. Quantitative Determination of Fluorinated Alkyl Substances by Large-Volume-Injection Liquid Chromatography Tandem Mass SpectrometryCharacterization of Municipal Wastewaters. *Environ. Sci. Technol.* **2006**, *40* (1), 289–295.

(216) Ahrens, L.; Felizeter, S.; Sturm, R.; Xie, Z.; Ebinghaus, R. Polyfluorinated compounds in waste water treatment plant effluents and surface waters along the River Elbe, Germany. *Mar. Pollut. Bull.* **2009**, *58* (9), 1326–1333.

(217) Möller, A.; Ahrens, L.; Surm, R.; Westerveld, J.; van der Wielen, F.; Ebinghaus, R.; de Voogt, P. Distribution and sources of polyfluoroalkyl substances (PFAS) in the River Rhine watershed. *Environ. Pollut.* **2010**, *158* (10), 3243–3250.

(218) Busch, J.; Ahrens, L.; Sturm, R.; Ebinghaus, R. Polyfluoroalkyl compounds in landfill leachates. *Environ. Pollut.* **2010**, *158* (5), 1467–1471.

(219) Huset, C. A.; Barlaz, M. A.; Barofsky, D. F.; Field, J. A. Quantitative determination of fluorochemicals in municipal landfill leachates. *Chemosphere* **2011**, *82* (10), 1380–1386.

(220) Skutlarek, D.; Exner, M.; Färber, H. Perfluorinated Surfactants in Surface and Drinking Waters (9 pp). *Environ. Sci. Pollut. Res.* **2006**, *13* (5), 299–307.

(221) Lasier, P. J.; Washington, J. W.; Hassan, S. M.; Jenkins, T. M. Perfluorinated chemicals in surface waters and sediments from northwest Georgia, USA, and their bioaccumulation in Lumbriculus variegatus. *Environ. Toxicol. Chem.* **2011**, *30* (10), 2194–2201.

(222) Benskin, J. P.; Muir, D. C. G.; Scott, B. F.; Spencer, C.; De Silva, A. O.; Kylin, H.; Martin, J. W.; Morris, A.; Lohmann, R.; Tomy, G.; et al. Perfluoroalkyl Acids in the Atlantic and Canadian Arctic Oceans. *Environ. Sci. Technol.* **2012**, *46* (11), 5815–5823.

(223) Veillette, J.; Muir, D. C. G.; Antoniades, D.; Small, J. M.; Spencer, C.; Loewen, T. N.; Babaluk, J. A.; Reist, J. D.; Vincent, W. F. Perfluorinated Chemicals in Meromictic Lakes on the Northern Coast of Ellesmere Island, High Arctic Canada. *Arctic* **2012**, *65* (3), 245–256.

(224) Nakayama, S. F.; Strynar, M. J.; Reiner, J. L.; Delinsky, A. D.; Lindstrom, A. B. Determination of Perfluorinated Compounds in the Upper Mississippi River Basin. *Environ. Sci. Technol.* **2010**, *44* (11), 4103–4109.

(225) Loi, E. I. H.; Yeung, L. W. Y.; Taniyasu, S.; Lam, P. K. S.; Kannan, K.; Yamashita, N. Trophic Magnification of Poly- and Perfluorinated Compounds in a Subtropical Food Web. *Environ. Sci. Technol.* **2011**, *45* (13), 5506–5513.

(226) Kwok, K. Y.; Yamazaki, E.; Yamashita, N.; Taniyasu, S.; Murphy, M. B.; Horii, Y.; Petrick, G.; Kallerborn, R.; Kannan, K.; Murano, K.; et al. Transport of Perfluoroalkyl substances (PFAS) from an arctic glacier to downstream locations: Implications for sources. *Sci. Total Environ.* **2013**, *447*, 46–55.

(227) Yamazaki, E.; Falandysz, J.; Taniyasu, S.; Hui, G.; Jurkiewicz, G.; Yamashita, N.; Yang, Y.-L.; Lam, P. K. S. Perfluorinated carboxylic and sulphonic acids in surface water media from the regions of Tibetan Plateau: Indirect evidence on photochemical degradation? *J. Environ. Sci. Health Part A* **2016**, *51* (1), 63–69.

(228) Müller, C. E.; Gerecke, A. C.; Alder, A. C.; Scheringer, M.; Hungerbühler, K. Identification of perfluoroalkyl acid sources in Swiss surface waters with the help of the artificial sweetener acesulfame. *Environ. Pollut.* **2011**, *159* (5), 1419–1426.

(229) Scott, B. F.; Moody, C. A.; Spencer, C.; Small, J. M.; Muir, D. C. G.; Mabury, S. A. Analysis for Perfluorocarboxylic Acids/Anions in Surface Waters and Precipitation Using GC−MS and Analysis of PFOA from Large-Volume Samples. *Environ. Sci. Technol.* **2006**, *40* (20), 6405–6410.

(230) De Silva, A. O.; Spencer, C.; Scott, B. F.; Backus, S.; Muir, D. C. G. Detection of a Cyclic Perfluorinated Acid, Perfluoroethylcyclohexane Sulfonate, in the Great Lakes of North America. *Environ. Sci. Technol.* **2011**, *45* (19), 8060–8066.

(231) Cai, M.; Zhao, Z.; Yin, Z.; Ahrens, L.; Huang, P.; Cai, M.; Yang, H.; He, J.; Sturm, R.; Ebinghaus, R.; et al. Occurrence of Perfluoroalkyl Compounds in Surface Waters from the North Pacific to the Arctic Ocean. *Environ. Sci. Technol.* **2012**, *46* (2), 661–668.

(232) Kim, S.-K.; Kannan, K. Perfluorinated Acids in Air, Rain, Snow, Surface Runoff, and Lakes: Relative Importance of Pathways to Contamination of Urban Lakes. *Environ. Sci. Technol.* **2007**, *41* (24), 8328–8334.

(233) Nguyen, V. T.; Reinhard, M.; Karina, G. Y.-H. Occurrence and source characterization of perfluorochemicals in an urban watershed RID A-1006-2008. *Chemosphere* **2011**, *82* (9), 1277–1285.

(234) Lin, Y.; Liu, R.; Hu, F.; Liu, R.; Ruan, T.; Jiang, G. Simultaneous qualitative and quantitative analysis of fluoroalkyl sulfonates in riverine water by liquid chromatography coupled with Orbitrap high resolution mass spectrometry. *J. Chromatogr. A* **2016**, *1435*, 66–74.

(235) González-Gaya, B.; Dachs, J.; Roscales, J. L.; Caballero, G.; Jiménez, B. Perfluoroalkylated Substances in the Global Tropical and Subtropical Surface Oceans. *Environ. Sci. Technol.* **2014**, *48* (22), 13076–13084.

(236) Ahrens, L.; Xie, Z.; Ebinghaus, R. Distribution of perfluoroalkyl compounds in seawater from Northern Europe, Atlantic Ocean, and Southern Ocean. *Chemosphere* **2010**, *78* (8), 1011–1016.

(237) Konwick, B. J.; Tomy, G. T.; Ismail, N.; Peterson, J. T.; Fauver, R. J.; Higginbotham, D.; Fisk, A. T. Concentrations and patterns of perfluoroalkyl acids in Georgia, USA surface waters near and distant to a major use source. *Environ. Toxicol. Chem.* **2008**, *27* (10), 2011–2018.

(238) Löfstedt Gilljam, J.; Leonel, J.; Cousins, I. T.; Benskin, J. P. Is Ongoing Sulfluramid Use in South America a Significant Source of Perfluorooctanesulfonate (PFOS)? Production Inventories, Environmental Fate, and Local Occurrence. *Environ. Sci. Technol.* **2016**, *50* (2), 653–659.

(239) Myers, A. L.; Crozier, P. W.; Helm, P. A.; Brimacombe, C.; Furdui, V. I.; Reiner, E. J.; Burniston, D.; Marvin, C. H. Fate, distribution, and contrasting temporal trends of perfluoroalkyl substances (PFASs) in Lake Ontario, Canada. *Environ. Int.* **2012**, *44*, 92–99.

(240) D'Eon, J. C.; Crozier, P. W.; Furdui, V. I.; Reiner, E. J.; Libelo, E. L.; Mabury, S. A. Observation of a Commercial Fluorinated Material, the Polyfluoroalkyl Phosphoric Acid Diesters, in Human Sera, Wastewater Treatment Plant Sludge, and Paper Fibers. *Environ. Sci. Technol.* **2009**, *43* (12), 4589–4594.

(241) Wang, S.; Huang, J.; Yang, Y.; Hui, Y.; Ge, Y.; Larssen, T.; Yu, G.; Deng, S.; Wang, B.; Harman, C. First Report of a Chinese PFOS Alternative Overlooked for 30 Years: Its Toxicity, Persistence, and Presence in the Environment. *Environ. Sci. Technol.* **2013**, *47* (18), 10163–10170.

Chapter Two

Identification of Novel Fluorinated Surfactants in Aqueous Film Forming Foams and Commercial Surfactant Concentrates

Lisa A. D'Agostino and Scott A. Mabury

Published as: *Environ. Sci. Technol.* **2014,** 48, 121−129. http://dx.doi.org/10.1021/es403729e

Contributions: Lisa D'Agostino was responsible for planning and executing the strategies for the identification of PFASs in AFFF and commercial surfactant concentrate samples and interpreted the resulting spectra. Acquisition of FTICR-MS data and advice on interpretation of mass spectra was provided by Karl Jobst. Lisa D'Agostino prepared this manuscript with editorial comments provided by Scott Mabury.

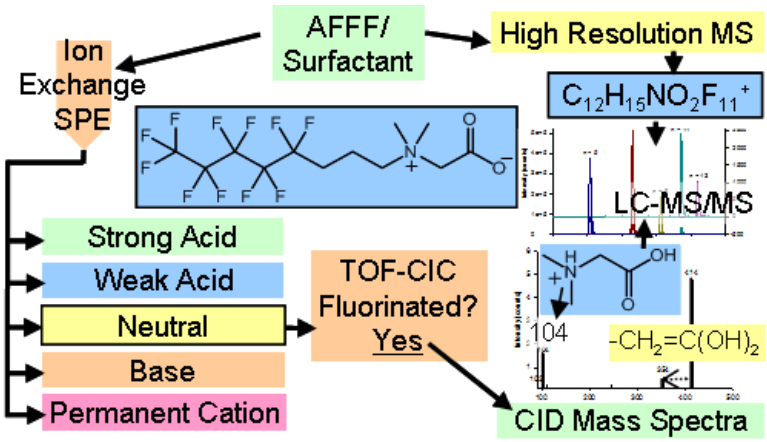

Reprinted with permission from *Environmental Science & Technology* **2014,** 48, 121−129.

2 Identification of Novel Fluorinated Surfactants in Aqueous Film Forming Foams and Commercial Surfactant Concentrates

2.1 Abstract

Recent studies comparing the results of total organofluorine-combustion ion chromatography (TOF-CIC) to targeted analysis of perfluoroalkyl and polyfluoroalkyl substances (PFASs) by liquid chromatography tandem mass spectrometry (LC-MS/MS) have shown that a significant yet variable portion of the total organofluorine in environmental and biological samples is in the form of unknown PFASs. A portion of this unknown organofluorine likely originates in proprietary fluorinated surfactants not included in LC-MS/MS analyses and not fully characterized by the environmental science community, which may enter the environment through use in aqueous film forming foams (AFFFs) for firefighting. Contamination of water, biota, and soils with various PFASs due to AFFF deployment has been documented. Ten fluorinated AFFF concentrates, 9 of which were obtained from fire sites in Ontario, Canada and two commercial fluorinated surfactant concentrates were characterized in order to identify novel fluorinated surfactants. Mixed-mode ion exchange solid phase extraction (SPE) fractionated fluorinated surfactants based on ionic character. High resolution mass spectrometry assigned molecular formulae to fluorinated surfactant ions, while collision induced dissociation (CID) spectra assisted structural elucidation. LC-MS/MS detected isomers and low abundance fluorinated chain lengths. In total, 12 novel and 10 infrequently reported PFAS classes were identified in fluorinated chain lengths from C3 to C15 for a total of 103 compounds. Further research should examine the environmental fate and toxicology of these PFASs, especially their potential as perfluoroalkyl acid (PFAA) precursors.

2.2 Introduction

Since the worldwide dissemination of perfluorooctane sulfonate (PFOS) was detected in human blood and in wildlife around the world in 2001, research into perfluoroalkyl and polyfluoroalkyl substances (PFASs) in the environment has been

extensive.[1–3] Nevertheless, there remains a great deal unknown about the identity of the specific PFASs present in environmental samples based on studies comparing general techniques for organofluorine analysis with targeted quantitation by liquid chromatography-tandem mass spectrometry (LC-MS/MS). Following an accidental AFFF release in Ontario, Canada in 2000, quantitative ^{19}F-NMR results showed approximately five-fold higher concentrations of materials giving signals similar to PFOS and perfluorooctanoate (PFOA) than did LC-MS/MS analysis of selected perfluoroalkyl carboxylates (PFCAs) and perfluoroalkane sulfonates (PFSAs) in surface water.[4] More recent studies also suffer from incomplete coverage of PFASs based on comparisons of TOF-CIC results with LC-MS/MS. Known PFASs accounted for approximately 11% of extractable organic fluorine (EOF) in shrimp in Hong Kong,[5] approximately 30 to 85% of EOF in human blood samples from around China,[6] 10 to 30% of organofluorine in sea water from Japan[7], and 2 to 44% of the anionic fraction of EOF in Lake Ontario surface sediments.[8]

AFFF, which is used in extinguishing hydrocarbon fuelled fires, is a potential source of incompletely characterized PFASs to the environment as it contains proprietary fluorinated surfactants,[9] which are typically not clearly listed on the Material Safety Data Sheet (MSDS) for an AFFF. Two fluorinated surfactants in AFFF that were characterized recently are the 6:2 fluorotelomer mercaptoalkylamido sulfonate (FTSAS; Figure 2.1I, n=6)[10,11] and the 6:2 fluorotelomer sulfonamide alkylbetaine (FTAB) marketed as Forafac 1157 (Figure 2.1L, n=6).[12,13] PFASs in AFFFs from United States military bases have been characterized using accurate masses from liquid chromatography-time-of-flight mass spectrometry (LC-TOF-MS) to assign molecular formulae and solely patent searching to assign structures.[14] Subsequently, groundwater from military bases decommissioned at least six years and AFFF samples were analyzed by LC-MS/MS for eight novel PFAS classes. Only FTSASs and structures shown in Figure 2.1R and 2.1T could be detected in groundwater.[15]

Prior to the electrochemical fluorination (ECF) PFOS phase out in 2002, AFFF was often formulated using ECF sulfonamide-based surfactants,[14,16] which may be precursors to PFSAs since N-ethyl perfluorooctane sulfonamido ethanol (EtFOSE)

biotransforms to PFOS in rats,[17] wastewater treatment plant (WWTP) sludge,[18] and marine sediments.[19] A number of fluorotelomer compounds, such as polyfluoroalkyl phosphate esters (PAPs),[20,21] 8:2 fluorotelomer acrylate,[22] 6:2 FTSA,[23] and the AFFF component 6:2 FTSAS[11] have been demonstrated to biotransform to PFCAs in WWTP sludge,[11,20,23] rats[21] and rainbow trout.[22] This suggests fluorotelomer-based surfactants, dominant in AFFF produced after 2002,[16] may be PFCA precursors. The potential for fluorinated surfactants to be PFAA precursors motivates identification of specific PFASs in AFFFs and commercial fluorinated surfactants to facilitate evaluation of this potential.

Weiner *et al.* recently examined AFFF samples from fire sites in Ontario, Canada and a commercial AFFF from 3M using ^{19}F-NMR, TOF-CIC, and LC-MS/MS analysis of known PFASs (i.e.: PFSAs; PFCAs; 6:2 and 8:2 FTSAs; and 4:2, 6:2, and 8:2 FTSASs)[11] and this study extends the characterization of many of the same samples by identifying unknown PFASs. Two mixed-mode ion exchange solid phase extraction (SPE) methods were developed to fractionate PFASs according to their ionic nature, simplifying samples for subsequent analysis and assisting in assigning ionic/ionizable functionalities. These methods were used along with TOF-CIC, quadrupole-time-of-flight mass spectrometry (qTOF-MS), Fourier transform ion cyclotron resonance mass spectrometry (FTICR-MS) and LC-MS/MS to identify 22 classes of novel or infrequently reported fluorinated surfactant in various fluorinated chain-lengths for a total of 103 compounds that may be released through use of AFFF or other applications. Structural assignments are supported by qTOF-MS CID spectra, which is a first for 18 of the PFASs.

2.3 Materials and Methods

2.3.1 Materials

The reagents, solvents and standards used are listed in the Supporting Information in Appendix A.

2.3.2 Samples

Foams 1 to 11 were an AFFF sample set collected by the Ontario Ministry of the Environment from sites where the AFFFs were used in firefighting in Ontario, Canada. Foams 6 and 9 were previously found to contain only residual organofluorine and were not examined further.[11] A commercial AFFF sample was obtained from 3M (St. Paul, MN, USA) and is called Foam 12. Two commercial fluorinated surfactant concentrates, referred to by their trade names, FS-330 and FS-1520, were from Mason Chemicals (Arlington Heights, IL, USA). Locations and dates of sample collection and relevant information from MSDSs are in Table A1 in Appendix A and sampling details are in Appendix A. Product literature for FS-330 and FS-1520 mention applications in alkaline cleaners, mining operations and photographic emulsions, coatings, and polishes.[24,25] FS-1520 is also marketed for use in hair conditioners, oil well stimulation fluids, and AFFFs.[25]

2.3.3 Ion Exchange SPE

Two SPE fractionation methods were developed with one utilizing Oasis weak anion exchange (WAX) SPE cartridges and the other utilizing Oasis weak cation exchange (WCX) SPE cartridges from Waters (Milford, MA) and are described in detail in Appendix A. Briefly, the sequence of elution solvents for WAX SPE was methanol to elute neutral, amphoteric, and cationic surfactants; 2% formic acid in methanol to elute weak acids (e.g.: carboxylates); methanol; and 1% NH_4OH in methanol to elute strong acids (e.g.: PFCAs, sulfonates). Excluding the second methanol rinse, these fractions are termed the neutral WAX, weak acid and strong acid fractions, respectively. WCX cartridges were eluted sequentially with methanol to elute neutral, amphoteric, and anionic surfactants; 2% NH_4OH in methanol to elute bases (e.g.: amines); methanol; and 2% formic acid in methanol to elute permanent cations (e.g.: quaternary ammoniums). Excluding the second methanol rinse, these fractions are named the neutral WCX, base, and permanent cation fractions, respectively. These procedures were developed using model compounds including, PFOA (strong acid), 7:3 fluorotelomer carboxylic acid (weak acid), perfluorooctane sulfonamide (non-ionic), N,N-dimethyldodecylamine

(base), cetyltrimethylammonium chloride (CTMA, permanent cation), 3-(N,N-dimethyloctylammonio)propanesulfonate (amphoteric), and Empigen BB detergent (amphoteric) with recovery and distribution of these compounds determined by LC-MS/MS as described in Appendix A. AFFF and commercial surfactant samples were extracted in batches with a solvent blank.

2.3.4 TOF-CIC

SPE fractions of AFFFs, commercial surfactants, and solvent blanks were analyzed by TOF-CIC as described previously[11,26] to screen for PFAS-containing fractions requiring further investigation. Method details are in Appendix A.

2.3.5 qTOF-MS

SPE fractions determined to contain organic fluorine using TOF-CIC were direct loop injected on an AB/Sciex QStar XL (MDS Sciex, Concord, ON, Canada) using electrospray ionization (ESI) in full scan and product ion scan modes (resolution ~8000). Detection of PFASs in SPE fractions was based on discrepancy with the theoretical mass to charge (*m/z*) less than 5 parts per million (*ppm*). Method details are in Appendix A.

2.3.6 FTICR-MS

Internally calibrated FTICR-MS spectra (resolution ~120,000) were generated for AFFFs and commercial surfactants diluted between 1000 and 100,000 times with methanol or 1:1 methanol: water in positive ion mode ESI (ESI+) and negative ion mode ESI (ESI-). Method details are provided in Appendix A.

2.3.7 LC-MS/MS

Several LC-MS/MS methods using both ESI+ and ESI- were developed in order to separate the SPE model compounds and the PFASs identified in AFFF and commercial surfactants as described in Appendix A. MS/MS transitions for model compounds and PFASs were developed through infusion of model compound solutions or SPE fractions for abundant chain length congeners and minor congeners were predicted from these results

(Tables A4 and A5 in Appendix A). Duplicate LC-MS/MS chromatograms of diluted AFFF and fluorinated surfactant samples were obtained and used qualitatively to assess the presence of PFASs and isomers.

2.3.8 Synthesis of N-(3-(dimethylamino)propyl)perfluorononanamide (DMAPFNAE)

DMAPNFAE (Figure 2.1A, *n*=8) was synthesized by amidation of perfluorononanoyl chloride with 3-(dimethylamino)-1-propylamine as described in Appendix A.

2.4 Results and Discussion

2.4.1 Analytical Strategies

Using both WAX and WCX SPE, average recoveries of all model compounds in corresponding fractions were acceptable and were 70 to 125% for all compounds except for CTMA, which had average recoveries of 135% (WCX) and 63% (WAX, Table A7 in Appendix A). For AFFF and fluorinated surfactant samples, total fluorine content of the SPE fractions by TOF-CIC is shown in Figure A22 in Appendix A.

In mass spectra, PFASs differing in fluorinated chain length are separated by 50 *Da* (-CF_2-) for ECF products or 100 *Da* (-CF_2CF_2-) for fluorotelomer products.[14,27] PFASs can also be identified by their low mass defects (approximately -0.1 to 0.15 *Da*)[14] caused by the negative mass defect of fluorine (-0.0016 *Da*) and their relatively high *m/z*, generally greater than 300. A mass defect is the difference between the accurate and whole number masses for an ion. Elemental formulae were generated based on accurate masses from FTICR-MS and qTOF-MS using Analyst 1.5.1 (MDS Sciex, Concord, ON, Canada) with even electron state, -0.5 to 10 double bond equivalents, a charge state of +1 or -1, 0-60 carbon, 5-40 fluorine, 0-100 hydrogen, 0-4 nitrogen, 0-26 oxygen, and the number of sulfur atoms suggested by isotope patterns. Likely formulae were selected based on a discrepancy from the theoretical *m/z* less than 1.5 *mDa* by FTICR-MS (preferably <1 *mDa*), apparent chain length congeners and (de)protonated ions also fitting

these criteria, and the dominant chain length congener having at least 9 fluorines. Preference was given to odd fluorine counts from single perfluoroalkyl chains, double bond equivalents lower than 5 and formulae with 13 or 17 fluorine atoms in the predominant congener indicative of C6 and C8 PFASs.

One instance where the lower resolution of the qTOF-MS could not adequately resolve congeners of the structures in Figure 2.1A and 2.1C differing by 59 *mDa*, while they could be resolved by FTICR-MS or WCX SPE fractionation, motivated the use of FTICR-MS. The combination of FTICR-MS and qTOF-MS was used for logistical reasons and a single high resolution mass spectrometer with CID capabilities could be used for other, similar studies. Identification of new classes of PFASs was limited by the relatively low sensitivity of qTOF-MS CID experiments and low mass accuracy for low intensity signals. Detection of minor chain lengths by LC-MS/MS was limited by instrumental detection limits and the need to perform substantial sample dilution to prevent instrument contamination. Only ESI was used, which may have prevented detection of PFASs with poor ionization efficiency in ESI and minor components whose ionization was suppressed during direct infusion of samples with high concentrations of other components.

2.4.2 Identified PFASs

Proposed structures and chain lengths of 22 classes of PFASs identified in AFFFs and surfactant concentrates with few or no literature reports are shown in Figure 2.1 with accurate masses for the apparent dominant congener of each in Table 2.1. The CID mass spectra discussed in following sections are in Figures A23-A30 in Appendix A. PFASs detected with each mass spectrometer in each sample are summarized in Table A2 in Appendix A, CID accurate masses are in Table A8 in Appendix A, and a summary of the PFAS classes identified in each sample and SPE fraction is in Table A3 in Appendix A.

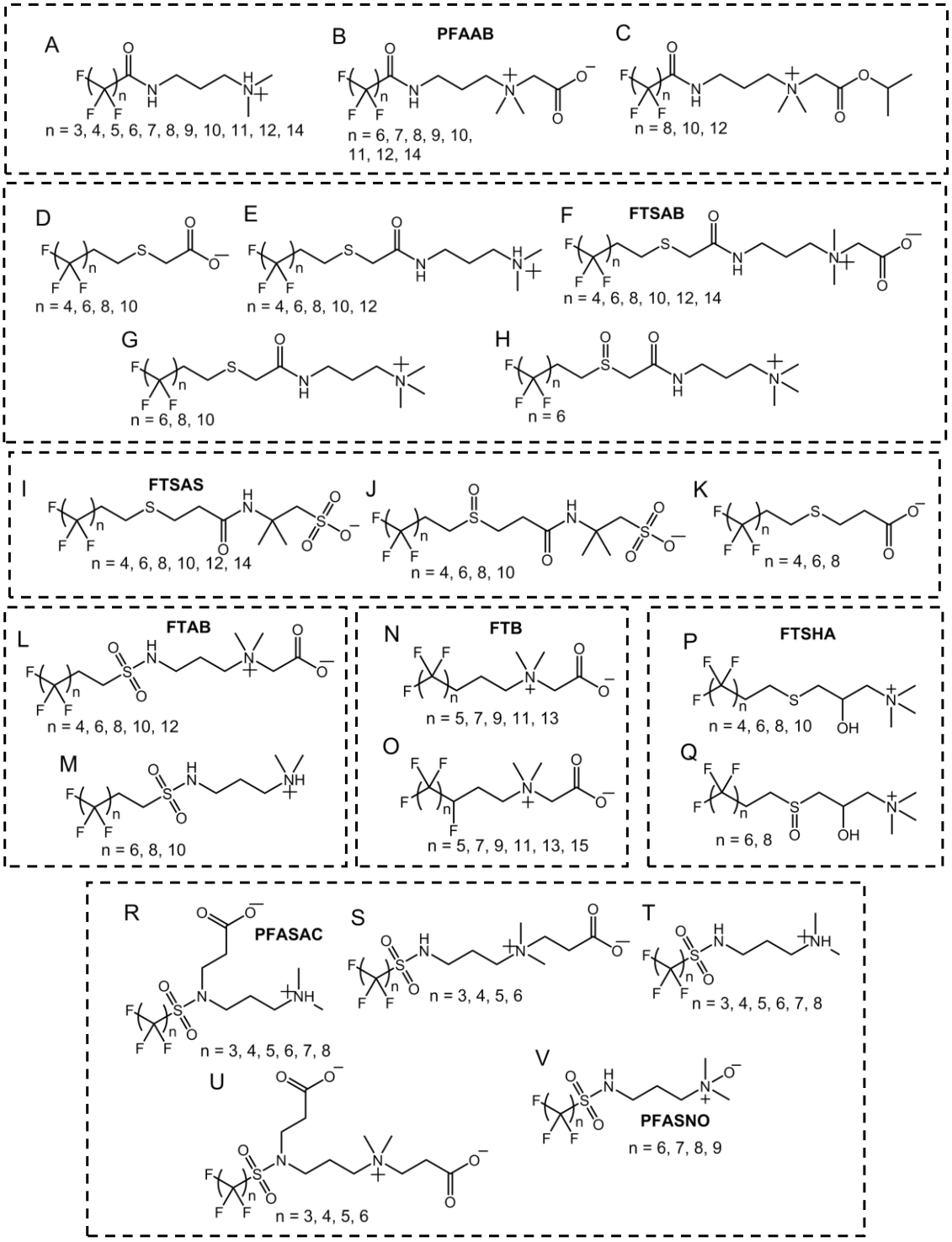

Figure 2.1: Structures and chain lengths observed for novel and infrequently reported PFASs in AFFF and commercial fluorinated surfactants.

Table 2.1: Accurate masses used in assigning molecular formulae to congeners with the highest apparent abundance for each structure

Structure	*n* =	Observed *m/z*	Formula	Theoretical *m/z*	Error (mDa)
A	8	549.0829	$C_{14}H_{14}ON_2F_{17}^{+1}$	549.0829	0.0
B	8	607.0887	$C_{16}H_{16}O_3N_2F_{17}^{+1}$	607.0884	0.3
C	8	649.1350	$C_{19}H_{22}O_3N_2F_{17}^{+1}$	649.1354	-0.4
D	6	436.9888	$C_{10}H_6O_2SF_{13}^{-1}$	436.9886	0.2
E	6	523.1084	$C_{15}H_{20}ON_2SF_{13}^{+1}$	523.1083	0.1
F	6	581.1138	$C_{17}H_{22}O_3N_2SF_{13}^{+1}$	581.1138	0.0
G	6	537.1241	$C_{16}H_{22}ON_2SF_{13}^{+1}$	537.1240	0.1
H	6	553.1185	$C_{16}H_{22}O_2N_2SF_{13}^{+1}$	553.1189	-0.4
I	6	586.0392	$C_{15}H_{17}O_4NS_2F_{13}^{-1}$	586.0397	-0.5
J	6	602.0343	$C_{15}H_{17}O_5NS_2F_{13}^{-1}$	602.0346	-0.3
K	6	451.0041*	$C_{11}H_8O_2SF_{13}^{-1}$	451.0043	-0.2
L	6	571.0926	$C_{15}H_{20}O_4N_2SF_{13}^{+1}$	571.0931	-0.5
M	6	513.0875	$C_{13}H_{18}O_2N_2SF_{13}^{+1}$	513.0876	-0.1
N	5	414.0921	$C_{12}H_{15}O_2NF_{11}^{+1}$	414.0922	-0.1
O	5	432.0825	$C_{12}H_{14}O_2NF_{12}^{+1}$	432.0827	-0.2
P	6	496.0974	$C_{14}H_{19}ONSF_{13}^{+1}$	496.0974	0.0
Q	6	512.0923*	$C_{14}H_{19}O_2NSF_{13}^{+1}$	512.0923	0.0
R/S	6	557.0780	$C_{14}H_{18}O_4N_2SF_{13}^{+1}$	557.0774	0.6
T	6	485.0566	$C_{11}H_{14}O_2N_2SF_{13}^{+1}$	485.0563	0.3
U	6	629.0996	$C_{17}H_{22}O_6N_2SF_{13}^{+1}$	629.0986	1.0
V	8	601.0445	$C_{13}H_{14}O_3N_2SF_{17}^{+1}$	601.0448	-0.3

All accurate masses were obtained by FTICR-MS except those marked by *, which were below detection limits in FTICR-MS but were detected in qTOF-MS analysis of SPE fractions. *n* is the fluorinated chain length.

2.4.3 PFASs in FS-330—Perfluoroalkylamido betaine (PFAAB)-related

The base fraction of FS-330 contained a series of ions with *m/z* 549, 649 and 749 in ESI+. Their occurrence in the base fraction and a 45 *Da* loss in the CID spectrum of *m/z* 549 (Figure A23c in Appendix A) consistent with dimethylamine is suggestive of a tertiary N,N-dimethylamine because this is a known neutral loss for tertiary N,N-dimethylamines.[28] Following dimethylamine, ethene was lost followed by CO. Loss of ethene suggests that a least two methylenes connect the amine to the amide implied by the molecular formula ($C_{14}H_{14}ON_2F_{17}^+$). Neutral loss of CO also suggests an amide since it has been observed with some amides.[29] Due to some uncertainty regarding the structure of *m/z* 549 and a straightforward synthesis, DMAPFNAE [Figure 2.1A, fluorinated chain length (*n*)=8][30] was synthesized and compared to *m/z* 549 in FS-330 to confirm its structure. The CID spectra were indistinguishable (Figure A31 in Appendix A) and DMAPFNAE co-eluted with *m/z* 549 from FS-330 in LC-MS/MS indicating that DMAPFNAE is in FS-330. FTICR-MS of FS-330 revealed ions consistent with **A** with *n*=6, 7, 8, 9, 10, 11, and 12 with no sulfur isotope peaks. The combination of even and odd chain lengths is unusual for a product that appears to be single isomers based on sharp LC-MS/MS peaks consistent with single isomers (Figure A1b in Appendix A). Single isomer polyfluorinated amides of structure **A** may have been made using linear PFCAs formed from fluorotelomer iodides through reaction with oleum, reaction with CO_2 in the presence of a catalyst, or a Grignard reaction or through another synthetic method.[31] C14 **A** was also detected by LC-MS/MS.

The neutral fractions of FS-330 contained *m/z* 607, 707, and 807 ions. The difference of 58 *Da* from **A** is consistent with addition of CH_2CO_2 to the tertiary amine forming a PFAAB. This is supported by the CID spectrum of *m/z* 607 in ESI+, which contains an *m/z* 104 fragment consistent with the protonated betaine fragment, $(CH_3)_2NH^+CH_2CO_2H$ (Figure A23b in Appendix A). The betaine structure proposed in Figure 2.1B agrees with the manufacturer's description of FS-330 as a fluoroaliphatic betaine surfactant. Neutral loss of $(CH_3)_2NCH_2CO_2H$ followed by ethene and CO occurs with *m/z* 607 forming the same *m/z* 504, 476, and 448 fragments as **A**, which substantiates the close relationship between these species. In ESI-, the CID spectrum of

m/z 605 contains an *m/z* 102 deprotonated betaine fragment [$(CH_3)_2NCH_2CO_2^-$] and $C_xF_{2x+1}^-$ fragments, including $C_8F_{17}^-$ indicating at least eight perfluorinated carbons are present (Figure A23a in Appendix A). Ions consistent with PFAABs with *n*=6, 7, 8, 9, 10, 11, and 12 were observed by FTICR-MS, which shows that PFAABs have odd and even congeners like intermediate and/or degradation product **A**. LC-MS/MS produced sharp peaks characteristic of a single isomer for PFAABs with *n*=6, 7, 8, 9, 10, 11, 12, 13, and 14 (Figure A2 in Appendix A).

An ion series in the permanent cation fraction of FS-330 corresponded to addition of C_3H_6 to the PFAAB series, likely through esterification of PFAABs by isopropanol solvent in FS-330.[32] The CID spectrum of *m/z* 649 shows a loss of propene, which can occur via a McLafferty rearrangement for the isopropyl ester (Figure 2.1C)[33,34] and the *m/z* 504 fragment observed with **A** and PFAAB (Figure A23d in Appendix A). The *m/z* 104 fragment [$(CH_3)_2NH^+CH_2CO_2H$] observed for PFAAB and its isopropyl ester are also present. **C** was observed in FS-330 with *n*=8, 10, and 12 by LC-MS/MS (Figure A3 in Appendix A).

2.4.4 PFASs in FS-1520— Fluorotelomerthioalkylamido betaine (FTSAB)-related

The weak acid fraction of FS-1520 contained *m/z* 437, 537, and 637 ions in ESI-. The CID spectrum for *m/z* 437 (Figure A24a in Appendix A) includes neutral losses of HF consistent with a fluorotelomer product[27] and a loss of CO_2 consistent with a carboxylic acid.[35] The *m/z* 91 fragment is likely $HSCH_2CO_2^-$ given it is a weak acid, which suggests one methylene separates the carboxylate from the sulfide implied by the molecular formula $C_{10}H_6O_2SF_{13}^-$. FTICR-MS results are consistent with the formula for the structure in Figure 2.1D with a sulfur isotope peak present for the abundant *m/z* 437 ion. Using LC-MS/MS, **D** was detected in FS-1520 with *n*=4, 6, 8, and 10 (Figure A4 in Appendix A).

Ions in the base fraction of FS-1520 had *m/z* 523, 623, and 723 in ESI+. The CID spectrum of *m/z* 523 (Figure A24b in Appendix A) contains a neutral loss of 45 *Da* that is likely dimethylamine, which indicates the basic functionality is likely a tertiary N,N-

dimethylamine. The *m/z* 393 fragment ($C_6F_{13}CH_2CH_2S{=}CH_2^+$) is suggestive of a fluorotelomer sulfide. The FTICR-MS accurate masses are consistent with the amide of **D** with 3-(dimethylamino)-1-propylamine shown in Figure 2.1E with sulfur isotope peaks for abundant ions as expected. **D** may be a product of the hydrolysis of the amide in **E**. Using LC-MS/MS, **E** with *n*=4, 6, 8, 10, and 12 was detected in FS-1520 (Figure A5 in Appendix A).

Neutral WAX and WCX fractions of FS-1520 contain ions of *m/z* 581, 681, and 781 in ESI+. These ions are 58 Da greater than the **E** amines, corresponding to the addition of CH_2CO_2 to the tertiary amine forming a FTSAB. Accurate masses were consistent with the structure in Figure 2.1F with *n*=6, 8, 10, and 12 and a sulfur isotope peak was present for the abundant *m/z* 581. The CID spectrum of *m/z* 581 (Figure A25a in Appendix A) includes a neutral loss of $(CH_3)_2NCH_2CO_2H$ and an *m/z* 104 fragment $[(CH_3)_2NH^+CH_2CO_2H]$ as expected for a betaine and an *m/z* 393 fragment ($C_6F_{13}CH_2CH_2S{=}CH_2^+$) consistent with a fluorotelomer sulfide. FTSABs are consistent with the manufacturer's description of FS-1520 as a fluoroaliphatic betaine surfactant.[25] LC-MS/MS detected FTSABs with *n*=4, 6, 8, 10, 12, and 14 (Figure A6 in Appendix A). However, FTSABs are inconsistent with the structure proposed for the same molecular formula in AFFF by Place and Field.[14] Their proposed structure does not fit FS-1520 as it would not be expected to produce the *m/z* 104 fragment as it is not a betaine and would not have **E** as an intermediate or degradation product since it would presumably be synthesized by Michael addition of a fluorotelomer thiol to an N-substituted maleic acid amide.[36]

The FTICR-MS spectrum of FS-1520 contains *m/z* 537, 637, and 737 ions in ESI+ corresponding to the addition of CH_2 to the amine **E** with a sulfur isotope peak for the abundant *m/z* 537. These ions appear in the permanent cation fraction. Thus, they are likely an N-methylated version of **E** shown in Figure 2.1G. CID of *m/z* 537 (Figure A25b in Appendix A) results in neutral loss of 59 *Da*, corresponding to trimethylamine, which supports the proposed N,N,N-trimethylammonium. The *n*=6, 8, and 10 congeners were detected by LC-MS/MS (Figure A7 in Appendix A). An additional *m/z* 553 ion corresponding to the addition of oxygen to **G** was also observed in the permanent cation

fraction. CID of *m/z* 553 (Figure A30c in Appendix A) results in loss of trimethylamine and an *m/z* 207 fragment consistent with a sulfenic acid-containing fragment of the sulfoxide in Figure 2.1H. Sulfenic acids are known to form in CID of sulfoxides, including methionine sulfoxide residues,[37] and this fragment provides evidence a sulfoxide is present. **H** with *n*=6 was detected by LC-MS/MS in 1,000,000-fold diluted FS-1520 indicating that the sulfoxide **H** is in FS-1520 (Figure A7 in Appendix A).

2.4.5 FTSAS-Related Structures

6:2 and 8:2 FTSASs (Figure 2.1I) were detected in Foams 1, 3, 4, 5, 8, and 11 by LC-MS/MS, consistent with previous quantitation of these FTSASs in these samples.[11] The 4:2 FTSAS was also detected in Foams 1, 3, 4, 8, and 11, while the previously unreported 10:2, 12:2, and 14:2 FTSASs were detected in some of these samples by LC-MS/MS (Figure A8 in Appendix A). The 6:2 FTSAS-sulfoxide (Figure 2.1J) identified previously[11] was detected in Foams 1, 3, 4, 5, 7, 8, and 11, while 4:2, 8:2, and 10:2 FTSAS-sulfoxides were detected in some of these AFFFs by LC-MS/MS (Figure A9 in Appendix A).

The weak acid fraction of Foam 8 contained an *m/z* 451 ion in ESI- corresponding to the acid formed through hydrolysis of the 6:2 FTSAS amide group (Figure 2.1K). The CID spectrum of *m/z* 451 (Figure A26 in Appendix A) includes a loss of 72 *Da*, which could be a loss of CO_2 and ethene from a carboxylate, and an *m/z* 105 fragment ($HSCH_2CH_2CO_2^-$), which suggests that two methylene groups separate a sulfide from a carboxylate in this weak acid. Additional losses of HF are characteristic of fluorotelomer PFASs.[27] Using LC-MS/MS, 6:2 **K** was found in Foams 4, 5, 8, and 11, while 4:2 and 8:2 **K** were detected in Foam 8 (Figure A10 in Appendix A). The detection of additional, low abundance fluorinated chain lengths by LC-MS/MS highlights the sensitivity of LC-MS/MS and its utility in detecting minor congeners.

2.4.6 FTAB-Related Structures

The 4:2, 6:2, 8:2, 10:2, and 12:2 FTABs (Figure 2.1L) were previously identified in AFFF.[14,15] Ions consistent with the 6:2 and 8:2 FTAB were observed in the WAX and WCX neutral fractions, which is consistent with an amphoteric species. CID spectra of

6:2 FTAB in ESI+ and ESI- (Figure A27a and b in Appendix A) both have neutral losses of 103 *Da* [$(CH_3)_2NCH_2CO_2H$]. In ESI-, *m/z* 569 (**L**) also loses HF or $C_6F_{13}CH{=}CH_2$. In ESI+, *m/z* 571 (**L**) loses ethene following loss of 103 *Da* and also produces an *m/z* 104 fragment [$(CH_3)_2NH^+CH_2CO_2H$], indicative of a betaine with one methylene separating acid from ammonium. Using LC-MS/MS, the FTABs detected were 6:2 and 8:2 in Foams 1, 3, 5, and 8; 10:2 and 12:2 in Foams 1 and 5; and 4:2 in Foam 5 (Figure A11 in Appendix A).

6:2 and 8:2 fluorotelomer sulfonamide amines (Figure 2.1M) were reported in association with FTABs as both synthetic intermediates and degradation products.[13–15,38] Ions consistent with 6:2 **M** were detected in Foams 1, 3, 5, and 8 and occurred in the base fraction, consistent with an amine. Sulfur isotope peaks consistent with FTABs and **M** were observed by FTICR-MS. In CID, *m/z* 513 (**M;** Figure A27c in Appendix A) loses 45 *Da* consistent with loss of dimethylamine, which suggests a tertiary N,N-dimethylamine, followed by loss of ethene similar to **A**, another tertiary N,N-dimethylamine with three methylene spacers. **M** was detected with *n*=6 in Foams 1, 3, 5, and 8 and with *n*=8 in Foams 1 and 5 by LC-MS/MS (Figure A12 in Appendix A). Summing 100 FTICR-MS spectra of 10,000-fold diluted Foam 1 enabled detection of an ion consistent with the previously unreported 10:2 **M**.

2.4.7 Fluorotelomer betaines (FTBs)

The FTBs shown in Figure 2.1N and 2.1O were previously reported in AFFF with *n*=5, 7, and 9[14,15] and may be synthesized through hydrogenation of unsaturated polyfluoroalkylamines.[39] Ions corresponding to **N** and **O** with *n*=5, 7, and 9 were detected in WAX and WCX neutral fractions of Foams 4 and 7 consistent with amphoteric surfactants. CID spectra of **N** and **O** (Figure A28 in Appendix A) are characterized by loss of 60 *Da*, which is likely the enol of acetic acid by a McLafferty rearrangement,[33,34] and an *m/z* 104 fragment [$(CH_3)_2NH^+CH_2CO_2H$], typical of betaines with one methylene spacer, including PFAABs, FTSABs, and FTABs. Signals at -200 *ppm* in ^{19}F-NMR spectra of Foams 4 and 7 are consistent with the -CHF- moiety in **O**.[11] Previously unreported congeners with *n*=11 and 13 for **N** and **O** and *n*=15 for **O** were also detected by LC-MS/MS (Figures A6 and A7 in Appendix A).

2.4.8 Fluorotelomerthiohydroxyl ammonium (FTSHA)-Related Structures

Foam 11 contained organofluorine in the permanent cation fraction attributed primarily to an FTSHA (Figure 2.1P) previously identified in AFFF with *n*=6 and 8,[14,15] based on accurate masses and a sulfur isotope peak observed for the abundant 6:2 congener. Additional ions 16 *Da* greater than FTSHAs with *n*=6 and 8 suggested the sulfide was oxidized to the sulfoxide as shown in Figure 2.1Q.

In CID, *m/z* 496 and 512 (Figure 2.2) corresponding to 6:2 FTSHA and **Q** both underwent a loss of 59 *Da* corresponding to trimethylamine, which is the only 59 *Da* tertiary amine that could be lost from a quaternary ammonium with one nitrogen atom and is a known loss for acetylcholine, which contains a quaternary N,N,N-trimethylammonium.[40] Following loss of trimethylamine, 6:2 FTSHA underwent a loss of formaldehyde or a loss of C_2H_4O, likely as ethenol through direct bond cleavage, producing an *m/z* 393 fragment also observed for the fluorotelomer sulfides in Figures 2.1E and 2.1F. **Q** (*m/z* 512) also loses its fluorotelomer tail forming a sulfenic acid-containing fragment with *m/z* 166. Fragmentation of sulfoxides forming sulfenic acids is known.[37] The sulfenic acid fragment subsequently loses HSOH, as reported for another sulfenic acid.[41] Using LC-MS/MS, 4:2, 6:2, 8:2, and 10:2 FTSHA were detected in Foam 11 (Figure A15 in Appendix A). Accelerated oxidation appeared to occur in the acidic methanol SPE fraction, allowing development of LC-MS/MS transitions for the sulfoxide **Q** which were used to detect 6:2 and 8:2 **Q** in 10,000-fold diluted Foam 11, which shows sulfoxides are present in the AFFF (Figure A16 in Appendix A).

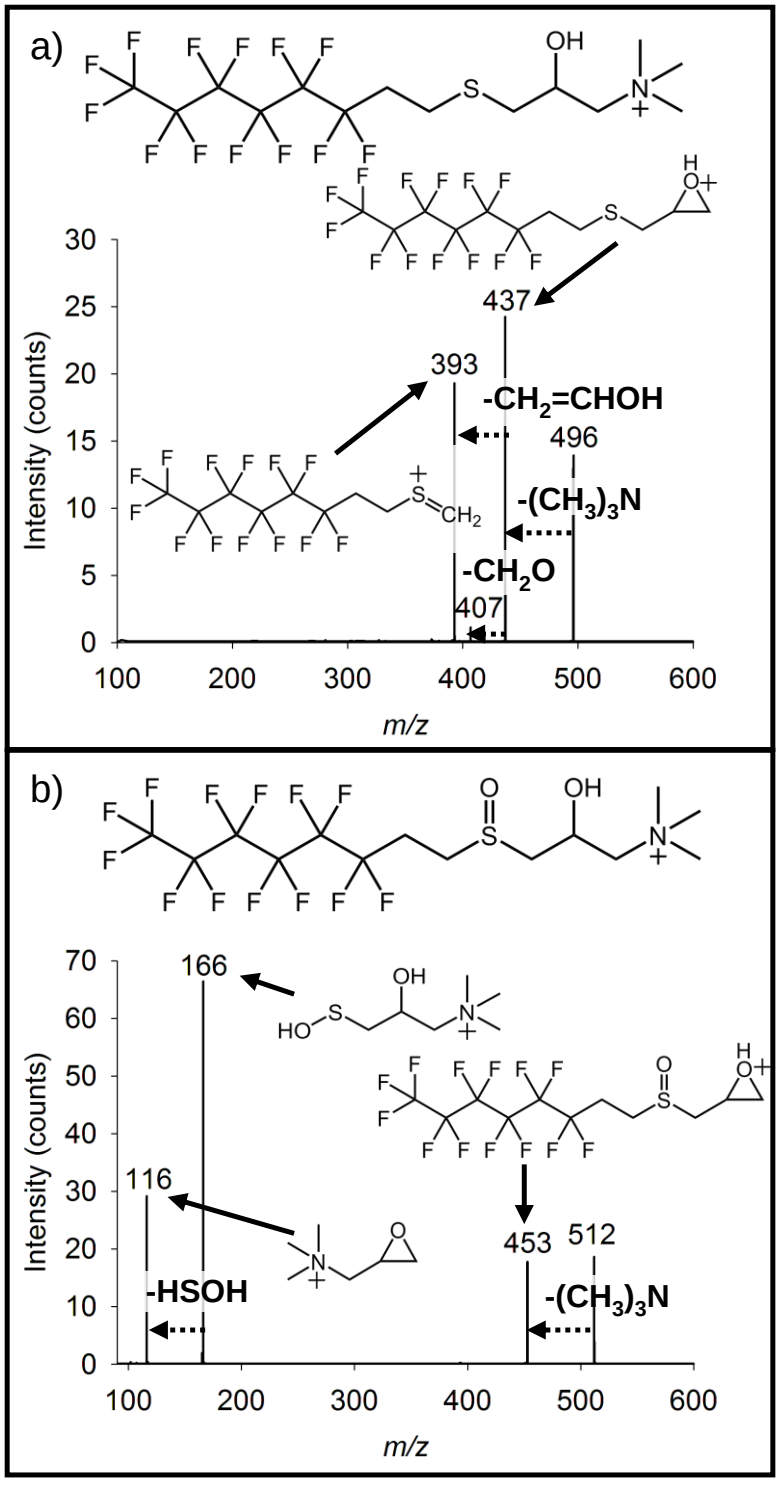

Figure 2.2: qTOF-MS CID spectrum of a) *m/z* 496 ion (6:2 FTSHA) in ESI+ with a collision energy of 40 V obtained using Foam 11 WAX neutral fraction and b) *m/z* 512 ion (Q, *n* = 6) in ESI+ with a collision energy of 30 V obtained using Foam 11 permanent cation fraction.

2.4.9 Perfluoroalkylsulfonamido-based Surfactants

A perfluoroalkylsulfonamido amino carboxylate (PFASAC) amphoteric surfactant (Figure 2.1R) and its amine intermediate (Figure 2.1T) in C4, C5, C6, C7, and C8 congeners[15] and a dicarboxylate side product (Figure 2.1U) in C5 and C6 versions were previously reported in AFFF[14] and described in a 3M patent.[42] Foams 2 and 12 contained ions corresponding to PFASAC, **T**, and **U** with characteristic sulfur isotope peaks. Consistent with their ionic natures, PFASACs occurred in WAX and WCX neutral fractions, **T** appeared in the base fraction and **U** occurred in the weak acid fraction.

In CID, *m/z* 555 and 557 (C6 PFASAC; Figure A29a and b in Appendix A) undergo sequential losses of CO_2 and ethene as occurred with **C**, which may be characteristic of at least two methylenes adjacent to a carboxylic acid. In ESI+, cleavage of the sulfonamide S-N bond yields an *m/z* 174 radical cation, which undergoes losses of dimethylamine or $\bullet CH_2CO_2H$. CID of sulfonamides is known to cleave S-N bonds forming resonance stabilized nitrogen radical cations[43] or cationic SO_2-containing fragments.[44] Instability of perfluorinated cations may drive radical formation in this case. Addition of acrylic acid to the amine rather than the sulfonamide on intermediate **T** produces the isomeric betaine in Figure 2.1S[42] and the *m/z* 118 fragment is probably $(CH_3)_2NH^+CH_2CH_2CO_2H$ from **S**.

In ESI-, *m/z* 483 (**T;** Figure A29c in Appendix A) primarily forms $C_xF_{2x+1}^-$ fragments characteristic of perfluoroalkane sulfonamido compounds.[45] In ESI+, *m/z* 485 (**T;** Figure A29d in Appendix A) loses dimethylamine and ethene followed by SO_2. Loss of SO_2 is known in CID of sulfonamides.[46] Cleavage of the S-N bond produces a 3-(dimethylamino)-1-propylamine radical cation (*m/z* 102). In ESI+, *m/z* 629 (**U**; Figure A30a in Appendix A) produces an *m/z* 187 fragment via a cyclic rearrangement and an *m/z* 118 fragment [$(CH_3)_2NH^+CH_2CH_2CO_2H$] consistent with addition of acrylic acid to the amine in PFASAC producing this betaine-containing side product.[42]

Using LC-MS/MS, PFASACs and **T** with *n*=3, 4, 5, 6, 7, and 8 and **U** with *n*=3, 4, 5, and 6 were detected in Foams 2 and 12 with multiple peaks due to branched isomers in ECF products (Figures A11, A12, and A13 in Appendix A). LC-MS/MS separated the

isobaric betaine **S** from PFASAC using the *m/z* 118 fragment revealing the presence of **S** with *n*=3, 4, 5, and 6, which eluted before the corresponding **R** congeners (Figure 2.3).

The Foam 10 MSDS lists N-3-(dimethylamino)propyl perfluoroctanesulfonamide N'-oxide potassium salt (Figure 2.1V, *n*=8), a pefluoroalkylsulfonamido amine oxide (PFASNO).[47] PFASNO was observed in Foams 5 and 10 with *n*=7 and 8 and a characteristic sulfur isotope peak by FTICR-MS. The C8 congener was detected in WAX and WCX neutral fractions consistent with an amphoteric surfactant. CID spectra of C8 PFASNO (Figure A30b and c in Appendix A) in both ESI+ and ESI- included loss of N,N-dimethylhydroxylamine, which is a typical neutral loss for N,N-dimethylamine oxides[48] and supports the amine oxide structure. In ESI+, loss of ethene follows loss of the amine oxide, which is analogous to losses of dimethylamine and ethene from **M** and may indicate three methylenes separate the amine oxide from the sulfonamide. Losses of SO_2 consistent with a sulfonamide[46] also occurred. In ESI-, cleavage of the S-N bond forms an *m/z* 483 ($C_8F_{17}SO_2^-$) fragment. Similar fragmentations have been observed for other sulfonamides.[35] $C_xF_{2x+1}^-$ and $SO_2NCH_2^-$ fragments are also present. Using LC-MS/MS, C6, C7, C8, and C9 PFASNOs were detected in Foams 5 and 10 (Figure A20 in Appendix A). Amine intermediates in preparing PFASNOs have structure **T**[49] and were detected with *n*=4, 5, 6, 7, and 8 in Foams 5 and 10 by LC-MS/MS.

Recently, polyfluorinated amides have been reported to occur in perfluoroalkane sulfonamido substances as byproducts of ECF synthesis.[50] In the FTICR-MS spectrum of Foam 12, a series of ions was observed corresponding to **A**, which is an amide version of **T**, with *n*=4, 5, 6, and 7. An ion corresponding to C7 **A** was observed in the base fraction and the FTICR-MS spectrum of Foam 2. Using LC-MS/MS, Foams 2 and 12 were found to contain compounds that undergo the **A** transitions for *n*=3, 4, 5, 6, 7, and 8 (Figure A1a in Appendix A) with broader peaks than FS-330 due to ECF branched isomers. The *n*=6, 7, and 8 congeners of **A** in Foam 12 had retention times within 11 seconds of those in FS-330 indicating that they probably share structure **A** (Figure A21 in Appendix A).

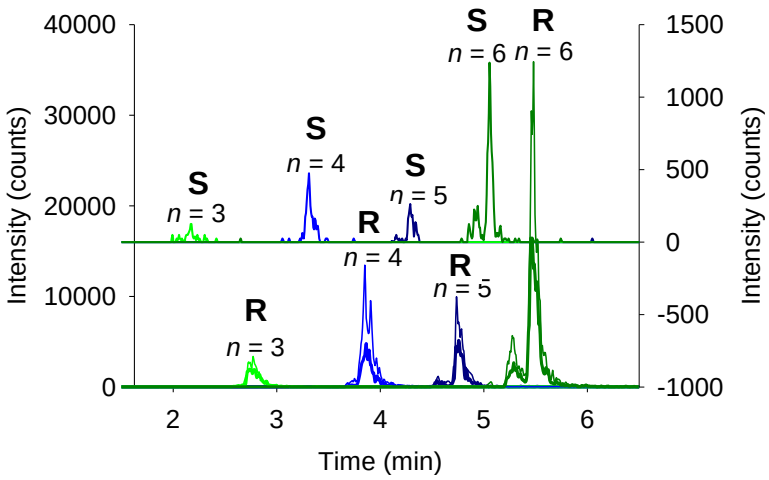

Figure 2.3: LC-MS/MS chromatograms of 50,000-times diluted Foam 12 showing transitions of the primary ECF amphoteric surfactant R and the isomeric side product betaine S. For R, the thin traces show transitions from $[M+H]^+$ to *m/z* 85 and the thick traces show the transitions from $[M+H]^+$ to *m/z* 129. For S, the traces show the transitions from $[M+H]^+$ to *m/z* 118.

2.4.10 Composition of AFFFs and Fluorinated Surfactant Concentrates

For the AFFF samples examined, there was no clear correlation between composition and manufacturer contrary to results reported for AFFFs used by the United States military.[14] For example, Foams 1, 3, and 8 were alike and contained FTSAS-related surfactants and FTAB-related surfactants but Foam 1 was from Hazard Control Technologies, while Foams 3 and 8 were from Angus Fire. Angus Fire also produced Foam 2, which was similar to the 3M Foam 12, as both contained PFSAs,[11] PFASAC-related surfactants, and **A**. However, 3M also produced Foam 10, which contains PFASNOs as an amphoteric component rather than PFASACs. Foams 4 and 11 were from Ansul Inc. and while both contain FTSASs, Foam 4 contains FTBs and Foam 11 contains FTSHA-related surfactants. Foams 6 and 9, which contain residual levels of organofluorine[11] were manufactured by Hazard Control Technologies and Angus Fire, respectively, indicating these manufacturers also produce "fluorine-free" firefighting foams. Apparently, identical AFFF components cannot be assumed for different formulas from the same manufacturer, at least with civilian products.

Generally, all fluorinated AFFFs, except Foams 5 and 7, contained two major classes of fluorinated surfactants plus intermediates, side products and/or degradation products of these surfactants. Foam 7 contained primarily FTBs with small amounts of **J**, while Foam 5 is a mixture of two AFFFs and contains PFSAs,[11] **T**, and PFASNO similar to Foam 10 and FTSASs, FTABs, and related surfactants similar to Foam 8. FS-330 and FS-1520 each contained a fluorinated amphoteric betaine as stated on product information as well as synthetic intermediates, side products, and/or breakdown products of these. This suggests that fluorinated intermediates, side products, and/or degradation products in AFFFs may originate in impure surfactant concentrates used to formulate them.

2.5 Environmental Implications

This investigation of AFFFs and commercial fluorinated surfactants highlights the enormous variety of PFASs that have been or are being produced. Impurities are common in the form of synthetic intermediates, side products, and/or degradation products. This greatly complicates the analysis of environmental samples for PFASs that are potential PFAA precursors since an enormous number of standards would be needed for complete quantitation of potential PFAA precursors. This highlights the utility of general analytical methods for organofluorine, including TOF-CIC.[6–8,26]

Environmental degradation of the PFASs discussed has not been investigated, except for 6:2 FTSAS (**I**) and 6:2 FTAB (**L**), which have been the subject of recent biodegradation experiments in WWTP sludge and marine organisms, respectively.[11,13] These studies indicated that 6:2 FTSAS biotransformation produces PFCAs,[11] while contamination of the 6:2 FTAB dose with PFCAs precluded confirmation of any PFCA production.[13] Previously other fluorotelomer surfactants, such as PAPs[20,21] and 6:2 FTSA,[23] have been shown to biotransform to PFCAs. Many PFASs discussed herein may be PFCA precursors based on hydrogenated carbons next to fluorinated carbons in their structures, including **D** through **H** and **I** through **Q**. Enzymatic hydrolysis of the amides in PFAAB and related surfactants would yield PFCAs directly as Seacat reported that rats dosed with N-methylperfluorooctanamide metabolized it to PFOA.[51]

Perfluoroalkane sulfonamido surfactants are potential PFSA precursors based on the reported biotransformation of EtFOSE to PFOS.[17–19] Therefore, **R** through **V** are likely candidates for biotransformation to PFSAs. Since all the ECF sulfonamide-based surfactants detected in this study were C9 or shorter, high hydrophobicity would not be expected to substantially slow their biodegradation as was reported for an EtFOSE-based phosphate diester with 16 perfluorinated carbons in marine sediment.[19] Further investigation of the biodegradation of the PFASs identified herein and their potential to biodegrade to PFAAs is warranted.

Chain lengths of the PFASs detected in AFFFs and commercial surfactants ranged from 3 to 15 perfluorinated carbons. Therefore, these PFASs are potentially precursors for PFAAs of a variety of chain lengths with different environmental fates and toxicological concerns associated with them. Sorption to sediments,[52,53] bioconcentration in rainbow trout,[54] and bioaccumulation in rainbow trout[55,56] and eels[53] have all been found to be influenced by the perfluorinated chain length and polar head group of PFAAs with increasing number of perfluorinated carbons positively correlated with sorption coefficients, bioconcentration factors, and bioaccumulation factors. Thus, the long-chain PFASs identified herein may be more bioaccumulative than short-chain congeners leading to significant accumulation of them or long-chain degradation products in biota. The toxicology of PFOS and PFOA has been investigated extensively,[57] but assessments of AFFF PFASs in the open literature are limited to a study of mixtures of FTAB congeners marketed as Forafac 1157 in turbot. These mixtures had different toxic modes of action, including immunosuppression and growth inhibition, depending on the mix of chain lengths applied.[12] Variable toxic effects depending on fluorinated chain length are supported by an investigation of the transcriptional effects of various long- and short-chain PFCAs and PFSAs in rat hepatoma cells that produced an unclear relationship between fluorinated chain-length and potential toxic effects.[58] Therefore, the toxicology of any chain-length congener detected in this study cannot necessarily be extrapolated to other congeners. The broad range of PFASs identified herein probably vary in sorption coefficient, bioaccumulation factor, and toxicology and require further investigation of their environmental fate and toxicology.

2.6 Acknowledgements

We thank Karl Jobst for obtaining FTICR-MS spectra and helpful discussions regarding interpretation of CID spectra and Patrick Crozier and Eric Reiner for collecting and donating AFFF samples (Ontario Ministry of the Environment, Etobicoke, ON). Leo Yeung assisted with TOF-CIC (University of Toronto). This work was funded by the Natural Sciences and Engineering Research Council of Canada.

2.7 References

(1) Giesy, J. P.; Kannan, K. Global distribution of perfluorooctane sulfonate in wildlife. *Environ. Sci.Technol.* **2001**, *35*, 1339–1342.

(2) Hansen, K. J.; Clemen, L. A.; Ellefson, M. E.; Johnson, H. O. Compound-specific, quantitative characterization of organic fluorochemicals in biological matrices. *Environ. Sci. Technol.* **2001**, *35*, 766–770.

(3) Buck, R. C.; Franklin, J.; Berger, U.; Conder, J. M.; Cousins, I. T.; de Voogt, P.; Jensen, A. A.; Kannan, K.; Mabury, S. A.; van Leeuwen, S. Perfluoroalkyl and polyfluoroalkyl substances in the environment: terminology, classification, and origins. *Integr. Environ. Assess. Manag.* **2011**, *7*, 513–541.

(4) Moody, C. A.; Martin, J. W.; Kwan, W. C.; Muir, D. C. G.; Mabury, S. A. Monitoring perfluorinated surfactants in biota and surface water samples following an accidental release of fire-fighting foam into Etobicoke Creek. *Environ.Sci.Technol.* **2002**, *36*, 545–551.

(5) Loi, E. I. H.; Yeung, L. W. Y.; Taniyasu, S.; Lam, P. K. S.; Kannan, K.; Yamashita, N. Trophic Magnification of poly- and perfluorinated compounds in a subtropical food web. *Environ. Sci. Technol.* **2011**, *45*, 5506–5513.

(6) Yeung, L. W. Y.; Miyake, Y.; Taniyasu, S.; Wang, Y.; Yu, H.; So, M. K.; Jiang, G.; Wu, Y.; Li, J.; Giesy, J. P.; Yamashita, N.; Lam, P. K. S. Perfluorinated compounds and total and extractable organic fluorine in human blood samples from China. *Environ.Sci.Technol.* **2008**, *42*, 8140–8145.

(7) Miyake, Y.; Yamashita, N.; Rostkowski, P.; So, M. K.; Taniyasu, S.; Lam, P. K. S.; Kannan, K. Determination of trace levels of total fluorine in water using combustion ion chromatography for fluorine: a mass balance approach to determine individual perfluorinated chemicals in water. *J.Chromatogr.A* **2007**, *1143*, 98–104.

(8) Yeung, L. W. Y.; De Silva, A. O.; Loi, E. I. H.; Marvin, C. H.; Taniyasu, S.; Yamashita, N.; Mabury, S. A.; Muir, D. C. G.; Lam, P. K. S. Pefluoroalkyl

substances and extractable organic fluorine in surface sediments and cores from Lake Ontario. *Environ. Int.* **2013**, *59*, 389–397.

(9) Moody, C.; Field, J. Perfluorinated surfactants and the environmental implications of their use in fire-fighting foams. *Environ.Sci.Technol.* **2000**, *34*, 3864–3870.

(10) Schultz, M. M.; Barofsky, D. F.; Field, J. A. Quantitative determination of fluorotelomer sulfonates in groundwater by LC MS/MS. *Environ.Sci.Technol.* **2004**, *38*, 1828–1835.

(11) Weiner, B.; Yeung, L. W. Y.; Marchington, E. B.; D'Agostino, L. A.; Mabury, S. A. Organic fluorine content in aqueous film forming foams (AFFFs) and biodegradation of the foam component 6:2 fluorotelomermercaptoalkylamido sulfonate (6:2 FTSAS). *Environ. Chem.* **2013**, 10, 486–493.

(12) Hagenaars, A.; Meyer, I. J.; Herzke, D.; Pardo, B. G.; Martinez, P.; Pabon, M.; De Coen, W.; Knapen, D. The search for alternative aqueous film forming foams (AFFF) with a low environmental impact: physiological and transcriptomic effects of two Forafac (R) Fluorosurfactants in Turbot. *Aquat.Toxicol.* **2011**, *104*, 168–176.

(13) Moe, M. K.; Huber, S.; Svenson, J.; Hagenaars, A.; Pabon, M.; Trümper, M.; Berger, U.; Knapen, D.; Herzke, D. The structure of the fire fighting foam surfactant Forafac®1157 and its biological and photolytic transformation products. *Chemosphere* **2012**, *89*, 869–875.

(14) Place, B. J.; Field, J. A. Identification of novel fluorochemicals in aqueous film-forming foams used by the US military. *Environ. Sci. Technol.* **2012**, *46*, 7120–7127.

(15) Backe, W. J.; Day, T. C.; Field, J. A. Zwitterionic, cationic, and anionic fluorinated chemicals in aqueous film forming foam formulations and groundwater from U.S. military bases by nonaqueous large-volume injection HPLC-MS/MS. *Environ. Sci. Technol.* **2013**, *47*, 5226–5234.

(16) Fire Fighting Foam Coalition AFFF Update; Issue 4 **2004**. http://www.fffc.org/images/AFFFupdate4.pdf

(17) Xie, W.; Wu, Q.; Kania-Korwel, I.; Tharappel, J. C.; Telu, S.; Coleman, M. C.; Glauert, H. P.; Kannan, K.; Mariappan, S. V. S.; Spitz, D. R.; Weydert, J.; Lehmler, H.-J. Subacute exposure to N-ethyl perfluorooctanesulfonamidoethanol results in the formation of perfluorooctanesulfonate and alters superoxide dismutase activity in female rats. *Arch.Toxicol.* **2009**, *83*, 909–924.

(18) Rhoads, K. R.; Janssen, E. M.-L.; Luthy, R. G.; Criddle, C. S. Aerobic biotransformation and fate of N-ethyl perfluorooctane sulfonamidoethanol (N-EtFOSE) in activated sludge. *Environ. Sci. Technol.* **2008**, *42*, 2873–2878.

(19) Benskin, J. P.; Ikonomou, M. G.; Gobas, F. A. P. C.; Begley, T. H.; Woudneh, M. B.; Cosgrove, J. R. Biodegradation of N-ethyl perfluorooctane sulfonamido ethanol (EtFOSE) and EtFOSE-based phosphate diester (SAmPAP diester) in marine sediments. *Environ. Sci. Technol.* **2013**, *47*, 1381–1389.

(20) Lee, H.; D'eon, J.; Mabury, S. A. Biodegradation of polyfluoroalkyl phosphates as a source of perfluorinated acids to the environment. *Environ.Sci.Technol.* **2010**, *44*, 3305–3310.

(21) D'eon, J. C.; Mabury, S. A. Exploring indirect sources of human exposure to perfluoroalkyl carboxylates (PFCAs): evaluating uptake, elimination, and biotransformation of polyfluoroalkyl phosphate esters (PAPs) in the rat. *Environ. Health Persp.* **2011**, *119*, 344-350.

(22) Butt, C. M.; Muir, D. C. G.; Mabury, S. A. Biotransformation of the 8:2 fluorotelomer acrylate in rainbow trout. 1. in vivo dietary exposure. *Environ. Toxicol. Chem.* **2010**, *29*, 2726–2735.

(23) Wang, N.; Liu, J.; Buck, R. C.; Korzeniowski, S. H.; Wolstenholme, B. W.; Folsom, P. W.; Sulecki, L. M. 6:2 Fluorotelomer sulfonate aerobic biotransformation in activated sludge of waste water treatment plants. *Chemosphere* **2011**, *82*, 853–858.

(24) Mason Chemical Company Masurf FS-330 **2007**.

(25) Mason Chemical Company Masurf FS-1520 **2007**.

(26) Rand, A. A.; Mabury, S. A. In vitro interactions of biological nucleophiles with fluorotelomer unsaturated acids and aldehydes: fate and consequences. *Environ. Sci. Technol.* **2012**, *46*, 7398–7406.

(27) Trier, X.; Granby, K.; Christensen, J. H. Tools to discover anionic and nonionic polyfluorinated alkyl surfactants by liquid chromatography electrospray ionisation mass spectrometry. *J. Chromatogr. A* **2011**, *1218*, 7094–7104.

(28) Fu, Q.; Li, L. J. Investigation of several unique tandem mass spectrometric fragmentation patterns of NFDEIDR, an Orcokinin analog, and its N-terminal dimethylated form. *Rapid Commun. Mass Spectrom.* **2006**, *20*, 553–562.

(29) Risoli, A.; Cheng, J. B. Y.; Verkerk, U. H.; Zhao, J.; Ragno, G.; Hopkinson, A. C.; Siu, K. W. M. Gas-phase fragmentation of protonated benzodiazepines. *Rapid Commun. Mass Spectrom.* **2007**, *21*, 2273–2281.

(30) Ovchinnikova, N. S.; Veraksich, O. V.; Pospelov, M. V.; Zhuravlev, L. T.; Glazunov, M. P.; Fokin, A. V. Mass-spectrometric study of fluoroalkylated and fluoroacylated alkylamines, ethylenediamines, and propylenediamines. *Russ. Chem. Bull.* **1986**, *35*, 752–756.

(31) Kissa, E. *Fluorinated Surfactants and Repellents*; Marcel Dekker: New York, 2001; Vol. 2nd ed., rev. and expanded.

(32) Mason Chemical Company Material Safety Data Sheet: Masurf FS-330 **2005**.

(33) McLafferty, F. W. Mass spectrometric analysis. Molecular rearrangements. *Anal. Chem.* **1959**, *31*, 82–87.

(34) McLafferty, F. W. *Interpretation of Mass Spectra*; University Science Books: Sausalito, Calif., 1993.

(35) Niessen, W. M. A. Fragmentation of toxicologically relevant drugs in negative-ion liquid chromatography–tandem mass spectrometry. *Mass Spectrom. Rev.* **2012**, *31*, 626–665.

(36) Ciba-Geigy AG Pefluoroalkyl compounds containing thio groups and fire-fighting compositions containing them. Great Britain 1,524,875, September 13, 1978.

(37) Reid, G. E.; Roberts, K. D.; Kapp, E. A.; Simpson, R. J. Statistical and mechanistic approaches to understanding the gas-phase fragmentation behavior of methionine sulfoxide containing peptides. *J. Proteome Res.* **2004**, *3*, 751–759.

(38) Hoffmann, D.; Stach, H. Perfluoro-alkyl-alkylene-sulfonamidoalkylene-dialkylamines and their quaternary ammonium salts; U.S. Patent 3,721,706, March 20, 1973.

(39) Prossel, G.; Knaup, W.; Wehowsky, F. Saturated fluoroalkylamines and their derivatives, and mixtures thereof. U.S. Patent 5,648,527, July 15, 1997.

(40) Lioe, H.; Barlow, C. K.; O'Hair, R. A. J. How does acetylcholine lose trimethylamine? A density functional theory study of four competing mechanisms. *J. Am. Soc. Mass Spectrom.* **2009**, *20*, 238–246.

(41) Shetty, V.; Spellman, D. S.; Neubert, T. A. Characterization by tandem mass spectrometry of stable cysteine sulfenic acid in a cysteine switch peptide of matrix metalloproteinases. *J. Am. Soc. Mass Spectrom.* **2007**, *18*, 1544–1551.

(42) Stern, R. M.; Guenthner, R.; Alm, R. R.; Wilkinson, T. K. Process for the preparation of fluoroaliphatic aminocarboxylate surfactants. U.S. Patent 5,144,069, September 1, 1992.

(43) Xu, G.; Huang, T.; Zhang, J.; Huang, J. K.; Carlson, T.; Miao, S. Investigation of collision-induced dissociations involving odd-electron ion formation under positive electrospray ionization conditions using accurate mass. *Rapid Commun.Mass Spectrom.* **2010**, *24*, 321–327.

(44) Klagkou, K.; Pullen, F.; Harrison, M.; Organ, A.; Firth, A.; Langley, G. J. Fragmentation pathways of sulphonamides under electrospray tandem mass spectrometric conditions. *Rapid Commun.Mass Spectrom.* **2003**, *17*, 2373–2379.

(45) Kuehl, D. W.; Rozynov, B. Chromatographic and mass spectral studies of perfluorooctanesulfonate and three perfluorooctanesulfonamides. *Rapid Commun.Mass Spectrom.* **2003**, *17*, 2364–2369.

(46) Sun, M.; Dai, W.; Liu, D. Q. Fragmentation of aromatic sulfonamides in electrospray ionization mass spectrometry: elimination of SO2 via rearrangement. *J.Mass Spectrom.* **2008**, *43*, 383–393.

(47) 3M Company Material Saftey Data Sheet: ATC-603 Light Water ATC3 AR-AFFF 3% **2005**.

(48) Holman, S. W.; Wright, P.; Langley, G. J. A rapid methodology for the characterization of dialkyl tertiary amine-N-oxide metabolites using structurally dependent dissociation pathways and reconstructed ion current chromatograms. *Anal. Chem.* **2010**, *82*, 2347–2354.

(49) Minnesota Mining and Manufacturing Company. Fluorinated amine oxides. G.B. Patent 1,202,612, January 10, 1973.

(50) Jackson, D. A.; Mabury, S. A. Polyfluorinated amides as a historical PFCA source by electrochemical fluorination of alkyl sulfonyl fluorides. *Environ. Sci. Technol.* **2013**, *47*, 382–389.

(51) Seacat, A. M. Toxicokinetic screen of FC methyl carboxamide (T-7483) in rats; 3M Medical Department Study T-7483.1; 3M Medical Department: St. Paul, MN, 2004.

(52) Higgins, C. P.; Luthy, R. G. Sorption of perfluorinated surfactants on sediments. *Environ. Sci. Technol.* **2006**, *40*, 7251–7256.

(53) Kwadijk, C. J. A. F.; Korytár, P.; Koelmans, A. A. Distribution of perfluorinated compounds in aquatic systems in The Netherlands. *Environ. Sci. Technol.* **2010**, *44*, 3746–3751.

(54) Martin, J. W.; Mabury, S. A.; Solomon, K. R.; Muir, D. C. G. Bioconcentration and tissue distribution of perfluorinated acids in rainbow trout (Oncorhynchus Mykiss). *Environ. Toxicol. Chem.* **2003**, *22*, 196–204.

(55) Martin, J. W.; Mabury, S. A.; Solomon, K. R.; Muir, D. C. G. Dietary accumulation of perfluorinated acids in juvenile rainbow trout (Oncorhynchus Mykiss). *Environ. Toxicol. Chem.* **2003**, *22*, 189–195.

(56) Lee, H.; De Silva, A. O.; Mabury, S. A. Dietary bioaccumulation of perfluorophosphonates and perfluorophosphinates in juvenile rainbow trout:

evidence of metabolism of perfluorophosphinates. *Environ. Sci. Technol.* **2012**, *46*, 3489–3497.

(57) Lau, C.; Anitole, K.; Hodes, C.; Lai, D.; Pfahles-Hutchens, A.; Seed, J. Perfluoroalkyl acids: A review of monitoring and toxicological findings. *Toxicol. Sci.* **2007**, *99*, 366–394.

(58) Naile, J. E.; Wiseman, S.; Bachtold, K.; Jones, P. D.; Giesy, J. P. Transcriptional effects of perfluorinated compounds in rat hepatoma cells. *Chemosphere* **2012**, *86*, 270–277.

Chapter Three

Aerobic Biodegradation of Two Fluorotelomer Sulfonamide-based Aqueous Film Forming Foam Components Produces Perfluoroalkyl Carboxylates

Lisa A. D'Agostino and Scott A. Mabury*

Contributions: Lisa D'Agostino synthesized the 6:2 FTAA and 6:2 FTAB standards, planned and executed the biodegradation experiments, and performed all sample analysis. The manuscript was prepared by Lisa D'Agostino with editorial input from Scott Mabury.

This is the peer reviewed version of the following article: Aerobic biodegradation of two fluorotelomer sulfonamide-based aqueous film forming foam components produces perfluoroalkyl carboxylates. **2017**, *Environ. Toxicol Chem.* DOI: 10.1002/etc.3750, which has been published in final form at http://onlinelibrary.wiley.com/doi/10.1002/etc.3750/full. This article may be used for non-commercial purposes in accordance with Wiley Terms and Conditions for Self-Archiving.

3 Aerobic Biodegradation of Two Fluorotelomer Sulfonamide-based Aqueous Film Forming Foam Components Produces Perfluoroalkyl Carboxylates

3.1 Abstract

The biodegradation of two common fluorotelomer surfactants used in aqueous film forming foams (AFFFs), 6:2 fluorotelomer sulfonamide alkylamine (FTAA) and 6:2 fluorotelomer sulfonamide alkylbetaine (FTAB), was investigated over 109 days with aerobic wastewater treatment plant (WWTP) sludge. Results show that biodegradation of 6:2 FTAA and 6:2 FTAB produces 6:2 fluorotelomer alcohol (FTOH), 6:2 fluorotelomer carboxylic acid (FTCA), 6:2 fluorotelomer unsaturated carboxylic acid (FTUCA), 5:3 FTCA, and short chain perfluoroalkyl carboxylates (PFCAs). Additional degradation products included 6:2 fluorotelomer sulfonamide (FTSAm), which was a major degradation product in the presence of either active or sterilized sludge, while 6:2 fluorotelomer sulfonate (FTSA) production was measured with sterilized sludge only. Six additional degradation products were tentatively identified by quadrupole time-of-flight mass spectrometry (qTOF-MS) and were attributed to *N*-dealkylation and oxidation of 6:2 FTAA.

3.2 Introduction

Aqueous film forming foam (AFFF) release is a known source of contamination in surface water[1,2], groundwater[3,4], soil[4], and biota[1,2] with perfluoroalkyl and polyfluoroalkyl substances (PFASs). Initially, the PFASs identified at AFFF impacted sites were limited to those that were known at the time, perfluoroalkyl carboxylates (PFCAs), perfluoroalkyl sulfonates (PFSAs), and fluorotelomer sulfonates (FTSAs)[1,3]. However, with the exception of PFSAs in AFFFs produced using electrochemical fluorination (ECF) prior to the perfluorooctane sulfonate (PFOS) phase out by 3M in 2001, these compounds are not the major PFASs in AFFFs[5,6]. Over the past several years numerous major PFASs in AFFFs have been identified[7,8]. However, even when including these newly identified PFASs, only about half of the total PFASs measured by an oxidation of precursors assay in aquifer solids, groundwater, and soil at an AFFF

impacted site were accounted for by known PFASs[4]. Degradation products of the more complex PFASs found in AFFFs[7,8] may be responsible for a significant portion of the unattributed PFASs in these samples. Studies investigating the degradation of PFASs recently identified in AFFFs are quite limited and include investigations of the biodegradation of fluorotelomer mercaptoalkylamido sulfonates (FTSASs) in wastewater treatment plant (WWTP) sludge[5] and soil[9], the aqueous photolysis of 6:2 fluorotelomer sulfonamide alkylbetaine (FTAB)[10,11], and the metabolism of 6:2 fluorotelomer sulfonamide alkylbetaine (FTAB) in blue mussels and turbot[10].

In an investigation of 10 fluorinated AFFFs used in Ontario, Canada, 6:2 FTAB was detected in four of the AFFFs and appeared to be the second most commonly utilized fluorotelomer AFFF component after 6:2 FTSAS[8]. 6:2 FTAB was always detected concomitantly with its synthetic intermediate 6:2 fluorotelomer sulfonamide alkylamine (FTAA)[8,12], which was measured in significant quantities ranging from 8-46% of the 6:2 FTAB in National Foams AFFFs[4,6]. Biodegradation of a number of fluorotelomer PFASs, including 8:2 FTOH[13], 6:2 FTOH[14,15], polyfluoroalkyl phosphate esters[16,17], 6:2 FTSA[18,19], and FTSASs[5,9] has been shown to yield PFCAs in mixed microbial cultures[13,14], soil[9,14,15], WWTP sludge[5,17–19], and rats[16]. Metabolism of 6:2 FTAB in blue mussels and turbot has only been investigated using the commercial product, Forafac 1157, and no production of PFCAs was observed above impurities present in the starting material[10]. In this study, the biodegradation of 6:2 FTAB and 6:2 FTAA were investigated in aerobic WWTP sludge. By synthesizing 6:2 FTAA and 6:2 FTAB in house, individual congeners were obtained for the biodegradation study with sufficient purity to detect PFCA production. The reported 6:2 FTAB degradation product, 6:2 fluorotelomer sulfonamide (6:2 FTSAm)[10], was also synthesized in order to quantify its formation during the study. By performing untargeted quadrupole time-of-flight mass spectrometry (qTOF-MS) analysis of extracts generated during the biodegradation study, further insight into the degradation products of 6:2 FTAB and 6:2 FTAA was obtained.

3.3 Materials and Methods

3.3.1 Materials and Synthesis

The chemicals, standards, and solvents utilized are listed in the Supporting Information (SI). Synthesis of 6:2 fluorotelomer sulfonyl chloride ($FTSO_2Cl$) was performed by sequentially adding 1 mmol of 6:2 fluorotelomer thiol (FTSH), 2.5 mmol of KNO_3, and 2.5 mmol of SO_2Cl_2 to 10 mL of dry acetonitrile under nitrogen in an ice-water bath[20]. The reaction mixture was allowed to stir for 3 hours, quenched with 12 ml of saturated $NaHCO_3$ in water, liquid-liquid extracted into methyl *tert*-butyl ether (MTBE), and dried with brine (saturated NaCl) and $MgSO_4$. The solvent was rotary evaporated under vacuum and 6:2 $FTSO_2Cl$ was used immediately in synthesis of 6:2 FTAA or 6:2 FTSAm.

To prepare 6:2 FTAA, 2.2 mmol of *N*,*N*-dimethylamino-1-propylamine was added to 2 mL of MTBE stirring on ice under N_2. A batch of 6:2 $FTSO_2Cl$ dissolved in approximately 7 mL of MTBE was added to the reaction mixture and stirred overnight while warming to room temperature. 6:2 FTAA was isolated by liquid-liquid extraction with MTBE and brine, then dried with brine and $MgSO_4$. MTBE was evaporated under vacuum initially and then under a gentle stream of nitrogen yielding 6:2 FTAA as a light yellow solid in 48% yield. The 6:2 FTAA used for the study had less than 2% impurity signals in ^{1}H NMR, no impurities detectable by ^{19}F NMR and contained less than 0.1 part per thousand (by weight) of PFCAs and less than 2 parts per thousand of 6:2 FTSA by LC-MS/MS.

Refluxing 0.4 mmol of 6:2 FTAA and 0.5 mmol of sodium chloroacetate in 2 mL of 80:20 ethanol: water for 24 hours yielded 6:2 FTAB. Crude 6:2 FTAB was obtained by evaporating the solvent under nitrogen followed by lyophilization. NaCl was removed by dissolving the crude 6:2 FTAB in 2-propanol with isolation of the supernatant by centrifugation. 2-propanol was then evaporated under N_2 and the 6:2 FTAB purified by repeated precipitation in MTBE with the precipitate isolated by centrifugation as described in Appendix B resulting in a 49% yield of 6:2 FTAB. The 6:2 FTAB used for the study had less than 2% impurity signals in ^{1}H-NMR, no impurities detectable by

fluorine NMR, and less than 0.5 parts per thousand each of 6:2 FTSA and PFCAs by LC-MS/MS.

Synthesis and isolation of 6:2 FTSAm was similar to 6:2 FTAA except that 10 mmol of NH_3 in tetrahydrofuran were used instead of *N*,*N*-dimethylamino-1-propylamine. The 6:2 FTSAm obtained in 60% yield contained less than 1% 6:2 FTSA by LC-MS/MS and less than 2 mol % of impurities by ^{1}H-NMR. . The 6:2 fluorotelomer unsaturated carboxylic acid (FTUCA) used for spiking positive controls was surplus from a previous study for which it was synthesized according to published methods[21]. Characterization data for synthesized 6:2 FTAB, 6:2 FTAA, and 6:2 FTSAm is provided in Appendix B.

The ^{19}F-NMR spectra of all the synthesized fluorotelomer sulfonamide PFASs have six signals representing six perfluoroalkyl carbons with no branched-chain -CF- signals, which is consistent with a single linear isomer of the perfluoroalkyl chain. No rearrangement of the perfluoroalkyl chain forming branches was expected during biodegradation.

3.3.2 WWTP Sludge Biodegradation Study

Mixed liquor was obtained from Ashbridges Bay Wastewater Treatment Plant in Toronto, Ontario, Canada and was kept aerated at room temperature prior to use for up to 21 d. The purge-and-trap setup using polypropylene bottles (Nalgene, Thermo Scientific, Rochester, NY, USA) with custom rubber septa fitted with 150 mg ORBO 605 Amberlight XAD-2 cartridges (Supelco, Bellefonte, PA, USA) and 20 gauge needles for air bubbling was similar to that described in previous studies[5,17]. The study included sixteen bottles each containing a total volume of 400 mL of mineral medium, which were divided into active experiments, sterile controls, surfactant only controls, mixed liquor blanks, and positive controls. Medium, biodegradation bottles, and mixed liquor for sterile controls were all autoclaved at 121°C for 30 minutes in a Steris SG-120 Scientific Gravity Sterilizer (Mentor, OH, USA), while vitamin and minerals solutions were sterilized by 0.2 μm syringe filtering. The active experiments (n = 3 each) contained 40 mL of washed mixed liquor and 600 μg of 6:2 FTAA or 6:2 FTAB from an ethanolic

spiking solution in 400 mL sulfate-free mineral medium. Sterile controls (n = 2 each) contained 40 mL of washed, autoclaved mixed liquor with 0.75 mg/mL of $HgCl_2$ and 0.75 mg/mL of NaN_3 as biocides as described in an earlier study[5] and 600 μg of 6:2 FTAA or 6:2 FTAB in 400 mL sulfate-free mineral medium. Surfactant only controls (n = 2) were spiked with 600 μg each of 6:2 FTAA and 6:2 FTAB in 400 mL sulfate-free mineral medium. Positive controls (n = 2) were identical to active experiments except they were spiked with 600 μg of 6:2 FTUCA initially and 400 μg of 6:2 FTUCA after 45 days to confirm the viability of the mixed liquor. All bottles were purged with air continuously for 109 days and were sampled 15 times over the course of the study. Further details on the biodegradation setup are in Appendix B.

The medium had a pH of 6.9, so 6:2 FTAA is expected to be protonated and have a single positive charge as protonated tertiary amines tend to have high pKas around 10[22], while 6:2 FTAB is expected to be zwitterionic with a positive charge on the ammonium and a negative charge on the carboxylate, since carboxylic acids adjacent to quaternary ammoniums have very low pKas around 2[23].

3.3.3 Extraction and analysis of aqueous phase

Aqueous phase samples (1 mL) were extracted by mixed mode weak anion exchange solid phase extraction (WAX-SPE) using Oasis WAX cartridges (6 cc, 200 mg, 30 μm) from Waters (Milford, MA). The cartridges were conditioned with 2 mL of 0.1% NH_4OH in methanol, 2 mL of methanol, and 2 mL of deionized water. Samples were acidified with 50 μL of 1.05% aqueous formic acid, loaded on the cartridges, and washed with 2 mL of 25 mM pH 5 ammonium acetate buffer. The cartridges were then dried on a vacuum manifold and eluted with a series of 4 mL and 1 mL of methanol for a fraction containing 6:2 FTAA and 6:2 FTAB and 4 mL of 0.1% NH_4OH in methanol for a fraction containing acidic degradation products. The fractions were evaporated to 2 mL each under a gentle stream of nitrogen. Aqueous phase extracts were analyzed by LC-MS/MS with a Waters Acquity UPLC-Sciex API 4000 system and a Kinetex XB-C18 column (4.6 x 50 mm, 2.6 μm, Phenomenex, Torrance, CA) using methods described in detail in Appendix B.

3.3.4 Extraction and analysis of XAD cartridges

XAD cartridges were extracted with 2 × 2 mL of ethyl acetate with 1 hour of sonication and analyzed by GC-MS for 6:2 FTOH as described in Appendix B with additional dilution and analysis of the XAD extracts for 6:2 FTSAm, 6:2 FTAA, and 6:2 FTAB by LC-MS/MS using methods described in Appendix B to determine losses due to spray formed by the purge setup.

3.3.5 Extraction and analysis of WWTP solids

After 109 days, the organic solids in each of the active experiment, sterile control, and mixed liquor blank bottles were isolated by centrifugation, frozen, and lyophilized. The mass of solids from each bottle was weighed and a 50 to 85 mg subsample of solids from each bottle was extracted with 3 × 2.5 mL of 0.1% NH_4OH in methanol[4], evaporated to 2 mL under nitrogen, cleaned up with Supelclean ENVI-Carb cartridges (1 mL, 100mg, Supelco, Bellefonte, PA), and evaporated to 4 mL. The solids extracts were analyzed by LC-MS/MS and further details of the extraction procedure are in Appendix B.

3.3.6 qTOF-MS Analysis

Direct injection on an AB/Sciex QStar XL qTOF-MS (Sciex, Concord, ON, Canada) in both positive ion mode (ESI+) and negative ion mode electrospray (ESI-) was used to examine a selection of XAD and organic solids extracts in order to tentatively identify additional degradation products formed from 6:2 FTAB and 6:2 FTAA. Mass spectra were collected between *m/z* 90 and 1000. External calibration of the mass spectrometer was performed using 10-times diluted Agilent Tune Mix for Ion Traps (Agilent Technologies, Wilmington, DE) in ESI+ and a mixture of PFCAs and fluorotelomer phosphate diesters (diPAPs) described previously in ESI-[8]. Plotting the mass spectra as mass defect plots on a CF_2 scale as described by Myers *et al.*[24], with the exception that nominal masses were determined by standard rounding rather than automatically rounding down, assisted in the identification of PFAS ions of interest based on their mass defects. Further details of the qTOF-MS settings and analysis of qTOF-MS data are provided in Appendix B.

3.3.7 Total organofluorine combustion ion chromatography (TOF-CIC)

All solids extracts and XAD extracts from the 21 days sampling point were analyzed by total organofluorine combustion ion chromatography (TOF-CIC) according to published methods[5,8,25] in order to gain insight into the proportion of organofluorine-containing degradation products covered by targeted, quantitative analyses. This method involves combusting sample extracts on a ceramic boat in an oven at 900 to 1000°C so organofluorine is mineralized as HF, absorbing the combustion products into aqueous solution with the HF dissolving as fluoride ions, determining the fluoride concentration by ion chromatography. Further details of the TOF-CIC method are included in Appendix B.

3.3.8 Quality Assurance of Data

The levels of 6:2 FTUCA, 6:2 fluorotelomer carboxylic acid (FTCA), 6:2 FTSA, perfluorobutanoate (PFBA), perfluoropentanoate (PFPeA), perfluorohexanoate (PFHxA), and perfluoroheptanoate (PFHpA) were quantified using mass labeled internal standards from Wellington Laboratories (Guelph, ON, Canada). Mass labeled standards were not available for 5:3 FTCA and 6:2 FTSAm, so mass labeled 6:2 FTUCA and perfluorooctane sulfonamide (FOSA), respectively, were used as surrogate internal standards. Quantification of 6:2 FTAB and 6:2 FTAA was done by matrix matched external calibration using aqueous phase, solids, or XAD extracts from mixed liquor blanks to prepare the calibration curves for extracts of the corresponding matrices. To assess the suitability of matrix matched external calibration, 6:2 FTAA and 6:2 FTAB were quantified from a spike and recovery in mineral medium treated with autoclaved, washed mixed liquor using both standard additions and matrix matched external standards. Matrix matched calibration was found to provide results within 2% of standard additions for 6:2 FTAA. Standard addition results were skewed 32% higher than expected for 6:2 FTAB, while matrix matched calibration provided an acceptable recovery (117 ± 3%). Results of the comparison between quantitation methods are in Table B2 in Appendix B.

Recoveries of FTCAs, 6:2 FTUCA, 6:2 FTSA, PFCAs, 6:2 FTAA, and 6:2 FTAB spiked at 10 ng/mL into mineral medium treated with autoclaved, washed mixed liquor were between 97 and 121% (n = 4, Table B3 in Appendix B). Recovery of 20 μg of 6:2 FTOH from a purge bottle containing autoclaved, washed mixed liquor in sulfate-free mineral medium that was purged for 24 hours was 79 ± 2% for the first XAD and rose to 90 ± 4% with a second XAD that was connected in series included (n = 3). A second XAD was used for all active experiment bottles throughout the study. Recoveries for 100 ng each of FTCAs, 6:2 FTUCA, 6:2 FTSA, and PFCAs and 1000 ng each of 6:2 FTAA and 6:2 FTAB spiked into blank, lyophilized mixed liquor solids were 75 to 115% (n = 3, Table B3 in Appendix B), while recoveries of these analytes and 1000 ng 6:2 FTSAm from autoclaved and washed wastewater treatment plant sludge that was subsequently lyophilized were 86 to 91% (n = 4, Table B3 in Appendix B).

. During the WAX-SPE extraction of aqueous samples for each time point, two solvent blanks of deionized water were also extracted to account for any contamination arising from the extraction process. For the XADs at each time point, three solvent blanks with no XAD resin were sonicated and transferred in the same manner as the extractions containing XAD resin to account for any contamination in the solvent or arising from solvent transfers. All analyses of extracts by LC-MS/MS or GC-MS were conducted in duplicate. The limits of detection (LODs) and limits of quantification (LOQs) for all analytes in the matrices that they were measured in are given in Table B4 in Appendix B. These are based on either the signal-to-noise (S/N) ratio with a S/N ratio of 3 for LOD and 10 for LOQ or on 3 times the mean blank signal for LOD and 10 times the mean blank signal for LOQ, where a signal was present in the procedural blanks. Methanolic aqueous phase extracts were sealed with parafilm and kept refrigerated at 4°C for a maximum of 7 weeks and otherwise were stored at -20°C, while all other extracts were stored at -20°C.

Duplicate analyses of four XAD extracts by TOF-CIC had relative standard deviations between 3.3 and 6.2% demonstrating the reproducibility of the method. Mixed liquor blank extracts were analyzed by TOF-CIC and were found to contain total organofluorine equivalent to between 0.005 and 0.15% of the 6:2 FTAB spiked into the

sterile controls and active experiments in the 21 day XAD extracts and between 0.12 and 0.44% of the organofluorine in the 6:2 FTAB spiked into the sterile controls and active experiments in the solids extract. For 6:2 FTAA, 6:2 FTAB, and 6:2 FTSAm standards, measurements by TOF-CIC determined between 94 and 106% of the expected organofluorine.

The positive control bottles demonstrated the viability of the microorganisms in the mixed liquor as the 6:2 FTUCA spikes were consumed with production of 5:3 FTCA (25 ± 16 mol % yield), PFHxA (1.4 ± 0.4 mol % yield), PFPeA (1.6 ± 1.3 mol % yield), and PFBA (0.34 ± 0.07 mol % yield).

Loss of material, including 6:2 FTAB and 6:2 FTAA, to the XAD cartridges in the purge set-up was an issue during the experiment. Once starting material was lost through purging, likely though its presence in spray droplets, it was unavailable to undergo further degradation. The extent and timing of these losses was variable between bottles and the cumulative losses of 6:2 FTAB and 6:2 FTAA to XADs in active experiments and sterile controls is plotted in Figures B1 and B2 in Appendix B. In summary, an average of 43 ± 8% of 6:2 FTAA and 29 ± 8% of 6:2 FTAB in active experiments and 1.2 ± 0.7% of 6:2 FTAA and 12 ± 1% of 6:2 FTAB in sterile controls was measured in the XAD extracts from throughout the course of the experiment. In one active experiment bottle with 6:2 FTAB, over 36% of the spiked 6:2 FTAB was detected in the XAD extracts over 31 days, while less than 4% of the spike remained as 6:2 FTAB in the aqueous phase (Figure B2a in Appendix B). This bottle lacked detectable production of aqueous phase degradation products throughout the study presumably due to large losses of 6:2 FTAB to the XAD early in the study with spray from vigorous bubbling (Figure B3 in Appendix B). It is therefore excluded from assessments of the products of 6:2 FTAB biodegradation. Additional starting material was also detected in the aqueous phase and solids extracts at the end of the experiment and for each bottle. Yields are given in the results as the mol % of the starting material that was not accounted for as intact material in the XADs cumulatively or in the aqueous phase or solids at the end of the experiment.

3.4 Results and Discussion

3.4.1 Production of PFCAs and PFCA-Precursors by Biodegradation

Previous studies have shown that FTOHs, FTCAs, and FTUCAs are precursors to persistent PFCAs and intermediates in the biodegradation of fluorotelomer compounds, such as 6:2 FTSA[18], FTSASs[5,9], and fluorotelomer phosphate esters (PAPs)[17]. Therefore, these compounds were monitored during the biodegradation study. The first of these products to evolve was 6:2 FTOH with greater production of 6:2 FTOH evident on the XADs of active experiments relative to sterile controls apparent after 21 days or less in the biodegradation of both 6:2 FTAA and 6:2 FTAB (Figure 3.1). Overall yields of 6:2 FTOH, as the sum of all 6:2 FTOH collected on XADs, were relatively low at 1.37 ± 0.12 mol % for 6:2 FTAA and 0.75 ± 0.18 mol % for 6:2 FTAB as a molar percentage of the starting materials not accounted for as intact starting material at the conclusion of the experiment. It should be noted that 6:2 FTOH evolution from the 6:2 FTAB bottle where no aqueous phase degradation product formation was detected was observed with 0.35 ± 0.03 mol % of the unaccounted for 6:2 FTAB converted to 6:2 FTOH over 31 days, indicating that active biodegradation was forming known PFCA precursors (Figure B3 in Appendix B).

With both 6:2 FTAA and 6:2 FTAB, a peak in the sum of aqueous 6:2 FTCA and 6:2 FTUCA concentrations was observed around 45 days in active experiments and subsequently decreased, which is consistent with their role as intermediates in biodegradation (Figure 3.1)[26,27]. The sum of 6:2 FTCA and 6:2 FTUCA is plotted since 6:2 FTCA spontaneously degrades to 6:2 FTUCA in methanol extracts over time[28]. In both active biodegradation experiments, 5:3 FTCA was a significant product observed and was produced in maximum yields of 4.01 ± 0.57 mol % with 6:2 FTAA and 0.76 ± 0.34 mol % with 6:2 FTAB. This is consistent with the result that 5:3 FTCA was the acidic product produced in the highest yields in biodegradation of 6:2 FTSAS in a similar WWTP mixed liquor and sulfate-free medium system[5]. Finally, production of PFCAs was observed in the aqueous phase with PFHxA and PFPeA production observed with both 6:2 FTAA and 6:2 FTAB in active experiments, while production of a low yield of PFBA (0.38 ± 0.04 mol %) that was between the LOD and LOQ was detectable

only with 6:2 FTAA. Yields of PFCAs were also higher with 6:2 FTAA at 0.95 ± 0.07 mol % for PFPeA and 0.76 ± 0.19 mol % for PFHxA than with 6:2 FTAB at 0.23 ± 0.14 mol% for PFPeA and 0.34 ± 0.12 mol% for PFHxA. Relatively low yields of PFCAs were also observed using sulfate-free medium in 6:2 FTSA biodegradation[19]. Production of PFHpA was not observed. This is the first confirmation that the FTOH to PFCAs biodegradation pathway can yield PFCAs from the fluorotelomer sulfonamide-based surfactants, 6:2 FTAB and 6:2 FTAA.

A number of additional intermediates that have been identified by other authors as part of biodegradation pathways forming PFCAs were not quantified due to a lack of standards, including fluorotelomer aldehydes, fluorotelomer ketones, and secondary FTOHs[13,18]. These PFASs may account for a portion of the missing 6:2 FTAA and 6:2 FTAB.

The production of 6:2 FTOH, 6:2 FTCA, 6:2 FTCA, 5:3 FTCA, and short chain PFCAs in the biodegradation of 6:2 FTAB and 6:2 FTAA contrasts with the known aerobic biodegradation pathway of *N*-ethyl perfluorooctane sulfonamido ethanol (EtFOSE) in which the carbon-sulfur bond remains[29]. This difference is as expected since the carbon-fluorine bonds on the carbon next to sulfur in EtFOSE would presumably strengthen the carbon-sulfur bond and inhibit oxidation as occurs with the fluorotelomer sulfonamides here to form 6:2 FTOH, where there are no carbon-fluorine bonds next to the sulfur.

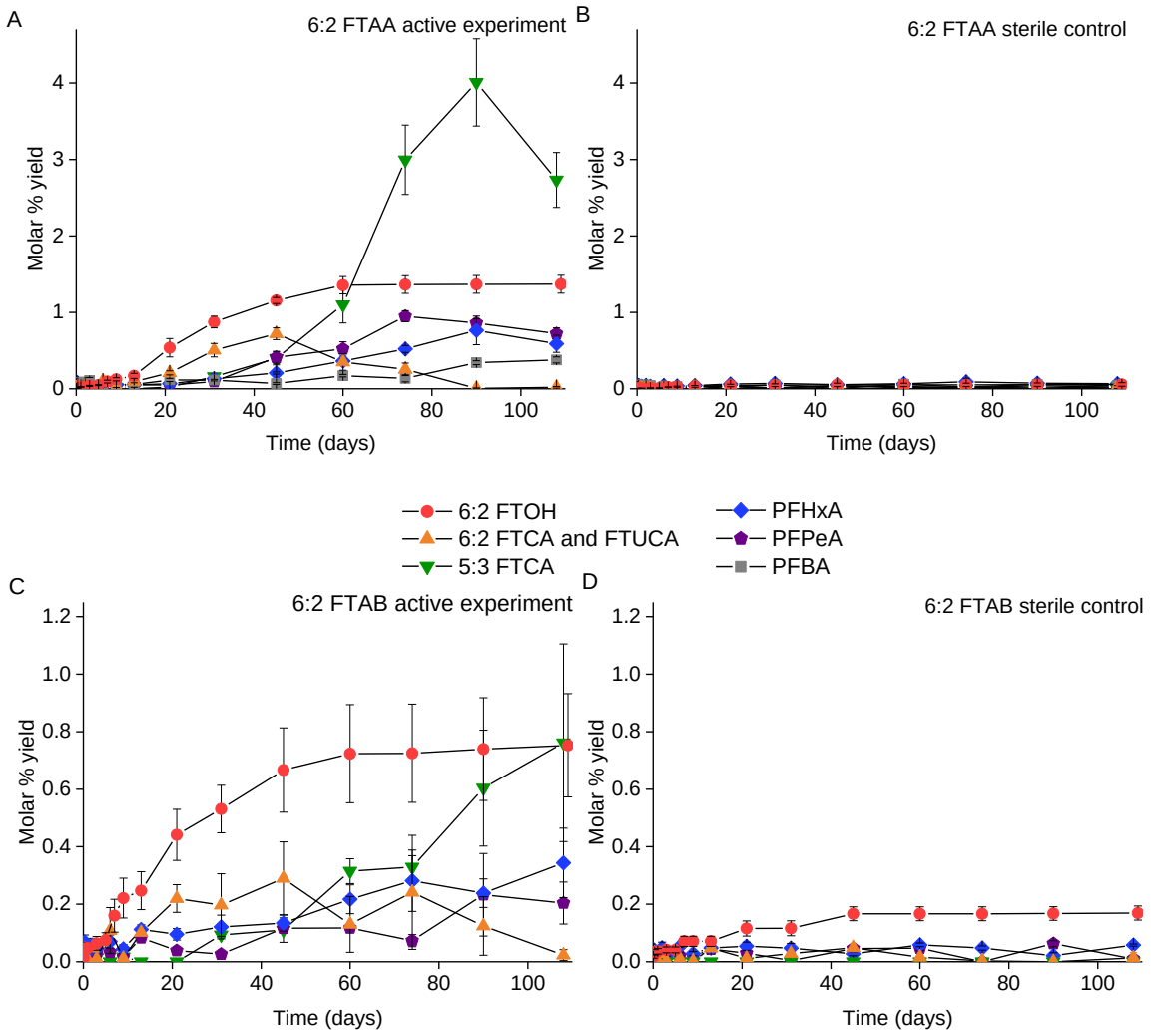

Figure 3.1: Time series of quantified products in the 6:2 FTOH to PFCAs degradation pathway for 6:2 FTAA a) active experiment (n = 3) and b) sterile control (n = 2), and 6:2 FTAB c) active experiment (n = 2) and d) sterile control (n = 2). 6:2 FTOH yield is the cumulative contents of all XADs over time analyzed by GC-MS, while other degradation product yields are the contents of the aqueous phase measured at each time point by LC-MS/MS. Error bars are standard errors.

3.4.2 6:2 FTSA

During the biodegradation study, an unexpected increase in aqueous 6:2 FTSA concentrations occurred in the sterile controls. Before the study, it was hypothesized that 6:2 FTSA might be a biodegradation product of 6:2 FTAA and 6:2 FTAB through an

enzymatic hydrolysis of the sulfonamide functional group since this would be akin to the formation of PFOS from EtFOSE and its degradation products[29]. FTSAs are also biodegradation products of FTSASs[5,9] and are a major component of documented PFAS contamination at AFFF-impacted sites[3,4,30]. Over the course of the study, there were no increasing trends in 6:2 FTSA concentrations for active experiments. This indicates that either 6:2 FTSA is not produced through biotic mechanisms from these PFASs, or relatively rapid biodegradation of 6:2 FTSA prevented its accumulation in the active experiments. The dramatic increase in 6:2 FTSA concentrations up to 4.9 ± 1.2 mol % of the missing 6:2 FTAA in the sterile controls was the initial indication that a degradation mechanism was active in the sterile controls (Figure 3.2A). This degradation mechanism was probably not biotic in nature because the sludge in the sterile controls appeared to be dead throughout the study since the sludge solids in the sterile controls did not stick to the experimental vessel or appear to grow as they did in the active experiments. Growth in the active experiment bottles was evident in the increased dry mass of the sludge solids at the end of the study in the active experiments (0.31 ± 0.05 g) compared to the sterile controls (0.14 ± 0.02 g).

3.4.3 6:2 FTSAm

The collection of full scan qTOF-MS spectra of selected solids and XAD extracts revealed a peak with high apparent abundance at *m/z* 426 in ESI- corresponding to the 6:2 FTSAm previously identified as a degradation product of 6:2 FTAB[10]. An authentic standard of 6:2 FTSAm was synthesized and used to quantify 6:2 FTSAm in XAD extracts, solids extracts, and aqueous extracts from the final time point. These analyses revealed that 6:2 FTSAm was a major product of the degradation of both 6:2 FTAA and 6:2 FTAB in both active experiments and sterile controls accounting for 6.9 ± 1.1 mol % of missing 6:2 FTAA and 0.9 ± 0.1 mol % of missing 6:2 FTAB in active experiments and 9.8 ± 1.1 mol % of missing 6:2 FTAA and 4.4 ± 0.9 mol % of missing 6:2 FTAB in sterile controls (Figure 3.2B). The presence of 6:2 FTSAm in the degradation pathway of 6:2 FTAB and 6:2 FTAA is similar to the degradation pathways of perfluorooctane sulfonamide-based substances, such as EtFOSE, which include FOSA[29].

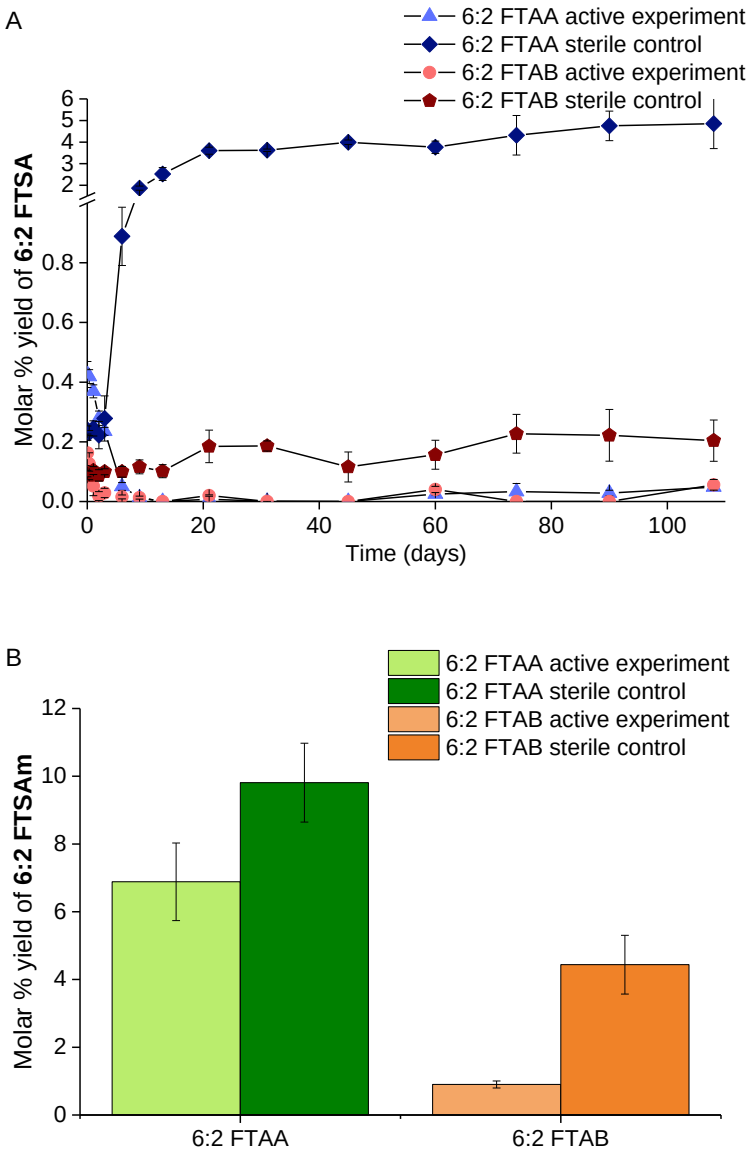

Figure 3.2: A. Molar percent yield of **6:2 FTSA** in aqueous phase over the course of the biodegradation study. B. Total molar percent yields of **6:2 FTSAm** during study as sum of XADs, aqueous phase at 108 days and biological solids at 109 days. Error bars are standard errors and n = 3 for 6:2 FTAA active experiment and n = 2 for all other data.

3.4.4 Abiotic Degradation of 6:2 FTAA and 6:2 FTAB

The overall product distributions of the degradation of 6:2 FTAA and 6:2 FTAB in active experiments and sterile controls are distinct from each other in that 6:2 FTSA formed in sterile controls, while 6:2 FTOH, 5:3 FTCA, and PFCAs formed over time in active experiments only (Figure 3.3). This difference in product distribution is further evidence that the degradation mechanism occurring in the sterile control bottles is distinct from the aerobic biodegradation in the active experiments. In performing qTOF-MS on selected solids and XAD extracts, the oxidative nature of the degradation mechanisms in both bottles is apparent since degradation product ions with additional oxygen atoms were observed for 6:2 FTAA (**1** and **4-6** in Figure 3.4, Table 3.1).

While the reaction mechanism leading to degradation in the sterile control is not known, the following possibilities may contribute to explaining the degradation observed. The degradation pathway in the sterile controls may involve activation of the molecular oxygen bubbled through the solutions by iron ions present in the mineral medium. The medium was prepared with 20 μM Fe(III), which could be reduced to Fe(II) through reactions with electron donors in the organic material[31] of the sterile sludge or perhaps through photoreduction, although the study took place indoors in translucent polypropylene bottles. Once Fe(II) formed, it could activate O_2 forming reactive oxygen species in the process of being oxidized itself in an Udenfriend-like process[32,33]. These reactive oxygen species could oxidatively degrade 6:2 FTAA or 6:2 FTAB. Non-enzymatic activation of O_2 by Fe(II) has been demonstrated to facilitate oxidative *N*-dealkylation reactions of the sort that could generate 6:2 FTSAm[34]. 6:2 FTSA may form through reaction of OH radicals with the sulfur center of the sulfonamide as was observed for gas phase *N*-methyl perfluorobutane sulfonamido ethanol[35].

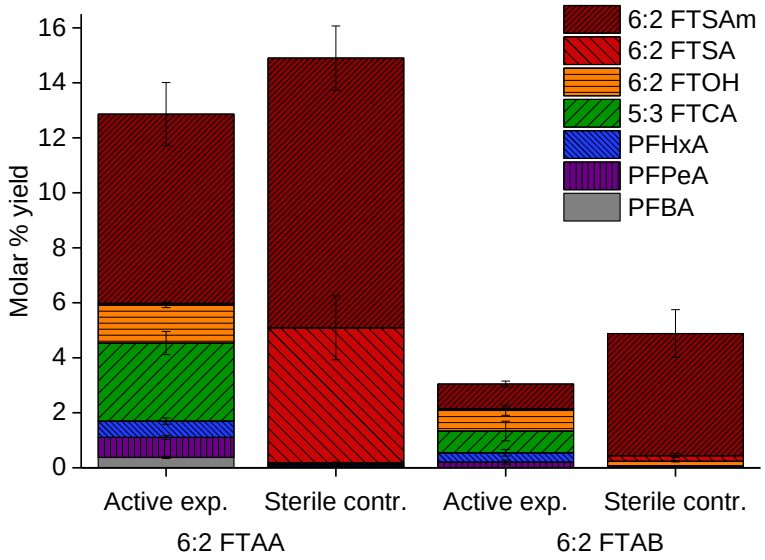

Figure 3.3: Overall product distributions from degradation of 6:2 FTAA (*n* = 3 for active experiments, *n* = 2 for sterile controls) and 6:2 FTAB (*n* = 2 for active experiments and sterile controls) as mol % yields using the sum of material in aqueous phase and solids at the end of the study and the cumulative total in XAD extracts. Error bars are standard errors. exp. = experiment; contr. = control

3.4.5 Additional Degradation Products for 6:2 FTAA

Selected XADs where high concentrations of 6:2 FTAA were measured were examined using qTOF-MS in an effort to tentatively identify additional fluorinated degradation products of 6:2 FTAA. This produced evidence of oxidative degradation of the *N*,*N*-dimethyl tertiary amine moiety in 6:2 FTAA. Proposed structures for these degradation products are labeled **1-6** in Figure 3.4A. These additional products result from oxidative *N*-dealkylations of the amine on any of the 3 α-carbons. As the tertiary amine has a lone pair of electrons in the non-protonated form, the dealkylation can proceed starting with a one electron oxidation of the nitrogen[36]. With 6:2 FTAA, single and double *N*-demethylation products **2** and **3** can be detected based on accurate mass by qTOF-MS in extracts from the active experiments and sterile controls (Table 3.1 and Figure B5a,c in Appendix B). The CID spectra of **2** and **3** in ESI+ are consistent with *N*-demethylations of 6:2 FTAA because they produce fragments of *m/z* 468 and 440

from loss of methylamine or ammonia followed by loss of ethene (Table B5 and Figure B7b,c in Appendix B), which are identical to the fragments produced by 6:2 FTAA[8]. **2** and **3** can also be detected by LC-MS/MS (Figure B8 in Appendix B). Overall, *N*-demethylation appears to be favored in sterile controls over active experiments with larger LC-MS/MS peaks for **2** and **3** in sterile control extracts (Table B6 in Appendix B).

The oxidative *N*-demethylation mechanism is further illuminated by the presence of an ion at *m/z* 529(+) and 527(-) in XADs from both sterile control and active experiment bottles that corresponds to hydroxylation of 6:2 FTAA (**1**, Table 3.1, Figure B5a,c,d in Appendix B). Since this ion produces fragments with *m/z* 468 and 440 in ESI+ (Table B5 and Figure B7a in Appendix B), identical to 6:2 FTAA, corresponding to loss of a hydroxylated secondary amine and ethene, it can be inferred that the hydroxylation occurs on an α-methyl group as would be intermediate in either enzymatic or non-enzymatic *N*-demethylation[34,36,37].

There is also evidence of *N*-dealkylation with loss of the amine moiety with *m/z* 498(-) ions corresponding to the resulting carboxylic acid oxidation product **6** detected in XADs from both active experiments and sterile controls (Table 3.1 and Figure B5b,d in Appendix B). The qTOF-MS CID spectrum of **6** is consistent with the proposed carboxylic acid with losses of HF consistent with a fluorotelomer structure, a neutral loss containing the sulfonamide and much of the head group, and an *m/z* 152(-) fragment containing the carboxylic acid and sulfonamide moieties resulting from neutral loss of 6:2 fluorotelomer olefin (Table B5 and Figure B7f in Appendix B). In addition, ions corresponding to the alcohol (**4**) and aldehyde (**5**) that would precede this acid in the oxidation pathway were detected occasionally, with the alcohol (**4)** detected in active experiments and the aldehyde (**5**) in sterile controls (Table 3.1 and Figure B5b,d in Appendix B). The qTOF-MS CID spectra of **4** and **5** include losses of HF and fragments at *m/z* 138(-) and *m/z* 136(-) corresponding to the neutral loss of 6:2 fluorotelomer olefin producing a fragment containing the alcohol or aldehyde and sulfonamide groups (Table B5 and Figure B7d,e in Appendix B). There were also neutral losses containing the aldehyde group of **5**, which was lost as C_2H_4O or C_3H_4O.

These degradation products cannot be seen by qTOF-MS in the 6:2 FTAA standards used for spiking, aside from **1** at less than 1% of the intensity of the parent compound in ESI+ (Figure B4a,b in Appendix B). In addition, only **1** and possibly **5** can be seen in XADs from the surfactant only controls containing large amounts of 6:2 FTAA. These results indicate the important role of sterile or active WWTP sludge in furthering the degradation of 6:2 FTAA forming degradation products **1**-**6** and that these are indeed degradation products and not impurities in the spike as the intensity observed for **1** greatly exceeds 1% of the intensity of the parent 6:2 FTAA in active experiment and sterile control XADs in ESI+ (Figure B5a,c in Appendix B).

Table 3.1: Accurate mass data from qTOF-MS used to assign molecular formulae to degradation products 1-6 of 6:2 FTAA

Degradation Product Number	Proposed Molecular Formula	ESI Mode	Observed *m/z*	Theoretical *m/z*	Error (*mDa*)	Extract Used
1	$C_{13}H_{18}F_{13}N_2O_3S^+$	ESI+	529.0821	529.0825	-0.4	Sterile Control XAD, *t*=21d
			529.0832		0.7	Active Experiment XAD, *t*=13d
	$C_{13}H_{16}F_{13}N_2O_3S^-$	ESI-	527.0687	527.0679	0.8	Sterile Control XAD, *t*=21d
			527.0724		4.5[a]	Active Experiment XAD, *t*=7d
2	$C_{12}H_{16}F_{13}N_2O_2S^+$	ESI+	499.0731	499.0719	1.2	Sterile Control Solids
			499.0722		0.3	Active Experiment XAD, *t*=74d
3	$C_{11}H_{14}F_{13}N_2O_2S^+$	ESI+	485.0605	485.0562	4.3[a]	Sterile Control Solids
			485.0571		0.9	Active Experiment XAD, *t*=74d
4	$C_{11}H_{11}F_{13}NO_3S^-$	ESI-	484.0247	484.0257	-1.0	Active Experiment XAD, *t*=21d
5	$C_{11}H_9F_{13}NO_3S^-$	ESI-	482.0111	482.0101	1.0	Sterile Control XAD, *t*=31d
6	$C_{11}H_9F_{13}NO_4S^-$	ESI-	498.0060	498.0050	1.0	Sterile Control XAD, *t*=21d
			498.0063		1.3	Active Experiment XAD, *t*=21d

a) low intensity and/or interference resulted in lower mass accuracy for these ions and samples.

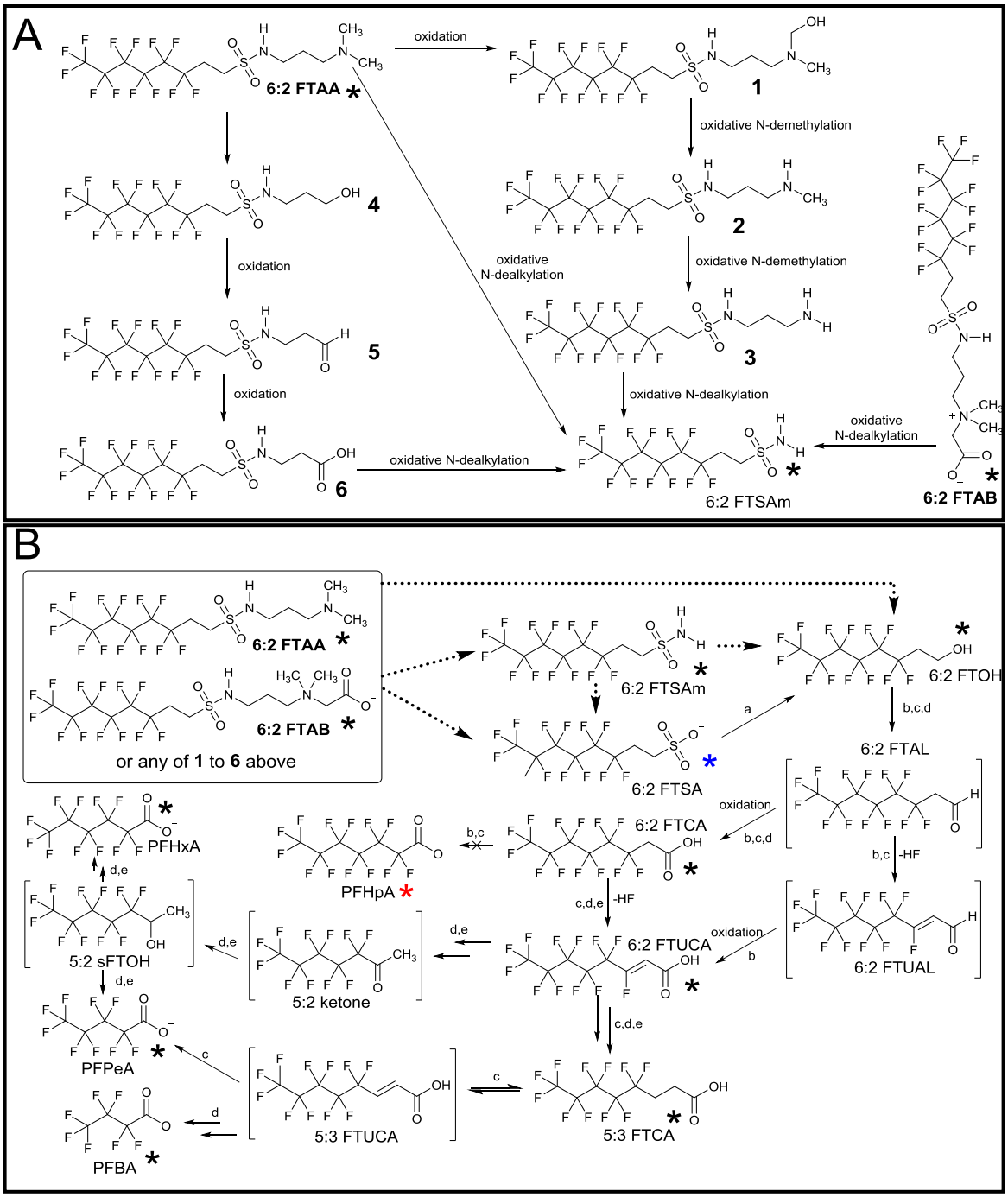

Figure 3.4: Proposed degradation pathways a) from 6:2 FTAB and 6:2 FTAA to 6:2 FTSAm and b) to PFCAs. Compounds labeled with * were quantified in this study. The blue * with 6:2 FTSA indicates that it accumulated only in sterile controls, while the red * with PFHpA indicates that production of this PFCA was not observed. Dashed arrows indicate possible pathways from 6:2 FTAA, 6:2 FTAB, or other sulfonamide-containing intermediates to 6:2 FTOH. Tentatively identified degradation products are labeled **1-6**

and corresponding qTOF-MS data and CID schemes are in Table B5 and Figure B5 and B7 in Appendix B. References for the pathways are: a) Marchington [19], b) Martin *et al.* [27], c) Butt *et al.*[26], d) Liu *et al.*[14], e) Wang *et al.*[18]

3.4.6 Additional Degradation Products for 6:2 FTAB

A previous study identified 6:2 FTAA and a number of metabolites resulting from *N*-dealkylation as metabolites of 6:2 FTAB in turbot and blue mussels[10]. In contrast to those results, only the starting material and 6:2 FTSAm could be identified in the qTOF-MS spectra of selected XAD extracts from 6:2 FTAB active experiments and sterile controls (Figure B4c,d in Appendix B). 6:2 FTAA was detected in some aqueous phase extracts but was not detected at or above its lowest calibration concentration, which places an upper bound on the production of 6:2 FTAA of approximately 0.15 mol % of the 6:2 FTAB spike. It does appear however, that there is a small enhancement in 6:2 FTAA concentrations in active experiment bottles relative to sterile controls from day 2 to day 31. Thus, it appears that formation of 6:2 FTAA may be a minor pathway in 6:2 FTAB biodegradation.

That 6:2 FTSAm is the only major product of 6:2 FTAB biodegradation with the sulfonamide group intact is consistent with the mechanism of cytochrome P-450 *N*-dealkylation. Since oxidation of amines typically occurs through electron transfer forming aminium radicals that favor deprotonation and oxidative *N*-dealkylation[36,37], 6:2 FTAB would not be expected to readily undergo *N*-dealkylation at the quaternary ammonium due to the lack of a lone pair of electrons. In addition, a cytochrome-P450 alkane hydroxylation mechanism that begins with homolytic H-abstraction from an alkyl carbon[36] would not be favorable around the quaternary ammonium due to the electron withdrawing effect of a permanent positive charge, which would be expected to deactivate the α-carbons toward H-abstraction. In contrast, the sulfonamide group has a lone pair of electrons and is somewhat removed from the positive charge and so could undergo *N*-dealkylation beginning with a one electron oxidation of the nitrogen lone pair to produce 6:2 FTSAm. The low probability of *N*-dealkylation at the quaternary ammonium would also apply to non-enzymatic oxidative *N*-dealkylation mechanisms

since loss of electrons from the cationic quaternary ammonium would be generally disfavored.

3.4.7 Overall Product Yields and Distribution

In the biodegradation study, more of the disappearance of 6:2 FTAA was accounted for by quantifiable degradation products (approximately 12 to 16 mol %) than for 6:2 FTAB (approximately 3 to 6 mol %, Figure 3.3). With the exception of the 6:2 FTAB active experiments, 6:2 FTSAm was the most prevalent degradation product accounting for more than 50% of quantifiable degradation products in both active experiments and sterile controls with 6:2 FTAA and in sterile controls with 6:2 FTAB. 6:2 FTOH, 5:3 FTCA, and short chain PFCAs accounted for 5.9 ± 0.5 mol % of the missing 6:2 FTAA in active experiments and 2.1 ± 0.4 mol % of the missing 6:2 FTAB in active experiments.

At the end of the experiment for both active experiments and sterile controls, only 1–9% of the 6:2 FTAA spike that was not accounted for by measurements of 6:2 FTAA in the XAD extracts was present in the aqueous phase or solids, whereas excluding the bottle with unusual losses, 33–74% of the 6:2 FTAB that was not accounted for in analysis of the XAD extracts remained in the aqueous phase or solids. This suggests that degradation of the 6:2 FTAA occurred faster and was more complete over 109 days than degradation of 6:2 FTAB, but due to losses the experiment does not enable a quantitative assessment of the differences in degradation rate. The higher concentrations of quantified degradation products and the detection of more tentatively identified degradation products in the bottles with 6:2 FTAA is consistent with faster biodegradation of 6:2 FTAA.

Overall mass recovery of the spiked starting materials, including that recovered as intact starting material on XADs or in the aqueous phase or solids at the conclusion of the experiment was 68 ± 13% for the active experiments with 6:2 FTAB used in determining product distributions, 57 ± 10% for sterile controls with 6:2 FTAB, 53 ± 6% for active experiments with 6:2 FTAA, and 17 ± 4% for sterile controls with 6:2 FTAA. However, this recovered mass was 96–99% intact 6:2 FTAB with 6:2 FTAB, 84–91% intact 6:2

FTAA in active experiments with 6:2 FTAA, and 13–15% intact 6:2 FTAA in sterile conctrols with 6:2 FTAA.

The loss of 6:2 FTAB to XADs is likely to be underestimated due to the hydrophobic nature of the styrene-divinylbenzene XAD resin and the hydrophilic nature of the amphoteric betaine group. The high breakthrough of 6:2 FTAB to the second XAD on active experiment bottles is evidence of the relatively poor trapping of 6:2 FTAB. With 6:2 FTAB, a median of 31% of the contents of the first XAD were found on the second XAD where the first XAD contained at least 0.5% of the spike (range: not detected–198%), while 6:2 FTAA had a median breakthrough of 0.07% of the first XAD (range: not detected–7.7%). Incomplete recovery of 6:2 FTAB lost to XADs may be an important factor in the low yield of 6:2 FTAB degradation products in the experiment as the missing 6:2 FTAB may be underestimated.

The relatively low mass balance in accounting for the disappearance of 6:2 FTAB and 6:2 FTAA likely arises from a number of additional factors. Non-quantifiable degradation products were also lost to XADs, including the 6:2 FTAA degradation products **1-6,** which were detected in XAD extracts but not quantified due to a lack of standards. Particularly in the case of 6:2 FTAA, this could represent a substantial quantity of the lost dosing material, given the detection of degradation products in XAD extracts with a relatively insensitive qTOF-MS technique. This is supported by TOF-CIC results for the t = 21 days XADs, which showed that for the three active experiment or sterile control bottles where more than 1% of the 6:2 FTAA spiked was found in the XAD at this time point, between 1.5 and 4.3 % of the organofluorine in the spike was accounted for by unknown organofluorine in the XAD at this single sampling time (Figure B9a in Appendix B). Losses of organofluorine on this order may have occured at numerous other sampling time points since loss of 6:2 FTAA to XADs exceeded 1% of the spike between 5 and 7 times for each active experiment bottle. This shows that a significant portion of the 6:2 FTAA spike was probably converted to non-quantifiable degradation products that were lost to the XAD cartridges. In contrast to the XAD extracts, the sludge solids extracts contained a relatively low proportion of the total spiked organofluorine as non-quantifiable compounds by TOF-CIC: 0.8 to 2% for active

experiments and sterile controls with 6:2 FTAA, 0.2 to 0.8% for active experiments with 6:2 FTAB, and no unknown organofluorine detected for sterile controls with 6:2 FTAB (Figure B9b in Appendix B).

Sorption of material to the bottles and septa could also account for a portion of the missing spike as it was not accounted for during the study. Preliminary testing determined that 12.3 ± 0.7% of a 600 μg 6:2 FTAA spike could be recovered by methanol extraction of the bottles and septa after 1 week of purging in aqueous buffer for a total recovery of 89 ± 4% of the 6:2 FTAA spike when including the aqueous phase and bottles and septa, so sorption would not be expected to account for the majority of the missing 6:2 FTAA. A 600 μg spike of 6:2 FTAB was fully recovered from the aqueous phase after one week of purging in preliminary testing (108 ± 2 %), so sorption to bottles was not likely to be significant for 6:2 FTAB in the biodegradation study.

Finally, 6:2 fluorotelomer unsaturated aldehyde (FTUAL), an α-β unsaturated carbonyl intermediate in the biodegradation of 6:2 FTOH, is known to bind to biological nucleophiles, including proteins, nucleophilic amino acids, and glutathione[25,38,39] forming adducts that were not analyzed using targeted LC-MS/MS methods. Covalent binding to protein in particular would put the organofluorine from degradation of 6:2 FTAA or 6:2 FTAB in a non-extractable form that would be insoluble in methanol. Thus, binding of the reactive intermediate 6:2 FTUAL to protein likely contributed to the incomplete mass balance in the biodgradation study.

3.5 Environmental Implications

The formation of 6:2 FTOH, 6:2 FTCA, 6:2 FTUCA, and PFCAs, especially PFHxA and PFPeA, in the active experiment bottles in the biodegradation study and the lack of formation of these degradation products in the sterile controls shows that 6:2 FTAA and 6:2 FTAB are PFCA precursors by microbial biodegradation. Ultimately, the fate of 6:2 FTAA and 6:2 FTAB by biodegradation is expected to be formation of PFCAs.

However, the biodegradation occurred relatively slowly during the biodegradation study as it took over a month to detect production of PFCAs in the aqueous phase. Therefore, 6:2 FTAA, 6:2 FTAB, or degradation products with an intact sulfonamide group are unlikely to be readily degraded to PFCAs in a WWTP and may persist for some time in the environment while exposed to aerobic microorganisms. In particular, 6:2 FTAB was still present in substantial quantities of at least 20% of the spike in the aqueous phase in two active experiment bottles at the end of the 109-day study. This suggests that 6:2 FTAB biodegrades quite slowly and may be relatively persistent under aerobic biodegradation conditions.

The most abundant of the quantifiable degradation products was 6:2 FTSAm, which may be thought of as a fluorotelomer analog of FOSA. Because of this structural similarity it may have similar physicochemical properties to FOSA and may be an environmentally important degradation intermediate for fluorotelomer sulfonamide-based PFASs, including 6:2 FTAB and 6:2 FTAA. FOSA is a neutral, hydrophobic, semi-volatile compound that is bioaccumulative and biomagnifies[40,41], and has been observed in the arctic atmosphere indicating that it likely undergoes atmospheric transport[42]. The disposition of 6:2 FTSAm in the environment has not been examined but could be of environmental concern if it is similar to FOSA. Research into the toxicology of FOSA has shown that it has toxic effects, such as activating peroxisome proliferator-activated receptor α[43] and uncoupling mitochondrial oxidative phosphorylation[44] in some systems. Little is known about the toxicology of 6:2 FTSAm, although one study found that it inhibits carbonic anhydrase with similar potency to FOSA[45]. The ultimate fate of 6:2 FTSAm is expected to be degradation to short chain PFCAs from C4 to C7.

Using samples from the biodegradation study, it was possible to tentatively identify six PFASs that are degradation products of 6:2 FTAA. The existence of multiple degradation products still bearing the fluorotelomer sulfonamide moiety suggests that if sites impacted by use of AFFF containing 6:2 FTAA are examined using targeted analytical methods for 6:2 FTAA and commonly targeted degradation products, such as PFCAs, FTCAs and FTUCAs, there is a strong possibility that the extent of

contamination with PFASs will be underestimated. The use of untargeted methods for assessing contamination with PFASs would be of particular utility in these instances. These methods could include TOF-CIC[5] and/or the oxidation of precursors assay[4]. Failure to consider PFAA precursors with untargeted analytical methods may lead to significant underestimation of the full potential for PFAA formation naturally over time and as a result of remediation efforts at AFFF impacted sites[30]. In one study of an AFFF-impacted site, approximately 40% of PFAA precursors in groundwater and 50% of PFAA precursors in aquifer solids and soils were quantified using LC-MS/MS analysis of known AFFF components, PFCAs, PFSAs, FTSAs, FOSA, and perfluorohexanesulfonamide [4]. Intermediate degradation products of AFFF components could account for a significant portion of the remaining unknown potential PFAA precursors.

3.6 Acknowledgements

We thank Anne L. Myers for providing 6:2 FTUCA synthesized previously. This work was supported by the Natural Sciences and Engineering Research Council of Canada through research grants to S.A.M. and a CGS-D postgraduate scholarship for L.A.D.

3.7 References

1. Moody CA, Martin JW, Kwan WC, Muir DCG, Mabury SA. 2002. Monitoring Perfluorinated Surfactants in Biota and Surface Water Samples Following an Accidental Release of Fire-Fighting Foam into Etobicoke Creek. *Environ. Sci. Technol.* 36:545–551.

2. de Solla SR, De Silva AO, Letcher RJ. 2012. Highly elevated levels of perfluorooctane sulfonate and other perfluorinated acids found in biota and surface water downstream of an international airport, Hamilton, Ontario, Canada. *Environ. Int.* 39:19–26.

3. Schultz MM, Barofsky DF, Field JA. 2004. Quantitative Determination of Fluorotelomer Sulfonates in Groundwater by LC MS/MS. *Environ. Sci. Technol.* 38:1828–1835.

4. Houtz EF, Higgins CP, Field JA, Sedlak DL. 2013. Persistence of Perfluoroalkyl Acid Precursors in AFFF-Impacted Groundwater and Soil. *Environ. Sci. Technol.* 47:8187–8195.

5. Weiner B, Yeung LWY, Marchington EB, D'Agostino LA, Mabury SA. 2013. Organic fluorine content in aqueous film forming foams (AFFFs) and biodegradation of the foam component 6 : 2 fluorotelomermercaptoalkylamido sulfonate (6 : 2 FTSAS). *Environ. Chem.* 10:486–493.

6. Backe WJ, Day TC, Field JA. 2013. Zwitterionic, Cationic, and Anionic Fluorinated Chemicals in Aqueous Film Forming Foam Formulations and Groundwater from U.S. Military Bases by Nonaqueous Large-Volume Injection HPLC-MS/MS. *Environ. Sci. Technol.* 47:5226–5234.

7. Place BJ, Field JA. 2012. Identification of Novel Fluorochemicals in Aqueous Film-Forming Foams Used by the US Military. *Environ. Sci. Technol.* 46:7120–7127.

8. D'Agostino LA, Mabury SA. 2014. Identification of Novel Fluorinated Surfactants in Aqueous Film Forming Foams and Commercial Surfactant Concentrates. *Environ. Sci. Technol.* 48:121–129.

9. Harding-Marjanovic KC, Houtz EF, Yi S, Field JA, Sedlak DL, Alvarez-Cohen L. 2015. Aerobic Biotransformation of Fluorotelomer Thioether Amido Sulfonate (Lodyne) in AFFF-Amended Microcosms. *Environ. Sci. Technol.* 49:7666–7674.

10. Moe MK, Huber S, Svenson J, Hagenaars A, Pabon M, Trümper M, Berger U, Knapen D, Herzke D. 2012. The structure of the fire fighting foam surfactant Forafac®1157 and its biological and photolytic transformation products. *Chemosphere*. 89:869–875.

11. Trouborst L, Mabury SA. Aqueous photolysis of 6:2 fluorotelomer sulfonamide alkylbetaine. *J Env Sci Prep*.

11. Hoffmann D, Stach H. 1973. Perfluoro-Alkyl-Alkylene-Sulfonamidoalkylene-Dialkylamines and Their Quaternary Ammonium Salts. U.S. 3,721,706

13. Dinglasan MJA, Ye Y, Edwards EA, Mabury SA. 2004. Fluorotelomer Alcohol Biodegradation Yields Poly- and Perfluorinated Acids. *Environ. Sci. Technol.* 38:2857–2864.

14. Liu J, Wang N, Szostek B, Buck RC, Panciroli PK, Folsom PW, Sulecki LM, Bellin CA. 2010. 6-2 Fluorotelomer alcohol aerobic biodegradation in soil and mixed bacterial culture. *Chemosphere*. 78:437–444.

15. Liu J, Wang N, Buck RC, Wolstenholme BW, Folsom PW, Sulecki LM, Bellin CA. 2010. Aerobic biodegradation of [14C] 6:2 fluorotelomer alcohol in a flow-through soil incubation system. *Chemosphere*. 80:716–723.

16. D'Eon JC, Mabury SA. 2007. Production of perfluorinated carboxylic acids (PFCAs) from the biotransformation of polyfluoroalkyl phosphate surfictants

(PAPS): Exploring routes of human contamination. *Environ. Sci. Technol.* 41:4799–4805.

17. Lee H, D'eon J, Mabury SA. 2010. Biodegradation of Polyfluoroalkyl Phosphates as a Source of Perfluorinated Acids to the Environment. *Environ. Sci. Technol.* 44:3305–3310.

18. Wang N, Liu J, Buck RC, Korzeniowski SH, Wolstenholme BW, Folsom PW, Sulecki LM. 2011. 6:2 Fluorotelomer sulfonate aerobic biotransformation in activated sludge of waste water treatment plants. *Chemosphere*. 82:853–858.

17. Marchington EB. 2008. Identification of Known and Novel Fluorinated Compounds in AFFF via 19F-NMR, LC-MS/MS, and LC-QUAD-TOFMS, and the Aerobic Biodegredation of 6:2 FTS. MSc Thesis. University of Toronto, Toronto, ON, Canada.

20. Park Y, Shin H, Kim Y. 1992. Convenient One-Pot Synthesis of Sulfonyl Chlorides from Thiols Using Sulfuryl Chloride and Metal Nitrate. *Chem. Lett.*:1483–1486. doi:10.1246/cl.1992.1483.

21. Achilefu S, Mansuy L, Selve C, Thiebaut S. 1995. Synthesis of 2H,2H-perfluoroalkyl and 2H-perfluoroalkenyl carboxylic acids and amides. *J. Fluor. Chem.* 70:19–26.

22. Perrin DD. 1972. *Dissociation constants of organic bases in aqueous solution*. Butterworths, London.

23. Weers JG, Rathman JF, Axe FU, Crichlow CA, Foland LD, Scheuing DR, Wiersema RJ, Zielske AG. 1991. Effect of the intramolecular charge separation distance on the solution properties of betaines and sulfobetaines. *Langmuir*. 7:854–867.

24. Myers AL, Jobst KJ, Mabury SA, Reiner EJ. 2014. Using mass defect plots as a discovery tool to identify novel fluoropolymer thermal decomposition products. *J. Mass Spectrom.* 49:291–296.

25. Rand AA, Mabury SA. 2012. In Vitro Interactions of Biological Nucleophiles with Fluorotelomer Unsaturated Acids and Aldehydes: Fate and Consequences. *Environ. Sci. Technol.* 46:7398–7406.

26. Butt CM, Muir DCG, Mabury SA. 2010. Elucidating the Pathways of Poly- and Perfluorinated Acid Formation in Rainbow Trout. *Environ. Sci. Technol.* 44:4973–4980.

27. Martin JW, Mabury SA, O'Brien PJ. 2005. Metabolic products and pathways of fluorotelomer alcohols in isolated rat hepatocytes. *Chem. Biol. Interact.* 155:165–180.

28. Loewen M, Halldorson T, Wang F, Tomy G. 2005. Fluorotelomer Carboxylic Acids and PFOS in Rainwater from an Urban Center in Canada. *Environ. Sci. Technol.* 39:2944–2951.

29. Rhoads KR, Janssen EM-L, Luthy RG, Criddle CS. 2008. Aerobic Biotransformation and Fate of N-Ethyl Perfluorooctane Sulfonamidoethanol (N-EtFOSE) in Activated Sludge. *Environ. Sci. Technol.* 42:2873–2878.

30. McGuire ME, Schaefer C, Richards T, Backe WJ, Field JA, Houtz E, Sedlak DL, Guelfo JL, Wunsch A, Higgins CP. 2014. Evidence of Remediation-Induced Alteration of Subsurface Poly- and Perfluoroalkyl Substance Distribution at a Former Firefighter Training Area. *Environ. Sci. Technol.* 48:6644–6652.

31. Melton ED, Swanner ED, Behrens S, Schmidt C, Kappler A. 2014. The interplay of microbially mediated and abiotic reactions in the biogeochemical Fe cycle. *Nat. Rev. Microbiol.* 12:797–808.

32. Udenfriend S, Clark CT, Axelrod J, Brodie BB. 1954. Ascorbic Acid in Aromatic Hydroxylation I. a Model System for Aromatic Hydroxylation. *J. Biol. Chem.* 208:731–740.

33. Burns JM, Craig PS, Shaw TJ, Ferry JL. 2010. Multivariate Examination of Fe(II)/Fe(III) Cycling and Consequent Hydroxyl Radical Generation. *Environ. Sci. Technol.* 44:7226–7231.

34. Locke RK, Mayer VW. 1974. Physical evidence for the oxidative demethylation in vitro of 1-naphthyl N-methylcarbamate by the udenfriend chemical hydroxylation system. *Biochem. Pharmacol.* 23:1979–1984.

35. D'eon JC, Hurley MD, Wallington TJ, Mabury SA. 2006. Atmospheric Chemistry of N-methyl Perfluorobutane Sulfonamidoethanol, C4F9SO2N(CH3)CH2CH2OH: Kinetics and Mechanism of Reaction with OH. *Environ. Sci. Technol.* 40:1862–1868.

36. Guengerich FP, MacDonald TL. 1990. Mechanisms of cytochrome P-450 catalysis. *FASEB J.* 4:2453–2459.

37. Guengerich FP. 2013. Kinetic deuterium isotope effects in cytochrome P450 oxidation reactions. *J. Label. Compd. Radiopharm.* 56:428–431.

38. Rand AA, Mabury SA. 2012. Assessing the structure–activity relationships of fluorotelomer unsaturated acids and aldehydes with glutathione. *Cell Biol. Toxicol.* 28:115–124.

39. Rand AA, Mabury SA. 2013. Covalent Binding of Fluorotelomer Unsaturated Aldehydes (FTUALs) and Carboxylic Acids (FTUCAs) to Proteins. *Environ. Sci. Technol.* 47:1655–1663.

40. Kelly BC, Ikonomou MG, Blair JD, Surridge B, Hoover D, Grace R, Gobas FAPC. 2009. Perfluoroalkyl Contaminants in an Arctic Marine Food Web: Trophic Magnification and Wildlife Exposure. *Environ. Sci. Technol.* 43:4037–4043.

41. Tomy GT, Pleskach K, Ferguson SH, Hare J, Stern G, MacInnis G, Marvin CH, Loseto L. 2009. Trophodynamics of Some PFCs and BFRs in a Western Canadian Arctic Marine Food Web. *Environ. Sci. Technol.* 43:4076–4081.

42. Stock NL, Furdui VI, Muir DCG, Mabury SA. 2007. Perfluoroalkyl Contaminants in the Canadian Arctic: Evidence of Atmospheric Transport and Local Contamination. *Environ. Sci. Technol.* 41:3529–3536.

43. Shipley JM, Hurst CH, Tanaka SS, DeRoos FL, Butenhoff JL, Seacat AM, Waxman DJ. 2004. trans-Activation of PPARα and Induction of PPARα Target Genes by Perfluorooctane-Based Chemicals. *Toxicol. Sci.* 80:151–160.

44. Starkov AA, Wallace KB. 2002. Structural Determinants of Fluorochemical-Induced Mitochondrial Dysfunction. *Toxicol. Sci.* 66:244–252.

45. Benfodda Z, Guillen F, Romestand B, Dahmani A, Blancou H. 2010. Synthesis and investigation of inhibition effect of fluorinated sulfonamide derivatives on carbonic anhydrase. *Eur. J. Med. Chem.* 45:1225–1229

Chapter 4

Aqueous Film Forming Foam-related Perfluoroalkyl and Polyfluoroalkyl Substances in Canadian Surface Waters

Lisa A. D'Agostino and Scott A. Mabury

Contributions: Lisa D'Agostino optimized the extraction and LC-MS/MS methods, performed sample extractions and analysis, and planned and executed sorption tests. Lisa D'Agostino prepared this chapter with input from Scott Mabury.

To be submitted to *Environmental Science & Technology*

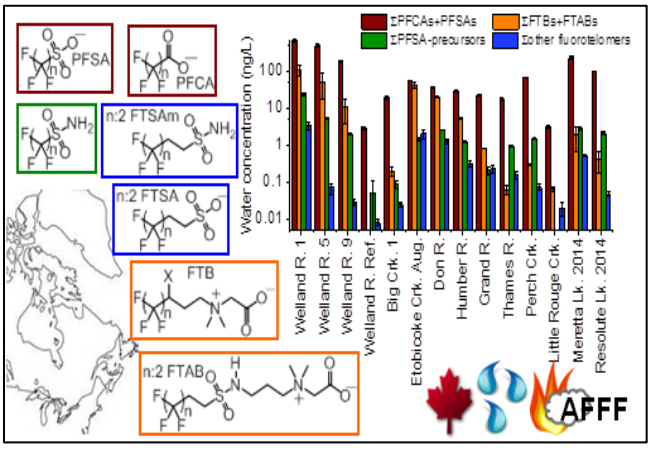

4 Aqueous Film Forming Foam-related Perfluoroalkyl and Polyfluoroalkyl Substances in Canadian Surface Waters

4.1 Abstract:

Few studies have investigated the presence of the dozens of perfluoroalkyl and polyfluoroalkyl substances (PFASs) recently identified in aqueous film forming foams (AFFFs) and as degradation products thereof in the environment, especially at sites without known AFFF-impacts. This exploratory survey of AFFF-related PFASs in surface waters from rural, urban, and AFFF-impacted sites in Canada revealed the presence of AFFF-related PFASs, including perfluorohexane sulfonamide (FHxSA), 6:2 fluorotelomer sulfonamide (FTSAm), fluorotelomer sulfonamide alkylbetaines (FTABs), fluorotelomer betaines (FTBs), 6:2 fluorotelomer mercaptoalkylamido sulfonate sulfone (FTSAS-SO_2), 6:2 fluorotelomerthiohydroxyl ammonium sulfoxide (FTSHA-SO), 6:2 fluorotelomer sulfonamide alkylamine (FTAA) and perfluoroalkane sulfonamido amphoterics. Detection of FHxSA in all urban and AFFF-impacted sites (0.04 to 18.5 ng/L) indicates the widespread presence of perfluorohexane sulfonate (PFHxS) precursors in Canadian waters. FTABs and FTBs were especially abundant with up to 15.5 to 33 ng/L of 6:2 FTAB in urban and AFFF-impacted water, while FTBs were only in AFFF-impacted sites (estimated maximum ΣFTBs 80 ng/L). Sediment samples from the AFFF-impacted Welland River indicated greater sorption of FTBs with longer perfluoroalkyl chains, while batch sorption experiments revealed enhanced sorption of basic 6:2 FTAA ($\log K_d$ = 1.43 ±0.01) compared to amphoteric 6:2 FTAB ($\log K_d$ = 0.634 ±0.008). By total organofluorine combustion ion chromatography (TOF-CIC), measured PFASs accounted for 0.3–64% of total organofluorine in these surface waters.

4.2 Introduction

Since 1999, AFFFs used to fight liquid-fuelled fires have been implicated in local environmental contamination with PFASs.[1] Most reports of PFASs at AFFF-impacted sites pertain to limited sets of PFASs, particularly perfluoroalkyl carboxylates (PFCAs),[1–11] perfluoroalkane sulfonates (PFSAs),[2–8,10–12] and/or fluorotelomer sulfonic acids

(FTSAs).[4,5,13] In early studies, AFFF was identified as an important local source of PFASs resulting in extreme concentrations of PFASs, such as up to 2,210,000 ng/L of perfluorooctane sulfonate (PFOS) in Etobicoke Creek immediately after an AFFF release from Toronto Pearson Airport in 2000,[3] up 920,000 ng/L of PFHxS and 14,600,000 ng/L of 6:2 FTSA in groundwater at Tyndall Air Force Base in Florida,[4] and up to 6,570,000 ng/L of perfluorooctanoate (PFOA) and in groundwater at Naval Air Station Fallon in Nevada.[1] Inputs of AFFF are also implicated in less extreme contamination of surface waters over longer time frames, including 290 ng/L of PFOS in Etobicoke Creek near the AFFF release site in 2009,[8] 45–64 ng/L of PFOS in Lake Niapenco downstream of Hamilton Airport in Ontario in 2010,[6] and 25 ng/L of PFHxS in Lake Bocksjön downstream of a military airport in Sweden.[11]

However, besides PFOS in AFFFs prepared from electrochemical fluorination products, these PFCAs, PFSAs, and FTSAs are not major fluorinated components in AFFFs.[14,15] More recently, over twenty additional classes of PFASs were identified in AFFFs and commercial fluorinated surfactant concentrates.[16,17] In degradation experiments with AFFF components, several degradation products have also been identified.[14,18–20] Reported detections and measurements of these recently identified AFFF components in the environment are limited. The 6:2 FTAA and 6:2 FTAB were detected in soil at a fire training area in Norway[19] and total concentrations of FTAAs and FTABs in river sediments in France were estimated at 0.055–13.5 ng/g.[21] Groundwater samples at three United States military bases were found to contain 6:2 fluorotelomer mercaptoalkylamido sulfonate (FTSAS) at concentrations up to 6900 ng/L, while 4:2 FTSAS was detected at one site at up to 490 ng/L.[22] The 6:2 FTSAS degradation product, 6:2 FTSAS-sulfone (6:2 FTSAS-SO_2), and FTSAS-related thioether and sulfone linked carboxylic acids have also been detected in AFFF-impacted groundwater from U.S. military bases.[23] Recently, a number of AFFF-related fluorotelomer PFASs have been reported in fish and sediment samples from the vicinity of a large oil fire, which was fought with AFFF in Lac Magentic, Quebec, Canada.[24] The fluorotelomer PFASs reported include FTSAs; 10:2 FTSAS, 10:2 FTSAS-sulfoxide (-SO), 8:2 and 10:2 fluorotelomer sulfonamides (FTSAms), 6:2 and 8:2 fluorotelomerthiohydroxyl ammonium sulfoxide (FTSHA) and FTSHA-SO; 6:2 through 12:2 FTAB, 6:2 through

10:2 FTAAs, demethyl 8:2 FTAA, and C7 through C13 fluorotelomer betaines (FTBs) at individual congener concentrations estimated at up to 20 ng/g in fish and 1.3 ng/g in sediment.[24]

On U. S. military bases with fire training areas, perfluorohexane sulfonamide alkylamine acid (FHxSAAA), perfluoropentane sulfonamide alkylamine acid (FPeSAAA), perfluorobutane sulfonamide alkylamine acid (FBSAAA), perfluorohexane sulfonamide alkylamine (FHxSAAm), perfluoropentane sulfonamide alkylamine (FPeSAAm), and perfluorobutane sulfonamide alkylamine (FBSAAm) were detected in some groundwater at concentrations up to 720 ng/L for the individual congeners.[22] In another study at a U. S. Air Force Base, FHxSAAm was detected in soil at up to 1600 ng/g and in aquifer solids at up to 14 ng/g.[15] At the same base, perfluorohexane sulfonamide (FHxSA), a likely degradation product of the perfluorohexane sulfonamido AFFF components, was detected in groundwater (up to 53,000 ng/L), soil (up to 1700 ng/g), and aquifer solids (up to 110 ng/g).[15]

Investigations of AFFF components in environmental samples have primarily targeted highly contaminated sites, especially U. S. military bases,[15,22,25] aside from the river sediments in France.[21] This study explores the presence of AFFF-related PFASs in surface water samples from a range of bodies of water in Canada, including urban rivers, rural sites, and AFFF-impacted sites in order determine how widespread these PFASs are in the environment. The AFFF-impacted sites investigated include the Welland River downstream of Hamilton Airport,[6,26] Etobicoke Creek downstream of Toronto Pearson Airport,[3,8] and Resolute and Meretta Lakes in Nunavut downstream of Resolute Bay Airport.[27,28] Sediments were also sampled from four sites along the Welland River and one reference site on Big Creek and analyzed for AFFF-related PFASs providing insight into sorptive AFFF components in this environment. Finally, batch sorption tests with 6:2 FTAB and 6:2 FTAA and an agricultural soil were performed as a preliminary investigation of the relative sorption of amphoteric versus basic PFASs.

4.3 Materials and Methods

4.3.1 Materials

6:2 FTAA, 6:2 FTAB, and 6:2 FTSAm were synthesized in house. As described in detail previously, 6:2 fluorotelomer sulfonyl chloride ($FTSO_2Cl$) was prepared by a one step synthesis from 6:2 fluorotelomer thiol, using KNO_3 and sulfuryl chloride. The 6:2 $FTSO_2Cl$ is then reacted with *N*,*N*-dimethylamino-1-propylamine to form 6:2 FTAA or with NH_3 in tetrahydrofuran to form 6:2 FTSAm. The 6:2 FTAA was used to prepare 6:2 FTAB by refluxing it with sodium chloroacetate.[20] A listing of the other solvents, chemicals, and standards used is provided in the Supporting Information (SI) in Appendix C.

4.3.2 Samples

Welland River 1-9 are sequential sites along the AFFF-impacted Welland River, while Big Creek 1–2 and Welland River Reference are rural sites not downstream of Hamilton Airport that were all sampled on October 22, 2015 with water collected in submerged 500 mL wide-mouth polypropylene bottles (Nalgene, Penfield, NY). Water samples from two AFFF-impacted arctic lakes, Resolute Lake and Meretta Lake, were collected in August 2012 and 2014 in 1 L polyethylene bottles (Kartell, Noviglio, Italy) by Environment and Climate Change Canada (ECCC) personnel. Rivers in Southern Ontario were sampled in conjunction with Ontario Ministry of the Environment and Climate Change (MOECC) sampling programs in 2015 with 500 mL polyethylene terephthalate jars used routinely for monitoring perfluoroalkyl acids (PFAAs). Of these rivers, Perch Creek, Thames River, Grand River, Humber River, and Don River are classified as urban and Etobicoke Creek has known AFFF-impacts. Additional rural samples were collected using 500 mL wide-mouth polypropylene bottles (Nalgene) from Little Rouge Creek in 2016 and Lake of Bays in 2015 some of which were used to for matrix spike and recovery. Samples were refrigerated at 4°C prior to extraction. Sampling dates and locations are in Figure C1 and Table C1 in Appendix C. Sediment samples were obtained in 500 mL wide-mouth polypropylene bottles (Nalgene) from four

Welland River sites and one Big Creek site. Sediments were frozen at -20°C and lyophilized prior to extraction.

4.3.3 Water Extraction

Water samples were extracted in the ALFONSE clean lab (UTSC) using Oasis WAX solid phase extraction (SPE) cartridges (6 cc, 200 mg, 30 μm; Waters, Milford, MA). The extraction protocol used to extract the approximately 500 mL water samples was a modification of existing methods[29] and is described fully in Appendix C. The cartridges were eluted with methanol for the neutral fraction followed by 0.1% NH_4OH in methanol for the acid fraction.

4.3.4 Sediment Extraction

Approximately 0.5 g subsamples of lyophilized sediment were weighed into polypropylene centrifuge tubes and extracted using a method with 0.1% NH_4OH in methanol based on Houtz *et al.*[15] with clean-up using 1mL/100mg Supelclean ENVI-Carb SPE cartridges (Supelco, Bellefonte, PA) in the ALFONSE clean lab. The extraction procedure is described in Appendix C.

4.3.5 Liquid chromatography-tandem mass spectrometry (LC-MS/MS)

Analysis of sample extracts for PFASs by LC-MS/MS was performed using an Acquity UPLC– Xevo TQ-S system (Waters, Milford, MA). A Waters Acquity UPLC BEH C18 column with 1.7 μm particles (2.1 mm x 75mm) and a mobile phase gradient of 10 mM ammonium acetate in deionized water and methanol were used. Further chromatography details are in Appendix C. The Xevo TQ-S was operated in positive and negative electrospray (ESI) mode with conditions described in Appendix C. Tandem mass spectrometry conditions for all PFASs analyzed are provided in Table C2 in Appendix C. Transitions for AFFF components were optimized by infusing dilutions of suitable AFFF extracts prepared previously[17] to determine suitable parameters. Screening LC-MS/MS runs were used to determine which PFASs may be present in sample extracts and included transitions for additional AFFF-components that were never detected.

4.3.6 Batch sorption tests for 6:2 FTAB and 6:2 FTAA

Batch sorption tests were performed with 6:2 FTAA and 6:2 FTAB in an agricultural soil. The tests were performed by shaking 9 g of air dried soil with 45 mL of 10 mM $CaCl_2$ in deionized water at 300 rpm overnight in a 50 mL polypropylene centrifuge tube (Falcon, Tewksbury, MA) and then spiking with up to 45 µL of 6:2 FTAA and 6:2 FTAB in methanol. The centrifuge tubes were then shaken at 300 rpm for 48 hours. To determine sorption kinetics and equilibration time, the aqueous phase of batch equilibration tubes spiked at 50 ng/mL were sampled 0.5, 4, 7, 24, 31, and 48 hours by centrifuging the tubes for 5 min at 4500 rpm and 30 min at 6000 rpm, collecting 90 µL of the aqueous phase, and diluting it 10-fold with methanol. For the sorption isotherm, additional batch equilibration tubes were spiked at 2 ng/mL, 10 ng/mL, 100 ng/mL, and 200 ng/mL with 6:2 FTAB and 6:2 FTAA and the aqueous phase was sampled by centrifuging the tubes as above with the aqueous phase diluted 3-fold with methanol for low concentrations and 10-fold for high concentrations. All sorption conditions were performed in triplicate with two soil blanks. Two soil-free tubes spiked with 6:2 FTAB and 6:2 FTAA were included in the kinetics experiment.

At the conclusion of the kinetics experiment, the aqueous phase was removed and the soil was sampled with one sample of approximately 0.7 g extracted using the same procedure as was used for sediments, except ENVICarb clean-up was not done and 2 mL extracts were diluted prior to analysis. A second subsample of at least 0.7 g was evaporated at 110°C until its mass stopped decreasing to determine the water content of the soil. Mass balances of 6:2 FTAB and 6:2 FTAA from the sorption kinetics experiment were 85 ±4% and 108 ±5%, respectively, therefore sorption coefficients for the sorption isotherms were calculated using aqueous phase concentrations.

4.3.7 TOF-CIC

Surface water extracts from each sampling location were analyzed by total organofluorine-combustion ion chromatography (TOF-CIC) using previously published procedures.[14,30] The acid extracts were also analyzed for inorganic fluoride by combining

100 μL of extract with 6.5 mL of deionized water and directly analyzing by ion chromatography using the TOF-CIC system.

4.3.8 Quality Assurance of Data

Analyses by LC-MS/MS were completed in at least duplicate (n =2–4). Quantification of PFASs was performed in several ways depending on the availability of standards. Perfluoropentanoate (PFPeA), perfluorohexanoate (PFHxA), perfluoroheptanoate (PFHpA), PFOA, PFHxS, PFOS, 4:2 FTSA, 6:2 FTSA, 8:2 FTSA, N-ethyl perfluorooctane sulfonamido acetic acid (EtFOSAA), and perfluorooctane sulfonamide (FOSA) were quantified using internal calibration with isotopically labeled standards. Perfluorobutane sulfonate (PFBS), perfluoropentane sulfonate (PFPeS), perfluoroheptane sulfonate (PFHpS), FHxSA, and 6:2 fluorotelomer sulfonamide (FTSAm) were quantified using structurally related surrogate mass-labeled internal standards: mass-labeled PFHxS for PFBS and PFPeS, mass-labeled PFOS for PFHpS, and mass-labeled FOSA for FHxSA and 6:2 FTSAm. For 6:2 FTAB and 6:2 FTAA, matrix matched calibration was used along with mass-labeled FOSA internal standard. Estimation of the concentrations of novel PFASs for which isolated standards were unavailable was performed by using calibration curves for 6:2 FTSA for sulfonic acid-containing compounds, EtFOSAA for carboxylic acid compounds, 6:2 FTAA for amine or quaternary ammonium compounds, and 6:2 FTAB for amphoteric compounds. To confirm the detection of AFFF components, two MS/MS transitions were used and retention times were matched to AFFF extracts containing those components from a previous study.[17]

The limit of detection (LOD) was defined as the concentration giving a signal-to-noise ratio of 3 in the sample matrix and the limit of quantitation (LOQ) was the concentration giving a signal-to-noise ratio of 10 in the sample matrix. The matrix LODs and LOQs are given in Table C4 in Appendix C. During each water extraction, two cartridge blanks were subjected to all portions of the extraction procedure except for sample loading to evaluate contamination of the extraction solvents and contained no PFASs above detection limits. Two field blanks from Welland River sampling were also

extracted and found to contain no PFASs above detection limits. For the sediment extraction, two solvent blanks containing no sediment were extracted along with the sediments and contained no PFASs above detection limits. Inter-day duplicate extractions were performed on Welland River 1, 2, 5, 6, 7, and 9; Welland River Reference; and Big Creek 1 water samples, while intra-day duplicate extractions were performed on all sediments and Little Rouge Creek water.

Recoveries for water extraction were determined by spiking approximately 500 mL surface water samples from relatively clean environments (n = 5, Little Rouge Creek and Lake of Bays) with 2.5 ng of FTSAs, EtFOSAA, FHxSA, FOSA, 6:2 FTSAm, 6:2 FTAA, and 6:2 FTAB and 25 ng of PFCAs and PFSAs in methanol, swirling to mix, and extracting the following day. The recoveries were between 71 and 96% for all PFASs and detailed results are shown in Table C3 in Appendix C. Recoveries from freeze dried sediment were determined by spiking approximately 0.5 g of sediment from Big Creek site 1 (n = 4) with 1 ng each of PFCAs, FTSAs, EtFOSAA, FOSA, FHxSA, 6:2 FTSAm, 6:2 FTAB, and 6:2 FTAA, and 5 ng each of PFSAs in 100 µL of methanol, vortexing to mix, and extracting the sediment the following day. Recoveries from sediment were 76 to 94 % for the PFASs, except for 6:2 FTAB, which had recoveries of 31 ±2%. Recoveries from sediment are shown in Table C3 in Appendix C and concentrations are reported without correction.

Table 4.1: Structures, names, and acronyms of PFASs detected in surface waters and/or sediments

Structure	Name	Acronym(s)
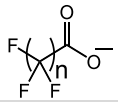	perfluoroalkyl carboxylate (PFCA)	PFPeA n = 4; PFHxA n = 5 PFHpA n = 6; PFOA n = 7
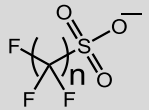	perfluoroalkane sulfonate (PFSA)	PFBS n = 4; PFPeS n = 5 PFHxS n =6; PFHpS n = 7 PFOS n =8
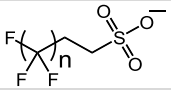	n:2 fluorotelomer sulfonic acid	n:2 FTSA (n = 4, 6, 8)
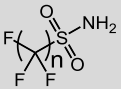	perfluoroalkane sulfonamide	FHxSA (n = 6) FOSA (n = 8)
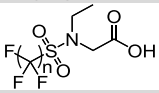	N-ethyl perfluorooctane sulfonamido acetic acid	EtFOSAA (n = 8)
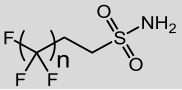	n:2 fluorotelomer sulfonamide	n:2 FTSAm (n = 6)
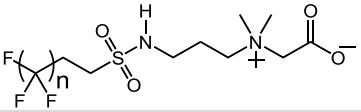	n:2 fluorotelomer sulfonamide alkylbetaine	n:2 FTAB (n = 4, 6, 8)
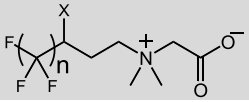	fluorotelomer betaine (FTB)	FTB CH_2 Cn (x = H) FTB CHF Cn (x = F) (n = 5, 7, 9)
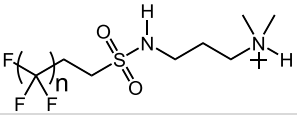	n:2 fluorotelomer sulfonamide alkylamine	n:2 FTAA (n = 6)
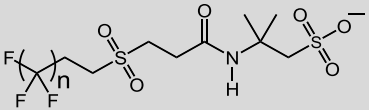	n:2 fluorotelomer mercaptoalkylamido sulfonate sulfone	n:2 FTSAS-SO2 (n = 6)
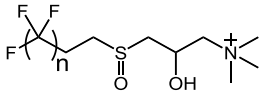	n:2 fluorotelomer thiohydroxylammonium sulfoxide	n:2 FTSHA-SO (n = 6)
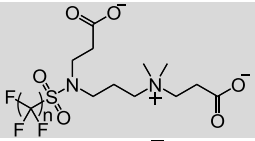	perfluoroalkane sulfonamide alkylamine diacid (FASADA)	FPrSADA (n = 3) FBSADA (n = 4) FPeSADA (n = 5) FHxSADA (n = 6)
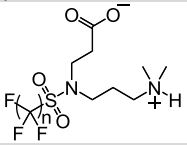	perfluoroalkane sulfonamide alkylamine acid (FASAAA)	FPrSAAA (n = 3) FBSAAA (n = 4) FPeSAAA (n = 5) FHxSAAA (n=6)
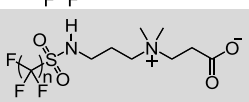	perfluoroalkane sulfonamide alkylbetaine (FASAB)	FPeSAB (n = 5) FHxSAB (n = 6)
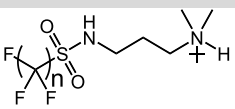	perfluoroalkane sulfonamide alkylamine (FASAAm)	FHxSAAm (n = 6)

4.4 Results and Discussion

4.4.1 PFAAs

Profiles of PFAAs in water samples were typically dominated by PFOS, PFPeA, PFHxA, and sometimes PFHxS (Figure 4.1A, Table C5 in Appendix C). Higher concentrations of PFPeA and PFHxA relative to PFHpA and PFOA suggest inputs from degradation of short chain fluorotelomers due to shifts in PFAS production, although greater sorption of longer chain PFCAs may be a factor.[31]

The PFHxS concentration is over half the PFOS concentration in most samples from Welland River and in samples from Resolute Lake, Meretta Lake, and Perch Creek. Since Welland River and Resolute and Meretta Lakes are known to have high PFOS concentrations due to AFFF impacts from airports,[6,27,28] the high concentrations of PFHxS may be due to degradation of perfluorohexane sulfonamido substances found in 3M AFFFs.[16,17,22] AFFF impacts to Perch Creek have not been reported, but Perch Creek runs alongside Sarnia Airport approximately 2.7 kilometers upstream from the sampling site and AFFF from the airport may be a source of PFOS and PFHxS.

Etobicoke Creek PFOS concentrations (10.5–16.7 ng/L) were 2 to 3 times lower than those reported for comparable locations in 2009 (32–41 ng/L) showing continuing attentuation of PFOS concentrations since an accidental AFFF spill in 2000.[8] Concentrations of PFOS (24–46 ng/L), PFHxS (13–30 ng/L), and PFOA (8–14 ng/L) found in Meretta and Resolute Lake samples from 2012 and 2014 were similar to measurements in 2005[27] and in 2010-11,[28] which likely indicates slow attenuation of PFAAs from the Arctic lakes and/or ongoing inputs to the lakes perhaps through runoff, since raw sewage inputs stopped in 1998.[32] Concentrations of PFOA and PFOS in Don River and PFOA in Humber River are 2–3-fold lower than 2007 measurements, while PFOS in Humber River decreased slightly (8.3 ng/L in 2007; 7.2 ±0.4 ng/L in 2015).[33] These decreases likely show effects of the PFOS phase-out [34] and reduced long-chain fluorotelomer use under the PFOA stewardship program.[35]

Compared to PFOS, PFBS, and PFCA concentrations reported for Welland River water sampled in 2010, water sampled in 2015 has lower concentrations of PFAAs

nearest Hamilton Airport and higher concentrations downstream.[6] For example, Welland River 1 had PFPeA conentrations of 270 ng/L in 2010[6] and 153 ±41 ng/L in 2015, while Welland River 5 had PFPeA concentrations of 2.4 ng/L in 2010[6] and 136 ±27 ng/L in 2015. This may be due to ongoing transport of PFSAs and PFCAs downstream of the airport and continuing degradation of PFAA precursors from AFFFs or perhaps differences in river flow between the two sampling times.

Among the rural sites without known AFFF-impacts, the Big Creek samples contained short-chain PFCAs and PFHxS at concentrations (4.8–6.6 ng/L of PFPeA, 0.45–1.26 ng/L of PFHxS) similar to urban sites without known AFFF-impacts (2.1–7.3 ng/L of PFPeA, 0.96–13.4 ng/L PFHxS), which suggests that the airport may be a source of PFASs to these sites to a lesser extent than to the Welland River. At the remaining rural sites, PFOA (0.30–0.65 ng/L) and PFOS (0.05–2.54 ng/L) were always detected, while PFPeA, PFHxA, PFHpA, PFBA, and PFPeA were detected in one or two rural samples each and were all below 1 ng/L.

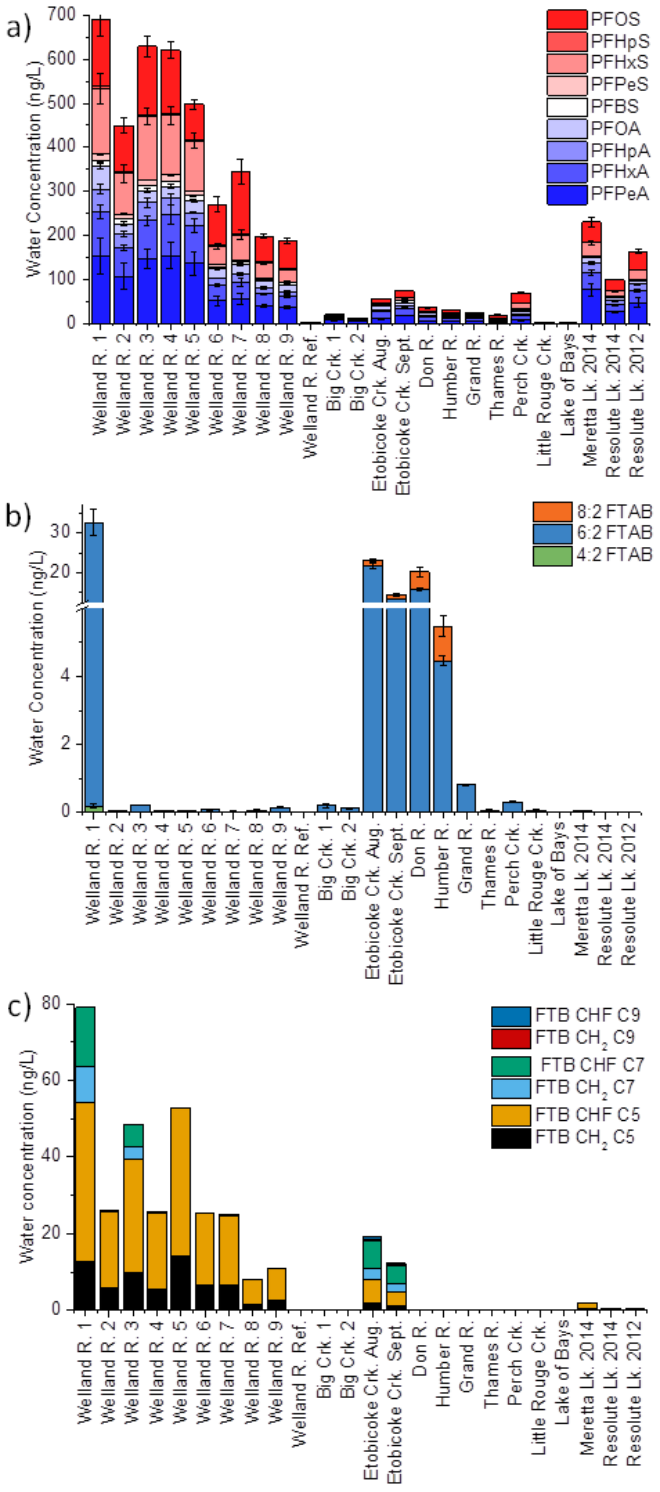

Figure 4.1: Concentrations of a) PFCAs and PFSAs, b) FTABs, and c) FTBs in surface water samples in ng/mL. Error bars are standard deviations and are excluded for clarity from the FTBs so patterns can be seen clearly despite uncertainty in estimated concentrations.

4.4.2 Fluorotelomer PFASs

Maximum concentrations of FTABs and FTBs were higher than for other fluorotelomer substances (Figure 4.1b/c; Table C7 in Appendix C). Previous environmental detections of FTABs are limited[19,21] and these are the first measurements of FTABs in surface waters. Welland River 1 had the highest 6:2 FTAB concentration (33 ±4 ng/L) but 6:2 FTAB concentrations rapidly decreased downstream to under 0.25 ng/L at sites 2–9 perhaps due to likely 6:2 FTAB photodegradation in sunlit waters, which was demonstrated in laboratory experiments.[36] Therefore, the relatively high concentrations of 6:2 FTAB (4.5–22 ng/L) and 8:2 FTAB (1.0–4.6 ng/L) in Etobicoke Creek, Don River, and Humber River are unexpected and suggest recent inputs of FTABs. Inputs may occur though runoff carrying FTABs stored in soils, wastewater treatment plant (WWTP) effluent, or AFFF use. Of these rivers, only Etobicoke Creek has known AFFF inputs from Toronto Pearson Airport, while North Toronto WWTP discharges into the Don River about 1.8 km upstream of the sampling site and Humber River receives urban and industrial runoff, sewer overflows, and effluent from a small WWTP over 32 km upstream. Since 6:2 FTAB was detected in all urban samples, either AFFF use is unanticipatedly widespread or additional applications of 6:2 FTAB lead to its presence in Ontario rivers through sources including WWTP effluent, combined sewer overflows, and septic fields. Possible additional applications of 6:2 FTAB include coating ceramics to prevent deposits as patented by DuPont[37] and are further suggested by Capstone FS-50, a "betaine partially fluorinated surfactant," marketed for applications including cleaning and floor care with identical properties to Capstone 1157 marketed for use in AFFFs, which is likely renamed Forafac 1157 containing mostly 6:2 FTAB.[19,38,39]

FTBs have only been reported in fish and sediments following an AFFF deployment previously[24] and were detected, in this study, in high estimated concentrations (ΣFTBs: 8–80 ng/L) in Welland River and Etobicoke Creek samples and lower concentrations (ΣFTBs: 0.3–2 ng/L) in Resolute and Meretta Lake samples (Figure 4.1c). These sites have known AFFF-impacts from upstream airports, which is probably the FTB source. An AFFF sample obtained from the Greater Toronto Airports Authority and dating from an AFFF deployment at an aircraft fire within meters of Etobicoke Creek

in 2005[13] contained FTBs.[17] This fire may be Etobicoke Creek's FTB source. FTB concentrations do not decrease nearly as rapidly as 6:2 FTAB concentrations downstream of Hamilton Airport, which suggests FTBs are less environmentally degradable than 6:2 FTAB perhaps due to the lack of an oxidizable sulfonamide nitrogen with a lone pair of electrons and the ability to absorb an actinic photon that may undergo direct or indirect photolysis or aerobic biodegradation.[20,36] Etobicoke Creek samples also have a greater proportion of C7 and C9 FTBs than Welland River samples, which may be due to AFFF formulation differences or greater sorption of longer chain congeners from Hamilton Airport.

Fluorotelomer PFASs other than betaines were detected at lower maximum concentrations (Figure C2a, Tables C6, C8 in Appendix C). Of these, 6:2 FTSA had the highest maximum concentration at 2.53 ±0.81 ng/L in Welland River 1 consistent with the association of 6:2 FTSA with AFFF-impacts.[4] However, 6:2 FTSA concentations in all other surface water samples were low (<0.45 ng/L) as were 4:2 and 8:2 FTSA concentrations (<0.13 ng/L). Concentrations of 6:2 FTSA were higher in Meretta Lake (0.42 ±0.01 ng/L) than Resolute Lake (0.05–0.12 ng/L), which is similar to measurements at these lakes in 2010-11.[28]

Detections of 6:2 FTAB degradation product 6:2 FTSAm (0.65–0.84 ng/L), [20] occured alongside substantial 6:2 FTAB concentrations. The amine-containing 6:2 FTAA (0.07–0.16 ng/L) and quaternary ammonium-containing 6:2 FTSHA-SO (estimated: 0.09–0.29 ng/L) were detected in some urban samples, which is the first environmental detection of 6:2 FTSHA-SO. The 6:2 FTSAS-SO_2 was observed in Don River, Humber River, Grand River, and Thames River samples with estimated concentrations (0.02–0.08 ng/L) below the LOQ, while Etobicoke Creek had estimated 6:2 FTSAS-SO_2 concentrations of 0.24–0.83 ng/L. This is the first detection of 6:2 FTSAS-SO_2 in surface water and its abundance in AFFF-impacted Etobicoke Creek is consistent with a dedgradation product of 6:2 FTSAS, an AFFF component.[4,18]

The only fluorotelomer PFASs detected in rural samples without known AFFF-impacts were 6:2 FTAB, which was detected in Big Creek (0.12–0.2 ng/L) and Little

Rouge Creek (0.07 ±0.01 ng/L), and 6:2 FTSA, which was detected in all samples except Lake of Bays at very low concentrations from 0.008 to 0.025 ng/L.

4.4.3 Perfluoroalkane sulfonamido substances in surface waters

Most PFASs in the Welland River had maximum concentrations nearest Hamilton Airport. However, FOSA and EtFOSAA had maximum concentrations at the sites furthest downstream (Figure 4.2a, Table C6 in Appendix C), which suggests the primary source of these perfluorooctane sulfonamido substances is not AFFF from Hamilton Airport. In contrast, FHxSA was found in maximum concentrations nearest Hamilton Airport, which suggests perfluorohexane sulfonamido precursors to FHxSA were used in AFFFs at the airport since perfluorohexane sulfonamido substances have been identified in AFFF concentrates[16,17,23] and FHxSA has been measured in AFFF-impacted groundwater, soil, and aquifer solids.[15,23,25]

In this first report of FHxSA in surface waters, detection of FHxSA occured outside areas with known AFFF-impacts as FHxSA was measured in all urban waters with concentrations ranging from 0.04 ±0.01 ng/L in Grand River to 0.94 ±0.04 ng/L in Perch Creek. At Meretta and Resolute Lakes, FHxSA concentrations were similar to downstream sections of the Welland River at 1.2–3.6 ng/L. Combined with substantial PFHxS concentrations, this suggests the lakes received inputs of AFFFs containing perfluorohexane sulfonamido substances.

Indeed, Welland River, Meretta Lake, and Resolute Lake samples also contained low concentrations of perfluoroalkane sulfonamido substances identified in AFFFs[16,17] with three to six perfluoroalkyl carbons (C3 to C6; Figure C2b, Tables C8-9 in Appendix C), but a broad suite of these C3 to C6 compounds was only detected in Welland River 1 (estimated Σ4.2 ng/L) with concentrations decreasing downstream. However, FHxSADA and FHxSAB could be detected in downstream samples at estimated concentrations under 0.65 ng/L in total. Resolute Lake and Meretta Lake samples had less than approximately 0.85 ng/L of these perfluoroalkane sulfonamido substances in total. The low concentrations of these PFASs are consistent with previous studies of AFFF-impacted groundwater that found only low concentrations of FHxSAAA and FBSAAA (<10 ng/L

each) in one highly contaminated groundwater sample, which contained 44,000 ng/L of PFOS.[15,22] Interestingly, perfluoroalkane sulfonamide alkylamines (FASAAms) were not detected in surface waters, while perfluoroalkane sulfonamide alkylamine diacids (FASADAs), and perfluoroalkane sulfonamide alkylbetaines (FASABs) make up a larger share in water than they do in AFFFs, where they are side products.[17,40] This absence of FASAAms may be due to enhanced sorption of amines on mineral cation exchange sites or faster degradation of amines becasue they have two oxidizable nitrogen atoms with lone pairs of electrons. The increased share of FASABs and FASADAs compared to perfluoroalkane sulfonamide alkylamine acids (FASAAAs) in water may be caused by inhibition of oxidation without a tertiary amine with a lone pair.

In rural water without known AFFF impacts, EtFOSAA was the most frequently detected perfluoroalkane sulfonamido substance in 3 out of 5 samples at 0.05–0.076 ng/L. In one Big Creek sample, FOSA and FHxSA were detected at less than 0.04 ng/L each.

4.4.4 PFASs in Sediments

The sediments collected from four sites on the Welland River and one site on Big Creek provide insight into the sediment water partitioning of AFFF-related PFASs (Table C10 in Appendix C). As Welland River 1 had the highest PFAS concentrations, it best illustrates the different PFAS profiles in sediment and water. The PFAA profile in sediment is dominated by PFOS, whereas the PFAA profile in water also has substantial PFHxS, PFHxA, and PFPeA (Figure C2c in Appendix C), due to the greater sorption of long-chain PFAAs, such as PFOS, compared to short-chain PFAAs. Based on the sediment and water concentrations of PFHxA, PFOA, PFHxS, PFHpS, PFOS, and FHxSA, which were detected in water and sediment in at least three sites, field-based sediment water distribution coefficients were calculated (Table C11 and Figure C3 in Appendix C). For the PFSAs, $\log K_d$ had an increasing trend with increasing chain-length with a slope of 0.53, which is similar to the slopes reported for C5 and higher PFCAs (0.46–0.51).[31] The $\log K_d$ for PFOA (C7; 0.55 ±0.06) is lower than for PFHpS (C7; 1.33 ±0.03), which is consistent with reports that PFSAs are more sorptive than PFCAs of equal chain-length.[31,41] Finally, FHxSA ($\log K_d$ = 1.03 ±0.06) had a higher distribution

coefficient than PFHxS ($\log K_d$ = 0.80 ±0.09), which is the same pattern as neutral FOSA having greater partitioning to sediment than anionic PFOS.[42]

The distribution of fluorotelomer substances between water and sediment at Welland River 1 (Figure 4.2b) demonstrates increased contributions of some PFASs, particularly C7 and C9 FTBs and 6:2 FTSAm in sediment. These are likely relatively more sorptive compounds, which is as expected given the uncharged, less water soluble nature of 6:2 FTSAm and the longer chain-lengths of the FTBs. Fluorotelomer substances that make up a smaller share of the profile in sediment than in water include C5 FTBs and 6:2 FTAB, which is likely due to reduced sorption of C5 and C6 zwitterionic betaines.

The only perfluorohexane sulfonamido AFFF component detected in sediment was a low concentration of FHxSAAm between the LOD and LOQ (approximately 0.09 ±0.06 ng/g) in Welland River 1 sediment. Combined with the lack of detection of FHxSAAm in water, it appears FHxSAAm is more sorptive than FHxSAB, FHxSAAA, and FHxSADA, which were all detected in water and not in sediment.

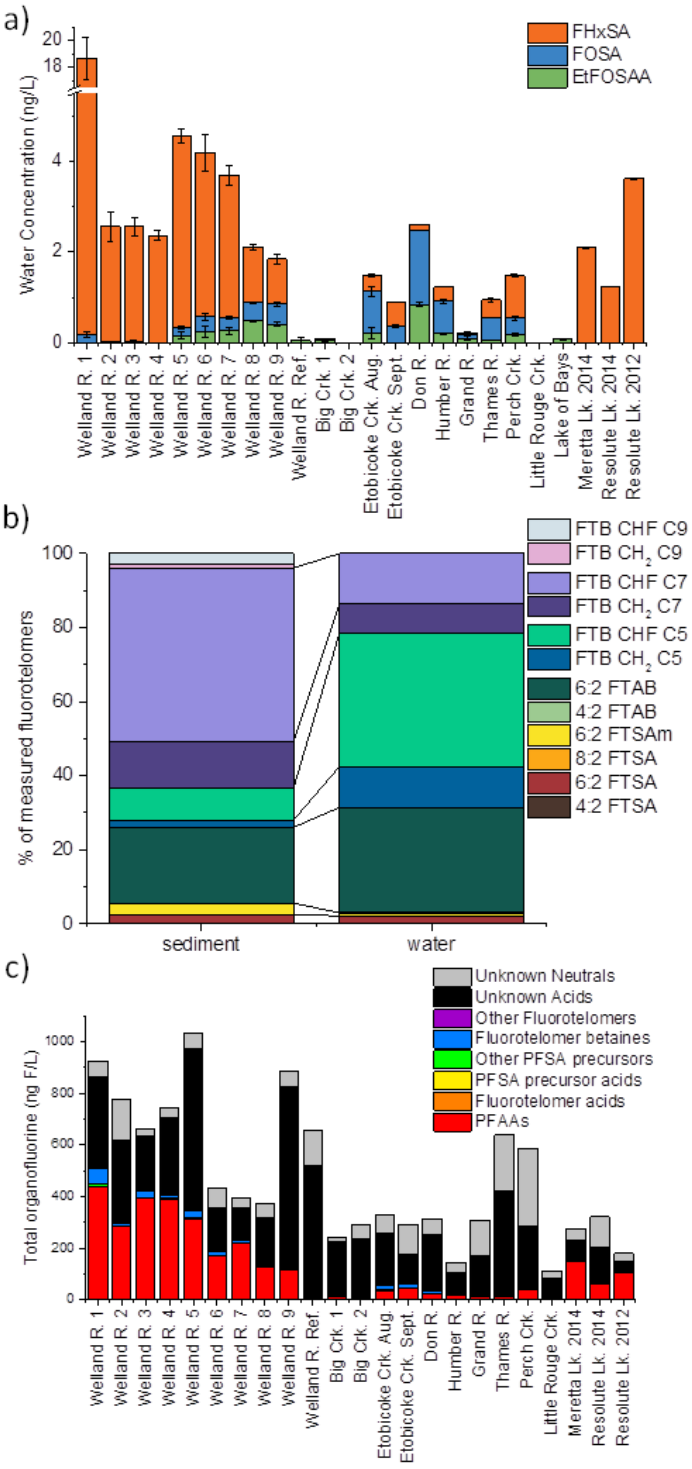

Figure 4.2: a) Concentrations of FHxSA, FOSA, and EtFOSAA in surface waters in ng/L with error bars showing standard deviations. b) Distribution of fluorotelomer substances in sediment and water from Welland River 1 sampling site. c) Total organofluorine in the

surface water extracts as measured by TOF-CIC plotted with the amount of total organofluorine accounted for by measured PFASs. PFAAs include PFCAs and PFSAs; fluorotelomer acids include FTSAs and 6:2 FTSAS-SO_2; PFSA precursor acids include FASADAs and EtFOSAA; other PFSA precursors include FHxSA, FOSA, FASAAAs, and FASABs; and fluorotelomer betaines include FTABs and FTBs. Unknown acids are organofluorine not accounted for by measured PFASs in the acids fraction and unknown neutrals are organofluorine not accounted for by measured PFASs in the neutral fraction.

4.4.5 Sorption of 6:2 FTAB and 6:2 FTAA to Agricultural Soil

Properties of the agricultural soil used are given in Table C12 in Appendix C. The kinetics plot for 6:2 FTAB and 6:2 FTAA sorption shows that 48 hours is a reasonable equilibration time because the aqueous concentration flattens out within 31 hours (Figure C4a in Appendix C). Control tubes with no soil show some sorption to the tubes with aqueous concentrations reduced by 17% for 6:2 FTAB and by 40% for 6:2 FTAA. However, kinetics experiment mass balances for 6:2 FTAB (85 ±4%) and 6:2 FTAA (108 ±5%) when incorporating extraction of the soil with aqueous phase analysis show sorption to containers is not significant in the presence of soil. The extent of sorption with a 1: 5 soil-to-water ratio was suitable for sorption measurements at 44 ±4% for 6:2 FTAB and 84±3% for 6:2 FTAA .[43]

Both 6:2 FTAB and 6:2 FTAA had linear sorption isotherms at spiking concentrations from 2 to 200 ng/mL with r^2 of 0.995 for 6:2 FTAB and 0.991 for 6:2 FTAA (Figure C4B and C in Appendix C). The soil-water distribution coefficient ($logK_d$) and organic carbon normalized distribution coefficient ($logK_{oc}$) for 6:2 FTAA ($logK_d$ = 1.43 ±0.01 (mean ±standard error), $logK_{oc}$ = 3.15 ±0.01) were greater than for 6:2 FTAB ($logK_d$ = 0.634 ±0.008, $logK_{oc}$ = 2.355 ± 0.008) in the agricultural soil. Sorption of 6:2 FTAA to soils and sediments may help to explain the much higher concentrations of 6:2 FTAB in surface water compared to 6:2 FTAA. However, the lack of detection of 6:2 FTAA in sediment at Welland River 1 suggests either sorption impeded its transport to the sampling site or faster biodegradation of 6:2 FTAA keeps its environmental concentrations low.[20] The higher sorption of 6:2 FTAA suggests that

electrostatic interactions between protonated 6:2 FTAA and cation exchange sites on soil contribute significantly to its sorption.

4.4.6 Total Organofluorine

Any measured inorganic fluoride was subtracted from the total fluoride measured by TOF-CIC in the acid fractions to obtain the total organofluorine concentrations in the acid fractions used in preparing Figure 4.2c). The percentage of the total organofluorine in the acid fraction that was not accounted for by the measured PFASs and is classified as unknown acids ranged from 30% to 99.7% and amounted to 44 to 700 ng/L of fluorine. The only significant contributors to the acid fraction total organofluorine were PFAAs. Shorter chain-lengths of PFAAs, which are inadequately retained in reverse phase liquid chromatography, may account for some unknown acids. In particular, trifluoroacetic acid (TFA) was the single most abundant PFCA in precipitation samples from Tsukuba, Japan[44] and Canada[45] by a large margin. Since TFA has been measured at variable concentrations up to hundreds of ng/L in surface waters,[46,47] TFA may account for a significant portion of the unknown acid fraction organofluorine. Perfluoropropionic acid (PFPrA) was the second most abundant PFCA in precipitation[44,45] and may account for additional unknown organofluorine in the acid fraction.

In the neutral fraction, fluorotelomer betaines (FTBs and FTABs) accounted for the largest portion of the total organofluorine of any measured PFASs at up to 44% of the neutral fraction organofluorine, while perfluoroalkane sulfonamido substances accounted for up to 10%, and other fluorotelomer substances accounted for 1% or less. The portion of neutral fraction organofluorine not accounted for by measured PFASs, the unknown neutrals, was 45 to 100%. Due to the lack of isolated standards for quantitation of FTBs, concentrations of FTBs have significant uncertainty and the share of organofluorine accounted for by FTBs may be larger or smaller than estimated.

Previously, total organofluorine in Lake Ontario surface sediments was found to be 56–98% unknown after measuring PFCAs and PFSAs.[48] This is similar to the 36–99.7% unknown organofluorine in surface waters in this study, several of which drain into Lake Ontario.

A study of AFFF-impacted groundwater using the oxidation of precursors assay found that unknown PFAA precursors accounted for 9% of total PFASs in very highly contaminated groundwater.[15] A substantially greater proportion of unidentified organofluorine was found in surface waters here. This may be partially due to sensitivity of the total organofluorine method to short chain PFCAs, including TFA. While 6:2 FTSA was 11% of the total PFASs in the groundwater study,[15] it is part of the fluorotelomer acids category accounting for at most 0.15% of the total organofluorine here. Perhaps the low relative proportion of FTSAs in surface waters compared to groundwater is related to surface water only loss processes, such as aqueous photolysis. Perfluoroalkane sulfonamido substances, categorized as PFSA precursors, account for a maximum of 1.44% of the total organofluorine in the Welland River 1 sample, which is close to the 3% of groundwater PFASs accounted for by FHxSA.[15] The FTABs and FTBs, which contribute between 2.5 and 6.2% of total organofluorine in eight samples from Welland River, Etobicoke Creek, and Don River are a unique finding of this study. Recently, Barzen-Hanson *et al.* identified 40 additional classes of PFASs in AFFF concentrates, commercial products, and AFFF-impacted groundwater, which may account for some of the unidentified organofluorine, particularly at AFFF impacted sites.[23]

4.5 Environmental Implications

This study shows that some PFASs associated with AFFFs are broadly distributed in Canadian surface waters and may be found in relatively high concentrations. In terms of compounds associated with perfluoroalkane sulfonamido AFFF components, FHxSA and PFHxS were detected in all the urban and AFFF-impacted sites investigated. This indicates that precursors to PFHxS are broadly present in urban and AFFF-impacted Canadian surface waters, while these classes of PFASs are rarely considered given that FHxSA has only been measured previously at highly AFFF-impacted U. S. military sites. Little is known about the biological or toxicological effects of FHxSA other than that it is a carbonic anhydrase inhibitor[49] and is toxic to red imported fire ants.[50] The detection of several perfluoroalkane sulfonamido AFFF components in AFFF-impacted surface waters in the Welland River, Resolute Lake, and Meretta Lake suggests that these

precursors likely contribute to the presence of FHxSA, PFHxS, PFPeS, and PFBS in these waters. However, it is likely that other as yet unidentified precursors contribute to the presence of FHxSA in urban surface waters and may include PFHxS precursors involved in the high serum PFHxS concentrations observed in a Canadian family who frequently used carpet treatments.[51] Since it was frequently detected, FHxSA may be a potentially useful marker of perfluorohexane sulfonamido substances for environmental monitoring. If the biodegradation of various perfluorohexane sulfonamido substances is like that of EtFOSE where FOSA is the longest lived intermediate,[52] then FHxSA is likely to be a particularly environmentally abundant PFHxS precursor.

The FTABs represent a large proportion of the PFASs characterized in some samples, including Don River where 6:2 and 8:2 FTAB constituted 36% of the organofluorine assigned to known PFASs, which is remarkable since 6:2 FTAB degrades by aqueous photolysis and biodegradation,[20,36] while PFCAs and PFSAs are fully persistent. The presence of 8:2 FTAB at 20 to 30% of the 6:2 FTAB concentration in Don River and Humber River water samples is significant because elimination of potential PFOA precursors, such as 8:2 FTAB, in emissions and products by 2015 was a goal of the PFOA Stewardship Program.[35] The FTBs were also detected in high estimated concentrations (up to 80 ng/L total) in AFFF-impacted waters. Together, FTBs and FTABs accounted for a maximum of 54% of organofluorine assigned to known PFASs in the August Etobicoke Creek sample. Thus, FTABs and FTBs represent significant sources of PFAS contamination in some surface waters and require more research on their potential sources in addition to AFFF, environmental fate including the degradability of FTBs, and toxicology.

The relatively low concentrations (<3.5 ng/L total) of fluorotelomer PFASs that are not betaines, including FTSAs, may indicate that these compounds lack stability to degradation in surface waters. This may be why FTSAs were not detected in surface waters from Hong Kong marine environments, while low concentrations were found in human blood[53] and levels of 6:2 FTSA were under 1.5 ng/L in surface water samples from Albany, NY,[54] the River Elbe in Germany,[55] and in thirteen rivers in China.[56]

Analysis of sediment samples from the Welland River revealed that while 6:2 FTAB and C5 FTBs are not especially sorptive and form a greater share of the fluorotelomer PFAS profile in water compared to sediment, C7 and C9 FTBs form a greater share of the fluorotelomer PFASs in sediment compared to water. This suggests that increasing to C7 or more enhances the sorption of fluorotelomer betaines, which is consistent with increasing sorption with increasing chain-lengths of PFCAs starting at C5 or C7 and above.[31] Batch sorption tests of 6:2 FTAB and 6:2 FTAA with an agricultural soil showed that the distribution coefficient of 6:2 FTAA is greater than that of any C6 PFAA studied in three soils and corresponds more closely to the distribution coefficient for a C8 to C10 or more PFAA,[31] which suggests that the sulfonamide alkylamine polar head group is more sorptive than a carboxylate, sulfonic acid, or sulfonamide alkylbetaine head group. Further research is needed to systematically examine the sorption of various chain-lengths of FTBs, FTABs, and FTAAs to different soils and sediments and compare them to other PFASs. This may help to elucidate some of the solute, sorbent, and solution specific parameters affecting the sorption of these PFASs beyond what is suggested by the limited results presented here.

In looking at the total organofluorine content of the water extracts, a large proportion of organofluorine was not characterized by measuring AFFF-related PFASs (36–99.7% of total organofluorine). Although a significant proportion of this may be made up of known PFASs, such as TFA, particularly in the acid fraction, between 4 and 51% of the unidentified organofluorine was in the neutrals fraction and may consist of PFASs used in commercial products other than the AFFF-related PFASs investigated here or degradation products of PFASs. This highlights the range of PFASs found in environmental samples and the difficulty of closing the mass balance of organofluorine by quantifying all the significantly contributing PFASs.

4.6 Acknowledgements

We thank Shane de Solla, Amila De Silva, and Cyril Cook (ECCC, Burlington, ON) for assistance with Welland River sampling, Paul Helm (MOECC, Etobicoke, ON) for providing Ontario urban water samples, and Derek Muir (ECCC, Burlington, ON) for

collecting Resolute and Meretta Lake samples. Leo W.Y. Yeung (University of Toronto) provided Little Rouge Creek samples and assistance with SPE. Funding was provided by the Natural Sciences and Engineering Research Council of Canada. L. A. D. received the Queen Elizabeth II/Edwin Walter and Margery Warren Graduate Scholarship in Science and Technology.

4.7 References

(1) Moody, C.; Field, J. Determination of perfluorocarboxylates in groundwater impacted by fire-fighting activity. *Environ. Sci. Technol.* **1999**, *33* (16), 2800–2806.

(2) Moody, C. A.; Kwan, W. C.; Martin, J. W.; Muir, D. C. G.; Mabury, S. A. Determination of Perfluorinated Surfactants in Surface Water Samples by Two Independent Analytical Techniques: Liquid Chromatography/Tandem Mass Spectrometry and 19F NMR. *Anal. Chem.* **2001**, *73* (10), 2200–2206.

(3) Moody, C. A.; Martin, J. W.; Kwan, W. C.; Muir, D. C. G.; Mabury, S. A. Monitoring Perfluorinated Surfactants in Biota and Surface Water Samples Following an Accidental Release of Fire-Fighting Foam into Etobicoke Creek. *Environ. Sci. Technol.* **2002**, *36* (4), 545–551.

(4) Schultz, M. M.; Barofsky, D. F.; Field, J. A. Quantitative Determination of Fluorotelomer Sulfonates in Groundwater by LC MS/MS. *Environ. Sci. Technol.* **2004**, *38* (6), 1828–1835.

(5) Norwegian Pollution Control Authority. *Screening of Polyfluorinated Organic Compounds at Four Fire Training Facilities in Norway*; 2444; 2008.

(6) de Solla, S. R.; De Silva, A. O.; Letcher, R. J. Highly elevated levels of perfluorooctane sulfonate and other perfluorinated acids found in biota and surface water downstream of an international airport, Hamilton, Ontario, Canada. *Environ. Int.* **2012**, *39* (1), 19–26.

(7) Karrman, A.; Elgh-Dalgren, K.; Lafossas, C.; Moskeland, T. Environmental levels and distribution of structural isomers of perfluoroalkyl acids after aqueous fire-fighting foam (AFFF) contamination. *Environ. Chem.* **2011**, *8* (4), 372–380.

(8) Awad, E.; Zhang, X.; Bhavsar, S. P.; Petro, S.; Crozier, P. W.; Reiner, E. J.; Fletcher, R.; Tittlemier, S. A.; Braekevelt, E. Long-Term Environmental Fate of Perfluorinated Compounds after Accidental Release at Toronto Airport. *Environ. Sci. Technol.* **2011**, *45* (19), 8081–8089.

(9) Kwadijk, C. J. A. F.; Kotterman, M.; Koelmans, A. A. Partitioning of Perfluorooctanesulfonate and Perfluorohexanesulfonate in the Aquatic Environment

After an Accidental Release of Aqueous Film Forming Foam at Schiphol Amsterdam Airport. *Environ. Toxicol. Chem.* **2014**, *33* (8), 1761–1765.

(10) Anderson, R. H.; Long, G. C.; Porter, R. C.; Anderson, J. K. Occurrence of select perfluoroalkyl substances at U.S. Air Force aqueous film-forming foam release sites other than fire-training areas: Field-validation of critical fate and transport properties. *Chemosphere* **2016**, *150*, 678–685.

(11) Filipovic, M.; Woldegiorgis, A.; Norström, K.; Bibi, M.; Lindberg, M.; Österås, A.-H. Historical usage of aqueous film forming foam: A case study of the widespread distribution of perfluoroalkyl acids from a military airport to groundwater, lakes, soils and fish. *Chemosphere* **2015**, *129*, 39–45.

(12) Moody, C.; Hebert, G.; Strauss, S.; Field, J. Occurrence and persistence of perfluorooctanesulfonate and other perfluorinated surfactants in groundwater at a fire-training area at Wurtsmith Air Force Base, Michigan, USA. *J. Environ. Monit.* **2003**, *5* (2), 341–345.

(13) Oakes, K. D.; Benskin, J. P.; Martin, J. W.; Ings, J. S.; Heinrichs, J. Y.; Dixon, D. G.; Servos, M. R. Biomonitoring of perfluorochemicals and toxicity to the downstream fish community of Etobicoke Creek following deployment of aqueous film-forming foam. *Aquat. Toxicol.* **2010**, *98* (2), 120–129.

(14) Weiner, B.; Yeung, L. W. Y.; Marchington, E. B.; D'Agostino, L. A.; Mabury, S. A. Organic fluorine content in aqueous film forming foams (AFFFs) and biodegradation of the foam component 6 : 2 fluorotelomermercaptoalkylamido sulfonate (6 : 2 FTSAS). *Environ. Chem.* **2013**, *10* (6), 486–493.

(15) Houtz, E. F.; Higgins, C. P.; Field, J. A.; Sedlak, D. L. Persistence of Perfluoroalkyl Acid Precursors in AFFF-Impacted Groundwater and Soil. *Environ. Sci. Technol.* **2013**, *47* (15), 8187–8195.

(16) Place, B. J.; Field, J. A. Identification of Novel Fluorochemicals in Aqueous Film-Forming Foams Used by the US Military. *Environ. Sci. Technol.* **2012**, *46* (13), 7120–7127.

(17) D'Agostino, L. A.; Mabury, S. A. Identification of Novel Fluorinated Surfactants in Aqueous Film Forming Foams and Commercial Surfactant Concentrates. *Environ. Sci. Technol.* **2014**, *48* (1), 121–129.

(18) Harding-Marjanovic, K. C.; Houtz, E. F.; Yi, S.; Field, J. A.; Sedlak, D. L.; Alvarez-Cohen, L. Aerobic Biotransformation of Fluorotelomer Thioether Amido Sulfonate (Lodyne) in AFFF-Amended Microcosms. *Environ. Sci. Technol.* **2015**, *49* (13), 7666–7674.

(19) Moe, M. K.; Huber, S.; Svenson, J.; Hagenaars, A.; Pabon, M.; Trümper, M.; Berger, U.; Knapen, D.; Herzke, D. The structure of the fire fighting foam surfactant

Forafac®1157 and its biological and photolytic transformation products. *Chemosphere* **2012**, *89* (7), 869–875.

(20) D'Agostino, L. A.; Mabury, S. A. Aerobic biodegradation of two fluorotelomer sulfonamide-based aqueous film forming foam components produces perfluoroalkyl carboxylates. *Environ. Toxicol. Chem.* **2017**, DOI: 10.1002/etc.3750

(21) Munoz, G.; Duy, S. V.; Labadie, P.; Botta, F.; Budzinski, H.; Lestremau, F.; Liu, J.; Sauvé, S. Analysis of zwitterionic, cationic, and anionic poly- and perfluoroalkyl surfactants in sediments by liquid chromatography polarity-switching electrospray ionization coupled to high resolution mass spectrometry. *Talanta* **2016**, *152*, 447–456.

(22) Backe, W. J.; Day, T. C.; Field, J. A. Zwitterionic, Cationic, and Anionic Fluorinated Chemicals in Aqueous Film Forming Foam Formulations and Groundwater from U.S. Military Bases by Nonaqueous Large-Volume Injection HPLC-MS/MS. *Environ. Sci. Technol.* **2013**, *47* (10), 5226–5234.

(23) Barzen-Hanson, K. A.; Roberts, S. C.; Choyke, S. J.; Oetjen, K.; McAlees, A.; Riddell, N.; McCrindle, R.; Ferguson, P. L.; Higgins, C. P.; Field, J. A. Discovery of 40 classes of per- and polyfluoroalkyl substances in historical aqueous film-forming foams (AFFFs) and AFFF-impacted groundwater. *Environ. Sci. Technol.* **2017**. DOI: 10.1021/acs.est.6b05843

(24) Munoz, G.; Desrosiers, M.; Duy, S. V.; Labadie, P.; Budzinski, H.; Liu, J.; Sauvé, S. Environmental Occurrence of Perfluoroalkyl Acids and Novel Fluorotelomer Surfactants in the Freshwater Fish Catostomus commersonii and Sediments Following Firefighting Foam Deployment at the Lac-Mégantic Railway Accident. *Environ. Sci. Technol.* **2017**. DOI: 10.1021/acs.est.6b05432

(25) McGuire, M. E.; Schaefer, C.; Richards, T.; Backe, W. J.; Field, J. A.; Houtz, E.; Sedlak, D. L.; Guelfo, J. L.; Wunsch, A.; Higgins, C. P. Evidence of Remediation-Induced Alteration of Subsurface Poly- and Perfluoroalkyl Substance Distribution at a Former Firefighter Training Area. *Environ. Sci. Technol.* **2014**, *48* (12), 6644–6652.

(26) Gewurtz, S. B.; Bhavsar, S. P.; Petro, S.; Mahon, C. G.; Zhao, X.; Morse, D.; Reiner, E. J.; Tittlemier, S. A.; Braekevelt, E.; Drouillard, K. High levels of perfluoroalkyl acids in sport fish species downstream of a firefighting training facility at Hamilton International Airport, Ontario, Canada. *Environ. Int.* **2014**, *67*, 1–11.

(27) Stock, N. L.; Furdui, V. I.; Muir, D. C. G.; Mabury, S. A. Perfluoroalkyl Contaminants in the Canadian Arctic: Evidence of Atmospheric Transport and Local Contamination. *Environ. Sci. Technol.* **2007**, *41* (10), 3529–3536.

(28) Lescord, G. L.; Kidd, K. A.; De Silva, A. O.; Williamson, M.; Spencer, C.; Wang, X.; Muir, D. C. G. Perfluorinated and Polyfluorinated Compounds in Lake Food

Webs from the Canadian High Arctic. *Environ. Sci. Technol.* **2015**, *49* (5), 2694–2702.

(29) Taniyasu, S.; Kannan, K.; So, M. K.; Gulkowska, A.; Sinclair, E.; Okazawa, T.; Yamashita, N. Analysis of fluorotelomer alcohols, fluorotelomer acids, and short- and long-chain perfluorinated acids in water and biota. *J. Chromatogr. A* **2005**, *1093* (1–2), 89–97.

(30) Rand, A. A.; Mabury, S. A. In Vitro Interactions of Biological Nucleophiles with Fluorotelomer Unsaturated Acids and Aldehydes: Fate and Consequences. *Environ. Sci. Technol.* **2012**, *46* (13), 7398–7406.

(31) Guelfo, J. L.; Higgins, C. P. Subsurface Transport Potential of Perfluoroalkyl Acids at Aqueous Film-Forming Foam (AFFF)-Impacted Sites. *Environ. Sci. Technol.* **2013**, *47* (9), 4164–4171.

(32) Douglas, M. S. V.; Smol, J. P. Eutrophication and recovery in the High Arctic: Meretta Lake (Cornwallis Island, Nunavut, Canada) revisited. *Hydrobiologia* **2000**, *431* (2-3), 193–204.

(33) D'eon, J. C.; Crozier, P. W.; Furdui, V. I.; Reiner, E. J.; Libelo, E. L.; Mabury, S. A. Perfluorinated phosphonic acids in Canadian surface waters and wastewater treatment plant effluent: Discovery of a new class of perfluorinated acids. *Environ. Toxicol. Chem.* **2009**, *28* (10), 2101–2107.

(34) Weppner, W. *Letter by William Weppner, 3M, to Charles Auer, EPA OPPT, regarding the Phase-out Plan for POSF-Based Products*; US EPA Public Docket EPA-HQ-OPPT-2002-0043-0009; 3M General Offices: St. Paul, MN, 2000.

(35) Stephen L. Johnson. PFOA Stewardship Program Invitation Letter, 2006.

(36) Trouborst, L.; Mabury, S. A. Aqueous photolysis of 6:2 fluorotelomer sulfonamide alkylbetaine. *J Env Sci Prep*.

(37) Erkenbrecher JR., Carl Willam; Longoria, John Mark; Reynolds, Richard Alan; Julian, Jennifer C.; DeLeo, Malcolm; Ochomogo, Maria Garcia. Prevention of deposits on ceramics. US20060094623, May 4, 2006.

(38) DuPont. Dupont Capstone Fluorosurfactant FS-50 Technical Information https://www.chemours.com/Capstone/en_US/assets/downloads/K-02043-2_Capstone_FS-50.pdf (accessed Oct 4, 2016).

(39) DuPont. Dupont Capston Fluorosurfactant 1157 Water-soluble additive for firefighting foam Technical Informtion https://www.chemours.com/Capstone/en_US/assets/downloads/H-97584-2_Capstone_1157.pdf (accessed Oct 4, 2016).

(40) Stern, R. M.; Guenthner, R. a; Alm, R. R.; Wilkinson, T. K. Process for the Preparation of Fluoroaliphatic Aminocarboxylate Surfactants. U.S. 5,144,069, September 1, 1992.

(41) Higgins, C. P.; Luthy, R. G. Sorption of Perfluorinated Surfactants on Sediments†. *Environ. Sci. Technol.* **2006**, *40* (23), 7251–7256.

(42) Ahrens, L. Partitioning of perfluorooctanoate (PFOA), perfluorooctane sulfonate (PFOS) and perfluorooctane sulfonamide (PFOSA) between water and sediment. *Chemosphere* **2011**, *85* (5), 731–737.

(43) OECD. *Test No. 106: Adsorption -- Desorption Using a Batch Equilibrium Method*; Organisation for Economic Co-operation and Development: Paris, 2000.

(44) Taniyasu, S.; Kannan, K.; Yeung, L. W. Y.; Kwok, K. Y.; Lam, P. K. S.; Yamashita, N. Analysis of trifluoroacetic acid and other short-chain perfluorinated acids (C2–C4) in precipitation by liquid chromatography–tandem mass spectrometry: Comparison to patterns of long-chain perfluorinated acids (C5–C18). *Anal. Chim. Acta* **2008**, *619* (2), 221–230.

(45) Scott, B. F.; Moody, C. A.; Spencer, C.; Small, J. M.; Muir, D. C. G.; Mabury, S. A. Analysis for Perfluorocarboxylic Acids/Anions in Surface Waters and Precipitation Using GC−MS and Analysis of PFOA from Large-Volume Samples. *Environ. Sci. Technol.* **2006**, *40* (20), 6405–6410.

(46) Scott, B. F.; MacTavish, D.; Spencer, C.; Strachan, W. M. J.; Muir, D. C. G. Haloacetic Acids in Canadian Lake Waters and Precipitation. *Environ. Sci. Technol.* **2000**, *34* (20), 4266–4272.

(47) Wujcik, C. E.; Cahill, T. M.; Seiber, J. N. Determination of Trifluoroacetic Acid in 1996−1997 Precipitation and Surface Waters in California and Nevada. *Environ. Sci. Technol.* **1999**, *33* (10), 1747–1751.

(48) Yeung, L. W. Y.; De Silva, A. O.; Loi, E. I. H.; Marvin, C. H.; Taniyasu, S.; Yamashita, N.; Mabury, S. A.; Muir, D. C. G.; Lam, P. K. S. Perfluoroalkyl substances and extractable organic fluorine in surface sediments and cores from Lake Ontario. *Environ. Int.* **2013**, *59*, 389–397.

(49) Benfodda, Z.; Guillen, F.; Romestand, B.; Dahmani, A.; Blancou, H. Synthesis and investigation of inhibition effect of fluorinated sulfonamide derivatives on carbonic anhydrase. *Eur. J. Med. Chem.* **2010**, *45* (3), 1225–1229.

(50) Meer, R. K. V.; Lofgren, C. S.; Williams, D. F. Fluoroaliphatic Sulfones: A New Class of Delayed-action Insecticides for Control of Solenopsis invicta (Hymenoptera: Formicidae). *J. Econ. Entomol.* **1985**, *78* (6), 1190–1197.

(51) Beesoon, S.; Genuis, S. J.; Benskin, J. P.; Martin, J. W. Exceptionally High Serum Concentrations of Perfluorohexanesulfonate in a Canadian Family are Linked to

Home Carpet Treatment Applications. *Environ. Sci. Technol.* **2012**, *46* (23), 12960–12967.

(52) Rhoads, K. R.; Janssen, E. M.-L.; Luthy, R. G.; Criddle, C. S. Aerobic Biotransformation and Fate of N-Ethyl Perfluorooctane Sulfonamidoethanol (N-EtFOSE) in Activated Sludge. *Environ. Sci. Technol.* **2008**, *42* (8), 2873–2878.

(53) Loi, E. I. H.; Yeung, L. W. Y.; Mabury, S. A.; Lam, P. K. S. Detections of Commercial Fluorosurfactants in Hong Kong Marine Environment and Human Blood: A Pilot Study. *Environ. Sci. Technol.* **2013**, *47* (9), 4677–4685.

(54) Kim, S.-K.; Kannan, K. Perfluorinated Acids in Air, Rain, Snow, Surface Runoff, and Lakes: Relative Importance of Pathways to Contamination of Urban Lakes. *Environ. Sci. Technol.* **2007**, *41* (24), 8328–8334.

(55) Ahrens, L.; Felizeter, S.; Sturm, R.; Xie, Z.; Ebinghaus, R. Polyfluorinated compounds in waste water treatment plant effluents and surface waters along the River Elbe, Germany. *Mar. Pollut. Bull.* **2009**, *58* (9), 1326–1333.

(56) Lin, Y.; Liu, R.; Hu, F.; Liu, R.; Ruan, T.; Jiang, G. Simultaneous qualitative and quantitative analysis of fluoroalkyl sulfonates in riverine water by liquid chromatography coupled with Orbitrap high resolution mass spectrometry. *J. Chromatogr. A* **2016**, *1435*, 66–74.

Chapter 5

Summary, Conclusions, and Future Work

5 Summary, Conclusions, and Future Work

5.1 Summary and Conclusions

The focus of this thesis is on perfluoroalkyl and polyfluoroalkyl substances (PFASs) that are found in aqueous film forming foams (AFFFs), which are used for fighting liquid fuelled fires. For approximately the last fifteen years, it has been known that use of AFFF in an area is associated with very high concentrations of PFASs, especially perfluorooctane sulfonate (PFOS), perfluorohexane sulfonate (PFHxS), perfluorooctanoate (PFOA), and 6:2 fluorotelomer sulfonic acid (FTSA), in groundwater[1–3] and surface water.[4] However, these PFASs are not major components of AFFFs, with the exception of PFOS in AFFFs prepared with electrochemical fluorination (ECF) products,[5,6] where PFSAs may make up 0.5 to 1.5% of the concentrate, while other PFASs are 1 to 5% of the concentrate according to a Material Safety Data Sheet.[7] Recent results comparing liquid chromatography-tandem mass spectrometry (LC-MS/MS) results to total organofluorine combustion ion chromatography (TOF-CIC)[5] and the total oxidizable precursors assay[6] have shown that PFSAs account for up to half the PFAS ingredients in ECF AFFFs. Therefore, to improve our understanding of AFFF components in the environment this thesis aimed to identify PFASs in AFFFs and commercial surfactant concentrates, determine the environmental fate of two AFFF-components under aerobic biodegradation conditions, and explore the presence of AFFF-related PFASs in a variety of surface water environments in Canada.

Uncertainties about the identities of PFASs used as the fluorinated surfactant components of AFFFs were addressed in Chapter 2. The identification of over 100 PFASs in AFFF and commercial surfactant concentrates using solid phase extraction (SPE), high resolution mass spectrometry (HR-MS), collision induced dissociation (CID) mass spectra, and LC-MS/MS was accomplished. Many important observations about the PFASs in AFFFs were made. Some of the AFFFs incorporated ECF products and some incorporated fluorotelomer PFASs, as expected based on earlier ^{19}F-nuclear magnetic resonance (NMR) spectra.[5] The perfluoroalkyl chain-lengths of PFASs in AFFFs spanned a large range from three to fifteen fluorinated carbons, while the major chain length congeners present tended to have either six or eight perfluoroalkyl carbons, which is

consistent with the PFASs first associated with AFFF-impacted sites.[1–4] Within AFFFs and commercial surfactant concentrates, synthetic intermediates, by-products, and degradation products were present along with the PFASs that were apparently the intended products. The approaches used to identify PFASs in AFFFs each contributed useful information with mixed-mode ion exchange SPE separating PFASs of different charge properties and reducing interferences, HR-MS enabling determination of molecular formulae and use of mass defect to select PFAS ions, CID mass spectra providing structural information about PFASs, and LC-MS/MS separating linear and branched isomers in ECF products and sensitively detecting low abundance perfluoroalkyl chain-lengths. Certain PFASs were found in more AFFFs than others with 6:2 fluorotelomer mercaptoalkylamido sulfonate (FTSAS) found in six of ten AFFFs, and 6:2 fluorotelomer sulfonamide alkylamine (FTAA) and 6:2 fluorotelomer sulfonamide alkyl betaine (FTAB) found in four of ten AFFFs. Overall, the identification of over one hundred PFASs in AFFFs and fluorinated surfactant concentrates reveals many PFASs that may be present in the environment and require more research as they generally have limited or no available information on their environmental chemistry, fate, or toxicology.

An investigation of the biodegradation of 6:2 FTAB and its synthetic intermediate 6:2 FTAA, which were detected in forty percent of AFFFs, with aerobic wastewater treatment plant (WWTP) sludge was undertaken in Chapter 3. This experiment revealed that under aerobic conditions, 6:2 FTAB and 6:2 FTAA can biodegrade to perfluoroalkyl carboxylates (PFCAs), including perfluorohexanoate (PFHxA) and perfluoropentanoate (PFPeA), and known PFCA precursors, including 6:2 fluorotelomer alcohol, 6:2 fluorotelomer carboxylic acid (FTCA), 6:2 fluorotelomer unsaturated carboxylic acid (FTUCA), and 5:3 FTCA. This is the first report of formation of PFCAs or known PFCA precursors from 6:2 FTAB and 6:2 FTAA and was enabled by synthesis and purification of 6:2 FTAB and 6:2 FTAA for the experiment. Biodegradation of 6:2 FTAB and 6:2 FTAA was apparently relatively slow with production of PFCAs observed after 21 to 45 days. Loss of 6:2 FTAA from the aqueous phase was apparently faster than for 6:2 FTAB, which had up to 60% still present in the aqueous phase after 109 days. Low yields of PFCAs and known PFCA precursors were found at 5.9 ± 0.5 mol % of the loss of 6:2 FTAA and 2.1 ± 0.4 mol % of the loss of 6:2 FTAB, although these number are affected

by poor mass recovery in the experiment. Another degradation product, 6:2 fluorotelomer sulfonamide (FTSAm), was synthesized and found to account for between 1 and 10% of the missing 6:2 FTAB or 6:2 FTAA, which made it generally the most abundant degradation product. Limited degradation to 6:2 FTSA and 6:2 FTSAm was observed in sterile controls, but formation of 6:2 FTOH, FTCAs, and PFCAs was limited to active biodegradation experiments. Using quadrupole time of flight mass spectrometry (qTOF-MS) and CID mass spectra, six additional degradation products of 6:2 FTAA were tentatively identified. These products may have contributed to the low mass balance in the experiment along with protein binding[8,9] and other known degradation products of 6:2 FTOH for which standards were unavailable.[10] The variety of degradation products identified highlights the difficulty of fully assessing PFAS contamination at AFFF impacted sites, which could include not only dozens of possible AFFF components identified in Chapter 2 but also numerous degradation products thereof.

In Chapter 4, the presence of AFFF-related PFASs in surface waters was investigated to help prioritize future research into the sources and environmental chemistry of these PFASs. Using the sensitivity of LC-MS/MS combined with sample concentration by SPE, PFCAs, perfluoroalkane sulfonates (PFSAs), FTSAs, and eleven other classes of PFASs were detected in Canadian surface waters. This survey was different from other investigations looking for newly identified AFFF components in groundwater[11,6,12] in that along with previously identified AFFF-impacted surface water, urban and rural surface waters were also examined. Among the findings in surface waters were that perfluorohexane sulfonamide (FHxSA), which was previously measured only at AFFF-impacted sites,[6,12]was present in all urban and AFFF-impacted sites indicating its perfluorohexane sulfonamido precursors are widespread. The fluorotelomer PFASs that were found at the highest maximum concentrations were those with betaine functional groups, including FTABs and fluorotelomer betaines (FTBs). The FTABs were measured in both urban and AFFF-impacted surface waters at concentrations up to 15.5 to 33 ng/L, whereas FTBs were detected only in AFFF-impacted surface waters with estimated total concentrations up to 80 ng/L. Other AFFF-components and degradation products thereof were detected at lower concentrations in surface waters, including 6:2 FTSAm, 6:2 FTSAS-sulfone (FTSAS-SO_2), 6:2 fluorotelomer thiohydroxylammonium sulfoxide

(FTSHA-SO), 6:2 FTAA, and some perfluoroalkane sulfonamido substances. Preliminary insights into sorption of AFFF-related PFASs were provided by extraction and measurement of sediments from the AFFF-impacted Welland River and soil batch sorption tests with 6:2 FTAB and 6:2 FTAA. The sediment samples had greater contributions from FTBs with seven or nine carbon perfluoroalkyl chains and smaller proportions with five carbon perfluoroalkyl chains than water samples, which suggests a trend of increasing sorption with increasing chain-length as has been observed for other PFASs.[13] The soil-water distribution coefficients for 6:2 FTAA and 6:2 FTAB in an agricultural soil suggest that amine-containing PFASs are more sorptive than betaine PFASs likely due to electrostatic interactions with soil cation exchange sites.

In this thesis, more than one hundred PFASs in twelve novel and ten infrequently reported classes were identified in AFFFs and commercial surfactant concentrates, ten classes of AFFF-related PFASs were detected and in both AFFF-impacted and urban surface waters, and the potential of two recently identified AFFF components 6:2 FTAB and 6:2 FTAA to aerobically biodegrade to PFCAs and known PFCA precursors was demonstrated for the first time.

5.2 Future Work

Further research is needed to address some knowledge gaps that remain in the subjects addressed in this thesis. In Chapter 3, unforeseen difficulties with experimental losses through the XAD cartridges due to vigorous air purging make the kinetics and yield calculations from the study more qualitative than quantitative. Therefore, a study using an improved apparatus to reduce losses due to air purging is needed to improve the accuracy of kinetic and yield measurements. This apparatus could address these problems by including more finely adjustable valves to control the flow of air so it is at a low level in all bottles that does not generate a spray from the surface.

The preliminary investigation of the sorption of 6:2 FTAA and 6:2 FTAB to an agricultural soil and the presence of FTBs in Welland River sediments should be extended to a systematic investigation of the sorption of several perfluoroalkyl chain-lengths of FTAAs, FTABs, and FTBs to a variety of soils and sediments in order to

investigate the dependence of their sorption on properties such as perfluoroalkyl chain-length, the cation exchange capacity of the sorbent, and the organic matter content of the soil or sediment. Side by side comparisons with PFSAs and PFCAs using the same soil or sediment would also be useful to confirm the greater tendency to sorb that FTABs and FTAAs seem to have for a given perfluoroalkyl chain length. Measurements of the soil-water distribution coefficients for other classes of PFASs identified in AFFFs are also needed, but FTBs, FTABs, and FTAAs should be a priority given the high concentrations of FTBs and FTABs in some surface water samples, and the fact that FTAAs are intermediates in the production of FTABs.

In Chapter 4, the slower attenuation of FTB concentrations moving downstream on the Welland River compared to the attenuation of 6:2 FTAB levels raises interesting questions about reason for this difference. The sorption experiments suggested above would determine if greater sorption of FTABs could be responsible for this difference, but another possibility is that FTBs are less degradable than FTABs in the environment. Since both biodegradation and aqueous photolysis[14] have been demonstrated to yield PFCAs from 6:2 FTAB, the biodegradation and aqueous photolysis of FTBs should be investigated to determine the extent to which they may be more persistent than FTABs in surface waters and WWTPs.

The 6:2 FTSAm was identified as an important degradation product of 6:2 FTAB and 6:2 FTAA in Chapter 3, while both 6:2 FTSAm and FHxSA were detected in AFFF-impacted and urban surface waters in Chapter 4. These neutral PFASs are likely relatively volatile and may partition into the gas phase. Because the 6:2 FTSAm is a new class of PFAS, it would be interesting to investigate the atmospheric chemistry of FTSAms in smog chamber experiments, since they would likely yield PFCAs and perhaps FTSAs similar to the atmospheric oxidation of N-methyl perfluorobutane sulfonamido ethanol (MeFBSE),[15] although FTSAs can undergo further environmental oxidation.[16] Measurements of FHxSA, 6:2 FTSAm, and 6:2 FTSA in the atmosphere in the gas phase, in particles, and in precipitation would be useful in determining the relevance of atmospheric transport and processing of these PFASs. Some published research suggests that FTSA inputs from the atmosphere, which may involve 6:2

FTSAm, are possible, since FTSAs were measured in the sediments of four non-AFFF impacted arctic lakes in Nunavut, Canada,[17] and up to 3.37 ng/L of 8:2 FTSA was measured in precipitation in Albany, NY, which was an order of magnitude higher than the maximum concentration measured in lake water.[18]

Finally, the unexpected detection of numerous AFFF-related PFASs in urban surface waters, especially the detection of high concentrations of FTABs in several samples requires further research to determine the sources of these compounds to urban surface waters. Quantification of AFFF-related PFASs, especially FTABs and FTAAs in WWTP influents and effluents may help to determine the impact of wastewater treatment on these compounds and if WWTP effluent is a source of AFFF-related PFASs. Further research to determine if the WWTPs receive wastewaters containing AFFF is also needed to help address the question of whether the AFFF-related PFASs, particularly 6:2 FTAB, are being used in other applications in urban environments, such as for institutional cleaning.[19]

In addition to the specific suggestions provided here, numerous other research questions also remain in regards to the PFASs that have been identified in AFFFs and various other aspects of their environmental fate, partitioning, bioaccumulation, and toxicology, which are generally little studied by the environmental science community at this point.

5.3 References

(1) Moody, C. A.; Field, J. A. Determination of Perfluorocarboxylates in Groundwater Impacted by Fire-Fighting Activity. Environ. Sci. Technol. 1999, 33 (16), 2800–2806.

(2) Moody, C.; Hebert, G.; Strauss, S.; Field, J. Occurrence and persistence of perfluorooctanesulfonate and other perfluorinated surfactants in groundwater at a fire-training area at Wurtsmith Air Force Base, Michigan, USA. J. Environ. Monit. 2003, 5 (2), 341–345.

(3) Schultz, M. M.; Barofsky, D. F.; Field, J. A. Quantitative Determination of Fluorotelomer Sulfonates in Groundwater by LC MS/MS. Environ. Sci. Technol. 2004, 38 (6), 1828–1835.

(4) Moody, C. A.; Martin, J. W.; Kwan, W. C.; Muir, D. C. G.; Mabury, S. A. Monitoring Perfluorinated Surfactants in Biota and Surface Water Samples Following an Accidental Release of Fire-Fighting Foam into Etobicoke Creek. Environ. Sci. Technol. 2002, 36 (4), 545–551.

(5) Weiner, B.; Yeung, L. W. Y.; Marchington, E. B.; D'Agostino, L. A.; Mabury, S. A. Organic fluorine content in aqueous film forming foams (AFFFs) and biodegradation of the foam component 6 : 2 fluorotelomermercaptoalkylamido sulfonate (6 : 2 FTSAS). Environ. Chem. 2013, 10 (6), 486–493.

(6) Houtz, E. F.; Higgins, C. P.; Field, J. A.; Sedlak, D. L. Persistence of Perfluoroalkyl Acid Precursors in AFFF-Impacted Groundwater and Soil. Environ. Sci. Technol. 2013, 47 (15), 8187–8195.

(7) 3M Company. Material Safety Data Sheet for FC-203FC Light Water (TM) AFFF; Document ID 07-1198-6. September 30, 1999.

(8) Rand, A. A.; Mabury, S. A. Covalent Binding of Fluorotelomer Unsaturated Aldehydes (FTUALs) and Carboxylic Acids (FTUCAs) to Proteins. Environ. Sci. Technol. 2013, 47 (3), 1655–1663.

(9) Rand, A. A.; Mabury, S. A. Protein Binding Associated with Exposure to Fluorotelomer Alcohols (FTOHs) and Polyfluoroalkyl Phosphate Esters (PAPs) in Rats. Environ. Sci. Technol. 2014, 48 (4), 2421–2429.

(10) Liu, J.; Wang, N.; Szostek, B.; Buck, R. C.; Panciroli, P. K.; Folsom, P. W.; Sulecki, L. M.; Bellin, C. A. 6-2 Fluorotelomer alcohol aerobic biodegradation in soil and mixed bacterial culture. Chemosphere 2010, 78 (4), 437–444.

(11) Backe, W. J.; Day, T. C.; Field, J. A. Zwitterionic, Cationic, and Anionic Fluorinated Chemicals in Aqueous Film Forming Foam Formulations and Groundwater from U.S. Military Bases by Nonaqueous Large-Volume Injection HPLC-MS/MS. Environ. Sci. Technol. 2013, 47 (10), 5226–5234.

(12) McGuire, M. E.; Schaefer, C.; Richards, T.; Backe, W. J.; Field, J. A.; Houtz, E.; Sedlak, D. L.; Guelfo, J. L.; Wunsch, A.; Higgins, C. P. Evidence of Remediation-Induced Alteration of Subsurface Poly- and Perfluoroalkyl Substance Distribution at a Former Firefighter Training Area. Environ. Sci. Technol. 2014, 48 (12), 6644–6652.

(13) Higgins, C. P.; Luthy, R. G. Sorption of Perfluorinated Surfactants on Sediments†. Environ. Sci. Technol. 2006, 40 (23), 7251–7256.

(14) Trouborst, L.; Mabury, S. A. Aqueous photolysis of 6:2 fluorotelomer sulfonamide alkylbetaine. J Env Sci Prep.

(15) D'eon, J. C.; Hurley, M. D.; Wallington, T. J.; Mabury, S. A. Atmospheric Chemistry of N-methyl Perfluorobutane Sulfonamidoethanol,

C4F9SO2N(CH3)CH2CH2OH: Kinetics and Mechanism of Reaction with OH. Environ. Sci. Technol. 2006, 40 (6), 1862–1868.

(16) Wang, N.; Liu, J.; Buck, R. C.; Korzeniowski, S. H.; Wolstenholme, B. W.; Folsom, P. W.; Sulecki, L. M. 6:2 Fluorotelomer sulfonate aerobic biotransformation in activated sludge of waste water treatment plants. Chemosphere 2011, 82 (6), 853–858.

(17) Lescord, G. L.; Kidd, K. A.; De Silva, A. O.; Williamson, M.; Spencer, C.; Wang, X.; Muir, D. C. G. Perfluorinated and Polyfluorinated Compounds in Lake Food Webs from the Canadian High Arctic. Environ. Sci. Technol. 2015, 49 (5), 2694–2702.

(18) Kim, S.-K.; Kannan, K. Perfluorinated Acids in Air, Rain, Snow, Surface Runoff, and Lakes: Relative Importance of Pathways to Contamination of Urban Lakes. Environ. Sci. Technol. 2007, 41 (24), 8328–8334.

(19) DuPont. Dupont Capstone Fluorosurfactant FS-50 Technical Information https://www.chemours.com/Capstone/en_US/assets/downloads/K-02043-2_Capstone_FS-50.pdf (accessed Oct 4, 2016).

Appendix A:

Supporting Information for Chapter Two

Identification of Novel Fluorinated Surfactants in Aqueous Film Forming Foams Used in Ontario, Canada and Commercial Surfactant Concentrates

Contents

Materials

All chemicals were used as received. [Glu^1]-Fibrinopeptide B human (≥90%), ammonium acetate (≥98%), perfluorooctanoic acid (PFOA, 96%), N,N-dimethyldodecylamine (DMDDA, 97%), cetyltrimethylammonium chloride (CTMA, 25 wt.% in H_2O), 3-(N,N-Dimethyloctylammonio)propanesulfonate inner salt (DMOAPS; ≥98%), Empigen BB detergent (~35% in H_2O, N-(Alkyl C_{10}-C_{16})-N,N-dimethylglycine betaine), methanesulfonic acid (≥99%), tetrahydrofuran, 3-(dimethylamino)-1-propylamine (99%), acetone-d_6, 4'-(trifluoromethoxy)acetanilide, trifluoroacetic acid (TFA, 99%), and perfluoropropionic acid (PFPrA, 97%) were purchased from Sigma-Aldrich (Oakville, Ontario, Canada). Omnisolv water, high performance liquid chromatography (HPLC) grade methanol, OmniSolv Methyl-t-Butyl Ether, and formic acid (98%) were purchased from EMD chemicals (Gibbstown, NJ). Ammonium hydroxide solution (28%) was purchased from BDH (Columbus, WI). 2H,2H,3H,3H-Perfluorodecanoic acid (7:3 fluorotelomer carboxylic acid, 7:3 FTCA, 97%), perfluorooctane sulfonamide (FOSA, 98%), and perfluorononanoyl chloride (97%) were purchased from SynQuest Labs Inc. (Alachua, FL). Sodium acetate (99%) was purchased from ACP Chemicals (Montreal, Quebec, Canada). Milli-Q water (18MΩ cm) was used for TOF-CIC and SPE extractions.

Sampling

AFFF samples 1 through 11 were obtained from the Ontario Ministry of the Environment (MOE). They were collected at fire sites in Ontario, Canada where they were deployed in polyethylene terephthalate (PET) bottles by either MOE personnel or the operators of the AFFF systems. The samples were obtained either from a holding tank after mixing the AFFF with water ("mixed") or from the original container of AFFF ("pure"). The "pure" and "mixed" samples are identified in Table A1 where known. Due to limitations in the sensitivity of the PFAS identification techniques and the chemically related PFASs identified in each sample, the PFASs identified in each sample are believed to be components of the AFFFs identified as currently occupying the holding tanks when "mixed" samples were taken and not carryover from previous contents of the tanks.

Mixed-Mode Ion Exchange SPE Methods

The cartridges used were Oasis weak anion exchange (WAX) SPE cartridges (6 cc, 200 mg, 30 μm) and Oasis weak cation exchange (WCX) SPE cartridges (6 cc, 200 mg, 30 μm) from Waters (Milford, MA). All extractions were performed using gravity to elute the cartridges. WAX cartridges were conditioned with 2 mL of 0.1% NH_4OH in methanol, 2 mL of methanol, and 2 mL of water. Samples were loaded as 2 mL of either 1000-fold diluted AFFF or 10,000-fold diluted FS-330 or FS-1520 in water with 0.04% formic acid. Foam 7 was diluted 2000-fold prior to extraction due to limited sample volume. The cartridges were then washed with 2 mL of pH 5 acetate buffer and dried under a flow of nitrogen. Elution solvents were 4 mL plus 2 mL of methanol, 4 mL of 2% formic acid in methanol, 2 mL of methanol, and 4 mL of 1% NH_4OH in methanol. WCX cartridges were conditioned with 2 mL of 0.1% formic acid in methanol, 2 mL of methanol, and 2 mL of water. Samples were loaded as for the WAX method, washed with 2 mL of pH 7.5 ammonium acetate buffer, and dried under a flow of nitrogen. Cartridges were then eluted with 4 mL plus 2 mL of methanol, 4 mL of 2% NH_4OH in methanol, 2 mL of methanol, and 4 mL of 2% formic acid in methanol.

Recoveries of the model compounds in fractions corresponding to their ionic nature without the additional 2 mL of methanol in the first elution were determined by LC-MS/MS using methods outlined in the LC-MS/MS section and in Tables S3 and S4. To determine recovery of model compounds, solutions with 2 μM each of PFOA, 7:3 FTCA, and FOSA; 6 μM each of DMOAPS and CTMA; 8 μM DMDDA and 12 μM Empigen BB in 0.04% aqueous formic acid were prepared and 2 mL aliquots were loaded on the SPE cartridges. These standard solutions were serially diluted to prepare 6 or 7 point external calibration curves to determine percent recovery by LC-MS/MS. Percent recoveries of model compounds were calculated taking into account the volume of the SPE fraction recovered in relation to the 2 mL of sample loaded and are shown in Table A7. To obtain adequate recoveries of DMDDA in basic methanol by WCX, the collected fraction was neutralized with 82 μL of 98% formic acid. This was necessary because it seemed that in the 1:1 methanol: water used to make up the LC-MS/MS samples, neutral DMDDA sorbed to container walls under basic conditions resulting in low recoveries of DMDDA.

The additional 2 mL of methanol used to elute the first fraction was added to prevent carryover of neutral fraction components into the weak acid or base fraction. The elution volume was optimized by extraction of Foam 12 samples by WAX and WCX SPE with additional 1 mL portions of each eluent collected separately analyzed by TOF-CIC to assess when organofluorine belonging in each fraction was fully eluted.

TOF-CIC Method

Fractions from the ion exchange SPE methods were analyzed using TOF-CIC methods described previously.[1,2] First, samples were combusted on a ceramic boat at 900-1000°C in an Automated Quick Furnace (AQF-100) automated combustion unit (Mitsubishi Chemical Analytech, Japan). The HF evolved from combustion of organic fluorine was collected in an aqueous absorption unit, dissociated to H^+ and F^-, and analyzed for F^- on an ICS-2100 ion chromatography system (Dionex Co. Ltd., Sunnyvale, CA, USA) with conductivity detection. In the furnace, the combustion gas was oxygen and the carrier gas was argon. IC was performed at a flow rate of 0.25 mL/min with a gradient that began at 2 mM of potassium hydroxide (KOH), held for 1 minute, increased to 40 mM KOH over 8 min., held for 3 min., immediately returned to 2mM KOH and remained at 2 mM until 18 minutes. An external calibration curve using 0.2, 2, 20, 100, and 200 ng F-/mL and an injection volume of 1.0 mL was used. Linearity of the calibration curve was good with $R^2 > 0.9999$. An internal standard, methanesulfonic acid (CH_3SO_3H), in the absorption solution corrected for any changes in the volume of the absorption solution during the combustion process.

TOF concentrations in the sample extracts were corrected using the TOF concentrations in solvent blanks extracted simultaneously and were multiplied by the volume of the SPE fraction to determine the mass of F in each fraction shown in Figure A22. Duplicate extraction and TOF-CIC analysis was performed with 2 AFFF samples for both WAX and WCX SPE and relative standard deviations were less than 10% for highly fluorinated fractions (containing >4 µg of F), which shows that SPE and TOF-CIC on AFFF samples was reproducible.

QTOF-MS Analysis

Direct loop injections on a AB/Sciex QStar XL mass spectrometer (MDS Sciex, Concord, ON, Canada) were made using a 100 μL/min flow of 50:50 methanol: 0.1% formic acid in water in positive ion mode electrospray (ESI+) or 50:50 methanol: aqueous 10 mM ammonium acetate in negative ion mode electrospray (ESI-) delivered by an 1100 series HPLC pump (Agilent Technologies, Inc., Santa Carla, CA, USA). Mass spectra were collected in full scan TOF mode and in product ion mode from *m/z* 90 to 1000. Additional mass spectra in product ion mode from *m/z* 50 to 1000 were collected to determine the molecular formulae of product ions used in LC-MS/MS with *m/z* between 50 and 90. The source temperature was set to 200ºC. The declustering potential was set to 60 V in ESI+ and -30V in ESI-. The focusing potential was set to 60V in ESI+ and -30V in ESI-. External calibrations for accurate masses were performed prior to each run using 10 times diluted ESI Tune Mix for Ion Traps (Agilent Technologies, Inc., Santa Carla, CA, USA) for ESI+; a mixture of PFCAs (TFA, PFPrA, PFOA) and Zonyl NF surfactant containing polyfluoroalkyl phosphate diesters (diPAPs) for ESI-; or product ions of Glu-fibrinopeptide for some ESI+ CID experiments.

FTICR-MS Method

Spectra were generated using a Varian FTICR-MS (Varian Inc., Walnut Creek, CA, USA) consisting of a Varian ESI source, Varian 920-MS, and a Varian 9.4 Tesla superconducting magnet. Samples consisted of 1000- to 100,000- fold diluted AFFF or commercial surfactant concentrate prepared with methanol in most cases and 1:1 methanol: water for Foam 8 since a precipitate formed in methanol. For ESI+ analysis, samples were mixed with ESI Tune Mix for Ion Traps (Agilent Technologies, Inc., Santa Carla, CA, USA) at a ratio of 100:1 or 50:1 (sample: tune mix) for internal calibration. Samples were infused at 2.5 to 5 μl/min with a syringe pump into the ESI source, where the ESI voltage was +3800 V in ESI+ and -3800 V in ESI-, while the cone voltage was +45 V in ESI+ and -45V in ESI-. FTICR-MS spectra were collected using direct mode (broadband) detection from *m/z* 150 to 1000 with an arbitrary waveform excitation, an acquisition time of 1049 ms and an analog to digital conversion rate of 2 MHz. This

resulted in a resolution of approximately 120,000 (full width at half maximum) at *m/z* 500. For most samples a single scan was collected, while for Foam 1, Foam 12, and FS-1520, 100 scans were summed in ESI+ and for Foam 12 and FS-330, 83 and 50 scans were summed, respectively, in ESI-. Internal mass calibration was performed using ions in ESI Tune Mix for Ion Traps in ESI+ or known PFASs in the samples in ESI-, such as PFSAs, FTSAs, and 6:2 FTSAS previously detected using LC-MS/MS[3] or $C_xF_{2x+1}^-$ fragments. Mass spectra were also screened for sodium adducts, which do not represent distinct fluorinated surfactants. Foam 7 was not analyzed by FTICR-MS due to limited sample volume.

LC-MS/MS Methods

The LC-MS/MS system used was a Water Acquity UPLC system with a Kinetex XB-C18 column (4.6 x 50 mm, 2.6 µm, 100Å) (Phenomenex, Torrance, CA), followed by mass analysis on an API 4000 triple quadrupole mass spectrometer (Applied Biosystems/MDS Sciex, Concord, ON, Canada). All methods used gradients of 10 mM ammonium acetate in water (A) and 10 mM ammonium acetate in methanol (B). In all LC-MS/MS methods, the ion source temperature was 550ºC, curtain gas was 10, ion source gas 1 was 40, ion source gas 2 was 40, and collision gas was 12. In all ESI+ methods, the ion source potential was 4500 V, the entrance potential was 10V, and the collision cell exit potential was 15V. In all ESI- methods, the ion source potential was -4500 V, the entrance potential was -10V, and the collision cell exit potential was -15V.

The LC gradients used are shown in Table A4. In all methods the flow rate was 0.5 mL/min and the injection volume was 30 µL. The gradients used for various analytes were: LC 1 for SPE model compounds in ESI+, LC 2 for SPE model compounds in ESI-, LC 3 for **I**, **J**, **K**, **M**, **N**, **O**, and **P**, LC 4 for **K**, LC 5 for **R** and **S**, LC 6 for **T** and **V**, LC 7 for **U** and LC 8 for **A**, **B**, **C**, **D**, **E**, **F**, **G**, and **H**. SPE extracts of model compounds were diluted 100-fold in 50:50 methanol: water prior to LC-MS/MS analysis. Typical dilutions of AFFF samples in 1:1 methanol: water prior to LC-MS/MS analysis were 10,000- to 50,000-fold, while FS-330 and FS-1520 were diluted 1,000,000-fold.

The MS/MS transitions for various analytes in ESI+ are shown in Table A5 and in ESI- are shown in Table A6. No more than 22 transitions were included and any one run using dwell times of 20 ms.

In the LC-MS/MS analysis of SPE fractions containing model compounds, both calibration standards and SPE fractions were analyzed in duplicate to determine recoveries in the SPE method. These recovery tests were performed for both WAX (n = 4) and WCX (n = 3) SPE. Calibration curves calculated using both analyses of the standards had good linearity with most R^2 values greater than 0.99 and all but one R^2 value greater than 0.95. Reproducibility was also acceptable with standard deviations for duplicate analyses of percent recovery within a trial less than 10% except for CTMA in one trial and standard deviations for peak areas of most standards less than 10%. To determine averages and standard deviations for recoveries, recoveries for both analyses of each trial were used.

Synthesis of N-(3-(dimethylamino)propyl)perfluorononanamide (DMAPFNAE)

Tetrahydrofuran (3 mL) and 3-(dimethylamino)-1-propylamine (3.6 mmol) were added to a round-bottom flask cooled in an ice bath. With stirring, perfluorononanoyl chloride (1.7 mmol) was added slowly to the round-bottom flask resulting in a white precipitate. After warming to room temperature, the tetrahydrofuran was evaporated under a gentle stream of nitrogen gas. The product was extracted with 5 mL of methyl *tert*-butyl ether (MTBE) and 5 mL of water. The MTBE layer was collected and the water layer was extracted with a second 5 mL of MTBE. The MTBE layers were combined, dried with anhydrous magnesium sulfate, and the MTBE was evaporated under a gentle stream of nitrogen gas resulting in DMAPNFAE as yellow oil. ^{19}F-NMR showed no detectable PFNA hydrolysis side product. ^{1}H NMR (400 MHz, acetone-d_6): δ 3.44 (quart, 2H), 2.48 (t, 2H), 2.25 (s, 6H), 1.77 (quint, 2H). ^{19}F NMR (377 MHz, acetone-d_6) δ = -80.8 (t, J=11.3 Hz, 3F, CF_3), -119.3 (m, 2F, CF_2), -121.3 to -122.4 [m, 10F, $(CF_2)_5$], -125.8 (m, 2F, CF_2). QTOF-MS: predicted for $C_{14}H_{14}ON_2F_{17}^+$ *m/z* 549.0829; measured *m/z* 549.0833; error 0.38 mDa.

References

(1) Rand, A. A.; Mabury, S. A. Covalent Binding of Fluorotelomer Unsaturated Aldehydes (FTUALs) and Carboxylic Acids (FTUCAs) to Proteins. *Environ. Sci. Technol.* 2013, *47* (3), 1655–1663.

(2) Rand, A. A.; Mabury, S. A. In Vitro Interactions of Biological Nucleophiles with Fluorotelomer Unsaturated Acids and Aldehydes: Fate and Consequences. *Environ. Sci. Technol.* 2012, *46* (13), 7398–7406.

(3) Weiner, B.; Yeung, L. W. Y.; Marchington, E. B.; D'Agostino, L. A.; Mabury, S. A. Organic fluorine content in aqueous film forming foams (AFFFs) and biodegradation of the foam component 6 : 2 fluorotelomermercaptoalkylamido sulfonate (6 : 2 FTSAS). *Environ. Chem.* 2013, *10* (6), 486–493.

Table A1: MSDS information of AFFF samples.

Sample ID	Collection Location, Date	AFFF Manufacturer, MSDS Date	AFFF name	Listed Fluorochemicals; Pure or Mixed?[f]
1	Toronto, 2004	Hazard Control Tech., 1997	F-500	no; mixed
2	Cobourg, 2005	Angus Fire, na	N-4210-21-900-4823 3	no; pure
3	Maxville, 2005	Angus Fire, 2004	Tridol S	fluorosurfactants 5-10%; mixed
4	GTAA, 2005	Ansul, 2002	Ansulite 3% AFFF DC-3	fluorosurfactants 5-12%; pure
5[a]	Thorold, 2007	Niagara 1-3: Angus Fire, 2000 Forexpan: Angus Fire, 1997	Niagara 1-3, Forexpan	Niagara 1-3: fluorosurfactants <5%; Forexpan: no; unknown
6	London, 2007	Hazard Control Tech., 2003	F-500	no; pure
7	Trenton, 2007	na	Na	na; unknown
8	Thorold, 2007[b]	Angus Fire, 2000	Niagara 1-3	fluorosurfactants < 5%; pure
9	Thorold, 2007[b]	Angus Fire, 2007	Hi Combat A	no; pure
10	Thorold, 2007[b]	3M, 2005	ATC-603 Light water	N-DMAP PFOSA potassium salt 1-5%c; fluoroaliphatic polymer 1-5%; residual organic fluoro-chemicals 0-1%; pure
11	Eastern ON, 2008	Ansul, 2006	Ansul Ansulite ARC	Fluorosurfactants; unknown
12	3M AFFF[d]	3M, 1999	FC-203FC Light water Brand AFFF	amphoteric fluoroalkylamide 1-5% residual fluorochemicals < 1% PFSA salts 0.5-1.5%; pure
FS-330	FS-330[d]	Mason Chemical Co., 2005	FS-330	fluoroaliphatic surfactants 30%[e]
FS-1520	FS-1520[d]	Mason Chemical Co., 2005	FS-1520	fluoroaliphatic betaine surfactant 20%[e]

na=not available. [a] Foam 5 is a foam mixture of Niagara 1-3 and Forexpam. [b] Samples 8-10 were collected on a later date than sample 5 from the same fire location. [c] N-dMAP-PFOSA = *N*-[3-(Dimethylamino)propyl] perfluorooctane sulfonamide, N'-oxide; CAS No. 178094-69-4. [d] Commercial products. [e] Masurf FS-fluorosurfactants do not contain PFOS. [f] "Pure" samples are from original AFFF containers, "mixed" samples are from holding tanks after mixing with water and "unknown" samples may be pure or mixed.

Table A2: Summary of Fluorinated Surfactant Ions Detected by FTICR-MS, QTOF-MS, and LC-MS/MS

Structure	*n* = i.e: Chain Length	Molecular Formula	Theor. m/z	Accurate Mass Results (FTICR-MS unless marked with * for QTOF-MS)			Observed in the following foams by:			SPE Fraction
				Observed m/z	Error (mDa)	Foam	FTICR-MS	QTOF-MS of SPE fractions	LC-MS/MS	
A 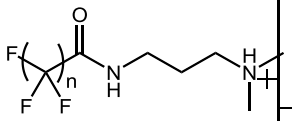	3	$C_9H_{14}ON_2F_7^{+1}$	299.0989						2, 12	
	4	$C_{10}H_{14}ON_2F_9^{+1}$	349.0957	349.0949	-0.8	12	12		2, 12	
	5	$C_{11}H_{14}ON_2F_{11}^{+1}$	399.0925	399.0923	-0.2	12	12		2, 12	
	6	$C_{12}H_{14}ON_2F_{13}^{+1}$	449.0893	449.0890	-0.3	12	12, FS-330		2, 12, FS-330	
	7	$C_{13}H_{14}ON_2F_{15}^{+1}$	499.0861	499.0864	0.3	12	2, 12, FS-330	2	2, 12, FS-330	Bases
	8	$C_{14}H_{12}ON_2F_{17}^{-1}$	547.0684	547.0684	0.0	FS-330	FS-330	FS-330		Bases
		$C_{14}H_{14}ON_2F_{17}^{+1}$	549.0829	549.0829	0.0	FS-330	FS-330	FS-330	2, 12, FS-330	Bases
	9	$C_{15}H_{14}ON_2F_{19}^{+1}$	599.0797	599.0796	-0.1	FS-330	FS-330		FS-330	
	10	$C_{16}H_{12}ON_2F_{21}^{-1}$	647.0620	647.0615	-0.5	FS-330	FS-330	FS-330		Bases
		$C_{16}H_{14}ON_2F_{21}^{+1}$	649.0765	649.0768	0.3	FS-330	FS-330	FS-330	FS-330	Bases
	11	$C_{17}H_{14}ON_2F_{23}^{+1}$	699.0733						FS-330	
	12	$C_{18}H_{14}ON_2F_{25}^{+1}$	749.0701	749.0702	0.1	FS-330	FS-330	FS-330	FS-330	Bases
	14	$C_{20}H_{14}ON_2F_{29}^{+1}$	849.0643						FS-330	
B 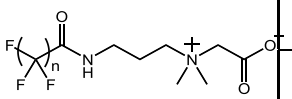 PFAAB	6	$C_{14}H_{14}O_3N_2F_{13}^{-1}$	505.0802	505.0796	-0.6	FS-330	FS-330			
		$C_{14}H_{16}O_3N_2F_{13}^{+1}$	507.0948						FS-330	
	7	$C_{15}H_{14}O_3N_2F_{15}^{-1}$	555.0770	555.0768	-0.2	FS-330	FS-330			
		$C_{15}H_{16}O_3N_2F_{15}^{+1}$	557.0916	557.0916	0.0	FS-330	FS-330		FS-330	
	8	$C_{16}H_{14}O_3N_2F_{17}^{-1}$	605.0739	605.0743	0.4	FS-330	FS-330	FS-330		Neutral

Structure	*n* = i.e: Chain Length	Molecular Formula	Theor. m/z	Accurate Mass Results (FTICR-MS unless marked with * for QTOF-MS)			Observed in the following foams by:			SPE Fraction
				Observed m/z	Error (mDa)	Foam	FTICR-MS	QTOF-MS of SPE fractions	LC-MS/MS	
B 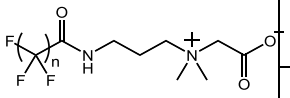 PFAAB	8	$C_{16}H_{16}O_3N_2F_{17}^{+1}$	607.0884	607.0887	0.3	FS-330	FS-330	FS-330	FS-330	Neutral
	9	$C_{17}H_{16}O_3N_2F_{19}^{+1}$	657.0852						FS-330	
	10	$C_{18}H_{14}O_3N_2F_{21}^{-1}$	705.0675	705.0673	-0.2	FS-330	FS-330	FS-330		Neutral
		$C_{18}H_{16}O_3N_2F_{21}^{+1}$	707.0820	707.0821	0.1	FS-330	FS-330	FS-330	FS-330	Neutral
	11	$C_{19}H_{16}O_3N_2F_{23}^{+1}$	757.0788						FS-330	
	12	$C_{20}H_{14}O_3N_2F_{25}^{-1}$	805.0611	805.0602	-0.9	FS-330	FS-330	FS-330		Neutral
		$C_{20}H_{16}O_3N_2F_{25}^{+1}$	807.0756	807.0754	-0.2	FS-330	FS-330	FS-330	FS-330	Neutral
	13	$C_{21}H_{16}O_3N_2F_{27}^{+1}$	857.0724						FS-330	
	14	$C_{22}H_{16}O_3N_2F_{29}^{+1}$	907.0692						FS-330	
C 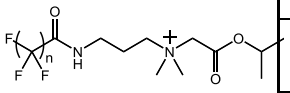	8	$C_{19}H_{22}O_3N_2F_{17}^{+1}$	649.1354	649.1350	-0.4	FS-330	FS-330	FS-330	FS-330	Permanent cation
	10	$C_{21}H_{22}O_3N_2F_{21}^{+1}$	749.1290	749.1286	-0.4	FS-330	FS-330	FS-330	FS-330	Permanent cation
	12	$C_{23}H_{22}O_3N_2F_{25}^{+1}$	849.1226						FS-330	
D 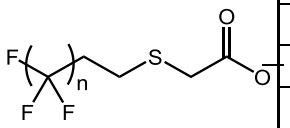	4	$C_8H_6O_2SF_9^{-1}$	336.9950						FS-1520	
	6	$C_{10}H_6O_2SF_{13}^{-1}$	436.9886	436.9888	0.2	FS-1520	FS-1520	FS-1520	FS-1520	Weak Acid
	8	$C_{12}H_6O_2SF_{17}^{-1}$	536.9823	536.9825	0.2	FS-1520	FS-1520	FS-1520	FS-1520	Weak Acid
	10	$C_{14}H_6O_2SF_{21}^{-1}$	636.9759	636.9761	0.2	FS-1520	FS-1520	FS-1520	FS-1520	Weak Acid
E 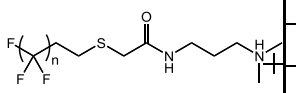	4	$C_{13}H_{20}ON_2SF_9^{+1}$	423.1147						FS-1520	
	6	$C_{15}H_{20}ON_2SF_{13}^{+1}$	523.1083	523.1084	0.1	FS-1520	FS-1520	FS-1520	FS-1520	Bases
	8	$C_{17}H_{20}ON_2SF_{17}^{+1}$	623.1019	623.1019	0.0	FS-1520	FS-1520	FS-1520	FS-1520	Bases
	10	$C_{19}H_{20}ON_2SF_{21}^{+1}$	723.0956	723.0961	0.5	FS-1520	FS-1520	FS-1520	FS-1520	Bases
	12	$C_{21}H_{20}ON_2SF_{25}^{+1}$	823.0892	823.0896	0.4	FS-1520	FS-1520		FS-1520	

Structure	*n* = i.e: Chain Length	Molecular Formula	Theor. m/z	Accurate Mass Results (FTICR-MS unless marked with * for QTOF-MS)			Observed in the following foams by:			SPE Fraction
				Observed m/z	Error (mDa)	Foam	FTICR-MS	QTOF-MS of SPE fractions	LC-MS/MS	
F 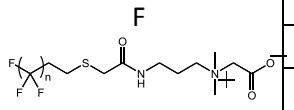 FTSAB	4	$C_{15}H_{22}O_3N_2SF_9^{+1}$	481.1202						FS-1520	
	6	$C_{17}H_{22}O_3N_2SF_{13}^{+1}$	581.1138	581.1138	0.0	FS-1520	FS-1520	FS-1520	FS-1520	Neutral
	8	$C_{19}H_{22}O_3N_2SF_{17}^{+1}$	681.1074	681.1078	0.4	FS-1520	FS-1520	FS-1520	FS-1520	Neutral
	10	$C_{21}H_{22}O_3N_2SF_{21}^{+1}$	781.1010	781.1018	0.8	FS-1520	FS-1520	FS-1520	FS-1520	Neutral
	12	$C_{23}H_{22}O_3N_2SF_{25}^{+1}$	881.0946	881.0950	0.4	FS-1520	FS-1520		FS-1520	
	14	$C_{25}H_{22}O_3N_2SF_{29}^{+1}$	981.0883						FS-1520	
G 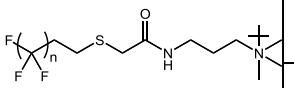	6	$C_{16}H_{22}ON_2SF_{13}^{+1}$	537.1240	537.1241	0.1	FS-1520	FS-1520	FS-1520	FS-1520	Permanent cation
	8	$C_{18}H_{22}ON_2SF_{17}^{+1}$	637.1176	637.1179	0.3	FS-1520	FS-1520	FS-1520	FS-1520	Permanent cation
	10	$C_{20}H_{22}ON_2SF_{21}^{+1}$	737.1121	737.1124	0.3	FS-1520	FS-1520	FS-1520	FS-1520	Permanent cation
H 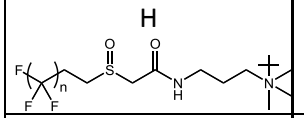	6	$C_{16}H_{22}O_2N_2SF_{13}^{+1}$	553.1189	553.1185	-0.4*	FS-1520		FS-1520	FS-1520	Permanent cation
I 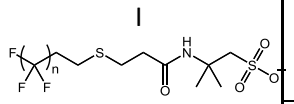 FTSAS	4	$C_{13}H_{17}O_4NS_2F_9^{-1}$	486.0461	486.0460	-0.1	11	1, 3, 4, 11	1, 3	1, 3, 4, 8, 11	Strong Acid
		$C_{13}H_{19}O_4NS_2F_9^{+1}$	488.0606						1, 3, 4, 11	
	6	$C_{15}H_{17}O_4NS_2F_{13}^{-1}$	586.0397	586.0392	-0.5	5	1, 3, 4, 5, 11	1, 3, 4, 5, 8, 11	1, 3, 4, 5, 8, 11	Strong Acid
		$C_{15}H_{19}O_4NS_2F_{13}^{+1}$	588.0542	588.0536	-0.6	1	1	1, 3, 4, 8, 11	1, 3, 4, 5, 8, 11	Strong Acid
	8	$C_{17}H_{17}O_4NS_2F_{17}^{-1}$	686.0333	686.0327	-0.6	11	1, 3, 4, 11	1, 3, 4, 11	1, 3, 4, 5, 8, 11	Strong Acid

Structure	*n* = i.e: Chain Length	Molecular Formula	Theor. m/z	Accurate Mass Results (FTICR-MS unless marked with * for QTOF-MS)			Observed in the following foams by:			SPE Fraction
				Observed m/z	Error (mDa)	Foam	FTICR-MS	QTOF-MS of SPE fractions	LC-MS/MS	
I 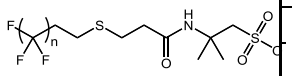 FTSAS	8	$C_{17}H_{19}O_4NS_2F_{17}^{+1}$	688.0479						1, 3, 4, 5, 8, 11	Strong Acid
	10	$C_{19}H_{17}O_4NS_2F_{21}^{-1}$	786.0269	786.0264	-0.5	11	11		1, 3, 4, 11	Strong Acid
		$C_{19}H_{19}O_4NS_2F_{21}^{+1}$	788.0415						3, 4, 11	
	12	$C_{21}H_{17}O_4NS_2F_{25}^{-1}$	886.0205						11	
	14	$C_{23}H_{17}O_4NS_2F_{29}^{-1}$	986.0141						11	
J 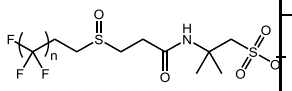	4	$C_{13}H_{17}O_5NS_2F_9^{-1}$	502.0410						1, 3, 4	
		$C_{13}H_{19}O_5NS_2F_9^{+1}$	504.0555						1	
	6	$C_{15}H_{17}O_5NS_2F_{13}^{-1}$	602.0346	602.0343	-0.3	1	1, 3, 4, 5, 11	1, 3, 4, 8, 11	1, 3, 4, 5, 7, 8,	Strong Acid
		$C_{15}H_{19}O_5NS_2F_{13}^{+1}$	604.0492	604.0487	-0.5	1	1	1, 3, 4, 8	1, 3, 4, 5, 8, 11	Strong Acid
	8	$C_{17}H_{17}O_5NS_2F_{17}^{-1}$	702.0282						1, 3, 4, 5, 7, 11	
		$C_{17}H_{19}O_5NS_2F_{17}^{+1}$	704.0428						1, 3, 4, 5, 11	
	10	$C_{19}H_{17}O_5NS_2F_{21}^{-1}$	802.0218						1, 4, 11	
		$C_{19}H_{19}O_5NS_2F_{21}^{+1}$	804.0364						11	
K 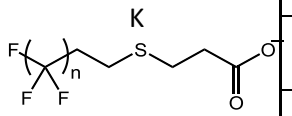	4	$C_9H_8O_2SF_9^{-1}$	351.0107						8	
	6	$C_{11}H_8O_2SF_{13}^{-1}$	451.0043	451.0041	-0.2*	8		8	4, 5, 8, 11	Weak Acid
	8	$C_{13}H_8O_2SF_{17}^{-1}$	550.9979						8	

Structure	*n* = i.e: Chain Length	Molecular Formula	Theor. m/z	Accurate Mass Results (FTICR-MS unless marked with * for QTOF-MS)			Observed in the following foams by:			SPE Fraction
				Observed m/z	Error (mDa)	Foam	FTICR-MS	QTOF-MS of SPE fractions	LC-MS/MS	
L 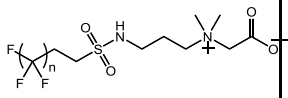 FTAB	4	$C_{13}H_{18}O_4N_2SF_9^{-1}$	469.0849							
		$C_{13}H_{20}O_4N_2SF_9^{+1}$	471.0995						5	
	6	$C_{15}H_{18}O_4N_2SF_{13}^{-1}$	569.0785	569.0780	-0.5	1	1, 3, 5	1, 3, 5, 8		Neutral
		$C_{15}H_{20}O_4N_2SF_{13}^{+1}$	571.0931	571.0926	-0.5	3	1, 3, 5	1, 3, 5, 8	1, 3, 5, 8	Neutral
	8	$C_{17}H_{18}O_4N_2SF_{17}^{-1}$	669.0721	669.0754	3.3*	1		1		Neutral
		$C_{17}H_{20}O_4N_2SF_{17}^{+1}$	671.0867	671.0874	0.7	1	1, 5	1, 5	1, 3, 5	Neutral
	10	$C_{19}H_{18}O_4N_2SF_{21}^{-1}$	769.0657							
		$C_{19}H_{20}O_4N_2SF_{21}^{+1}$	771.0803	771.0796	-0.7	1	1		1, 5	
	12	$C_{21}H_{20}O_4N_2SF_{25}^{+1}$	871.0739						1, 5	
M 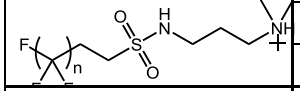	6	$C_{13}H_{18}O_2N_2SF_{13}^{+1}$	513.0876	513.0875	-0.1	3	1, 3, 5	1, 3, 5, 8	1, 3, 5, 8	Base
	8	$C_{15}H_{18}O_2N_2SF_{17}^{+1}$	613.0812	613.0805	-0.7	1	1	1	1, 5	Base
	10	$C_{17}H_{18}O_2N_2SF_{21}^{+1}$	713.0748	713.0741	-0.7	1	1			
N 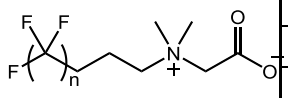 FTB	5	$C_{12}H_{15}O_2NF_{11}^{+1}$	414.0922	414.0921	-0.1	4	4	4, 7	4, 7	Neutral
	7	$C_{14}H_{15}O_2NF_{15}^{+1}$	514.0858	514.0858	0.0	4	4	4, 7	4, 7	Neutral
	9	$C_{16}H_{15}O_2NF_{19}^{+1}$	614.0794	614.0779	-1.5	4	4	4	4, 7	Neutral
	11	$C_{18}H_{15}O_2NF_{23}^{+1}$	714.0730						4, 7	
	13	$C_{20}H_{15}O_2NF_{27}^{+1}$	814.0666						4, 7	
O 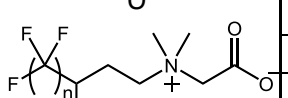 FTB	5	$C_{12}H_{14}O_2NF_{12}^{+1}$	432.0827	432.0825	-0.2	4	4	4, 7	4, 7	Neutral
	7	$C_{14}H_{14}O_2NF_{16}^{+1}$	532.0764	532.0760	-0.4	4	4	4, 7	4, 7	Neutral
	9	$C_{16}H_{14}O_2NF_{20}^{+1}$	632.0700	632.0701	0.1	4	4	4, 7	4, 7	Neutral
	11	$C_{18}H_{14}O_2NF_{24}^{+1}$	732.0636	732.0632	-0.4*	7		7	4, 7	Neutral
	13	$C_{20}H_{14}O_2NF_{28}^{+1}$	832.0572						4, 7	
	15	$C_{22}H_{14}O_2NF_{32}^{+1}$	932.0508						7	

Structure	*n* = i.e: Chain Length	Molecular Formula	Theor. m/z	Accurate Mass Results (FTICR-MS unless marked with * for QTOF-MS)			Observed in the following foams by:			SPE Fraction
				Observed m/z	Error (mDa)	Foam	FTICR-MS	QTOF-MS of SPE fractions	LC-MS/MS	
P 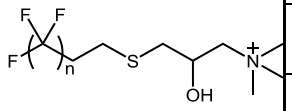 FTSHA	4	$C_{12}H_{19}ONSF_9^{+1}$	396.1038						11	
	6	$C_{14}H_{19}ONSF_{13}^{+1}$	496.0974	496.0974	0.0	11	11	11	11	Permanent cation
	8	$C_{16}H_{19}ONSF_{17}^{+1}$	596.0910	596.0920	1.0	11	11		11	
	10	$C_{18}H_{19}ONSF_{21}^{+1}$	696.0847						11	
Q 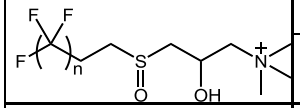	6	$C_{14}H_{19}O_2NSF_{13}^{+1}$	512.0923	512.0923	0.0*	11		11	11	Permanent cation
	8	$C_{16}H_{19}O_2NSF_{17}^{+1}$	612.0860	612.0876	1.6*	11		11	11	Permanent cation
R/S 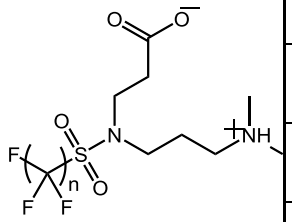 PFASAC 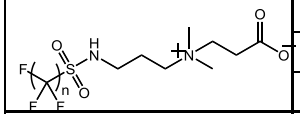	3	$C_{11}H_{16}O_4N_2SF_7^{-1}$	405.0725	405.0726	0.1	12	12	2		Neutral
		$C_{11}H_{18}O_4N_2SF_7^{+1}$	407.0870	407.0870	0.0	12	2, 12	2, 12	2, 12	Neutral
	4	$C_{12}H_{16}O_4N_2SF_9^{-1}$	455.0693	455.0695	0.2	12	12	2		Neutral
		$C_{12}H_{18}O_4N_2SF_9^{+1}$	457.0838	457.0840	0.2	12	2, 12	2, 12	2, 12	Neutral
	5	$C_{13}H_{16}O_4N_2SF_{11}^{-1}$	505.0661	505.0663	0.2	12	12	2		Neutral
		$C_{13}H_{18}O_4N_2SF_{11}^{+1}$	507.0806	507.0810	0.4	12	2, 12	2, 12	2, 12	Neutral
	6	$C_{14}H_{16}O_4N_2SF_{13}^{-1}$	555.0629	555.0633	0.4	12	2, 12	2, 12		Neutral
		$C_{14}H_{18}O_4N_2SF_{13}^{+1}$	557.0774	557.0780	0.6	12	2, 12	2, 12	2, 12	Neutral
	7	$C_{15}H_{18}O_4N_2SF_{15}^{+1}$	607.0742	607.0745	0.3	12	2, 12		2, 12	
	8	$C_{16}H_{18}O_4N_2SF_{17}^{+1}$	657.0710	657.0714	0.4	12	2, 12		2, 12	
T 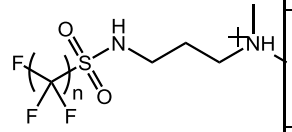	3	$C_8H_{12}O_2N_2SF_7^{-1}$	333.0513	333.051	-0.3	12	2, 12	2, 12		Bases
		$C_8H_{14}O_2N_2SF_7^{+1}$	335.0659	335.0658	-0.1	12	2, 12	2, 12	2, 12	Bases
	4	$C_9H_{12}O_2N_2SF_9^{-1}$	383.0481	383.048	-0.1	12	2, 12	2, 12		Bases
		$C_9H_{14}O_2N_2SF_9^{+1}$	385.0627	385.0627	0.0	12	2, 12	2, 12	2, 12, 5, 10	Bases
	5	$C_{10}H_{12}O_2N_2SF_{11}^{-1}$	433.0449	433.045	0.1	12	2, 12	2, 12		Bases

Structure	*n* = i.e: Chain Length	Molecular Formula	Theor. m/z	Accurate Mass Results (FTICR-MS unless marked with * for QTOF-MS)			Observed in the following foams by:			SPE Fraction
				Observed m/z	Error (mDa)	Foam	FTICR-MS	QTOF-MS of SPE fractions	LC-MS/MS	
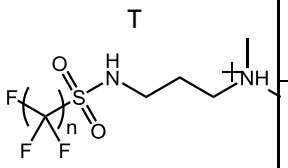 T	5	$C_{10}H_{14}O_2N_2SF_{11}^{+1}$	435.0595	435.0596	0.1	12	2, 12	2, 12	2, 12, 5, 10	Bases
	6	$C_{11}H_{12}O_2N_2SF_{13}^{-1}$	483.0417	483.042	0.3	12	2, 12	2, 12		Bases
		$C_{11}H_{14}O_2N_2SF_{13}^{+1}$	485.0563	485.0566	0.3	12	2, 12, 5, 10	2, 12	2, 12, 5, 10	Bases
	7	$C_{12}H_{12}O_2N_2SF_{15}^{-1}$	533.0386	533.039	0.4	12	12			Bases
		$C_{12}H_{14}O_2N_2SF_{15}^{+1}$	535.0531	535.0526	-0.5	12	12		2, 12, 5, 10	Bases
	8	$C_{13}H_{12}O_2N_2SF_{17}^{-1}$	583.0354	583.036	0.6	12	12			Bases
		$C_{13}H_{14}O_2N_2SF_{17}^{+1}$	585.0499	585.0501	0.2	12	2, 12, 5, 10	5, 10	2, 12, 5, 10	Bases
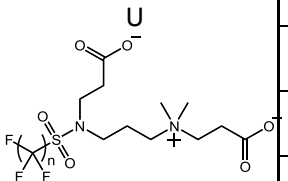 U	3	$C_{14}H_{22}O_6N_2SF_7^{+1}$	479.1081	479.1084	0.3	12	12	2, 12	2, 12	Weak Acids
	4	$C_{15}H_{22}O_6N_2SF_9^{+1}$	529.1049	529.1059	1.0	12	2, 12	2, 12	2, 12	Weak Acids
	5	$C_{16}H_{22}O_6N_2SF_{11}^{+1}$	579.1017	579.1023	0.6	12	2, 12	2, 12	2, 12	Weak Acids
	6	$C_{17}H_{22}O_6N_2SF_{13}^{+1}$	629.0986	629.0996	1.0	12	2, 12	2, 12	2, 12	Weak Acids
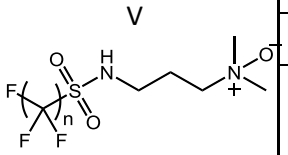 V PFASNO	6	$C_{11}H_{14}O_3N_2SF_{13}^{+1}$	501.0512						5, 10	
	7	$C_{12}H_{14}O_3N_2SF_{15}^{+1}$	551.0480	551.0481	0.1	5	5, 10		5, 10	
	8	$C_{13}H_{12}O_3N_2SF_{17}^{-1}$	599.0303	599.0298	-0.5	5	5, 10	5, 10	5, 10	Neutral
		$C_{13}H_{14}O_3N_2SF_{17}^{+1}$	601.0448	601.0445	-0.3	5	5, 10	5, 10	5, 10	Neutral
	9	$C_{14}H_{14}O_3N_2SF_{19}^{+1}$	651.0416						5, 10	

Table A3: Summary of SPE fractions and samples where the 22 classes of PFASs detected were found.

Sample ID	Neutral*	Weak Acids	Strong Acids	Bases	Permanent Cations
1	L		I, J	M	
2	R, S	U	PFSAs[3]	A, T	
3	L		I, J	M	
4	N, O	K	I, J		
5	L, V	K	I, J, PFSAs[3]	M, T	
7	N, O		J		
8	L	K	I, J	M	
10	V		PFSAs[3]	T	
11		K	I, J		P, Q
12	R, S	U	PFSAs[3]	A, T	
FS-330	B			A	C
FS-1520	F	D		E	G, H

* Neutral refers to compounds found in both the WAX and WCX neutral fractions

3. Weiner *et al.*[3] measured large quantities of PFSAs in these samples by LC-MS/MS, which were also detected in this work

Table A4: LC Gradients used in LC-MS/MS analysis. A: 10 mM ammonium acetate in water; B: 10 mM ammonium acetate in methanol

LC Gradient	LC 1	LC 2	LC 3	LC 4	LC 5	LC 6	LC 7	LC 8
Time (min)	0.0	0.0	0.0	0.0	0.0	0.0	0.0	0.0
Composition	65% A: 35% B	40% A: 60% B	50% A: 50% B	50% A: 50% B	50% A: 50% B	60% A: 40% B	60% A: 40% B	50% A: 50% B
Time (min)	4.5	1.0	5.0	5.0	6.0	6.0	6.0	5.0
Composition	35% A: 65% B	5% A: 95% B	5% A: 95% B	5% A: 95% B	5% A: 95% B	5% A: 95% B	5% A: 95% B	5% A: 95% B
Time (min)	5.0	3.5	8.0	7.0	7.0	8.0	7.0	9.0
Composition	5% A: 95% B	5% A: 95% B	5% A: 95% B	5% A: 95% B	5% A: 95% B	5% A: 95% B	60% A: 40% B	5% A: 95% B
Time (min)	8.0	4.0	9.0	8.0	8.0	9.0	9.0	10.0
Composition	5% A: 95% B	40% A: 60% B	50% A: 50% B	50% A: 50% B	50% A: 50% B	60% A: 40% B	60% A: 40% B	50% A: 50% B
Time (min)	8.5	5.5	11.0	10.0	10.0	11.0		12.0
Composition	65% A: 35% B	40% A: 60% B	50% A: 50% B	50% A: 50% B	50% A: 50% B	60% A: 40% B		50% A: 50% B
Time (min)	10.0							
Composition	65% A: 35% B							

Table A5: MS/MS Transitions for SPE Model Compounds and Identified FTSASs in ESI+.

Target Analyte	Mass Transition	Dwell (ms)	Declustering Potential (V)	Collision Energy (V)
dimethyldodecylamine	214.2>46.1**	20	92	42
	214.2>57.1	20	92	36
Empigen BB C12	272.1>104.1**	20	85	28
	272.1>85.1	20	85	30
Empigen BB C14	300.3>104.1**	20	85	30
	300.3>85.1	20	85	32
Empigen BB C16	328.4>104.1**	20	75	32
3-(N,N-dimethyloctylammonio) propanesulfonate	280.1>168.1**	20	90	32
	280.1>123.1	20	90	37
cetyltrimethylammonium	284.4>60.1	20	95	47
	284.4>57.1	20	95	47
A; *n* = 3	299.0>254.1	20	90	30
	299.0>226.1	20	90	40
A; *n* = 4	349.0>304.1	20	90	33
	349.0>276.1	20	90	43
A; *n* = 5	399.0>354.1	20	90	36
	399.0>326.1	20	90	46
A; *n* = 6	449.0>404.1	20	90	39
	449.0>376.1	20	90	48
A; *n* = 7	499.0>454.1	20	92	42
	499.0>426.1	20	92	51
A; *n* = 8	549.0>504.1*	20	92	44
	549.0>476.1*	20	92	54
A; *n* = 9	599.0>554.0	20	90	46
	599.0>526.0	20	90	56
A; *n* = 10	649.0>604.0*	20	85	49
	649.0>576.0*	20	85	59
A; *n* = 11	699.0>654.0	20	85	52
	699.0>626.0	20	85	62
A; *n* = 12	749.0>704.0*	20	80	55
	749.0>676.0*	20	80	64
A; *n* = 14	849.0>804.0	20	80	58
	849.0>776.0	20	80	68
B; *n* = 6	507.0>404.0	20	100	35
	507.0>376.0	20	100	53

Target Analyte	Mass Transition	Dwell (ms)	Declustering Potential (V)	Collision Energy (V)
B; *n* = 7	557.0>454.0	20	100	38
	557.0>426.0	20	100	54
B; *n* = 8	607.0>504.1*	20	94	40
	607.0>476.0*	20	94	57
B; *n* = 9	657.0>554.0	20	100	42
	657.0>526.0	20	100	58
B; *n* = 10	707.0>604.0*	20	112	45
	707.0>576.0*	20	112	60
B; *n* = 11	757.0>654.0	20	100	47
	757.0>626.0	20	100	62
B; *n* = 12	807.0>704.0*	20	95	49
	807.0>675.9*	20	95	64
B; *n* = 13	857.0>754.0	20	100	51
	857.0>726.0	20	100	66
B; *n* = 14	907.0>804.0	20	95	55
	907.0>776.0	20	95	67
C; *n* = 8	649.1>607.1*	20	90	35
	649.1>504.0*	20	90	47
C; *n* = 10	749.1>707.0*	20	85	41
	749.1>604.1*	20	85	52
C; *n* = 12	849.0>807.0*	20	90	45
	849.0>704.0*	20	90	56
E; *n* = 4	423.1>378.1	20	94	40
	423.1>293.1	20	94	55
E; *n* = 6	523.1>478.1*	20	90	39
	523.1>393.0*	20	90	60
E; *n* = 8	623.1>578.1*	20	88	44
	623.1>493.1*	20	88	66
E; *n* = 10	723.1>678.1*	20	82	50
	723.1>593.1*	20	82	74
E; *n* = 12	823.1>778.1	20	82	55
	823.1>693.1	20	82	78
F; *n* = 4	481.1>378.1	20	70	26
	481.1>293.1	20	70	54
F; *n* = 6	581.2>478.1*	20	70	30
	581.2>393.1*	20	70	62
F; *n* = 8	681.1>578.1*	20	80	34
	681.1>493.1*	20	80	70

Target Analyte	Mass Transition	Dwell (ms)	Declustering Potential (V)	Collision Energy (V)
F; *n* = 10	781.1>678.0*	20	90	41
	781.1>593.0*	20	90	74
F; *n* = 12	881.1>778.1*	20	70	48
	881.1>693.1*	20	70	78
F; *n* = 14	981.1>878.1	20	80	54
	981.1>793.1	20	80	82
G; *n* = 2	337.1>278.1	20	74	26
G; *n* = 4	437.1>378.1	20	75	30
G; *n* = 6	537.1>478.1*	20	75	34
G; *n* = 8	637.1>578.1*	20	85	39
G; *n* = 10	737.1>678.1*	20	95	45
G; *n* = 12	837.1>778.1	20	100	50
G; *n* = 14	937.1>878.1	20	105	55
H; *n* = 2	353.1>207.2	20	70	26
	353.1>158.2	20	70	28
H; *n* = 4	453.1>207.2	20	70	30
	453.1>158.2	20	70	32
H; *n* = 6	553.1>207.2*	20	75	32
	553.1>158.2*	20	75	37
H; *n* = 8	653.1>207.2*	20	75	37
	653.1>158.2*	20	75	42
H; *n* = 10	753.0>207.2*	20	62	44
	753.0>158.2*	20	62	48
H; *n* = 12	853.0>207.2	20	70	50
	853.0>158.2	20	70	54
H; *n* = 14	953.0>207.2	20	70	55
	953.0>158.2	20	70	59
I, *n* = 4	488.3>307.1	20	85	45
	488.3>154.1	20	85	28
I, *n* = 6	588.3>407.1*	20	90	50
	588.1>154.1*	20	90	32
I, *n* = 8	688.3>507.1	20	95	55
	688.3>154.1	20	95	36
I, *n* = 10	788.3>607.1	20	98	58
	788.3>154.1	20	98	40
I, *n* = 12	888.3>707.1	20	104	62
	888.3>154.1	20	104	44

Target Analyte	Mass Transition	Dwell (ms)	Declustering Potential (V)	Collision Energy (V)
J, *n* = 4	504.2>208.2	20	90	25
	504.2>351.1	20	90	23
J, *n* = 6	604.2>208.2*	20	95	29
	604.2>451.1*	20	95	27
J, *n* = 8	704.2>208.2	20	100	33
	704.2>551.1	20	100	31
J, *n* = 10	804.2>208.2	20	105	37
	804.2>651.1	20	105	35
L, *n* = 4	471.2>340.0	20	110	40
	471.2>104.1	20	110	45
L, *n* = 6	571.2>440.0*	20	114	43
	571.2>104.1*	20	114	50
L, *n* = 8	671.2>540.0	20	114	45
	671.2>104.1	20	114	55
L, *n* = 10	771.2>640.0	20	120	50
	771.2>104.1	20	120	60
L, *n* = 12	871.2>740.0	20	124	55
	871.2>104.1	20	124	65
M, *n* = 4	413.2>340.1	20	85	40
	413.2>86.1	20	85	55
M, *n* = 6	513.2>440.1*	20	90	45
	513.2>86.1*	20	90	60
M, *n* = 8	613.2>540.1	20	95	50
	613.2>86.1	20	95	65
M, *n* = 10	713.2>640.1	20	100	55
	713.2>86.1	20	100	70
M, *n* = 12	813.2>740.1	20	105	60
	813.2>86.1	20	105	75
N; *n* = 5	414.0>58.1*	20	112	75
	414.0>104.1*	20	112	42
N; *n* = 7	514.0>58.1*	20	124	82
	514.0>104.1*	20	124	50
N; *n* = 9	614.1>58.1*	20	145	98
	614.1>104.1*	20	145	59
N; *n* = 11	714.1>58.1	20	150	104
	714.1>104.1	20	150	65

Target Analyte	Mass Transition	Dwell (ms)	Declustering Potential (V)	Collision Energy (V)
N; *n* = 13	814.1>58.1	20	155	110
	814.1>104.1	20	155	70
O; *n* = 5	432.0>58.1*	20	120	80
	432.0>372.1*	20	120	50
O; *n* = 7	532.0>58.1*	20	128	88
	532.0>472.1*	20	128	58
O; *n* = 9	632.1>58.1*	20	146	104
	632.1>572.0*	20	146	65
O; *n* = 11	732.1>58.1	20	150	110
	732.1>672.0	20	150	70
O; *n* = 13	832.1>58.1	20	152	113
	832.1>772.0	20	152	75
O; *n* = 15	932.1>58.1	20	155	116
	932.1>872.0	20	155	79
P; *n* = 4	396.0>337.1	20	115	36
	396.0>293.1	20	115	46
P; *n* = 6	496.0>437.1*	20	118	40
	496.0>393.1*	20	118	51
P; *n* = 8	596.0>537.1	20	118	45
	596.0>493.1	20	118	55
P; *n* = 10	696.0>637.1	20	120	50
	696.0>593.1	20	120	60
Q; *n* = 4	412.0>166.1	20	65	30
	412.0>116.2	20	65	32
Q; *n* = 6	512.0>166.1*	20	70	34
	512.0>116.2*	20	70	36
Q; *n* = 8	612.0>166.1	20	75	38
	612.0>116.2	20	75	40
Q; *n* = 10	712.0>166.1	20	78	43
	712.0>116.2	20	78	45
R; *n* = 3	407.2>129.2*	20	85	38
	407.2>85.1*	20	85	45
R; *n* = 4	457.1>129.1*	20	90	42
	457.1>85.1*	20	90	52
R; *n* = 5	507.2>129.1*	20	100	44
	507.2>85.1*	20	100	58

Target Analyte	Mass Transition	Dwell (ms)	Declustering Potential (V)	Collision Energy (V)
R; *n* = 6	557.3>129.1*	20	100	47
	557.3>85.1*	20	100	58
R; *n* = 7	607.2>129.1	20	100	50
	607.2>85.1	20	100	60
R; *n* = 8	657.2>129.1	20	100	52
	657.2>85.1	20	100	63
S; *n* = 3	407.2>118.2*	20	85	42
S; *n* = 4	457.1>118.2*	20	90	44
S; *n* = 5	507.2>118.2*	20	100	50
S; *n* = 6	557.3>118.2*	20	100	52
T; *n* = 3	335.1>85.1*	20	75	37
	335.1>70.1*	20	75	60
T; *n* = 4	385.1>85.1*	20	80	42
	385.1>70.1*	20	80	68
T; *n* = 5	435.0>85.1*	20	80	48
	435.0>70.1*	20	80	74
T; *n* = 6	485.1>85.1*	20	90	52
	485.1>70.1*	20	90	80
T; *n* = 7	535.1>85.1	20	100	56
	535.1>70.1	20	100	86
T; *n* = 8	585.1>85.1	20	110	60
	585.1>70.1	20	110	94
T; *n* = 9	635.1>85.1	20	115	64
	635.1>70.1	20	115	98
U; *n* = 3	479.2>187.3*	20	100	46
	479.2>129.2*	20	100	42
U; *n* = 4	529.3>187.3*	20	100	48
	529.3>129.2*	20	100	45
U; *n* = 5	579.2>187.3*	20	100	52
	579.2>129.2*	20	100	50
U; *n* = 6	629.3>187.3*	20	100	55
	629.3>129.2*	20	100	51
V; *n* = 6	501.0>348.1	20	110	50
	501.0>58.2	20	110	86
V; *n* = 7	551.0>398.1	20	120	54
	551.0>58.2	20	120	90

Target Analyte	Mass Transition	Dwell (ms)	Declustering Potential (V)	Collision Energy (V)
V; *n* = 8	601.0>448.1*	20	130	58
	601.0>58.2*	20	130	94
V; *n* = 9	651.0>498.1	20	135	62
	651.0>58.2	20	135	98

** indicates quantifying transitions ad * indicates transitions optimized by infusing an SPE fraction.

n = fluorinated chain length of the congener

Table A6: MS/MS Transitions for SPE Model Compounds and Identified FTSASs in ESI-

Target Analyte	Mass Transition	Dwell (ms)	Declustering Potential (V)	Collision Energy (V)
PFOA	413.0>368.9**	30	-35	-15
7:3 FTCA	441.0>337.0**	30	-40	-17
FOSA	497.9>78.0**	30	-80	-85
	497.9>477.9	30	-80	-38
D; *n* = 4	336.9>276.9	20	-48	-16
	336.9>90.9	20	-48	-26
D; *n* = 6	436.9>376.9*	20	-52	-17
	436.9>90.0*	20	-52	-30
D; *n* = 8	537.0>476.9*	20	-58	-18
	537.0>90.9*	20	-58	-35
D; *n* = 10	637.1>576.9*	20	-62	-20
	637.1>90.9*	20	-62	-40
D; *n* = 12	737.1>676.9	20	-66	-22
	737.1>90.9	20	-66	-45
D; *n* = 14	837.1>776.9	20	-70	-23
	837.1>90.9	20	-70	-48
D; *n* = 16	837.1>776.9	20	-70	-24
	837.1>90.9	20	-70	-49
I, *n* = 4	486.1>206.0	20	-100	-45
	486.1>134.9	20	-100	-52
I, *n* = 6	586.1>206.0*	20	-110	-54
	586.1>134.9*	20	-110	-62

Target Analyte	Mass Transition	Dwell (ms)	Declustering Potential (V)	Collision Energy (V)
I, *n* = 8	686.1>206.0*	20	-125	-64
	686.1>134.9*	20	-125	-76
I, *n* = 10	786.1>206.0	20	-130	-74
	786.1>134.9	20	-130	-82
I, *n* = 12	886.1>206.0	20	-135	-80
	886.1>134.9	20	-135	-90
I, *n* = 14	986.1>206.0	20	-140	-82
	986.1>134.9	20	-140	-92
J, *n* = 4	502.1>205.9	20	-70	-50
	502.1>256.0	20	-70	-32
J, *n* = 6	602.1>205.9*	20	-76	-56
	602.1>256.0*	20	-76	-37
J, *n* = 8	702.1>205.9	20	-85	-62
	702.1>256.0	20	-85	-42
J, *n* = 10	802.1>205.9	20	-90	-68
	802.1>256.0	20	-90	-48
K, *n* = 4	351.0>105.0	20	-64	-18
	351.0>278.9	20	-64	-21
K, *n* = 6	451.0>105.1*	20	-68	-21
	451.0>378.9*	20	-68	-25
K, *n* = 8	551.0>105.1	20	-72	-24
	551.0>478.9	20	-72	-29

** indicates quantifying transitions and * indicates transitions optimized by infusing an SPE fraction

n = fluorinated chain length of the congener

Table A7: Percent Recoveries for Model Compounds in Ion Exchange Solid Phase Extraction Methods

Compound	WAX; (*n* = 4)		WCX; (*n* = 3)	
	Fraction	% Recovery ± Std. Dev.	Fraction	% Recovery ± Std. Dev.
PFOA	Strong Acid	90 ± 11	Neutral	103 ± 3
7:3 FTCA	Weak Acid	79 ± 14	Neutral	110 ± 8
FOSA	Neutral	82 ± 9	Neutral	101 ± 3
dimethyldodecylamine	Neutral	73 ± 5	Base	93 ± 4
Empigen BB C12	Neutral	113 ± 4	Neutral	124 ± 3
Empigen BB C14	Neutral	94 ± 6	Neutral	105 ± 6
Empigen BB C16	Neutral	88 ± 10	Neutral	101 ± 5
3-(N,N-dimethyloctylammonio) propanesulfonate	Neutral	90 ± 6	Neutral	104 ± 6
cetyltrimethylammonium	Neutral	63 ± 11	Permanent cation	135 ± 6

Table A8: Accurate mass data for fragment ions of fluorinated surfactants in AFFFs and fluorinated surfactant concentrates.

					Fragment Ion Characteristics				
Structure ID	ESI Mode	Precursor Ion	Collision Energy (V)	Sample	Nominal Mass	Molecular Formula	Observed m/z	Theoretical m/z	Error (mDa)
A; *n* = 8	ESI+	549	50	Base, FS-330	119	C2F5+1	118.9891	118.9915	-2.37
					131	C3F5+1	130.9930	130.9915	1.53
					169	C3F7+1	168.9897	168.9883	1.43
					448	C9H3NF17+1	448.0003	447.9989	1.44
					476	C10H3ONF17+1	475.9951	475.9938	1.33
					504	C12H7ONF17+1	504.0240	504.0251	-1.07
					549	C14H14ON2F17+1	549.0786	549.0829	-4.30
B; *n* = 8	ESI-	605	-30	WCX Neutral, FS-330	102	C4H8O2N-1	102.0542	102.0561	-1.85
					169	C3F7-1	168.9881	168.9894	-1.27
					219	C4F9-1	218.9850	218.9862	-1.18
					269	C5F11-1	268.9831	268.9830	0.12
					419	C8F17-1	418.9724	418.9734	-1.00
					428	C9OF16-1	427.9689	427.9699	-1.01
					475	C10H2ONF17-1	474.9866	474.9870	-0.44
					502	C12H5ONF17-1	502.0108	502.0105	0.28
					507	C10H2O3NF17-1	506.9770	506.9769	0.13
					531	C13H8ON2F17-1	531.0384	531.0371	1.33
					546	C14H11ON2F17-1	546.0586	546.0605	-1.94
					605	C16H14O3N2F17-1	605.0780	605.0739	4.15
	ESI+	607	40	WCX Neutral, FS 330	104	C4H10O2N+1	104.0702	104.0706	-0.40
					448	C9H3NF17+1	448.0003	447.9989	1.44
					476	C10H3ONF17+1	475.9965	475.9938	2.73
					504	C12H7ONF17+1	504.0248	504.0251	-0.27
					607	C16H16O3N2F17+1	607.0873	607.0895	-2.20

Fragment Ion Characteristics

Structure ID	ESI Mode	Precursor Ion	Collision Energy (V)	Sample	Nominal Mass	Molecular Formula	Observed m/z	Theoretical m/z	Error (mDa)
C; *n* = 8	ESI+	649	30	Quat. Ammonium, FS-330	104	C4H10O2N+1	104.0707	104.0706	0.10
					146	C7H16O2N+1	146.1173	146.1176	-0.26
					504	C12H7ONF17+1	504.0239	504.0251	-1.17
					607	C16H16O3N2F17+1	607.0854	607.0884	-3.00
					649	C19H22O3N2F17+1	649.1325	649.1354	-2.85
D; *n* = 6	ESI-	437	-20	Weak Acid, FS-1520	91	C2H3O2S-1	90.9844	90.9859	-1.52
					273	C9SF7-1	272.9641	272.9614	2.66
					293	C9HSF8-1	292.9637	292.9677	-3.97
					313	C9H2SF9-1	312.9759	312.9739	2.00
					333	C9H3SF10-1	332.9818	332.9801	1.67
					377	C10H3O2SF10-1	376.9706	376.9700	0.64
					397	C10H4O2SF11-1	396.9760	396.9762	-0.18
					417	C10H5O2SF12-1	416.9844	416.9824	1.99
					437	C10H6O2SF13-1	436.9914	436.9886	2.76
E; *n* = 6	ESI+	523	40	Base, FS-1520	393	C9H6SF13+1	392.9984	392.9977	0.69
					478	C13H13ONSF13+1	478.0535	478.0505	3.02
					523	C15H20ON2SF13+1	523.1111	523.1083	2.80
F; *n* = 6	ESI+	581	30	WCX Neutral, FS-1520	104	C4H10O2N+1	104.0679	104.0706	-2.70
					393	C9H6SF13+1	392.9983	392.9977	0.59
					478	C13H13ONSF13+1	478.0514	478.0505	0.92
					581	C17H22O3N2SF13+1	581.1095	581.1138	-4.30
G; *n* = 6	ESI+	537	30	Quat. Ammonium, FS-1520	478	C13H13ONSF13+1	478.0518	478.0505	1.32
					537	C16H22ON2SF13+1	537.1227	537.1240	-1.28

Fragment Ion Characteristics

Structure ID	ESI Mode	Precursor Ion	Collision Energy (V)	Sample	Nominal Mass	Molecular Formula	Observed m/z	Theoretical m/z	Error (mDa)
H; *n* = 6	ESI+	553	30	Quat. Ammonium, FS-1520	99	C5H9ON+1	99.0667	99.0679	-1.17
					148	C5H10O2NS+1	148.0445	148.0427	1.82
					158	C8H18ON2+1	158.1431	158.1414	1.74
					207	C8H19O2N2S+1	207.1146	207.1162	-1.57
					494	C13H13O2NSF13+1	494.0506	494.0454	5.21
					553	C16H22O2N2SF13+1	553.1236	553.1189	4.71
I; *n* =6	ESI-	586	-40	Strong Acid, Foam 1	135	C4H7O3S-1	135.0095	135.0121	-2.64
					152	C4H10O3NS-1	152.0378	152.0387	-0.89
					206	C7H12O4NS-1	206.0492	206.0493	-0.05
					586	C15H17O4NS2F13-1	586.0381	586.0397	-1.59
	ESI+	588	30	Strong Acid, Foam 3	154	C4H12O3NS+1	154.0533	154.0532	0.06
					407	C10H8SF13+1	407.0140	407.0134	0.64
					588	C15H19O4NS2F13+1	588.0533	588.0542	-0.94
J; *n* = 6	ESI-	602	-30	Strong Acid, Foam 1	152	C4H10O3NS-1	152.0373	152.0387	-1.39
					206	C7H12O4NS-1	206.0490	206.0493	-0.25
					256	C7H14O5NS2-1	256.0309	256.0319	-0.99
					602	C15H17O5NS2F13-1	602.0338	602.0346	-0.80
	ESI+	604	30	Strong Acid, Foam 1	136	C4H10O2NS+1	136.0429	136.0427	0.22
					154	C4H12O3NS+1	154.0560	154.0532	2.76
					208	C7H14O4NS+1	208.0653	208.0638	1.49
					451	C11H8O2SF13+1	451.0000	451.0032	-3.19
					604	C15H19O5NS2F13+1	604.0502	604.0492	1.04
K; *n* = 6	ESI-	451	-20	Weak Acid, Foam 8	105	C3H5O2S-1	105.0010	105.0016	-0.57
					339	C8H2SF11-1	338.9700	338.9707	-0.70
					359	C8H3SF12-1	358.9812	358.9769	4.27
					379	C8H4SF13-1	378.9860	378.9832	2.84
					451	C11H8O2SF13-1	451.0014	451.0043	-2.89

Fragment Ion Characteristics

Structure ID	ESI Mode	Precursor Ion	Collision Energy (V)	Sample	Nominal Mass	Molecular Formula	Observed m/z	Theoretical m/z	Error (mDa)
L; *n* = 6	ESI-	569	-20	WAX Neutral, Foam 3	179	C6H15O2N2S-1	179.0880	179.0860	2.03
					223	C7H15O4N2S-1	223.0738	223.0758	-2.00
					446	C11H8O2NSF12-1	446.0095	446.0090	0.54
					466	C11H9O2NSF13-1	466.0195	466.0152	4.31
					549	C15H17O4N2SF12-1	549.0718	549.0723	-0.49
					569	C15H18O4N2SF13-1	569.0737	569.0785	-4.82
	ESI+	571	40	WCX Neutral, Foam 3	104	C4H10O2N+	104.0700	104.0706	-0.60
					440	C9H7O2NSF13+	439.9996	439.9984	1.16
					468	C11H11O2NSF13+	468.0309	468.0297	1.16
					571	C15H20O4N2SF13+1	571.0907	571.0931	-2.40
M; *n* = 6	ESI+	513	40	Base, Foam 8	440	C9H7O2NSF13+1	439.9969	439.9984	-1.54
					468	C11H11O2NSF13+1	468.0288	468.0297	-0.94
					513	C13H18O2N2SF13+1	513.0868	513.0876	-0.80
N; *n* = 5	ESI+	414	45	WCX Neutral, Foam 4	102	C4H8O2N+1	102.0505	102.0550	-4.45
					104	C4H10O2N+1	104.0697	104.0706	-0.90
					354	C10H11NF11+1	354.0696	354.0710	-1.44
					414	C12H15O2NF11+1	414.0932	414.0922	1.00
O; *n* = 5	ESI+	432	45	WCX Neutral, Foam 4	102	C4H8O2N+1	102.0540	102.0550	-0.95
					104	C4H10O2N+1	104.0689	104.0706	-1.70
					372	C10H10NF12+1	372.0583	372.0616	-3.31
					432	C12H14O2NF12+1	432.0833	432.0827	0.60
P; *n* = 6	ESI+	496	40	WAX Neutral, Foam 11	393	C9H6F13S+	392.9980	392.9977	0.28
					407	C10H8SF13+1	407.0100	407.0134	-3.36
					437	C11H10OSF13+1	437.0243	437.0239	0.37
					496	C14H19ONSF13+1	496.0970	496.0974	-0.40

Fragment Ion Characteristics

Structure ID	ESI Mode	Precursor Ion	Collision Energy (V)	Sample	Nominal Mass	Molecular Formula	Observed m/z	Theoretical m/z	Error (mDa)
Q; *n* = 6	ESI+	512	30	Quat. Ammonium, Foam 11	116	C6H14ON+1	116.1052	116.1070	-1.79
					166	C6H16O2NS+1	166.0890	166.0896	-0.63
					453	C11H10O2SF13+1	453.0197	453.0188	0.86
					512	C14H19O2NSF13+1	512.0933	512.0923	0.96
R and **S**; *n* = 6	ESI-	555	-20	WCX Neutral, Foam 12	483	C11H12O2N2SF13-1	483.0403	483.0417	-1.44
					555	C14H16O4N2SF13-1	555.0671	555.0629	4.23
	ESI+	557	50	WCX Neutral, Foam 12	115	C6H15N2+1	115.1219	115.1230	-1.07
					118	C5H12O2N+1	118.0852	118.0863	-1.06
					129	C6H11O2N+1	129.0776	129.0784	-0.83
					174	C8H18O2N2+1	174.1369	174.1363	0.62
					485	C11H14O2N2SF13+1	485.0612	485.0562	5.00
					557	C14H18O4N2SF13+1	557.0794	557.0774	2.00
T; *n* = 6	ESI-	483	-30	Base, Foam 12	119	C2F5-1	118.9939	118.9926	1.34
					163	C5H11O2N2S-1	163.0526	163.0547	-2.07
					169	C3F7-1	168.9877	168.9894	-1.67
					183	C5H12O2N2SF-1	183.0614	183.0609	0.50
					319	C6F13-1	318.9800	318.9798	0.21
					483	C11H12O2N2SF13-1	483.0411	483.0417	-0.64
	ESI+	485	50	Base, Foam 12	102	C5H14N2+1	102.1196	102.1152	4.45
					348	C7H3NF13+1	348.0022	348.0052	-3.04
					412	C7H3O2NSF13+1	411.9845	411.9671	17.36*
					485	C11H14O2N2SF13+1	485.0576	485.0562	1.40

Fragment Ion Characteristics

Structure ID	ESI Mode	Precursor Ion	Collision Energy (V)	Sample	Nominal Mass	Molecular Formula	Observed m/z	Theoretical m/z	Error (mDa)
U; *n* = 6	ESI+	629	50	Weak Acid, Foam 12	117	C5H11O2N+1	117.0740	117.0784	-4.43
					118	C5H12O2N+1	118.0860	118.0863	-0.26
					129	C6H11O2N+1	129.0757	129.0784	-2.73
					144	C7H14O2N+1	144.1010	144.1019	-0.91
					187	C9H19O2N2+1	187.1442	187.1441	0.10
					629	C17H22O6N2SF13+	629.0954	629.0985	-3.10
V; *n* = 8	ESI-	599	-30	WCX Neutral, Foam 10	92	CH2O2NS-1	91.9808	91.9812	-0.37
					219	C4F9-1	218.9866	218.9862	0.42
					419	C8F17-1	418.9739	418.9734	0.50
					483	C8O2SF17-1	482.9332	482.9353	-2.10
					538	C11H5O2NSF17-1	537.9744	537.9775	-3.10
					584	C12H9O3N2SF17-1	584.0054	584.0068	-1.39
					599	C13H12O3N2SF17-1	599.0313	599.0303	1.03
	ESI+	601	50	WCX Neutral, Foam 10	119	C2F5+1	118.9909	118.9915	-0.57
					131	C3F5+1	130.9917	130.9915	0.23
					169	C3F7+1	168.9894	168.9883	1.13
					331	C7F13+	330.9795	330.9787	0.81
					448	C9H3NF17 +	448.0032	447.9989	4.34
					476	C11H7NF17+1	476.0333	476.0302	3.14
					512	C9H3O2NSF17+1	511.9641	511.9608	3.34
					540	C11H7O2NSF17+1	539.9880	539.9921	-4.06
					583	C13H12O2N2SF17+1	583.0384	583.0343	4.15
					601	C13H14O3N2SF17+1	601.0521	601.0448	7.30

* This peak has poor mass accuracy due to its low intensity. *n* = fluorinated chain length of the congener

a)

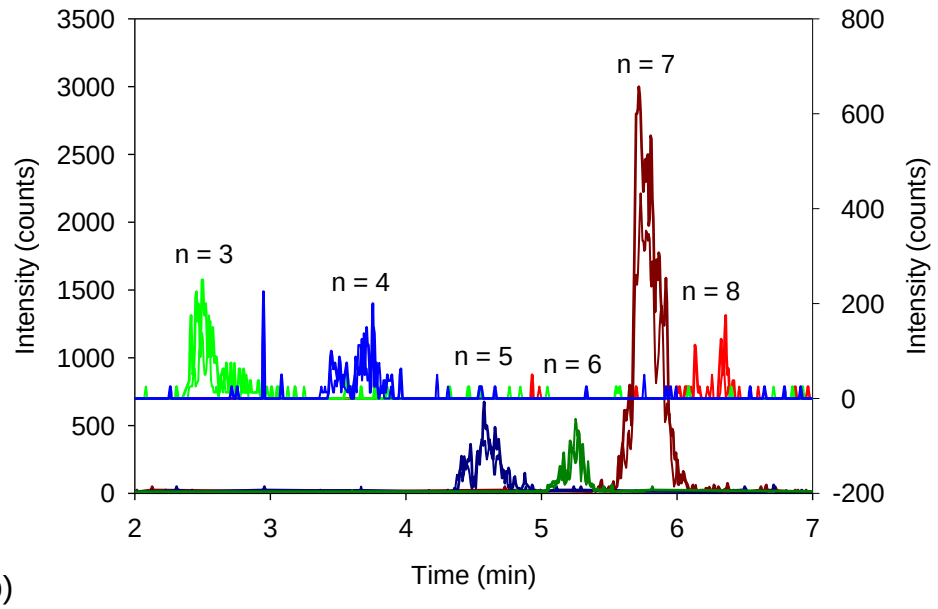

b)

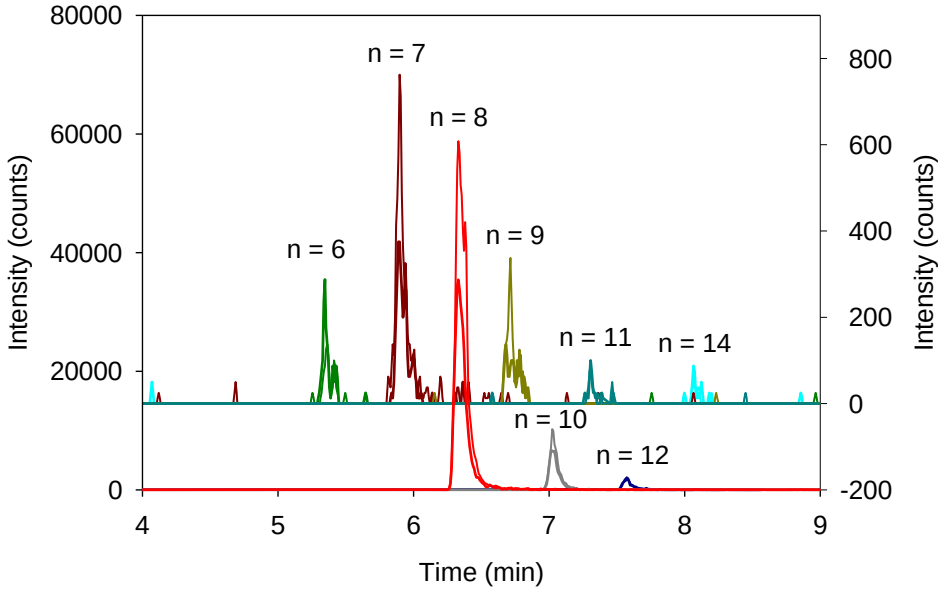

Figure A1: LC-MS/MS chromatograms for A components in (a) 50,000-fold diluted Foam 12 and (b) 20-fold diluted FS-330 base fraction. Fine traces are loss of 45 from [M+H]+ and thick traces are loss of 73 from [M+H]+.

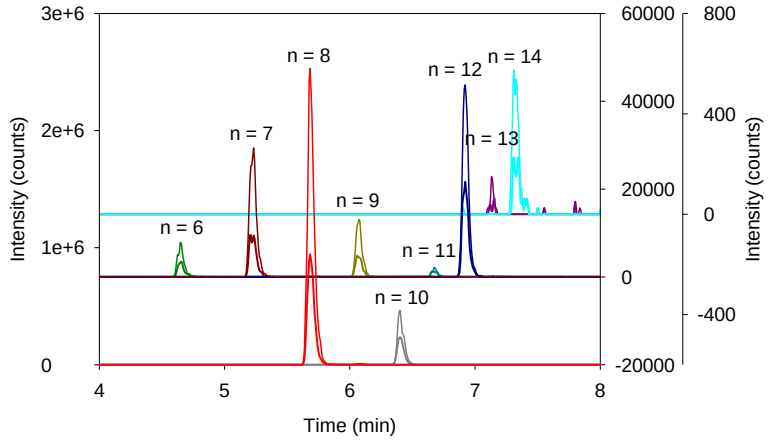

Figure A2: LC-MS/MS chromatograms for B (PFAAB) components in 100-fold diluted FS-330 WCX neutral fraction. Fine traces are loss of 103 from [M+H]+ and thick traces are loss of 131 from [M+H]+.

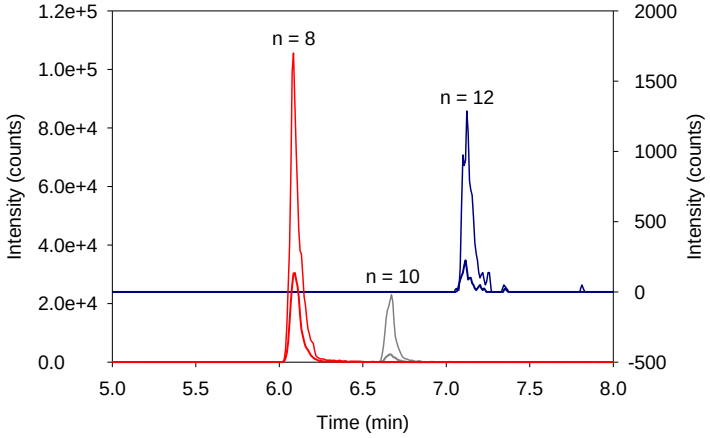

Figure A3: LC-MS/MS chromatograms for C components in 1,000,000-fold diluted FS-330. Fine traces are loss of 145 from M^+ and thick traces are loss of 42 from M^+.

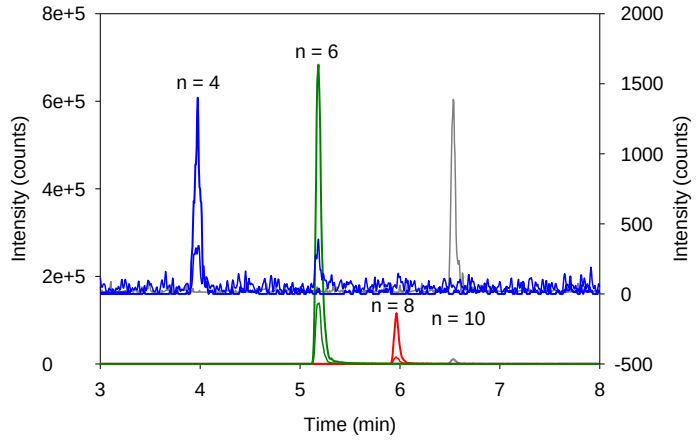

Figure A4: LC-MS/MS chromatograms for D components in 1,000,000-fold diluted FS-1520. Fine traces are loss of 60 from $[M-H]^-$ and thick traces are transition from $[M-H]^-$ to *m/z* 91.

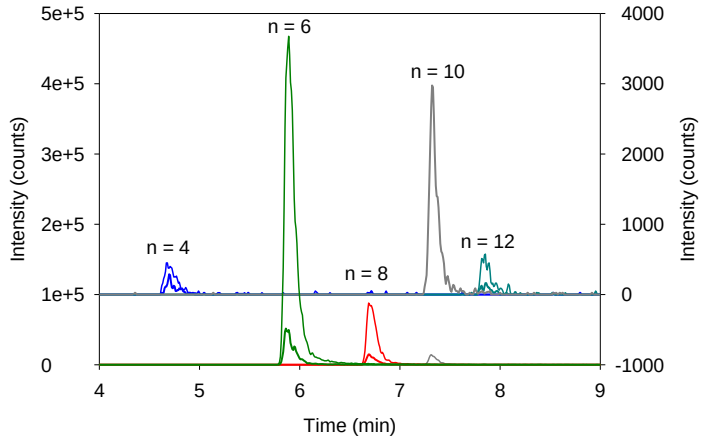

Figure A5: LC-MS/MS chromatograms for E components in 1,000,000-fold diluted FS-1520. Fine traces are loss of 45 from $[M+H]^+$ and thick traces are loss of 130 from $[M+H]^+$.

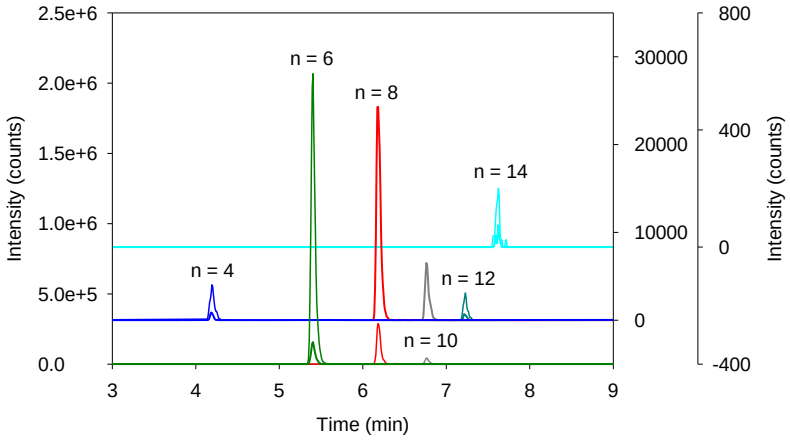

Figure A6: LC-MS/MS chromatograms for F (FTSAB) components in 1,000,000-fold diluted FS-1520. Fine traces are loss of 103 from $[M+H]^+$ and thick traces are loss of 188 from $[M+H]^+$.

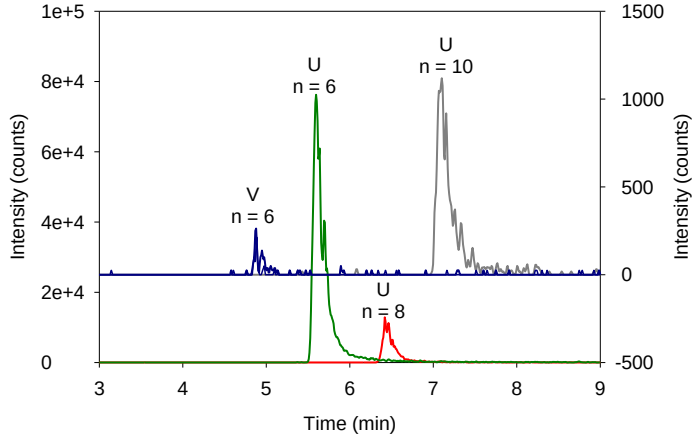

Figure A7: LC-MS/MS chromatograms for G and H components in 1,000,000-fold diluted FS-1520. For G, traces are loss of 59 from M^+. For H, thin traces are transition to *m/z* 158 from M^+ and thick traces are transition to *m/z* 207 from M^+.

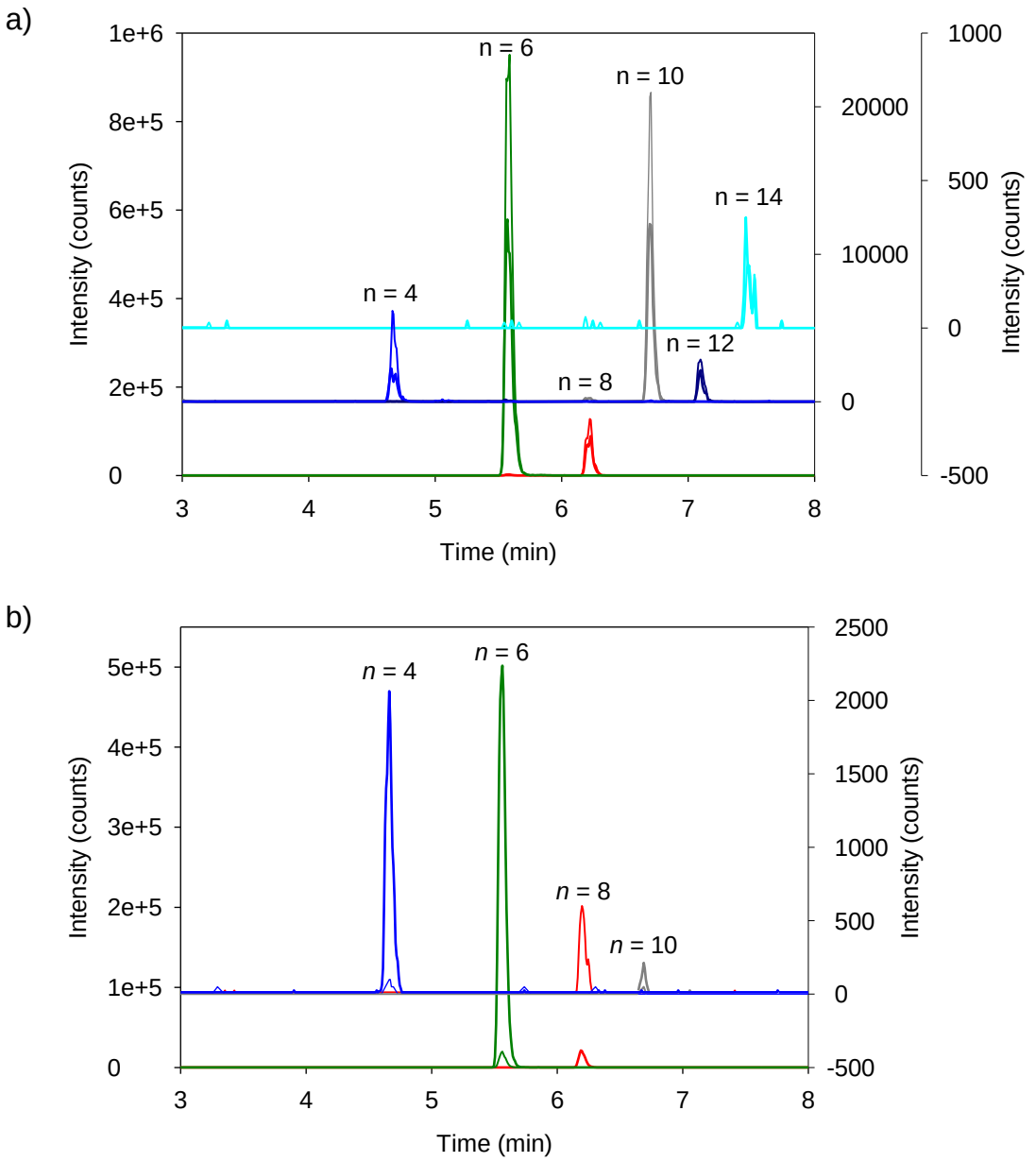

Figure A8: LC-MS/MS chromatograms for x:2 FTSAS (I) components. a) Chromatograms for 10,000-fold diluted Foam 11 in ESI-. Fine traces are transitions from [M-H]- to *m/z* 135 and thick traces are transitions form [M-H]- to *m/z* 206. b) Chromatograms for 50,000-fold diluted Foam 3 in ESI +. Fine traces are loss of 181 from $[M+H]^+$ and thick traces are transition from $[M+H]^+$ to *m/z* 154.

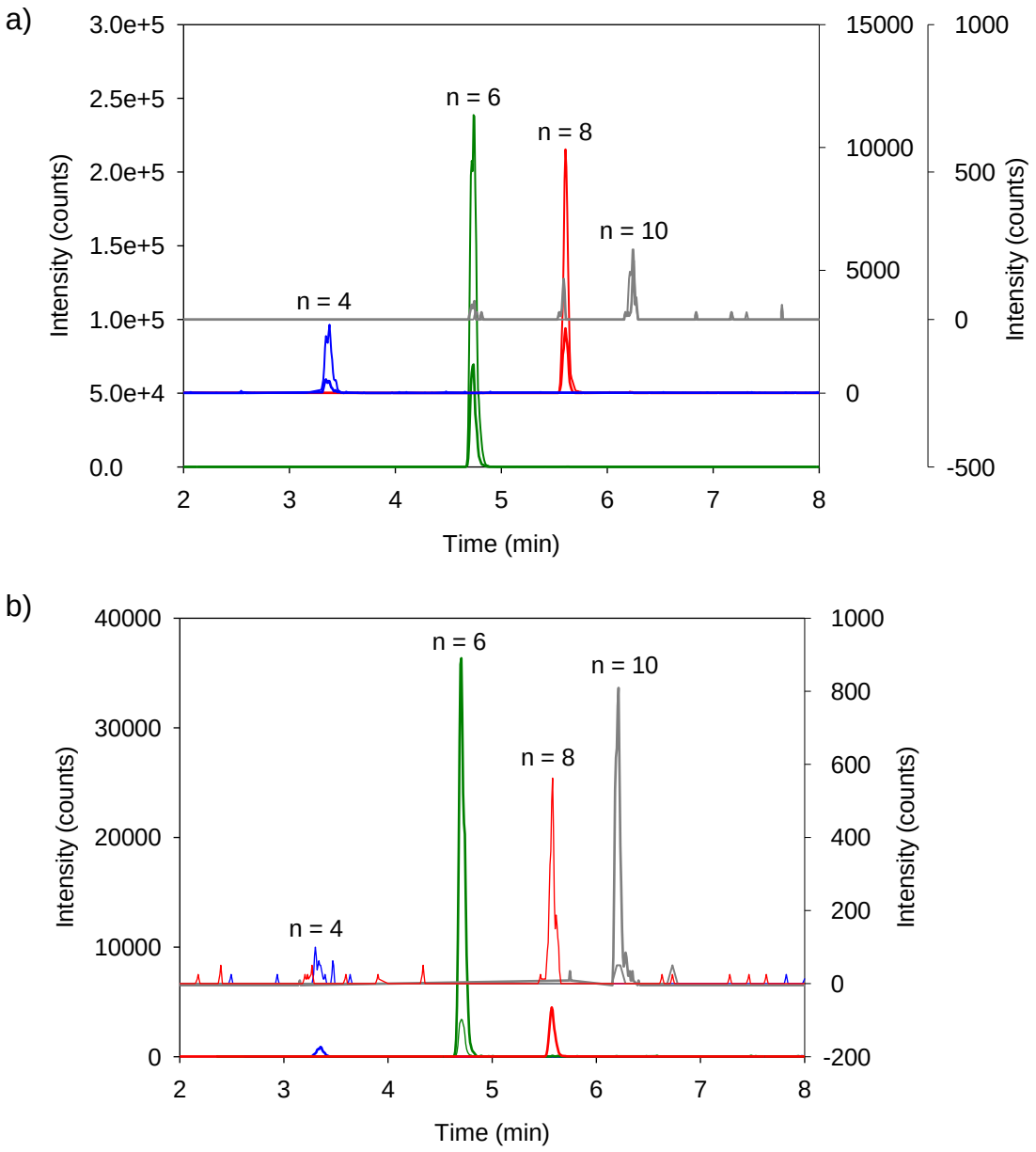

Figure A9: LC-MS/MS chromatograms for x:2 FTSAS sulfoxide (J) components. a) Chromatograms for 50,000-fold diluted Foam 1 in ESI-. Fine traces are transitions from [M-H]- to *m/z* 256 and thick traces are transitions from [M-H]- to *m/z* 206. b) Chromatograms for 50,000-fold diluted Foam 1 (for n = 4) and in 10,000-fold diluted Foam 11 (for n = 6, 8, 10) in ESI+. Fine traces are loss of 153 from $[M+H]^+$ and thick traces are transition from $[M+H]^+$ to *m/z* 208.

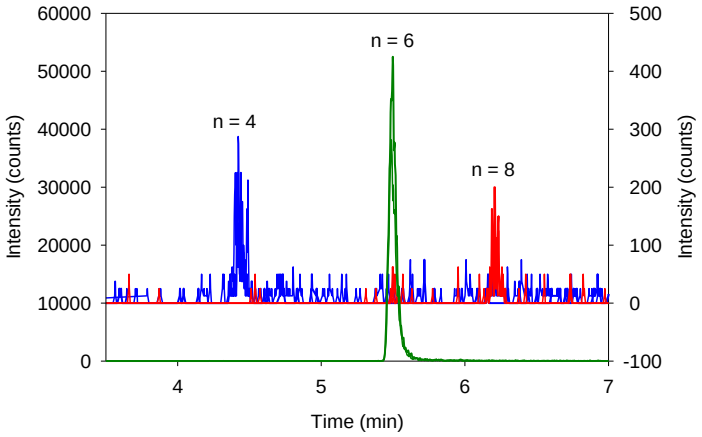

Figure A10: LC-MS/MS chromatograms for K components in 50,000-fold diluted Foam 8. Fine traces are loss of 72 from $[M-H]^-$ and thick traces are transition from $[M-H]^-$ to *m/z* 105.

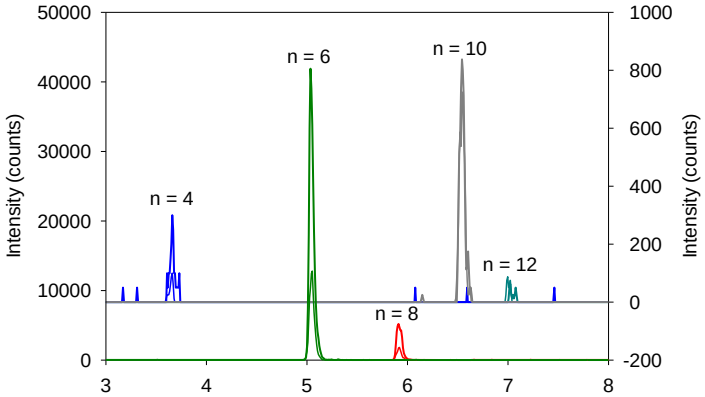

Figure A11: LC-MS/MS chromatograms for x:2 FTAB (L) components in 50,000-fold diluted Foam 5. Fine traces are transition from [M+H]+ to m/z 104 and thick traces are loss of 131 from [M+H]+.

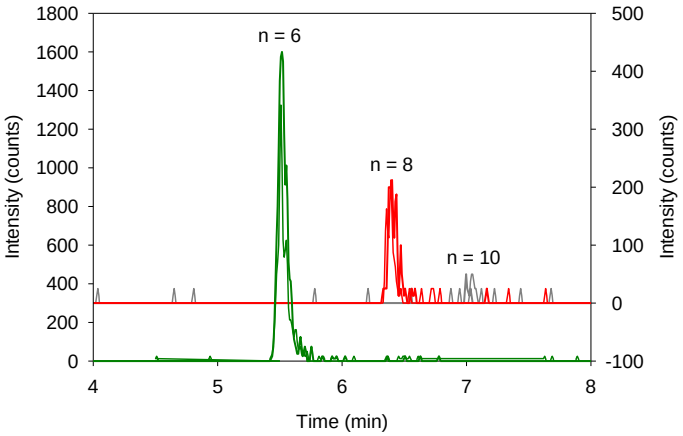

Figure A12: LC-MS/MS chromatograms for M components in 50,000-fold diluted Foam 1. Fine traces are transition from $[M+H]^+$ to *m/z* 86 (CH_2=$CHCH_2NH(CH_3)_2^+$; *m/z* 86.0987; 2.27 mDa error) and thick traces are loss of 73 from $[M+H]^+$.

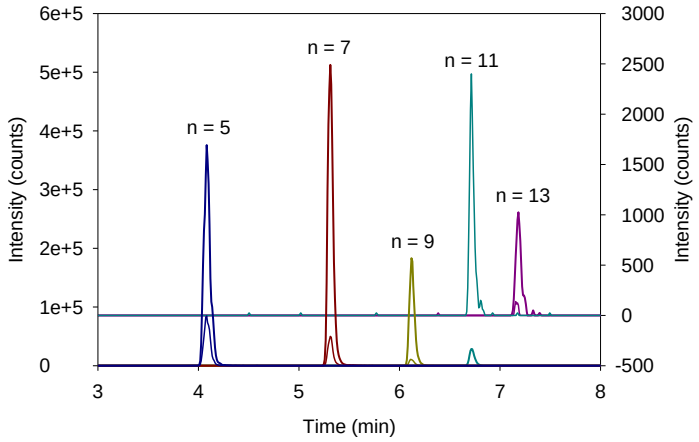

Figure A13: LC-MS/MS chromatograms for N (FTB) components in 10,000-fold diluted Foam 4. Fine traces are transition from $[M+H]^+$ to *m/z* 104 and thick traces are transition from $[M+H]^+$ to *m/z* 58 [$(CH_3)_2N^+=CH_2$; *m/z* 58.0652; 0.07 mDa error].

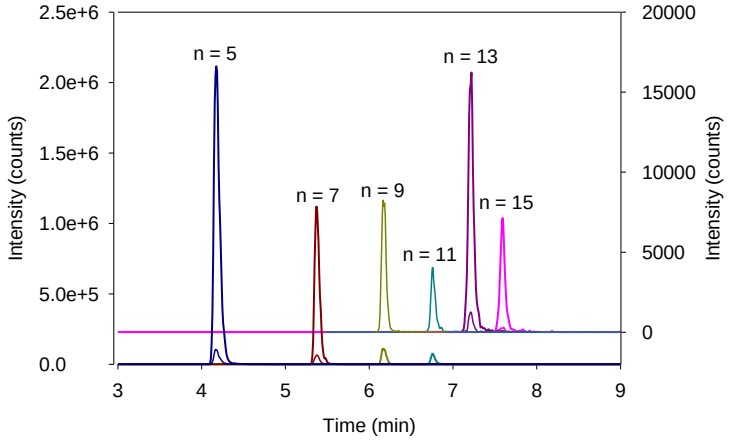

Figure A14: LC-MS/MS chromatograms for O (FTB) components in 10,000-fold diluted Foam 7. Fine traces are loss of 60 from $[M+H]^+$ and thick traces are transition from $[M+H]^+$ to *m/z* 58 [$(CH_3)_2N^+=CH_2$; *m/z* 58.0653; 0.17 mDa error].

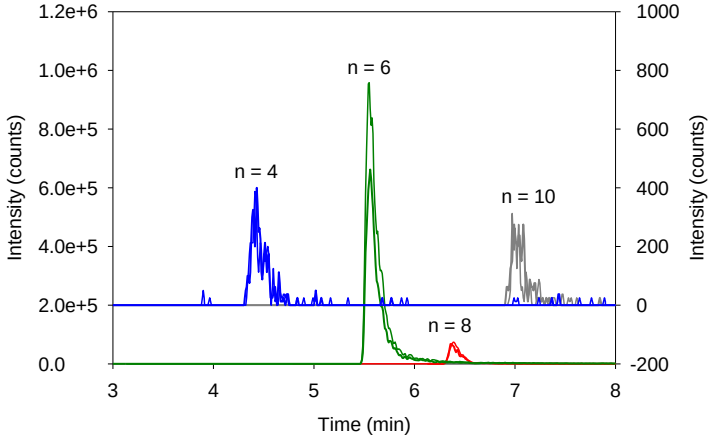

Figure A15: LC-MS/MS chromatograms for P (x:2 FTSHA) components in 10,000-fold diluted Foam 11. Fine traces are loss of 59 from M^+ and thick traces are loss of 103 from M^+.

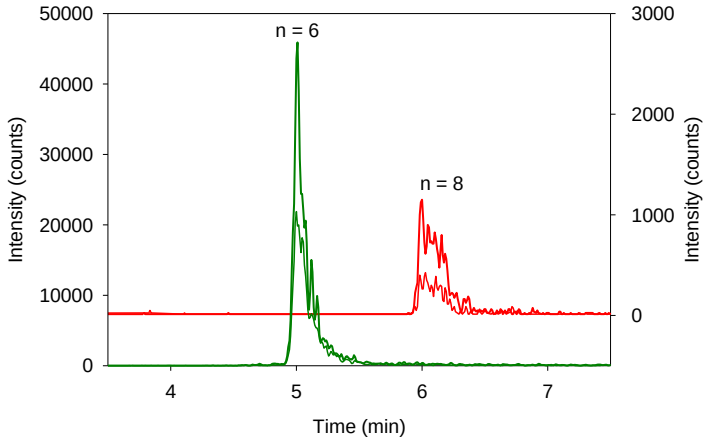

Figure A16: LC-MS/MS chromatograms for Q components in 10,000-fold diluted Foam 11. Fine traces are transition from M^+ to *m/z* 116 and thick traces are transition from M^+ to *m/z* 166.

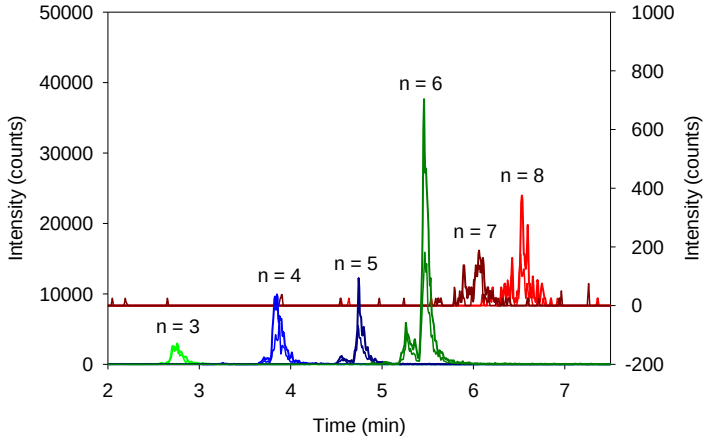

Figure A17: LC-MS/MS chromatograms for PFASAC (R) components in 50,000-fold diluted Foam 12. Fine traces are transition from $[M+H]^+$ to *m/z* 129 and thick traces are transition from $[M+H]^+$ to *m/z* 85 ($C_5H_{11}N^{\bullet+}$; *m/z* 85.0877; -0.9 mDa error).

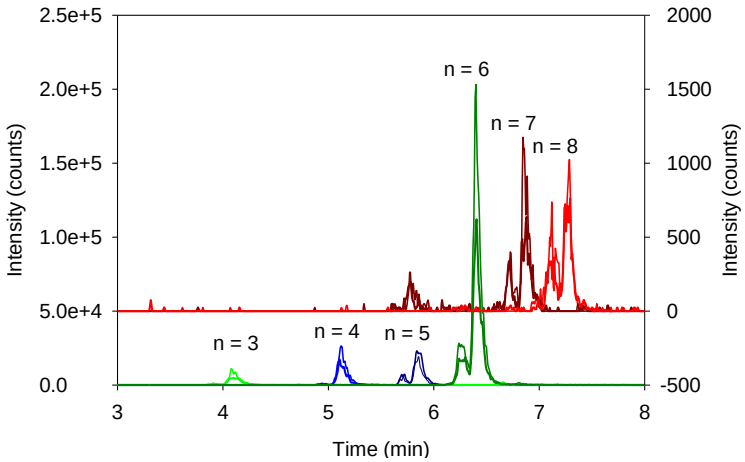

Figure A18: LC-MS/MS chromatograms for T tertiary amine ECF components in 50,000-fold diluted Foam 12. Fine traces are transition from $[M+H]^+$ to *m/z* 85 ($C_5H_{11}N^{\bullet+}$; *m/z* 85.0886; 0 mDa error) and thick traces are transition from $[M+H]^+$ to *m/z* 70 ($C_4H_8N^+$; *m/z* 70.0645; -0.63 mDa error).

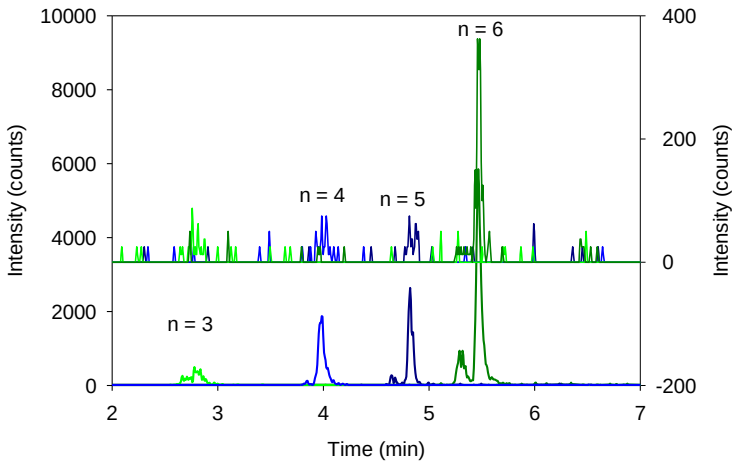

Figure A19: LC-MS/MS chromatograms for U dicarboxylic ECF components in 50,000-fold diluted Foam 12. Fine traces are transition from $[M+H]^+$ to *m/z* 129 and thick traces are transition from $[M+H]^+$ to *m/z* 187.

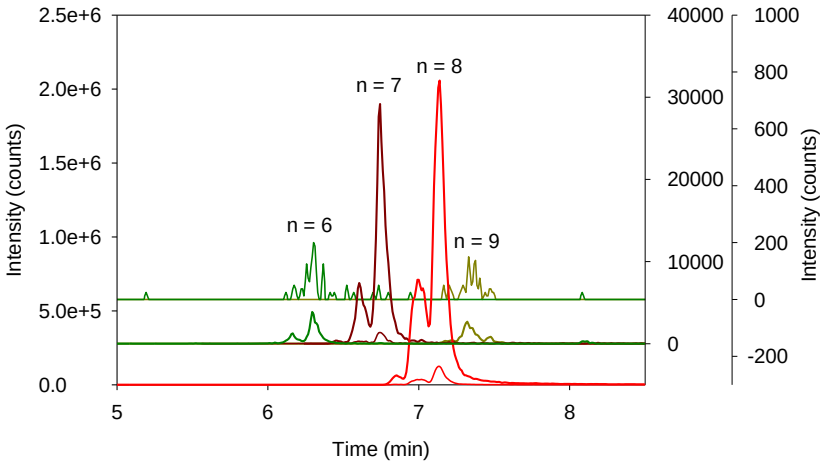

Figure A20: LC-MS/MS chromatograms for PFASNO (V) components in 50,000-fold diluted Foam 10. Fine traces are loss of 153 from $[M+H]^+$ and thick traces are transition from $[M+H]^+$ to *m/z* 58 ($C_3H_8N^+$; *m/z* 58.0652; 0.07 mDa error).

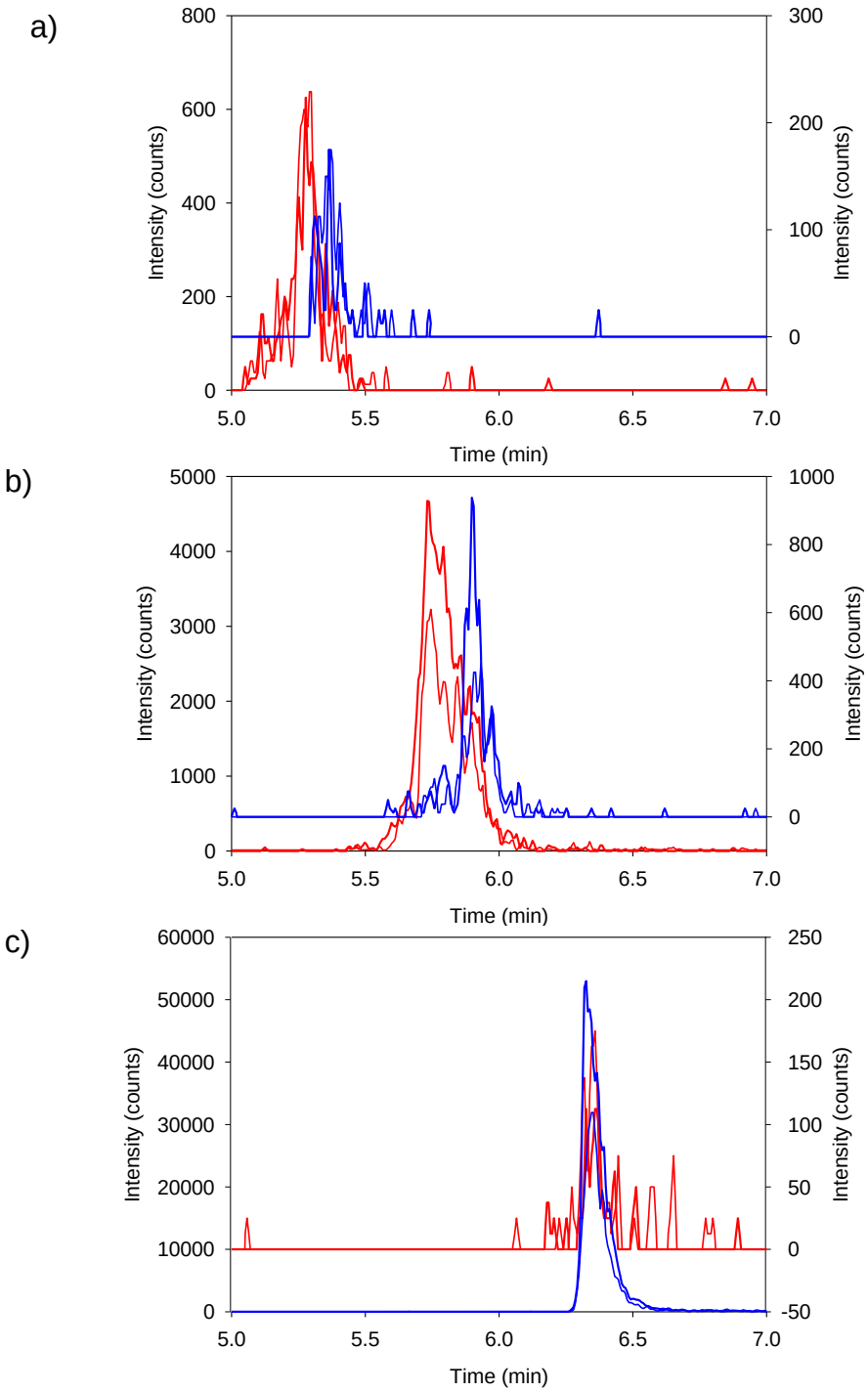

Figure A21: Overlay of LC-MS/MS chromatograms for **A** obtained with 50,000-times diluted Foam 12 (red) and 20-times diluted FS-330 base fraction (blue) for a) n = 6 **A** with transitions from *m/z* 449 to 404 (thick) and 376 (fine), b) n = 7 **A** with transitions from *m/z* 499 to 454 (thick) and 426 (fine), c) n = 8 **A** with transitions from *m/z* 549 to 504 (thick) and 476 (fine).

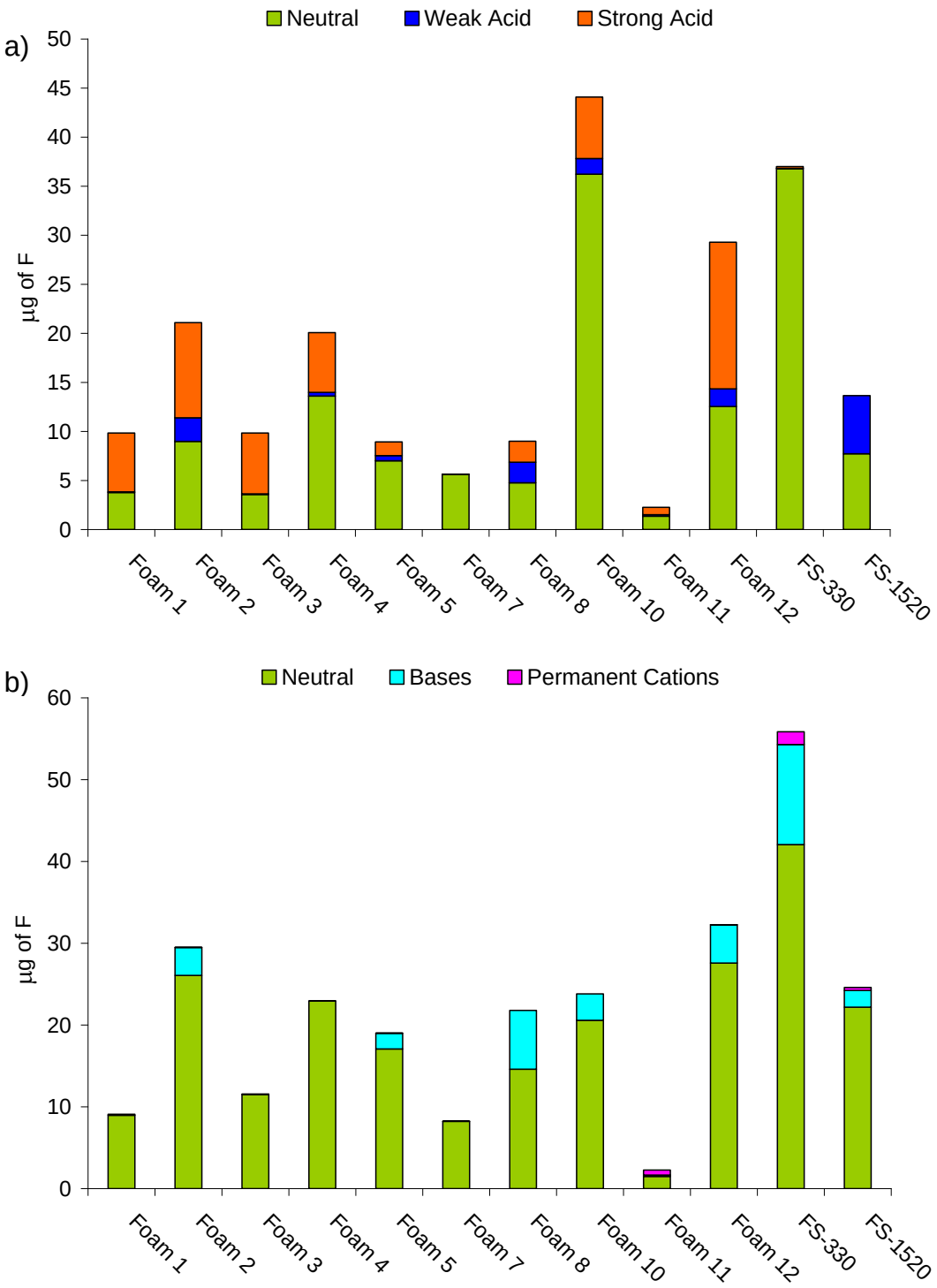

Figure A22: Graph of the total fluorine content of each fraction obtained by a) WAX SPE and b) WCX SPE as determined by TOF-CIC.

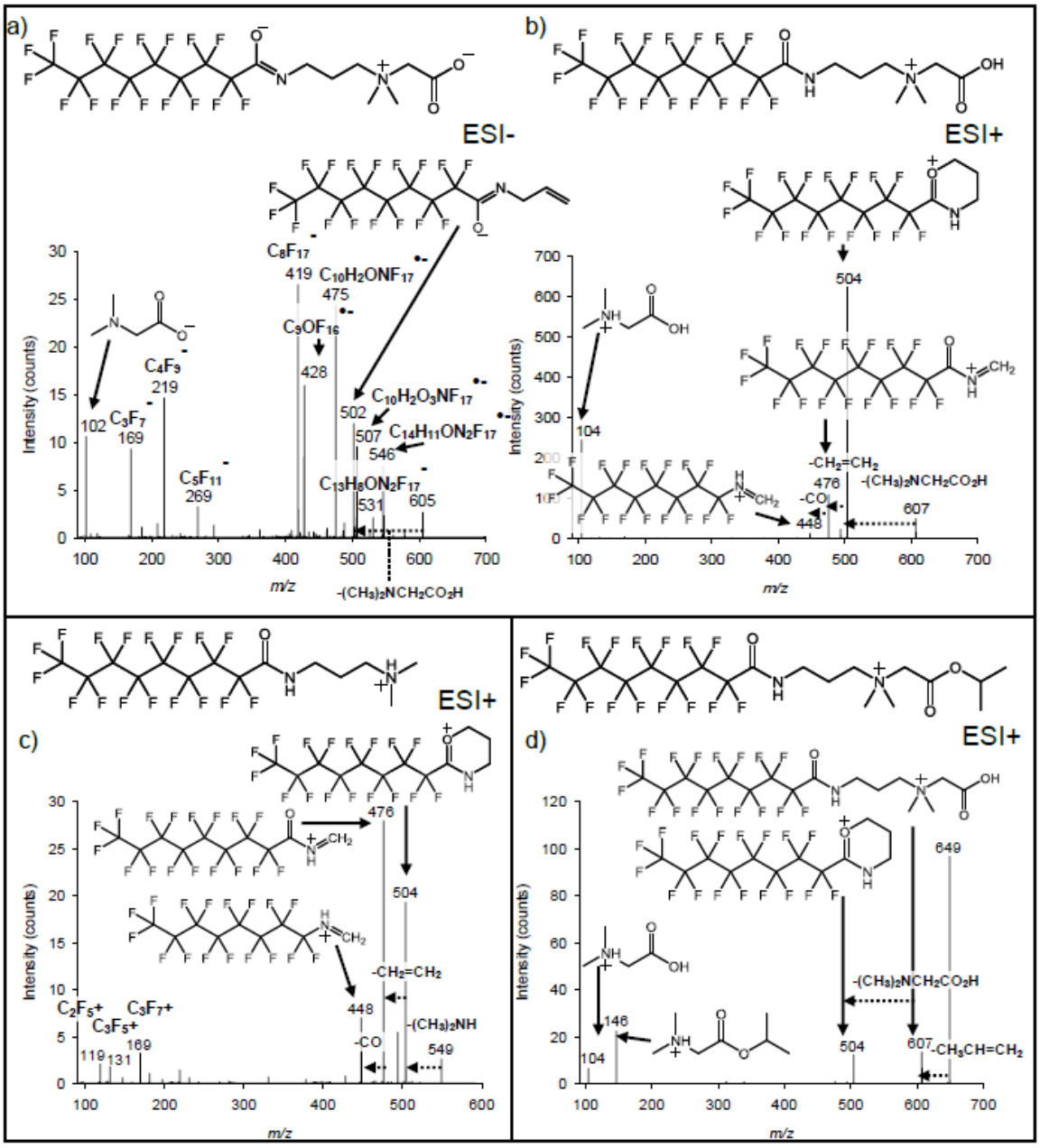

Figure A23: QTOF-MS CID spectra of **A**, **B** (PFAAB) and **C** using a) *m/z* 605 ion (**B**, *n* = 8) in ESI- with a collision energy of -30 V obtained using FS-330 WCX neutral fraction; b) *m/z* 607 ion (**B**, *n* = 8) in ESI+ with a collision energy of 40 V obtained using FS-330 WCX neutral fraction; c) *m/z* 549 ion (**A**, *n* = 8) in ESI+ with a collision energy of 50 V obtained using FS-330 base fraction; and d) m/z 649 ion (**C**, *n* = 8) in ESI+ with a collision energy of 30V obtained using FS-330 permanent cation fraction.

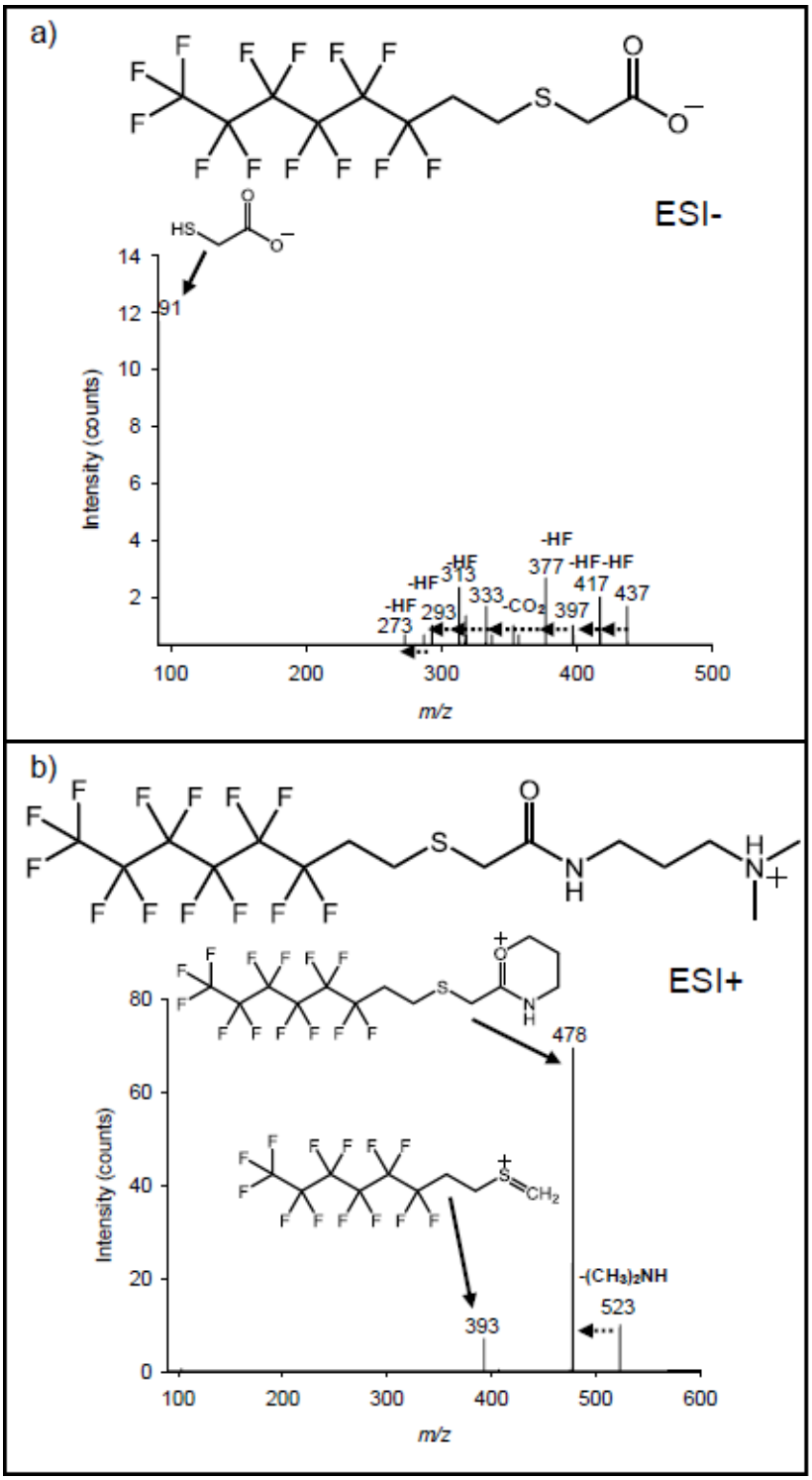

Figure A24: QTOF-MS CID spectra of **D** and **E** using a) *m/z* 437 ion (**D**, *n* = 6) in ESI- with a collision energy of -20 V obtained using FS-1520 WCX neutral fraction and b) *m/z* 523 ion (**E**, *n* = 6) in ESI+ with a collision energy of 40 V obtained using FS-1520 base fraction.

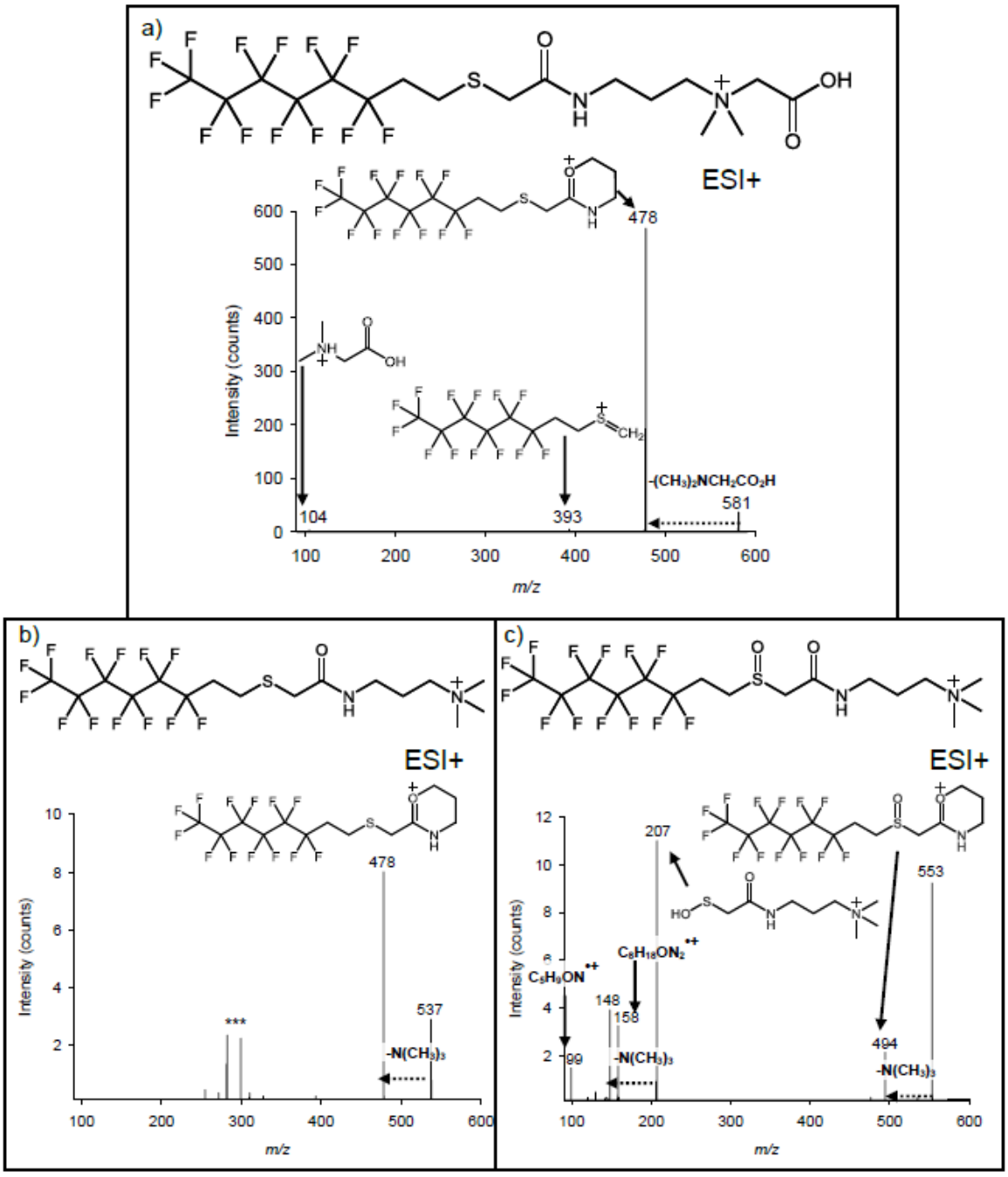

Figure A25: QTOF-MS CID spectra of **F** (FTSAB), **G** and **H** using a) *m/z* 581 ion (**F**, *n* = 6) in ESI+ with a collision energy of 30 V obtained using FS-1520 WCX neutral fraction; b) *m/z* 537 ion (**G**, *n* = 6) in ESI+ with a collision energy of 30 V obtained using FS-1520 permanent cation fraction; and c) *m/z* 553 ion (**H**, *n* = 6) in ESI+ with a collision energy of 30 V obtained using FS-1520 permanent cation fraction.

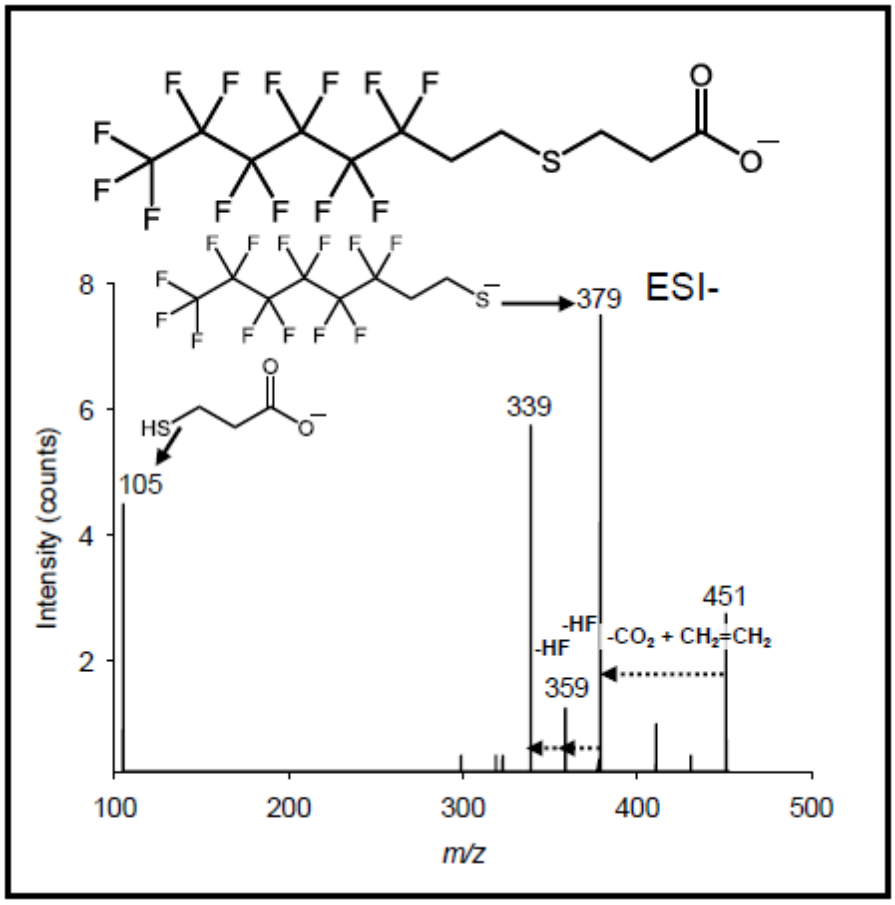

Figure A26: QTOF-MS CID spectrum of **K** as *m/z* 451 ion (*n* = 6) in ESI- with a collision energy of -20 V obtained using Foam 8 weak acid fraction.

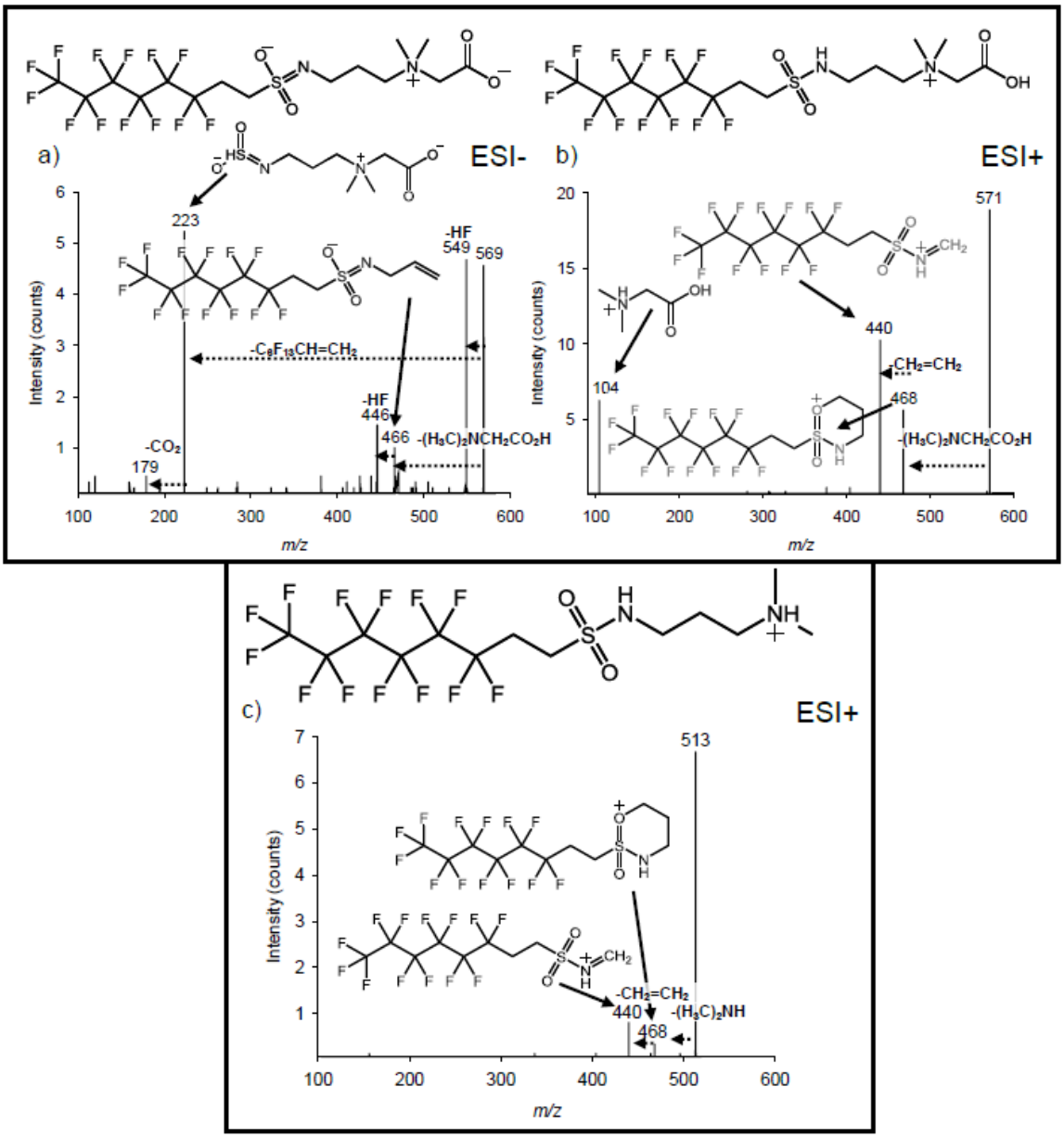

Figure A27: QTOF-MS CID spectra of **L** (6:2 FTAB) and **M** using a) *m/z* 569 ion (**L**, *n* = 6) in ESI- with a collision energy of -20 V obtained using Foam 3 WAX neutral fraction; b) *m/z* 571 ion (**L**, *n* = 6) in ESI+ with a collision energy of 40 V obtained using Foam 3 WCX neutral fraction; and c) *m/z* 513 ion (**M**, *n* = 6) in ESI+ with a collision energy of 40 V obtained using Foam 8 base fraction.

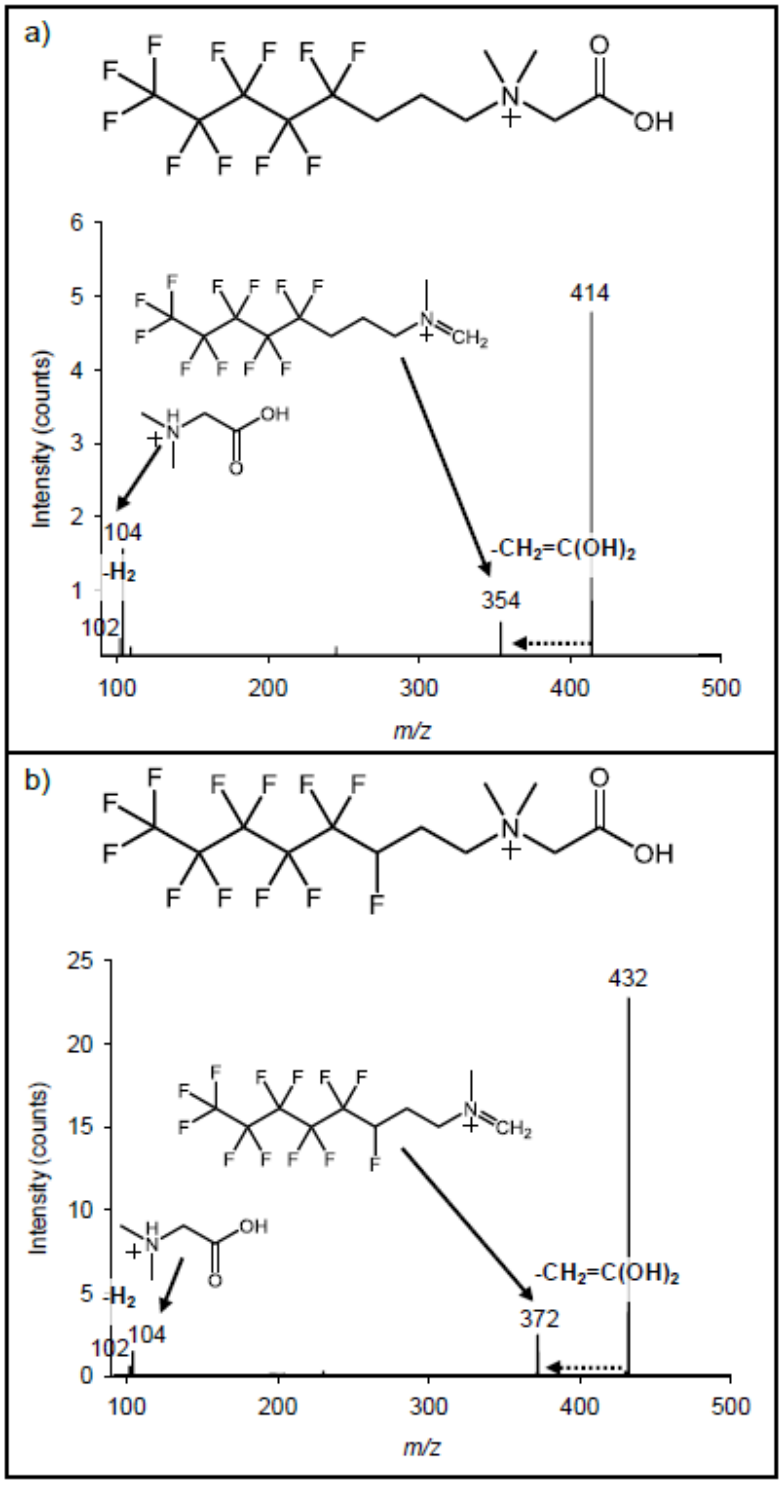

Figure A28: QTOF-MS CID spectra of FTBs **N** and **O** using a) *m/z* 414 ion (**N**, *n* = 5) in ESI+ with a collision energy of 45 V obtained using Foam 4 WCX neutral fraction and b) *m/z 432* ion (**O**, *n* = 5) in ESI+ with a collision energy of 45 V obtained using Foam 4 WCX neutral fraction.

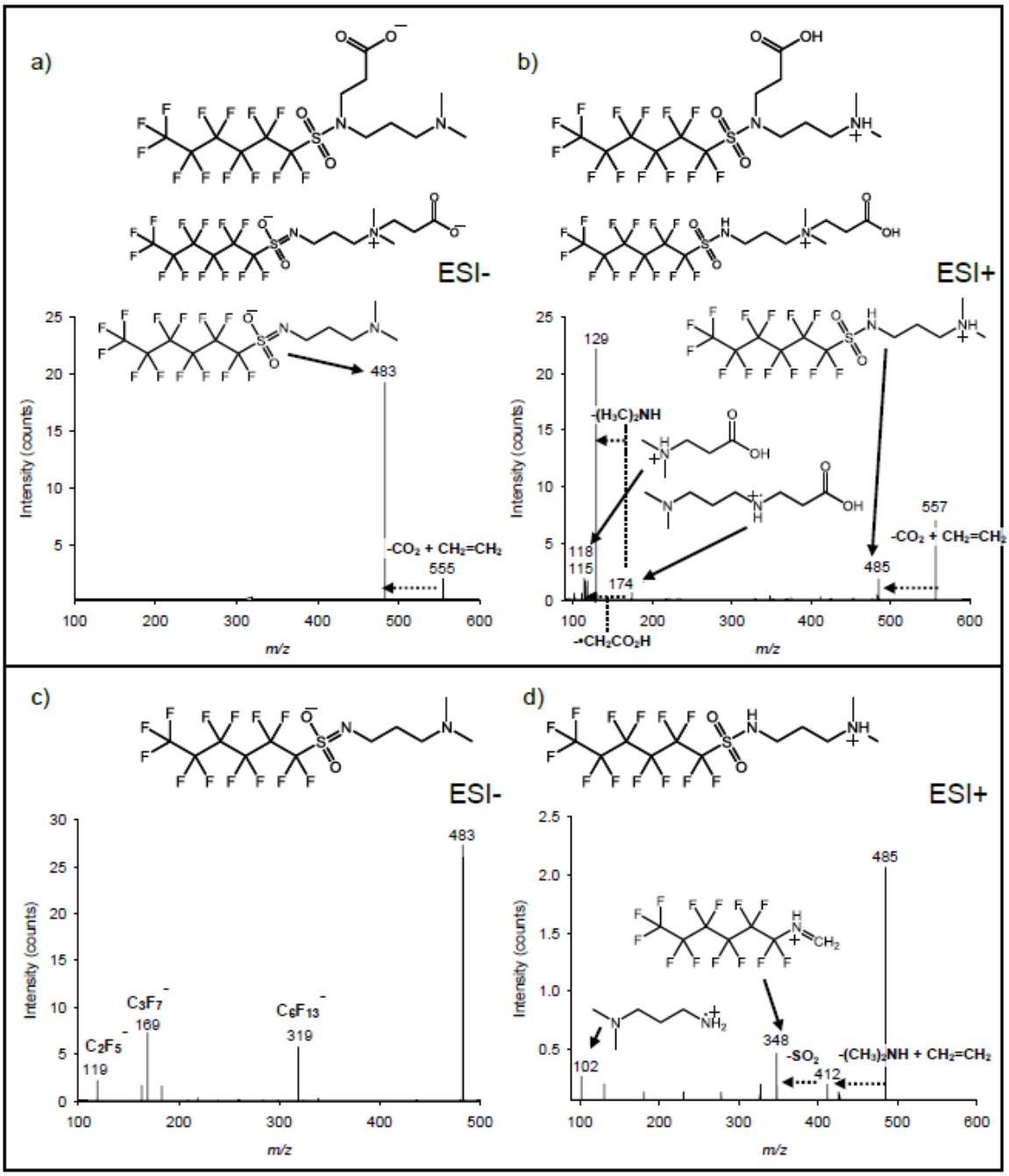

Figure A29: QTOF-MS CID spectra of **R** (PFASAC), **S**, and **T** using a) *m/z* 555 ion (**R/S**, *n* = 6) in ESI- with a collision energy of -20 V obtained using Foam 12 WCX neutral fraction; b) *m/z* 557 ion (**R/S**, *n* = 6) in ESI+ with a collision energy of 50 V obtained using Foam 12 WCX neutral fraction; c) *m/z* 483 ion (**T**, *n* = 6) in ESI- with a collision energy of -30V obtained using Foam 12 base fraction and d) m/z 485 ion (**T**, *n* = 6) in ESI+ with a collision energy of 50V obtained using Foam 12 base fraction.

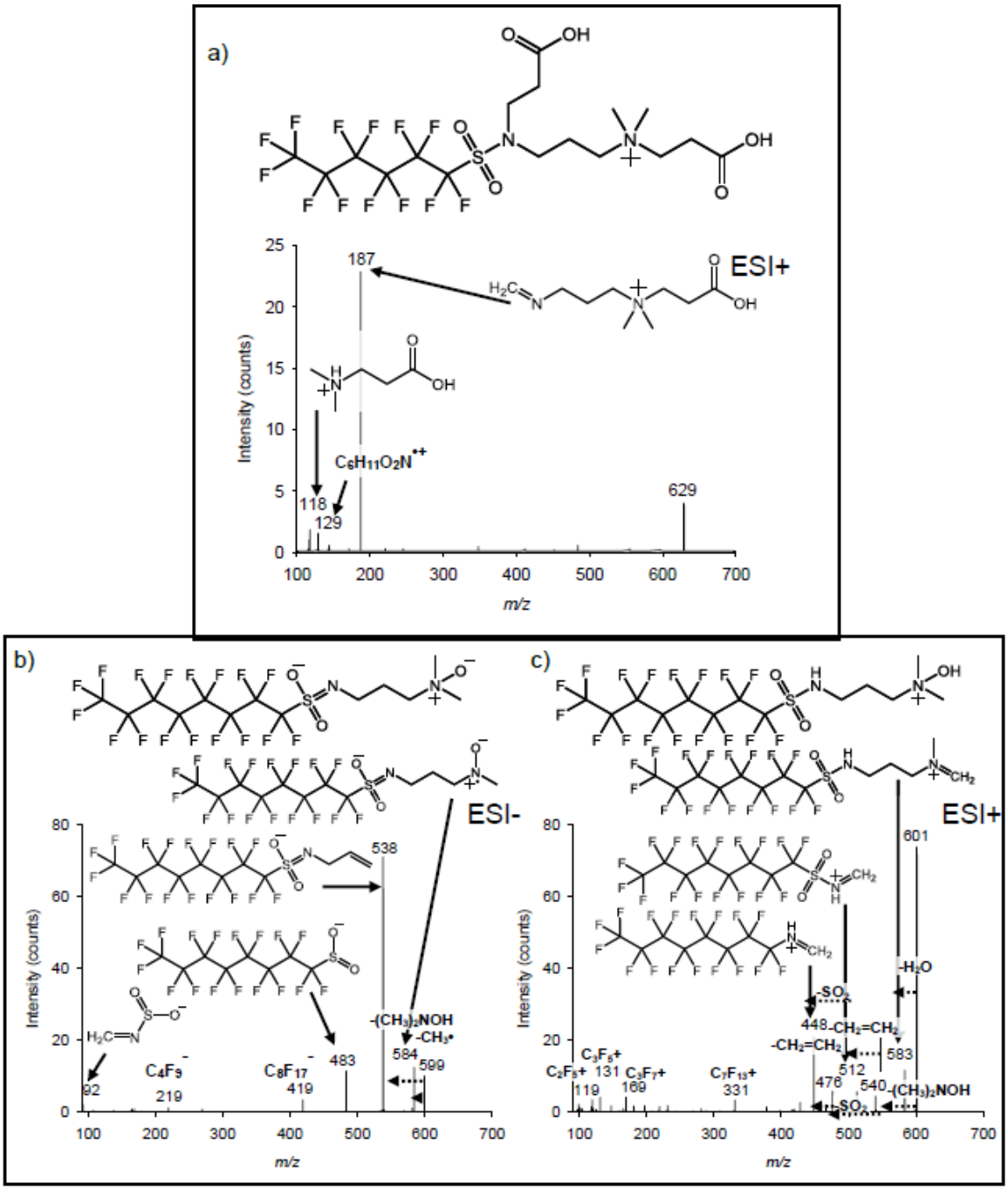

Figure A30: QTOF-MS CID spectra of **U** and **V** using a) *m/z* 629 ion (**U**, *n* = 6) in ESI+ with a collision energy of 50V obtained using Foam 12 weak acid fraction; b) *m/z* 599 ion (**V**, *n* = 8) in ESI- with a collision energy of -30V obtained using Foam 10 WCX neutral fraction and c) *m/z* 601 ion (**V**, *n* = 8) in ESI+ with a collision energy of 50V obtained using Foam 10 WCX neutral fraction.

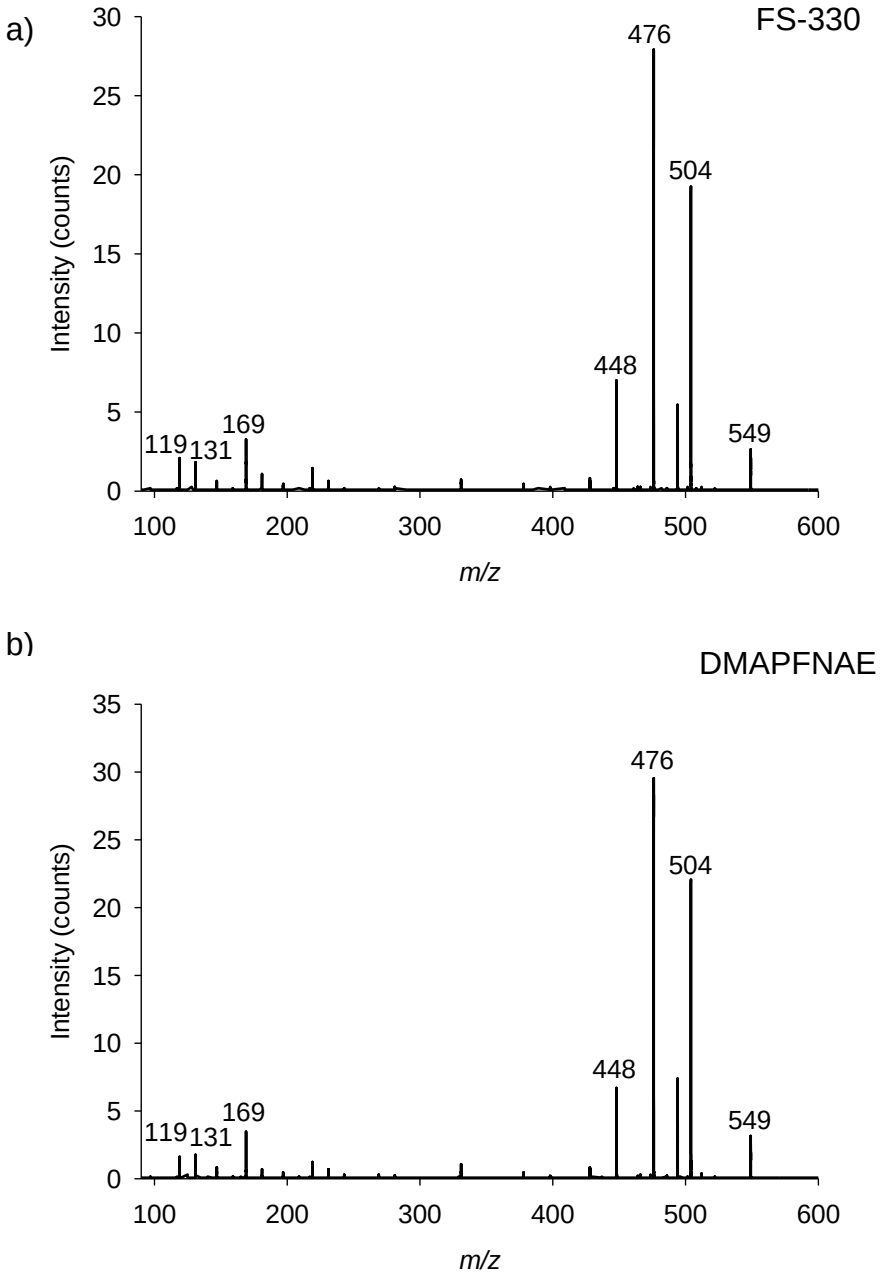

Figure A31: QTOF-MS CID spectra for synthetic and FS-330 *m/z* 549 ion in ESI+ with a collision energy of 50V using a) FS-330 base fraction (*m/z* of product ions: 549.0786, 504.0240, 475.9951, 448.0003, 168.9897, 130.9930, 118.9891) and b) synthetic N-(3-(dimethylamino)propyl)perfluorononanamide **(**DMAPFNAE) (*m/z* of product ions: 549.0788, 504.0227, 475.9946, 448.0010, 168.9896, 130.9908, 118.9906).

Appendix B:

Supporting Information for Chapter Three

Aerobic Biodegradation of Two Fluorotelomer Sulfonamide-based Aqueous Film Forming Foam Components Produces Perfluoroalkyl Carboxylates

Contents

Analytical Standards

Native analytical standards of 6:2 fluorotelomer alcohol (FTOH), 6:2 fluorotelomer sulfonate (FTSA), 6:2 fluorotelomer carboxylic acid (FTCA), 6:2 fluorotelomer unsaturated carboxylic acid (FTUCA), 5:3 FTCA, perfluoroheptanoic acid (PFHpA), perfluorohexanoic acid (PFHxA), perfluoropentanoic acid (PFPeA), and perfluorobutanoic acid (PFBA) were obtained from Wellington Laboratories (Guelph, Canada). Mass labelled standards of $^{13}C_8$-perfluorooctane sulfonamide (FOSA), $^{13}C_4$-6:2 FTOH, $^{13}C_2$-6:2 FTSA, $^{13}C_2$-6:2 FTCA, $^{13}C_2$-6:2 FTUCA, $^{13}C_4$-PFHpA, $^{13}C_2$-PFHxA, $^{13}C_5$-PFPeA, and $^{13}C_4$-PFBA were also from Wellington Laboratories (Guelph, Canada).

Chemicals Used

6:2 fluorotelomer thiol (FTSH), sulfuryl chloride, anhydrous acetonitrile, N,N-dimethylamino-1-propylamine, and 0.4 M ammonia in tetrahydrofuran were from Sigma Aldrich (Oakville, Canada). 6:2 FTOH (SynQuest Laboratories, Alachua, FL, USA) was used to spike high concentrations for spike and recovery tests. HPLC grade methanol and OmniSolv ethyl acetate were obtained from EMD Millipore (Billerica, MA, USA) and deionized water was obtained from a Purelab flex water purification system (ELGA, Woodridge, IL, USA).

Method for Purification of 6:2 FTAB by Precipitation

Crude 6:2 FTAB is first dissolved in 0.5 mL of methanol. A brief sonication (10 min.) may be used to break up clumps and dissolve the 6:2 FTAB. The methanol solution is then dropped into 10 mL of MTBE in a polypropylene centrifuge tube resulting in a white precipitate, which is allowed to finish precipitating for 10 minutes prior to a 10 minute centrifugation at 6000 rpm. The supernatant is removed and the precipitate is dissolved in methanol and precipitated again. The process is repeated multiple times (e.g.: 5 to 7 times) until adequate removal of unreacted 6:2 FTAA from the 6:2 FTAB is achieved.

Characterization of Synthesized Standards

6:2 fluorotelomer sulfonamide alkylamine (FTAA):

^{1}H NMR (400 MHz, chloroform-*d*): δ 1.73 (2H, $CH_2C\underline{H}_2CH_2$, multiplet), δ 2.24 (6H, $-N(C\underline{H}_3)_2$, singlet), δ 2.48 (2H, $-CH_2C\underline{H}_2N(CH_3)_2$, triplet), δ 2.62 (2H, $-CF_2C\underline{H}_2CH_2-$, triplet), δ 3.22 (2H, $-SO_2C\underline{H}_2CH_2-$, multiplet), δ 3.26 (2H, $-NHC\underline{H}_2CH_2-$, triplet)

^{19}F NMR (377 MHz, chloroform-*d*): δ -80.68 (3F, $-CF_3$, triplet of triplets), δ -113.56 (2F, $CH2C\underline{F}_2CF_2$, multiplet), δ -121.76 (2F, CF_2, multiplet), δ -122.75 (2F, CF_2, multiplet), δ -123.18 (2F, CF_2, multiplet), δ -126.02 (2F, CF_2, multiplet)

qTOF-MS: ESI+ theoretical *m/z* of $C_{13}H_{18}N_2O_2F_{13}S^+$ is 513.0875; *m/z* 513.0885 found

6:2 fluorotelomer sulfonamide alkylbetaine (FTAB):

^{1}H NMR (400 MHz, methanol-d_4): δ 2.03 (2H, $CH_2C\underline{H}_2CH_2$, multiplet), δ 2.70 (2H, $-CF_2C\underline{H}_2-$, multiplet), δ 3.22 (2H, $-SO_2NHC\underline{H}_2CH_2-$, triplet), δ 3.28 (6H, $-N(C\underline{H}_3)_2$, singlet), δ 3.40 (2H, $-SO_2C\underline{H}_2CH_2-$, multiplet), δ 3.70 (2H, $-CH_2C\underline{H}_2N(CH_3)_2-$, multiplet), δ 3.84 (2H, $(CH_3)_2NC\underline{H}_2CO_2$, singlet)

^{19}F NMR (377 MHz, methanol-d_4): δ -80.68 (3F, $-CF_3$, triplet of triplets), δ -113.02 (2F, $CH2C\underline{F}_2CF_2$, multiplet), δ -121.15 (2F, CF_2, multiplet), δ -122.15 (2F, CF_2, multiplet), δ -122.55 (2F, CF_2, multiplet), δ -125.58 (2F, CF_2, multiplet)

qTOF-MS: ESI(+) theoretical *m/z* of $C_{15}H_{20}N_2O_4F_{13}S^+$ is 571.0931; *m/z* 571.0936 found

6:2 fluorotelomer sulfonamide (FTSAm):

^{1}H NMR (400 MHz, acetone-d_6): δ 2.77 (2H, $-CF_2C\underline{H}_2-$, multiplet), δ 3.41 (2H, $-C_6F_{13}CH_2C\underline{H}_2-$, multiplet), δ 6.43 (2H, $-SO_2N\underline{H}_2-$, broad singlet)

^{19}F NMR (377 MHz, acetone-d_6): δ -80.85 (3F, $-CF_3$, triplet of triplets), δ -113.27 (2F, $CH2C\underline{F}_2CF_2$, multiplet), δ -121.58 (2F, CF_2, multiplet), δ -122.56 (2F, CF_2, multiplet), δ -123.06 (2F, CF_2, multiplet), δ -125.92 (2F, CF_2, multiplet)

qTOF-MS: ESI- theoretical *m/z* of $C_8H_5NO_2F_{13}S^-$ is 425.9838; *m/z* 425.9823 found

Mineral Medium

A sulfate-free mineral medium based on that reported in van Hamme *et al.* was used.[1] The mineral medium contained 1.60 g of K_2HPO_4, 0.40 g of KH_2PO_4, 5 g of sodium acetate, 1.55 g of NH_4Cl, 0.09 g of $CaCl_2{\cdot}2H_2O$, 0.165 g of $MgCl_2{\cdot}6H_2O$ and 4 g of glucose per litre of deionized water. The medium and all biodegradation bottles were

autoclaved for 30 minutes at 121°C in a Steris SG-120 Scientific Gravity Sterilizer (Mentor, OH, USA). The medium also contained 5.0 mL/L of Wolfe's minerals and 1.0 mL/L of Pfennig's vitamins added after autoclaving by filtration through a 0.2-µm nylon syringe filter (Chromatographic Specialties, Brockville, Canada). The Wolfe's minerals were composed of 50 mg/L of $AlCl_3$, 67 mg/L of $CaCl_2 \cdot 2H_2O$, 4.0 mg/L of $CuCl_2$, 1.0 g/L of $FeCl_3 \cdot 6H_2O$, 5.1 g/L of $MgCl_2 \cdot 6H_2O$, 0.808 g/L of $MnCl_2 \cdot 4H_2O$, 40 mg/L of $Na_2MoO_4 \cdot 2H_2O$, 1.0 g/L of NaCl, 1.5 g/L of trisodium nitrilo(tri)acetate monohydrate, and 80 mg/L of $ZnCl_2$ in deionized water. The Pfennig's vitamins contained 10 mg/L of biotin, 50 mg/L of *p*-aminobenzoic acid, 100 mg/L of thiamine hydrochloride, and 50 mg/L of vitamin B12 in deionized water.

Biodegradation Setup

The mixed liquor was collected from Ashbridges Bay Wastewater Treatment Plant in Toronto, Ontario, Canada, which is the largest wastewater treatment plant in the City of Toronto. The mixed liquor was shaken prior to dispensing it to re-suspend the solids. To wash the mixed liquor, 40 mL portions of mixed liquor (either active or autoclaved) were transferred to 50 mL centrifuge tubes and centrifuged at 6000 rpm for 20 min. The supernatant was removed with a transfer pipet, and the tubes were topped up to 40 mL with mineral medium. The tubes were vortex mixed, then centrifuged for 20 min at 6000 rpm, the supernatant was removed, and the wash with mineral medium was repeated a second time. The solids were suspended in 40 mL of mineral medium and added to the biodegradation experiment bottles. The bottles containing mineral medium and washed mixed liquor, where needed, were purged overnight prior to spiking with 6:2 FTAB, 6:2 FTAA, and/or 6:2 FTUCA. The biocide used was 300 mg of $HgCl_2$ and 300 mg of NaN_3 as described for an earlier study[2]. However, this mixture is not recommended due to safety concerns with mixing azides and heavy metals.

The air purge for the polypropylene bottles in the biodegradation experiment was delivered through a 20 gauge needle inserted through the septum of each bottle. The air was house air that passed through a Tylan RO-32 mass flow controller (San Diego, CA, USA) and a Supelpure HC charcoal filter (Supelco, Bellefonte, PA, USA), and a bubbler

with deionized water to humidify the air and reduce evaporative losses prior to being delivered through Tygon tubing and a series of valves to the biodegradation vessels.

LC-MS/MS Methods

Most LC-MS/MS analysis was performed using a Waters Acquity UPLC coupled to an API 4000 triple quadrupole mass spectrometer (Sciex, Concord, Ontario). The analytical column was a Kinetex XB-C18 (4.6 x 50 mm, 2.6 μm, 100Å, Phenomenex, Torrance, CA) with a Security Guard Ultra C18 guard cartridge (Phenomenex, Torrance, CA). The mobile phase solvents were 10 mM ammonium acetate in water (A) and 10 mM ammonium acetate in methanol (B) at 0.5 mL/min. In all methods, the source temperature was 550°C, the curtain gas setting was 10, the collision gas setting was 12, and source gases 1 and 2 were set to 40. For positive electrospray (ESI+) methods, the ionization source potential was 4500 V, the entrance potential was 10 V, and the collision cell exit potential was 15V. For negative electrospray (ESI-) methods, the ionization source potential was -4500V, the entrance potential was -10 V, and the collision cell exit potential was -15 V. The injection volume used was 30 μL and for gradients beginning at 50% A: 50% B the sample composition was 50% H_2O: 50 % methanol, while for gradients beginning at 70% A: 30% B sample composition was 60% H_2O: 40% methanol.

Three gradient profiles were used to analyze different components by LC-MS/MS. For analysis of 6:2 FTAA, 6:2 FTAB, and related transitions in ESI+, the gradient began at 50% A: 50% B, changed to 5% A: 95% B over 3 minutes, held for 1.5 minutes, returned to 50% A: 50% B over 0.5 minutes, and equilibrated for 2.0 minutes. For analysis of FTCAs, 6:2 FTUCA, 6:2 FTSA, and PFCAs, the gradient started at 70% A: 30% B, transitioned to 5% A: 95% B over 3.0 minutes, held for 2.0 minutes, returned to 70% A: 30% B over 0.5 minutes, and equilibrated for 2.0 minutes. For analysis of 6:2 FTSAm, the gradient was identical to that for 6:2 FTAA and 6:2 FTAB except that the hold at 5% A: 95% B was 2.0 minutes instead of 1.5 minutes. A table of compound specific multiple reaction monitoring (MRM) parameters is included as Table B4.

Some preliminary experiments were analyzed by LC-MS/MS using an Agilent 1100 series HPLC (Agilent Technologies, Wilmington, DE) coupled to an API 4000

triple quadrupole mass spectrometer (Sciex, Concord, ON, Canada). The same HPLC column, mobile phase composition, and API 4000 mass spectrometer settings were used for these analyses as with the Acquity system. For analysis of 6:2 FTAA, 6:2 FTAB, and degradation products in ESI+, the gradient program began at 50% A: 50% B, changed to 5% A: 95% B over 3 minutes, held for 2 minutes, returned to 50% A: 50% B over 0.5 minutes, and equilibrated for 2.0 minutes. For analysis of FTCAs, 6:2 FTUCA, 6:2 FTSA, and PFCAs in ESI-, the gradient program was identical to that used with the Acquity UPLC system.

Because the API 4000 LC-MS/MS was not available to analyze the repeat spike and recovery experiment using wet, autoclaved, washed wastewater treatment plant sludge, these samples were analyzed using a Waters Acquity UPLC-Xevo TQS (Waters, Cambridge, MA) with an Acquity UPLC BEH C18 column with 1.7 μm particles (2.1 mm x 75mm, Waters, Cambridge, MA). The gradient program was run at 0.5 mL/min with 10 mM ammonium acetate in deionized water (A) and methanol (B) beginning at 90% A: 10% B, changing to 22% A: 78% B over 7 min., transitioning to 10% A: 90% B over 0.4 min., returning to 90% A: 10% B over 0.1 min., and remaining at 90% A: 10% B for 3 min. for a run time of 10.5 min. Matrix matched calibration using blank sludge extracts was performed with internal standards as in analyses for the main biodegradation experiment. With the Xevo TQS, the source temperature was 150°C, the desolvation temperature was 500°C, the cone gas flow was 150 L/hr, the desolvation gas flow was 650 L/hr, the collision gas flow was 0.15-0.12 mL/min, and the nebulizer gas flow was 5.5 Bar. The source offset was 50 V, while the the capillary voltage was 3.43 kV in ESI+ and -2.48 kV in ESI-. Injection volume was 2 μL. The MS/MS transitions used in with the Xevo TQS are included in Table S1.

GC-MS Method

An Agilent 7890A gas chromatography system coupled to an Agilent 5975C inert XL EI/CI MSD (Agilent Technologies, Wilmington, DE) in positive methane chemical ionization (CI) mode was used to analyze XAD extracts for 6:2 FTOH. Using the system autosampler, injections were 1 μL in splitless mode into an inert double gooseneck inlet liner. The analytical column was an Agilent DB-1701 column (Agilent Technologies,

Wilmington, DE) with dimensions 30 m × 0.25 mm × 0.15 μm. The oven program began at 50°C, held at 50°C for 2 minutes, increased at 12°C per minute to 150°C, and then increased at 30°C per minute to 250°C for a run time of 14.67 minutes. The carrier gas was helium at a constant flow rate of 1.2 mL per minute, the inlet temperature was 250°C, and the MSD transfer line was kept at 280°C. The MSD was operated with a solvent delay of 3.5 minutes. Quantification of 6:2 FTOH was by internal standard calibration in selected ion monitoring mode with *m/z* 365.0 monitored for 6:2 FTOH and *m/z* 369.0 monitored for $^{13}C_4$-6:2 FTOH with dwell times of 50 msec each. A CI autotune was performed prior to analysis of each set of samples.

Solids Extraction Procedure

Based on the procedures of Houtz *et al.*[3], to extract organic solids from the biodegradation experiment, 50 to 85 mg of lyophilized solids from each bottle was weighed into a 15 mL polypropylene centrifuge tube. 2.5 mL of 0.1% NH_4OH in methanol was added to each tube, vortex mixed for 20 seconds, sonicated for 30 minutes, and shaken for 2 hours 360 rpm. The tubes were then centrifuged for 5 minutes at 6000 rpm and the supernatant was collected with a transfer pipet. The extraction procedure was repeated two more times and the combined extract was evaporated to 2 mL. The extracts were cleaned up with Supelclean ENVI-carb cartridges (1mL, 100 mg, Supelco, Bellefonte, PA, USA) that were conditioned with 3 × 1 mL of methanol, loaded with 2 mL of extract, and eluted with 4 × 1 mL of methanol. The extracts collected during both sample loading and elution were then evaporated to 4 mL under a gentle stream of nitrogen.

A repeat spike and recovery experiment conducted by spiking autoclaved, washed wastewater treatment plant solids, freezing those solids at -20°C, lyophilizing those solids overnight and then extracting them as described previously.

qTOF-MS Method

qTOF-MS measurements were made using a AB/Sciex QStar XL mass spectrometer (MDS Sciex, Concord, ON, Canada) with direct loop injections and solvent

flow delivered with an Agilent 1100 series HPLC pump (Agilent Technologies, Wilmington, DE). Solvent flow was delivered at 100 µL per minute and consisted of 50% methanol: 50% 0.1% formic acid in water for ESI+ measurements and 50% methanol : 50% 10 mM ammonium acetate in water for ESI- measurements. The source temperature was 200°C, the declustering potential was 60 V (ESI+) or -30 V (ESI-), the focusing potential was 60 V (ESI+) or -30 V (ESI-), and the ionization potential was 4200 V (ESI+) or -4200 V (ESI-).

qTOF-MS Data Analysis

Using CF2 scale mass defect plots[4], it is possible to quickly and easily focus attention on a region of highly fluorinated PFASs, which have relatively high *m/z* greater than 350 and low mass defects on the CF_2 scale between -0.05 and 0.15. Compared to the parent compounds, fluorinated degradation products tended to have lower mass defects due to oxidation (O has a negative mass defect) and shortening of the hydrocarbon head group (H has a positive mass defect). In identifying possible degradation products, it was important to consider whether the ions observed were adducts or fragments of 6:2 FTAB, 6:2 FTAA, or a degradation product. Along these lines, Na^+ and K^+ adducts and known product ions of 6:2 FTAB and 6:2 FTAA were observed in ESI+ and do not represent distinct degradation products. In ESI-, Cl^- and NO_3^- adducts were identified along with many fragment ions resulting from losses of HF from anions of fluorotelomer substances, which occur relatively readily in the source used. Molecular formulae were assigned to possible degradation products using Analyst 1.5.1 (Sciex, Concord, ON) by considering formulas with even electron state, a charge of +1 or -1, -0.5 to 10 double bond equivalents, 0 to 25 carbon, 8 to 13 fluorine, 0 to 100 hydrogen, 0 to 4 nitrogen, 0 to 8 oxygen, and 0 to 1 sulfur. The probable molecular formula was chosen based on error in the accurate mass less than 3 *mDa* and whether the molecular formula could be assigned to a chemically reasonable modification of the starting 6:2 FTAB or 6:2 FTAA. For product ion scans, only molecular formulas consisting of atoms present in the putative parent compound were considered to assign the molecular formulae of fragment ions and accurate mass errors of 5 *mDa* or less were preferred.

TOF-CIC Method

Selected extracts of sludge solids and XADs were analyzed by total organofluorine combustion ion chromatography (TOF-CIC), as described in detail elsewhere[2,5]. In this technique samples were loaded on a ceramic boat and combusted at 900-1000°C with oxygen as a combustion gas and argon as carrier gas in an Automated Quick Furnace (AQF-100) automated combustion unit (Mitsubishi Chemical Analytech, Japan). Organofluorine in the samples produces HF during combustion, which is collected in an aqueous absorption unit that dissociates it to F^- and H^+. F^- is then analyzed by ion chromatography with an ICS-2100 ion chromatography system (Dionex Co. Ltd., Sunnyvale, CA, USA) using methane sulfonic acid in the absorption solution as an internal standard.

Table B1: MRM Parameters for LC-MS/MS Analysis ([a] indicates quantifying transition)

Analyte	ESI Mode	API 4000 MRM Transition(s)	API 4000 Declustering Potential (V)	API 4000 Collision Energy (V)	Xevo TQS MRM Transition(s)	Xevo TQS Cone Voltage (V)	Xevo TQS Collision Energy (V)
6:2 FTAB	+	571.2>440.0[a] 571.2>104.1	114 114	43 50	570.90>440.00[a] 570.90>104.06	50 50	30 30
6:2 FTAA	+	513.2>440.1[a] 513.2>86.1	90 90	45 60	512.90>439.98[a] 512.90>85.93	40 40	30 34
Degradation product **2**	+	499.0>440.0 499.0>58.1	105 105	42 70	na		
Degradation product **3**	+	485.0>440.1 485.0>58.1	80 80	38 70	na		
6:2 FTSAm	-	425.8>345.9[a] 425.8>406.0	-60 -60	-32 -12	425.95>365.99[a] 425.95>345.90	-28 -28	-16 -22
$^{13}C_8$-FOSA	-	505.9>78.0[a] 505.9>485.9	-80 -80	-85 -38	506.00>78.00	-66	-28
6:2 FTSA	-	427.0>81.0[a] 427.0>406.8	-100 -100	-65 -32	427.10>407.08[a] 427.10>81.00	-38 -38	-22 -32
$^{13}C_2$-6:2 FTSA	-	429.0>81.0[a] 429.0>408.8	-100 -100	-65 -32	428.84>81.00	-86	-32
6:2 FTCA	-	376.9>292.9	-23	-13	na		
$^{13}C_2$-6:2 FTCA	-	379.0>294.0	-23	-13	na		
6:2 FTUCA	-	356.9>292.9	-28	-15	357.03>293.05	-10	-10
$^{13}C_2$-6:2 FTUCA	-	359.0>294.0	-28	-15	359.00>294.00	-10	-10
5:3 FTCA	-	341.0>237.0	-28	-15	240.97>216.95 240.97>236.91[a]	-46 -46	-22 -12
PFHpA	-	362.8>318.97	-27	-13	363.00>169.00 363.00>319.00[a]	-30 -30	-19 -10
$^{13}C_4$-PFHpA	-	366.8>321.97	-27	-13	367.10>168.98	-30	-19
PFHxA	-	312.8>268.9	-20	-13	313.00>269.00	-26	-10
$^{13}C_2$-PFHxA	-	314.8>269.8	-20	-13	315.00>270.00	-26	-10
PFPeA	-	262.8>218.97	-20	-13	263.03>219.04	-24	-8
$^{13}C_5$-PFPeA	-	267.8>222.97	-20	-13	268.10>223.03	-24	-8
PFBA	-	212.8>168.9	-25	-13	212.90>168.90	-30	-11
$^{13}C_4$-PFBA	-	217.0>172.0	-25	-13	216.90>171.90	-30	-11

Table B2: Comparison of results of quantitation of 6:2 FTAA and 6:2 FTAB in matrix spike and recovery by matrix matched external calibration and standard additions (n = 4)

Analyte	Matrix Matched Calibration Average Recovery (± standard deviation)	Standard Additions Average Recovery (± standard deviation)
6:2 FTAA	97 ± 5 %	95 ± 5 %
6:2 FTAB	117 ± 3 %	132 ± 9 %

Table B3: Percent Recoveries of Analytes Analyzed by LC-MS/MS from mixed liquor treated medium "Aqueous Phase" and blank sludge "Solids" (mean ± standard deviation; n =4 for aqueous phase, n = 3 for solids)

Analyte	% Recovery from Aqueous Phase	% Recovery from pre-lyophilized Solids	% Recovery from wet solids
6:2 FTAB	117 ± 3	92 ± 13	86 ± 5
6:2 FTAA	97 ± 5	75 ± 12	91 ± 4
6:2 FTSAm	--	--	88 ± 4
6:2 FTSA	119 ± 15	89 ± 10	89 ± 6
6:2 FTCA	114 ± 15	--	--
6:2 FTUCA	111 ± 8	105 ± 35	87 ± 6
5:3 FTCA	106 ± 12	96 ± 21	86 ± 10
PFHpA	121 ± 11	115 ± 18	90 ± 4
PFHxA	104 ± 7	95 ± 20	91 ± 6
PFPeA	107 ± 9	114 ± 14	88 ± 7
PFBA	112 ± 9	113 ± 24	91 ± 10

Table B4: LOD and LOQ for Quantified Analytes in Matrix

Analyte	LOD (aq) (ng/mL)	LOQ (aq) (ng/mL)	LOD (solids) (ng/g)	LOQ (solids) (ng/g)	LOD (XAD) ng	LOQ (XAD) ng
6:2 FTAB	0.2	0.7	20	60	20	70
6:2 FTAA	0.4	1.2	20	60	30	100
6:2 FTSAm	0.2	0.6	40	120	40	110
6:2 FTSA	0.1	0.4	9	30	--	--
6:2 FTOH	--	--	--	--	10	40
6:2 FTCA	0.15	0.5	--	--	--	--
6:2 FTUCA	0.03	0.1	0.9	3	--	--
5:3 FTCA	0.03	0.1	1	4	--	--
PFHpA	0.03	0.1	1	4	--	--
PFHxA	0.04	0.15	2	8	--	--
PFPeA	0.03	0.1	4	10	--	--
PFBA	0.4	1.5	9	30	--	--

Table B5: Mass Spectral Data Table for qTOF-MS

Structure ID	ESI Mode	Precursor Ion	Collision Energy (V)	Sample	Precursor/ Product	Observed *m/z*	Molecular Formula	Theoretical m/z	Error (mDa)
6:2 FTAA	ESI-	511	-20	synthesized standard	Precursor	511.0741	C13H16F13N2O2S-	511.0730	1.1
					Product	491.0676	C13H15F12N2O2S-	491.0668	0.8
					Product	471.0622	C13H14F11N2O2S-	471.0605	1.7
					Product	451.0525	C13H13F10N2O2S-	451.0543	-1.8
					Product	431.0497	C13H12F9N2O2S-	431.0481	1.6
					Product	367.0910	C13H12F9N2-	367.0862	4.8
					Product	347.0780	C13H11F8N2-	347.0799	-1.9
					Product	327.0769	C13H10F7N2-	327.0737	3.2
					Product	165.0708	C5H13N2O2S-	165.0703	0.5
6:2 FTSAm	ESI-	426	-10	synthesized standard	Precursor	425.9842	C8H5F13NO2S-	425.9838	0.4
					Product	405.9785	C8H4F12NO2S-	405.9776	0.9
					Product	385.9693	C8H3F11NO2S-	385.9714	-2.1
					Product	365.9668	C8H2F10NO2S-	365.9652	1.6
1	ESI+	529	40	AE #3, 6:2 FTAA, XAD, t=45 days	Precursor	529.0849	C13H18F13N2O3S+	529.0825	2.4
					Product	468.0286	C11H11O2NSF13+	468.0297	-1.1
					Product	439.9973	C9H7O2NSF13+	439.9984	-1.1
	ESI-	527	-20	SC #1, 6:2 FTAA, XAD, t=21 days	Precursor	527.0687	C13H16F13N2O3S-	527.0679	0.8
					Product	507.0585	C13H15F12N2O3S-	507.0617	-3.2
					Product	467.0453	C13H13F10N2O3S-	467.0492	-3.9
					Product	447.041	C13H12F9N2O3S-	447.043	-2
					Product	446.0058	C11H8NO2F12S-	446.0089	-3.1
					Product	426.0057	C11H7NO2F11S-	426.0027	3.0
					Product	322.0282	C11H5F9N-	322.0283	-0.1
					Product	181.0614	C5H13N2O3S-	181.0652	-3.8
					Product	120.0108	C3H6NO2S-	120.0124	-1.6

Structure ID	ESI Mode	Precursor Ion	Collision Energy (V)	Sample	Precursor/ Product	Observed *m/z*	Molecular Formula	Theoretical m/z	Error (mDa)
2	ESI+	499	30	SC #1, 6:2 FTAA, solids extract	Precursor	499.0731	C12H16N2O2F13S+	499.0719	1.2
					Product	468.0359	C11H11O2NSF13+	468.0297	6.2[a]
					Product	439.9994	C9H7O2NSF13+	439.9984	1.0
3	ESI+	485	30	SC #1, 6:2 FTAA, solids extract	Precursor	485.0516	C11H14N2O2F13S+	485.0562	-4.6
					Product	468.0309	C11H11O2NSF13+	468.0297	1.2
					Product	439.9984	C9H7O2NSF13+	439.9984	0.0
4	ESI-	484	-10	AE #1, 6:2 FTAA, XAD, t=7 days	Precursor	484.0235	C11H11NO3F13S-	484.0257	-2.2
					Product	464.0177	C11H10NO3F12S-	464.0195	-1.8
					Product	444.0079	C11H9NO3F11S-	444.0132	-5.3
					Product	138.0224	C3NO3SH8-	138.0230	-0.6
5	ESI-	482	-20	SC #1, 6:2 FTAA, solids extract	Precursor	482.0090	C11H9NO3F13S-	482.0101	-1.1
					Product	462.0033	C11H8NO3F12S-	462.0038	-0.5
					Product	421.9948	C11H6NO3F10S-	421.9914	3.4
					Product	397.9863	C9H3NO2F11S-	397.9714	14.9[a]
					Product	385.9651	C8H3NO2F11S-	385.9714	-6.3[a]
					Product	365.9653	C8H2NO2F10S-	365.9652	0.1
					Product	325.9397	C8NO2F8S-	325.9527	-13[a]
					Product	136.0053	C3NO3SH6-	136.0073	-2.0
6	ESI-	498	-20	AE #3, 6:2 FTAA, XAD, t=45 days	Precursor	498.0070	C11H9NO4F13S-	498.0050	2.0
					Product	457.9935	C11H7NO4F11S-	457.9925	1.0
					Product	417.9846	C11H5NO4F9S-	417.9801	4.5
					Product	322.9958	C8H2OF11-	322.9935	2.3
					Product	302.9853	C8HOF10-	302.9873	-2.0
					Product	151.0024	C3H6NO4S-	152.0023	0.1

a) These fragment ions have a higher error in observed accurate mass compared to theoretical accurate mass for the assigned fragment due to low intensity signals.

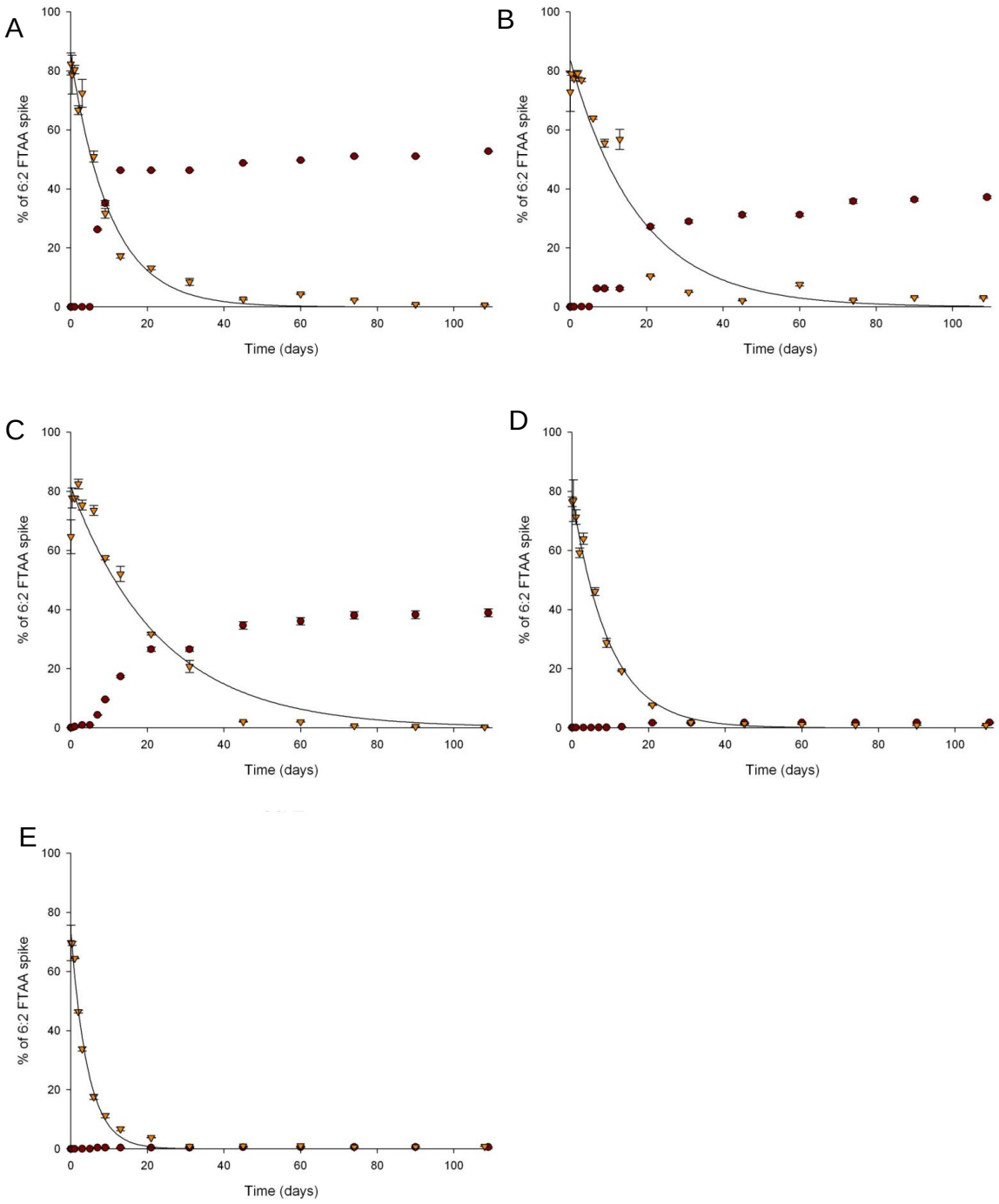

Figure B1: Loss of 6:2 FTAA from aqueous phase (▲) and cumulative amount of 6:2 FTAA recovered on XADs (●). Fitted curves are shown to highlight trends and error bars are standard deviations. Graphs are for: a) active experiment 1, b) active experiment 2, c) active experiment 3, d) sterile control 1, and e) sterile control 2.

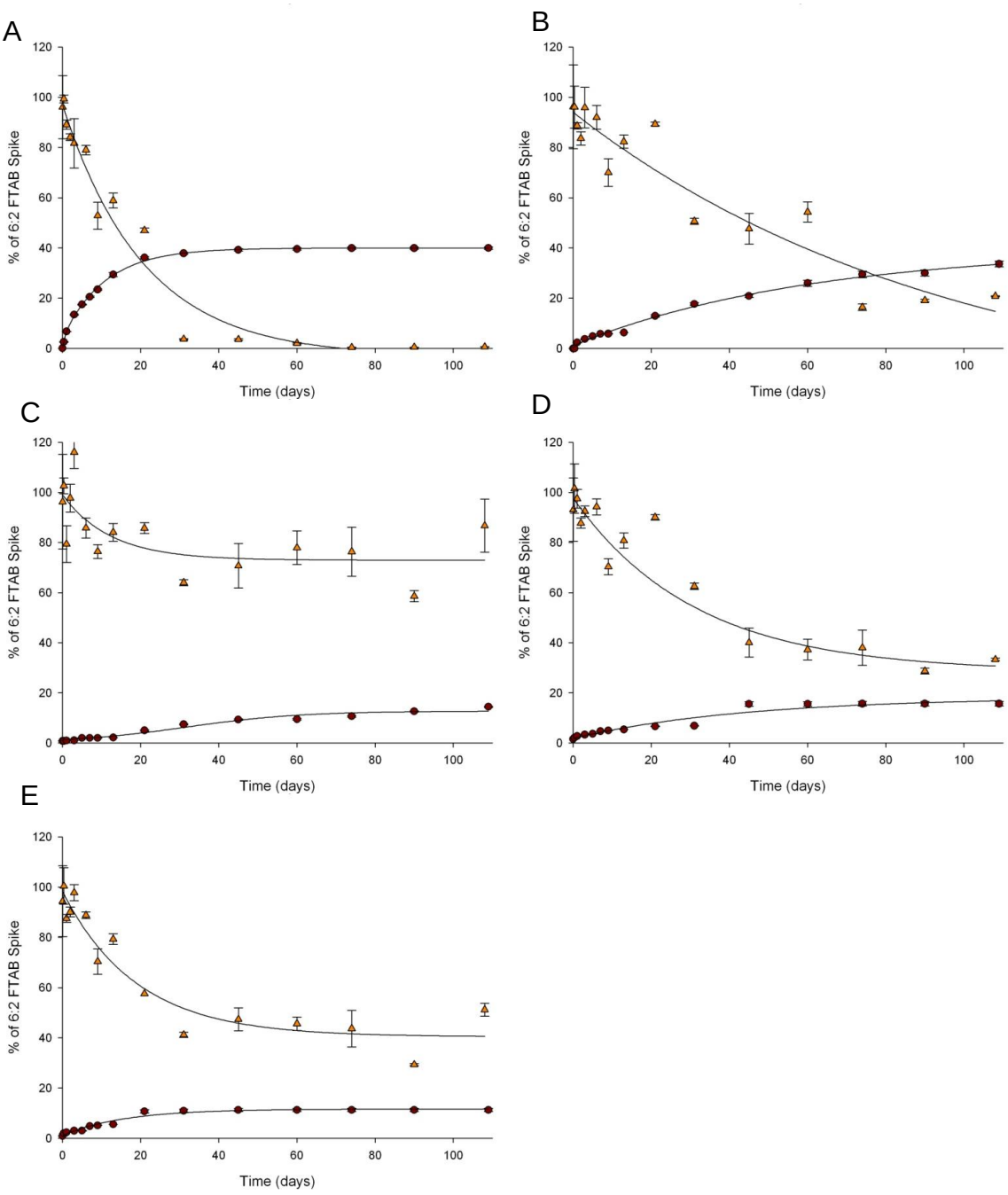

Figure B2: Loss of 6:2 FTAB from aqueous phase (▲) and cumulative amount of 6:2 FTAA recovered on XADs (●). Fitted curves are shown to highlight trends and error bars are standard deviations. Graphs are for: a) active experiment 1, b) active experiment 2, c) active experiment 3, d) sterile control 1, and e) sterile control 2.

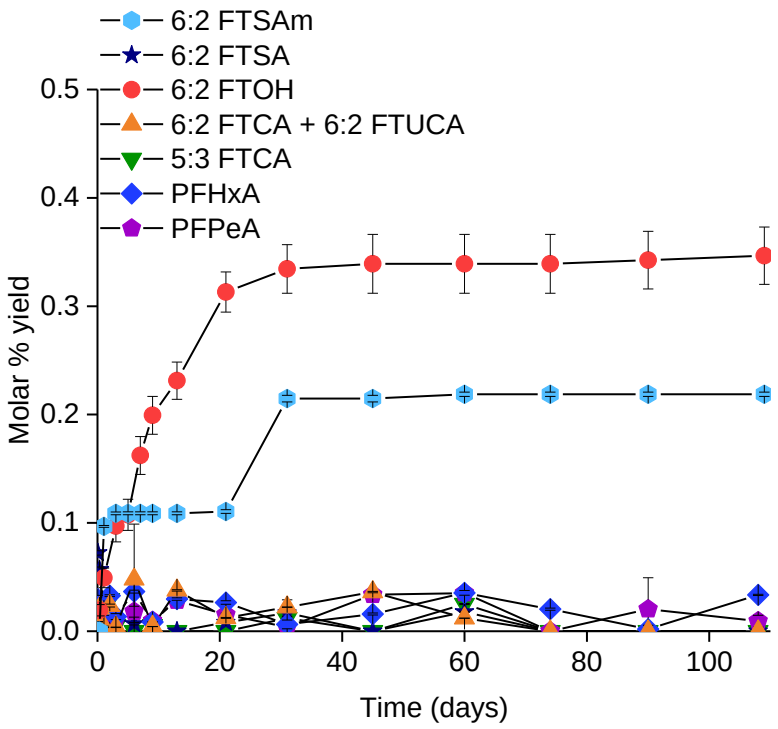

Figure B3: Time series of quantified products in the biodegradation study for the 6:2 FTAB active experiment where less than 4% of 6:2 FTAB remained in the aqueous phase after 31 days as a percentage of the 6:2 FTAB not accounted for as intact 6:2 FTAB at the end of the experiment. 6:2 FTOH and 6:2 FTSAm yields are the cumulative contents of all XADs over time, while all other yields are the contents of the aqueous phase at individual time points. Error bars are standard deviations for replicate analyses of extracts.

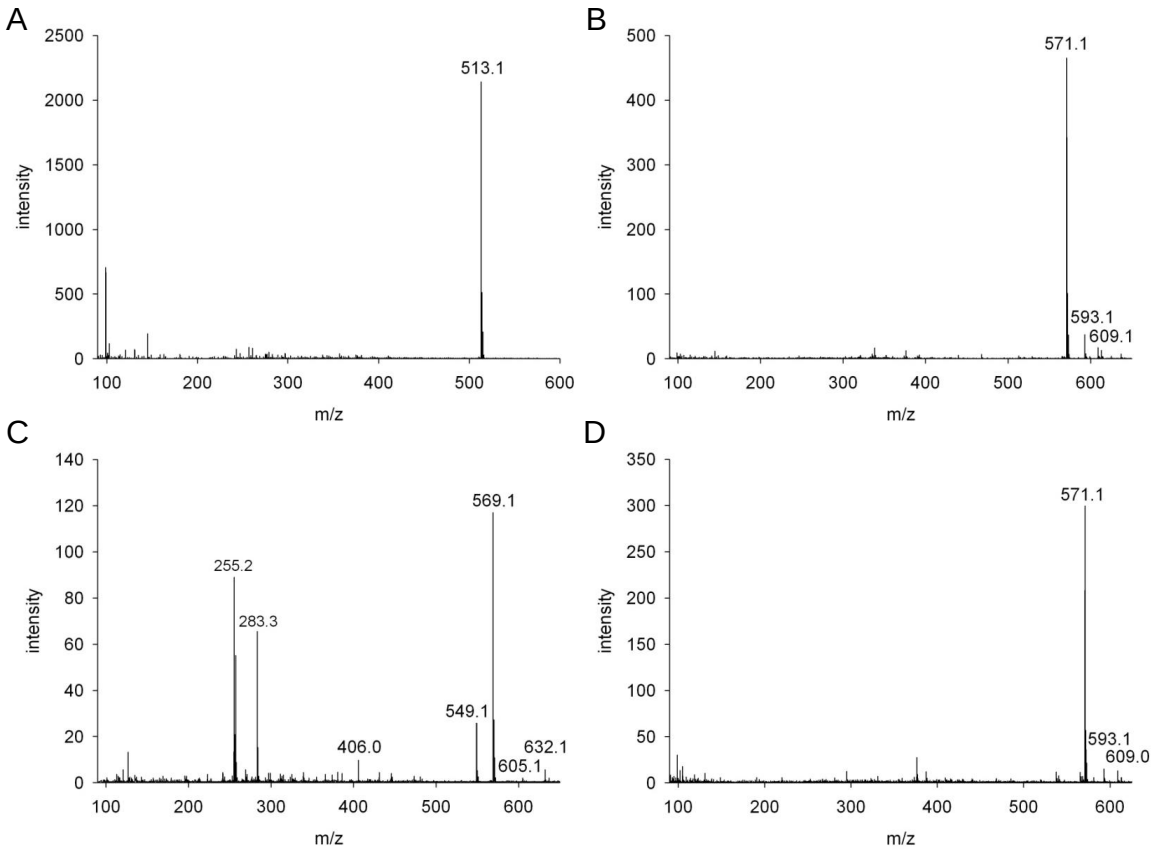

Figure B4: Selected qTOF-MS spectra of: a) 5 ppm dilution of 6:2 FTAA standard used to spike for biodegradation study in ESI+ (*m/z* 513.0776 is 6:2 FTAA). b) 5 ppm dilution of 6:2 FTAB standard used to spike for biodegradation study in ESI+ (*m/z* 571.0914 is 6:2 FTAB, *m/z* 593.0796 is a sodium adduct of 6:2 FTAB, *m/z* 609.0504 is a potassium adduct of 6:2 FTAB). c) XAD extract from sterile control 1 with 6:2 FTAB from t = 45 days in ESI- (*m/z* 569.0797 is 6:2 FTAB, *m/z* 549.0744 is a fragment of 6:2 FTAB [6], *m/z* 405.9791 is a fragment of 6:2 FTSAm, *m/z* 605.0600 is a chloride adduct of 6:2 FTAB, m/z 632.0794 is a nitrate adduct of 6:2 FTAB, 255.2 and 283.3 are non-fluorinated ions). d) XAD extract from active experiment 2 with 6:2 FTAB from t = 31 days in ESI+ (*m/z* 571.0876 is 6:2 FTAB, *m/z* 593.0766 is a sodium adduct of 6:2 FTAB, *m/z* 609.0489 is a potassium adduct of 6:2 FTAB).

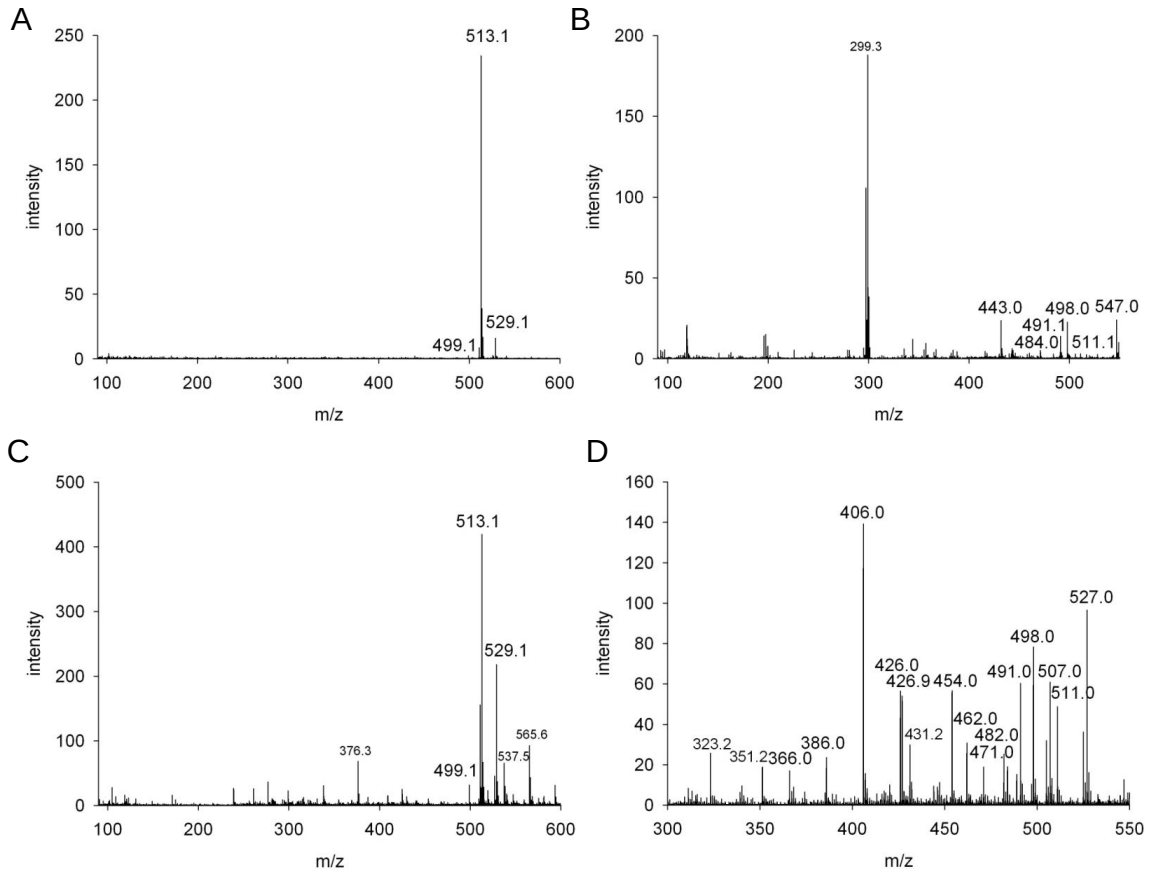

Figure B5: Selected qTOF-MS spectra of: a) XAD extract from active experiment 3 with 6:2 FTAA at t = 45 days in ESI+ (*m/z* 513.0896 is 6:2 FTAA, *m/z* 529.0849 is degradation product **1**, *m/z* 499.1 is degradation product **2**). b) XAD extract from active experiment 3 with 6:2 FTAA at t = 21 days in ESI- (*m/z* 547.0465 is a chloride adduct of 6:2 FTAA, *m/z* 511.0788 is 6:2 FTAA, *m/z* 498.0063 is degradation product **6**, *m/z* 491.0664 is a fragment of 6:2 FTAA, *m/z* 484.0 is degradation product **4**, *m/z* 444.0129 is a fragment of degradation product **4**). c) XAD extract from sterile control 1 with 6:2 FTAA at t = 21 days in ESI+ (*m/z* 529.0811 is degradation product **1**, *m/z* 513.0864 is 6:2 FTAA, *m/z* 499.0687 is degradation product **2**, others are non-fluorinated ions) d) XAD extract from sterile control 1 with 6:2 FTAA at t = 21 days in ESI- (*m/z* 527.0687 is degradation product **1**, *m/z* 511.0652 is 6:2 FTAA, *m/z* 507.0622 is a fragment of degradation product **1**, *m/z* 498.0046 is degradation product **6**, *m/z* 491.0649 is a fragment of 6:2 FTAA, *m/z* 482.0050 is degradation product **5**, *m/z* 471.0529 is a fragment of 6:2 FTAA, *m/z* 461.9927 is a fragment of degradation product **5**, *m/z* 453.9769 is a degradation product with the formula $C_9H_5NO_3F_{13}S^-$, *m/z* 426.9677 is 6:2 FTSA, *m/z* 425.9824 is 6:2 FTSAm, *m/z* 405.9772, *m/z* 385.9770, and 365.9653 are fragments of 6:2 FTSAm.

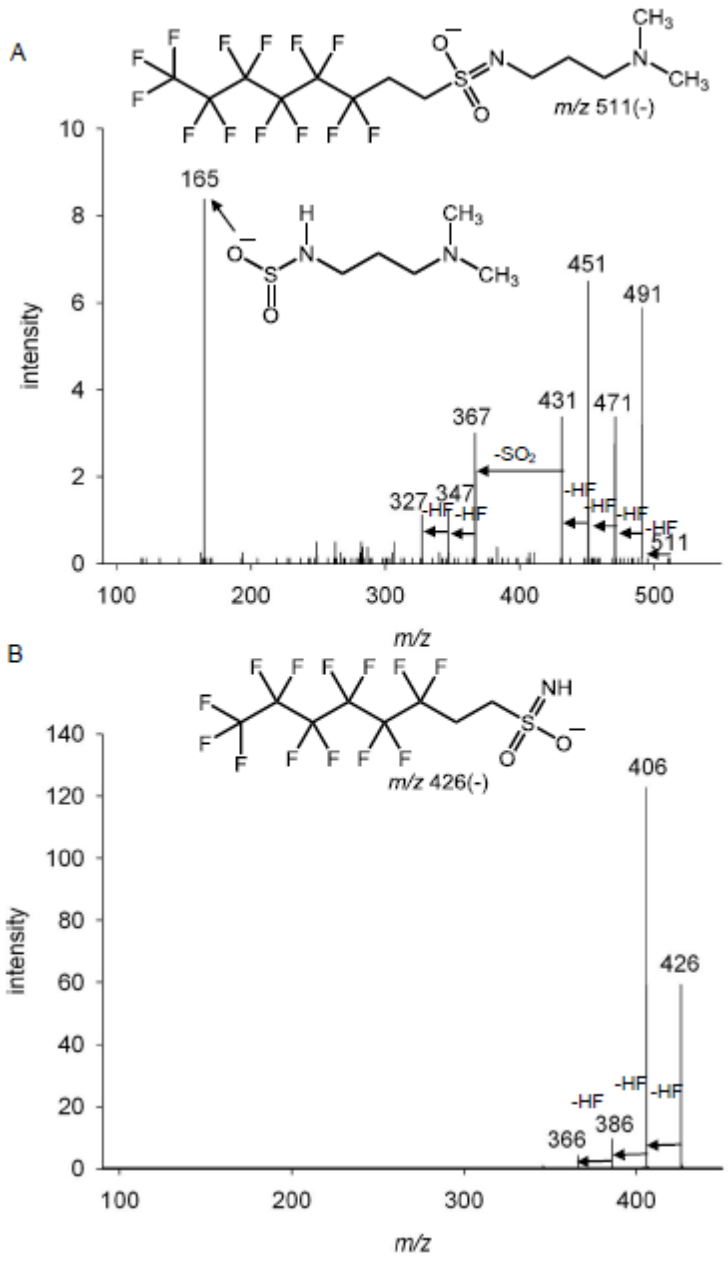

Figure B6: qTOF-MS CID mass spectra of A) 6:2 FTAA in ESI- using the synthesized standard with a collision energy of -20V and B) 6:2 FTSAm in ESI- using the synthesized standard with a collision energy of -10V.

A

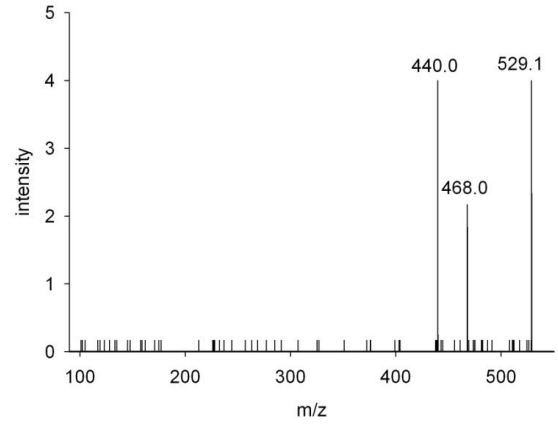
intensity
m/z
440.0
529.1
468.0

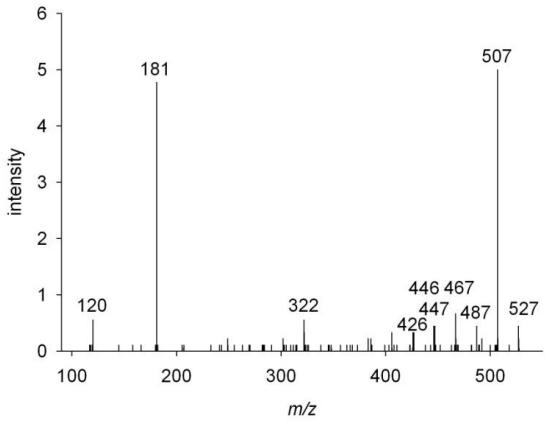
intensity
m/z
181
507
120
322
446 467
447
426
487
527

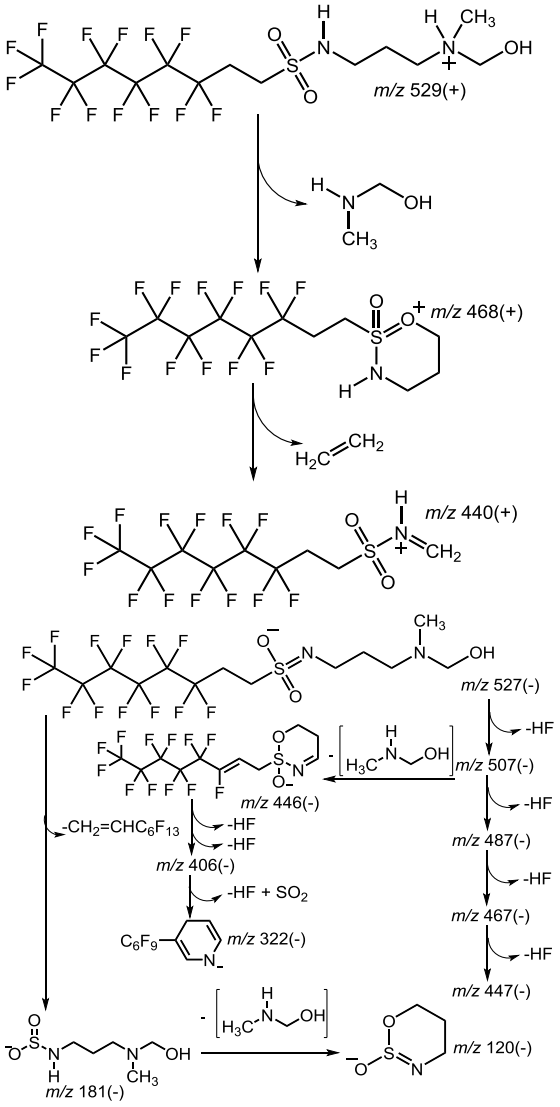
m/z 529(+)
m/z 468(+)
m/z 440(+)
m/z 527(-)
m/z 507(-)
m/z 446(-)
m/z 487(-)
m/z 467(-)
m/z 447(-)
m/z 406(-)
m/z 322(-)
m/z 181(-)
m/z 120(-)
-HF
-HF + SO2
-CH2=CHC6F13

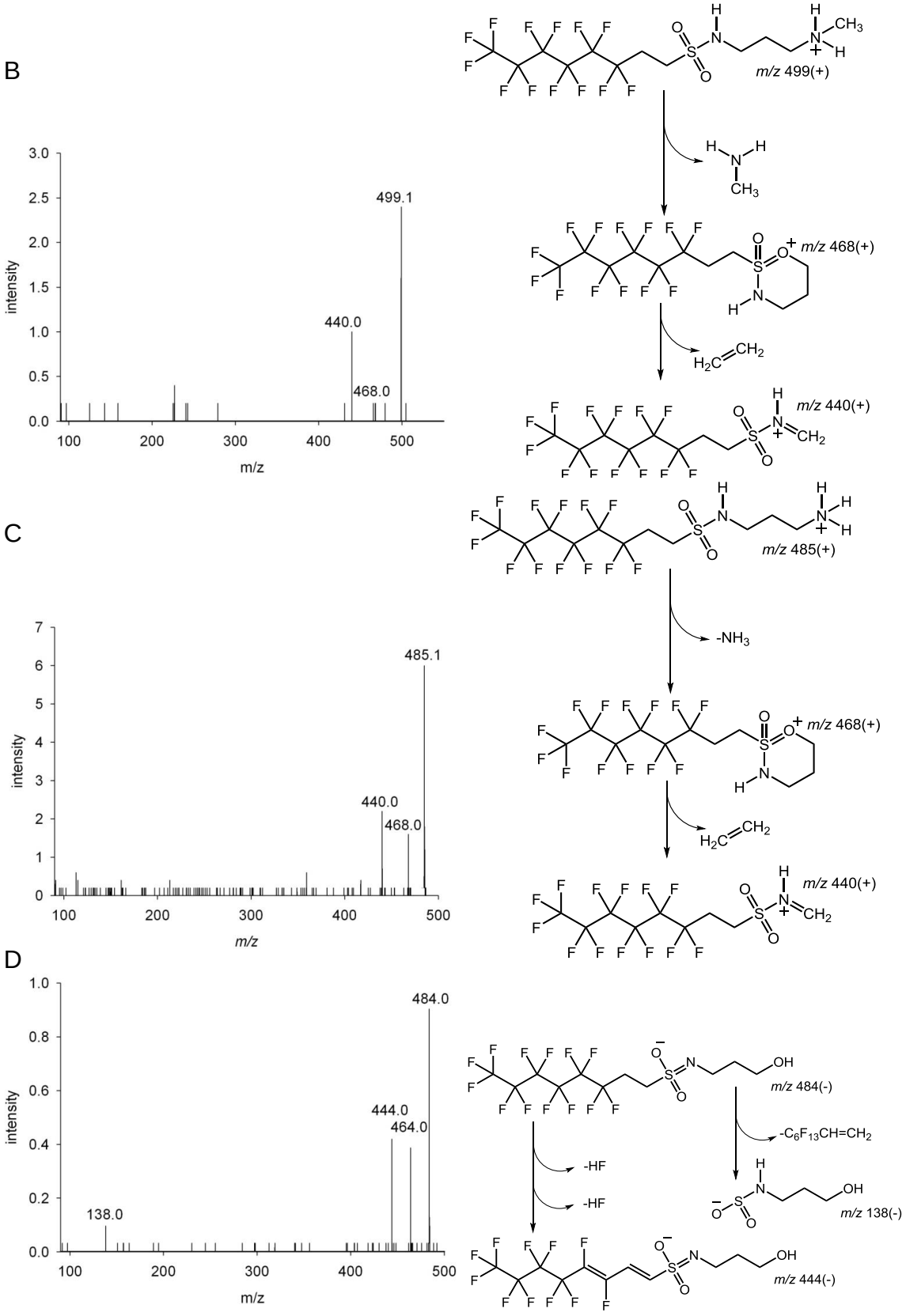
B
3.0
2.5
2.0
1.5
1.0
0.5
0.0
intensity
499.1
440.0
468.0
100
200
300
400
500
m/z
m/z 499(+)
m/z 468(+)
m/z 440(+)
C
7
6
5
4
3
2
1
0
intensity
485.1
440.0
468.0
100
200
300
400
500
m/z
m/z 485(+)
-NH3
m/z 468(+)
m/z 440(+)
D
1.0
0.8
0.6
0.4
0.2
0.0
intensity
484.0
444.0
464.0
138.0
100
200
300
400
500
m/z
m/z 484(-)
-HF
-HF
-C6F13CH=CH2
m/z 138(-)
m/z 444(-)

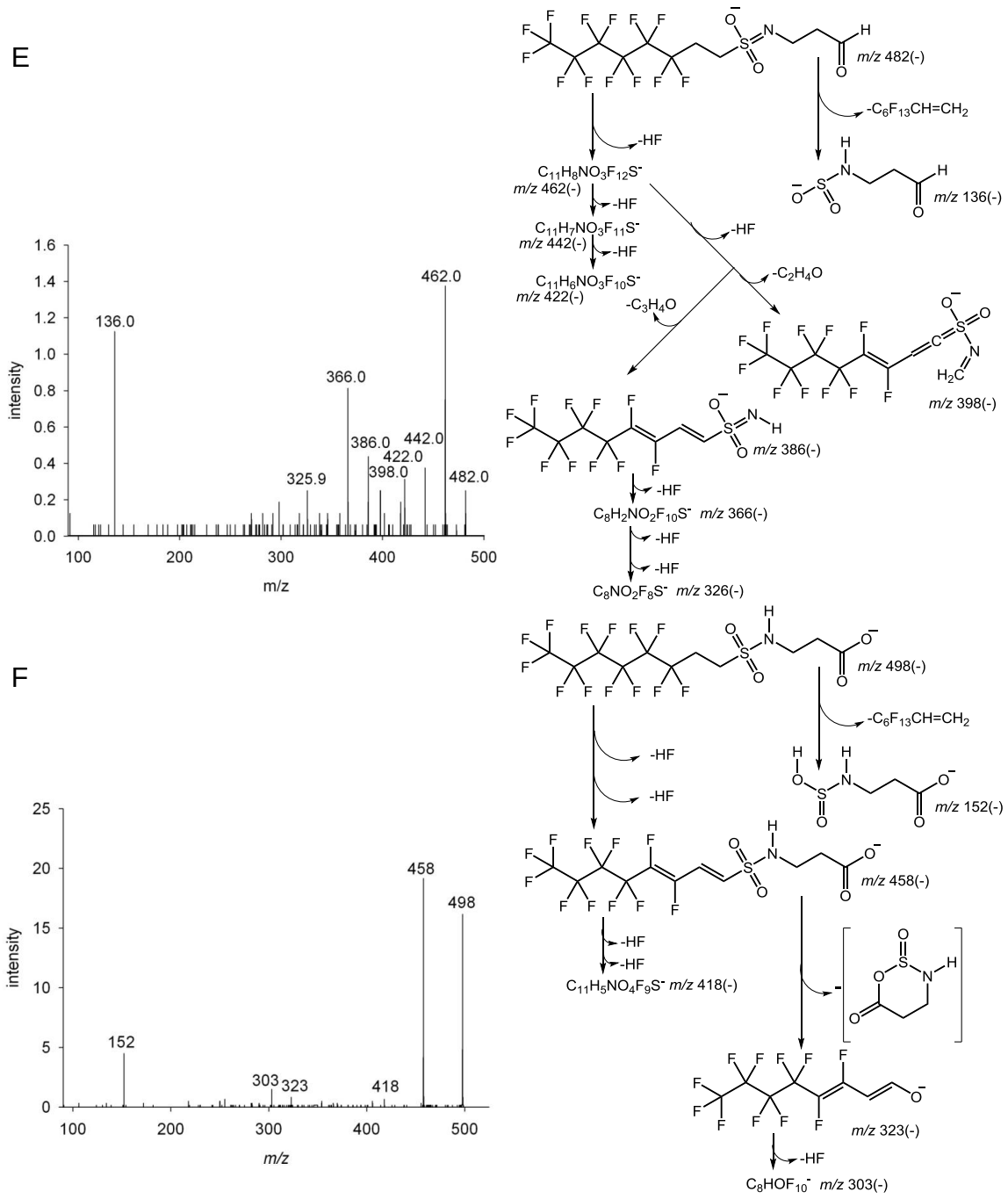

Figure B7: qTOF-MS CID spectra and schemes for collision induced dissociation (CID) pathways observed for tentatively identified degradation products of 6:2 FTAA. a) CID scheme for 1, b) CID scheme for 2, c) CID scheme for 3, d) CID scheme for 4, e) CID scheme for 5, and f) CID scheme for 6.

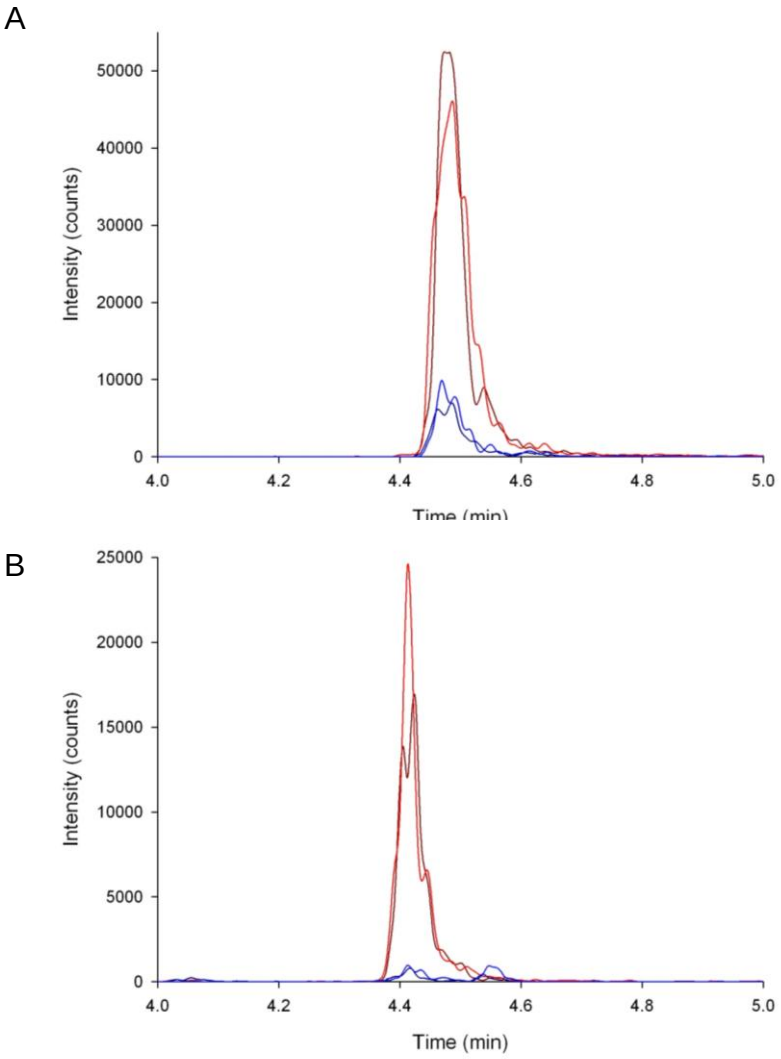

Figure B8: Extracted ion chromatograms for N-demethylation products of 6:2 FTAA a) 2 and b) 3 showing sterile control #2 solids with 6:2 FTAA in red and active experiment #2 solids with 6:2 FTAA in blue. An extra peak of unknown origin is visible at higher retention time with the active experiment for 3. Mass spectral transitions to 58 and 440 are shown for each analyte.

Table B6: Peak areas and retention times for N-demethylation products of 6:2 FTAA in solids extracts normalized to the proportion of total solids in each bottle extracted (average ± standard deviation)

	499>440		499>58		485>440		485>58	
	Peak Area	**Time (min)**	**Peak Area**	**Time (min)**	**Peak Area**	**Time (min)**	**Peak Area**	**Time (min)**
AE	(8.8 ± 7.4) x 10^4	4.48	(7.3 ± 6.3) x 10^4	4.49	(5.0 ± 5.8) x 10^3	4.42	(4.1 ± 4.8) x 10^3	4.41
SC	(8.3 ± 2.2) x 10^5	4.48	(7.6 ± 1.9) x 10^5	4.48	(1.9 ± 0.3) x 10^5	4.42	(1.5 ± 0.2) x 10^5	4.42

AE = active experiment; SC = sterile control

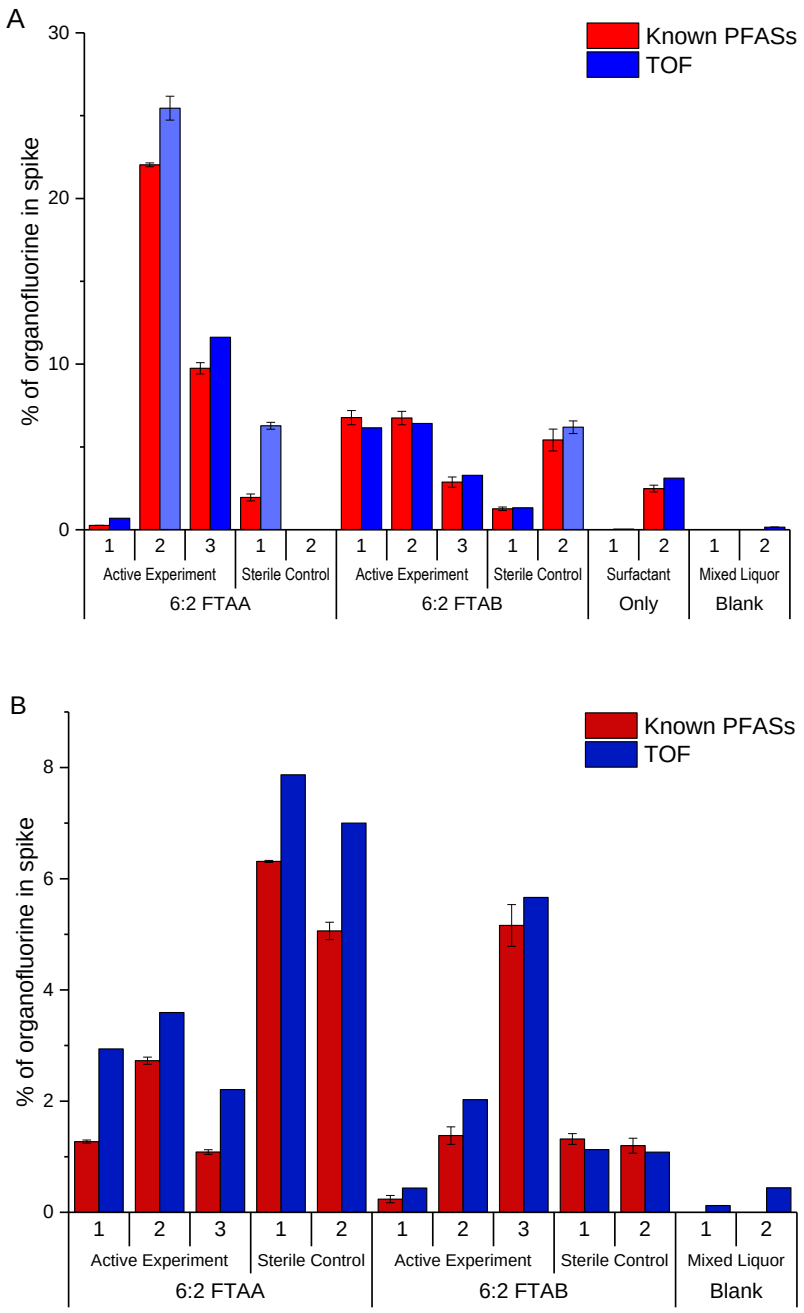

Figure B9: Percentage of the organofluorine in the 6:2 FTAB or 6:2 FTAA spike detected by TOF-CIC (blue) and analysis of known PFASs by LC-MS/MS and GC-MS in A) XAD extracts from the t = 21 days time point and B) extracts of the sludge solids at the end of the experiment. Error bars on red bars are standard deviations for the analysis of known PFASs, while error bars on light blue bars are standard deviations for replicate analyses by TOF-CIC, where they were conducted.

References

1. Hamme JDV, Fedorak PM, Foght JM, Gray MR, Dettman HD. 2004. Use of a Novel Fluorinated Organosulfur Compound To Isolate Bacteria Capable of Carbon-Sulfur Bond Cleavage. *Appl. Environ. Microbiol.* 70:1487–1493.

2. Weiner B, Yeung LWY, Marchington EB, D'Agostino LA, Mabury SA. 2013. Organic fluorine content in aqueous film forming foams (AFFFs) and biodegradation of the foam component 6 : 2 fluorotelomermercaptoalkylamido sulfonate (6 : 2 FTSAS). *Environ. Chem.* 10:486–493.

3. Houtz EF, Higgins CP, Field JA, Sedlak DL. 2013. Persistence of Perfluoroalkyl Acid Precursors in AFFF-Impacted Groundwater and Soil. *Environ. Sci. Technol.* 47:8187–8195.

4. Myers AL, Jobst KJ, Mabury SA, Reiner EJ. 2014. Using mass defect plots as a discovery tool to identify novel fluoropolymer thermal decomposition products. *J. Mass Spectrom.* 49:291–296.

5. Rand AA, Mabury SA. 2012. In Vitro Interactions of Biological Nucleophiles with Fluorotelomer Unsaturated Acids and Aldehydes: Fate and Consequences. *Environ. Sci. Technol.* 46:7398–7406.

6. D'Agostino LA, Mabury SA. 2014. Identification of Novel Fluorinated Surfactants in Aqueous Film Forming Foams and Commercial Surfactant Concentrates. *Environ. Sci. Technol.* 48:121–129.

Appendix C

Supporting Information for Chapter Four:

Aqueous Film Forming Foam-related Perfluoroalkyl and Polyfluoroalkyl Substances in Canadian Surface Waters

Contents

Materials

The methanol used was LC-MS grade and obtained from EMD Millipore (Billerica, MA, USA) and Fisher Scientific (Waltham, MA, USA) . Deionized water was generated using a Purelab flex water purification system (ELGA, Woodridge, IL, USA). 28% NH_4OH (ACS grade), perfluorohexane sulfonamide (FHxSA), and ammonium acetate for HPLC were all from Sigma Aldrich (St. Louis, MO, USA). 6:2 fluorotelomer sulfonamide (FTSAm), 6:2 fluorotelomer sulfonamide alkyl betaine (FTAB), and 6:2 fluorotelomer sulfonamide alkyl amine (FTAA) were synthesized in house as describe previously.[1]

Native standards of perfluoroalkyl carboxylate (PFCA) mixture (MXA), perfluoroalkane sulfonate (PFSA) mixture (MXA), perfluoropentane sulfonate (PFPeS), and perfluoroheptane sulfonate (PFHpS), 4:2 fluorotelomer sulfonic acid (FTSA), 6:2 FTSA, 8:2 FTSA, N-ethyl perfluorooctane sulfonamido ethanol acetic acid (EtFOSAA), and perfluorooctane sulfonamide (FOSA) were obtained from Wellington Laboratories (Guelph, ON, Canada). Mass labelled standards of labelled PFCA/PFSA mixture (MXA), $^{13}C_5$-perfluoropentanoate (PFPeA), $^{13}C_4$ -perfluoroheptanoate (PFHpA), $^{13}C_2$-4:2 FTSA, $^{13}C_2$-6:2 FTSA, $^{13}C_2$-8:2 FTSA, D_5-EtFOSAA, and $^{13}C_8$ -FOSA were also from Wellington Laboratories.

Extraction of Water

Oasis WAX cartridges (6 cc, 200 mg, 30 μm; Waters, Milford, MA) cartridges were conditioned with 2 mL of 0.1% NH_4OH in methanol, 2 mL of methanol, and 2 mL of deionized water. Surface water samples were then loaded, cartridges were rinsed with 2 mL of 25 mM ammonium acetate in deionized water, and dried by centrifugation and under vacuum. The cartridges were then eluted with 4 mL of methanol for the neutral fraction followed by 4 mL of 0.1% NH_4OH in methanol for the acid fraction. The extracts were evaporated under a gentle stream of nitrogen to a little less than 1 mL and made up to 1 mL with methanol. Extracts were stored at -20°C.

Extraction of Sediment

In the ALFONSE clean lab, the approximately 0.5g sediment subsamples were extracted three times with 2.5 mL of 0.1% NH_4OH in methanol by vortex mixing 20 sec, sonicating 30 min, shaking at 300 rpm for 1 hour, and centrifuging at 4500 rpm for 15 min. The supernatants from each extraction were combined and evaporated to approximately 2 mL under a gentle stream of nitrogen. The extracts were then cleaned up using 1mL/100mg Supelclean ENVI-Carb cartridges (Supelco, Bellefonte, PA). The cartridges were conditioned with 3 x 1 mL of methanol. While collecting the final extract, the extracts were loaded and eluted with 4 x 1 mL of methanol. The cleaned up extracts were then evaporated to less than 1 mL under a gentle stream of nitrogen, made up to 1 mL with methanol, and stored at -20°C.

LC-MS/MS

The column was a Waters Acquity UPLC BEH C18 column with 1.7 µm particles (2.1 mm x 75mm) used with a flow rate of 0.5 mL/min and a column temperature of 60°C. The mobile phase consisted of 10 mM ammonium acetate in deionized water (A) and methanol (B) and the gradient started at 90% A: 10% B, changed to 22% A: 78% B over 7 min, changed to 10% A: 90 %B over 0.4 min, returned to 90% A: 10% B in 0.1 min, and held at 90% A: 10% B for 3 min for a total run time of 10.5 min. Injection volumes were 2 µL.

In positive mode electrospray ionization (ESI+) the electrospray voltage was 3300 V and in negative ion mode electrospray ionization (ESI-) the electrospray voltage was -2480 V. The nebulizing nitrogen gas was 5.5 Bar, desolvation gas was nitrogen at 650 L/hr, cone nitrogen gas flow rate was 150 L/hr, and the helium collision gas flow rate was 0.12–0.15 mL/min. The Xevo TQ-S was operated in MRM mode with dwell times of at least 0.01 sec per transition. Multiple reaction monitoring (MRM) transitions that were used in this study are given in Table C2.

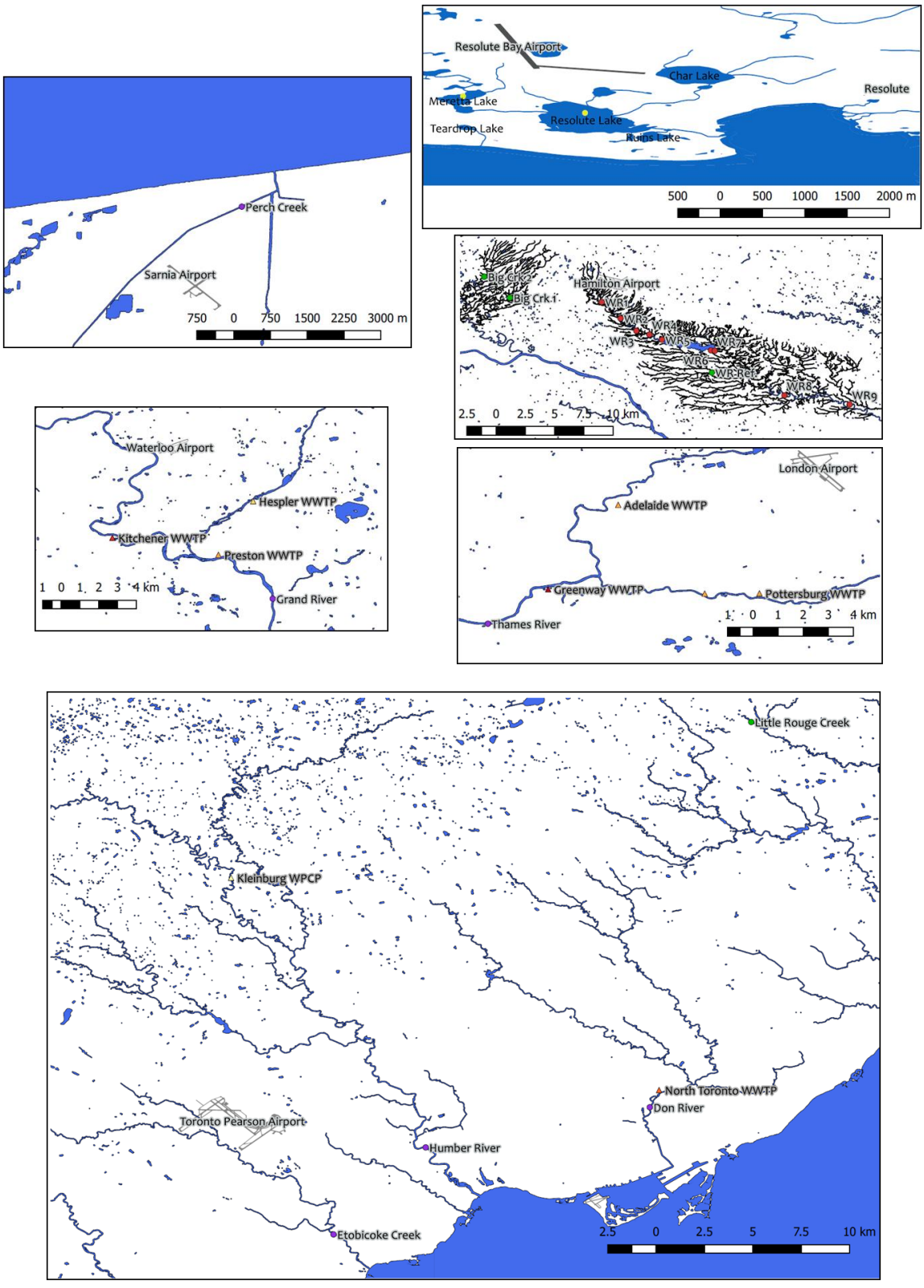

Figure C1: Maps showing sampling sites and upstream airports and wastewater treatment plants.

Table C1: Sampling dates and locations

Location	Coordinates	Date(s)
Welland R. 1	43.1508, -79.9446	Oct. 22, 2015
Welland R. 2	43.1333, -79.9246	Oct. 22, 2015
Welland R. 3	43.1206, -79.9083	Oct. 22, 2015
Welland R. 4	43.1168, -79.8947	Oct. 22, 2015
Welland R.5	43.1113,-79.8815	Oct. 22, 2015
Welland R. 6	43.1001,-79.8298	Oct. 22, 2015
Welland R. 7	43.0995,-79.8259	Oct. 22, 2015
Welland R. 8	43.0528,-79.7529	Oct. 22, 2015
Welland R. 9	43.0432, -79.6844	Oct. 22, 2015
Welland R. Ref.	43.0768, -79.8288	Oct. 22, 2015
Big Crk. 1	43.1552,-80.0408	Oct. 22, 2015
Big Crk. 2	43.1775,-80.0678	Oct. 22, 2015
Etobicoke Crk.	43.6071, -79.5645	Aug. 10, 2015; Sept. 29, 2015
Don R.	43.6885, -79.3622	Sept. 29, 2015
Humber R.	43.6628, -79.5055	Sept. 29, 2015
Grand R.	43.3589, -80.3162	Aug. 6, 2015
Thames R.	42.9584, -81.3112	July 7, 2015
Perch Crk.	43.0195, -82.2976	July 8, 2015
Little Rouge Crk.	43.1775, -80.0678	Feb. 6, 2016
Meretta Lk.	74.695, -94.993	Aug. 4, 2014
Resolute Lk.	74.687, -94.942	Aug. 1 2012; Aug. 6, 2014
Lake of Bays	45.2395, -78.9135	Sept. 27, 2015

Table C2: Tandem mass spectrometry transitions for all AFFF-related PFASs monitored

Compound	ESI Mode	Mass Transition	Cone Voltage (V)	Collision Energy (V)
PFPeA	–	263.03>219.04	24	8
M-PFPeA	–	268.10>223.03	24	8
PFHxA	–	313.00>269.00	26	10
M-PFHxA	–	315.00>270.00	26	10
PFHpA	–	363.00>169.00	30	19
		363.00>319.00[q]	30	10
M-PFHpA	–	367.10>168.98	30	19
PFOA	–	413.00>168.90	30	18
		413.00>369.00[q]	30	10
M-PFOA	–	417.00>372.00	30	10
PFBS	–	299.00>80.00[q]	40	30
		299.00>99.00	40	31
PFPeS	–	349.00>80.00[q]	42	32
		349.00>99.00	42	31
PFHxS	–	399.00>80.00[q]	45	33
		399.00>99.00	45	31
M-PFHxS	–	403.00>103.00	45	30
PFHpS	–	449.00>80.00[q]	48	34
		449.00>98.90	48	34
PFOS	–	499.00>80.00[q]	60	39
		499.00>99.00	60	38
M-PFOS	–	503.00>80.00	60	39
EtFOSAA	–	584.03>418.99	20	18
M-EtFOSAA	–	589.03>418.99	44	20
4:2 FTSA	–	327.03>81.00	60	30
		327.03>307.07[q]	60	20
M-4:2 FTSA	–	329.03>81.00	60	30
6:2 FTSA	–	427.10>81.00	38	32
		427.10>407.08[q]	38	22
M-6:2 FTSA	–	428.84>81.00	86	32
8:2 FTSA	–	527.10>81.00	68	34
		527.10>507.13[q]	68	26
M-8:2 FTSA	–	529.10>81.00	68	34
FHxSA	–	398.00>78.00	62	26
FOSA	–	498.00>78.00	66	28
M-FOSA	–	506.00>78.00	66	28
6:2 FTSAm*	–	425.65>345.90	28	22
		425.65>365.99[q]	28	16
4:2 FTAB	+	470.90>340.00	50	30
		470.90>104.06	50	30
6:2 FTAB*	+	570.90>440.00[q]	50	30
		570.90>104.06	50	30
8:2 FTAB*	+	670.90>539.99	96	32
		670.90>104.06	96	32

Compound	ESI Mode	Mass Transition	Cone Voltage (V)	Collision Energy (V)
FTB CH_2 C5*	+	413.78>58.10	36	30
		413.78>104.13	36	28
FTB CHF C5*	+	431.78>58.10	40	32
		431.78>372.05	40	32
FTB CH_2 C7*	+	513.84>58.17	82	36
		513.84>104.06	82	32
FTB CHF C7*	+	531.71>58.10	50	36
		531.71>472.05	50	38
FTB CH_2 C9	+	613.84>58.17	82	36
		613.84>104.06	82	32
FTB CHF C9	+	631.71>58.10	50	36
		631.71>572.05	50	38
6:2 FTAA*	+	512.90>439.98[q]	40	30
		512.90>85.93	40	34
4:2 FTSAS-SO_2	–	517.80>206.00	50	35
		517.80>151.97	50	40
6:2 FTSAS-SO_2[a]	–	617.80>206.00	50	35
		617.80>151.97	50	40
8:2 FTSAS-SO_2	–	717.80>206.00	50	35
		717.80>151.97	50	40
6:2 FTSHA-SO	+	511.84>166.08	50	20
		511.84>116.15	50	24
FHxSADA*	+	628.97>187.20	40	36
		628.97>70.06	40	56
FPeSADA*	+	579.03>187.14	60	34
		579.03>70.06	60	52
PBSADA	+	529.03>187.14	60	34
		529.03>70.06	60	52
PPrSADA	+	479.03>187.14	60	34
		479.03>70.06	60	52
FHxSAAA*	+	556.97>129.03	52	30
		556.97>84.96	52	34
FPeSAAA*	+	506.90>129.09	60	30
		506.90>85.02	60	30
FBSAAA	+	456.90>129.09	60	30
		456.90>85.02	60	30
FPrSAAA	+	406.90>129.09	60	30
		406.90>85.02	60	30
FHxSAB	+	556.97>118.00	52	32
		556.97>84.96	52	34
FPeSAB	+	506.90>118.00	60	30
		506.90>85.02	60	30
FBSAB	+	456.90>118.00	60	30
		456.90>85.02	60	30

Compound	ESI Mode	Mass Transition	Cone Voltage (V)	Collision Energy (V)
FPrSAB	+	406.90>118.00	60	30
		406.90>85.02	60	30
FHxSAAm*	+	484.84>85.02	60	30
		484.84>70.06	60	34
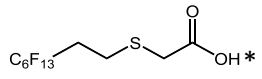	–	436.71>90.93	22	15
		436.71>376.98	22	11
6:2 FTSAS*	–	585.71>135.01	90	42
		585.71>206.00	90	35
6:2 FTSAS-SO*	–	601.78>255.98	62	24
		601.78>151.97	62	40
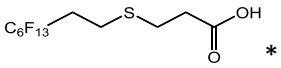	–	450.65>378.96	32	15
		450.65>338.99	32	14
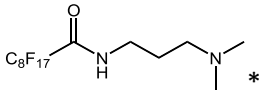	+	548.90>504.00	42	28
		548.90>475.98	42	34
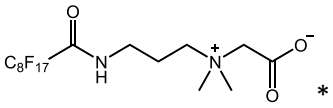	+	606.84>504.02	36	26
		606.84>104.06	36	22
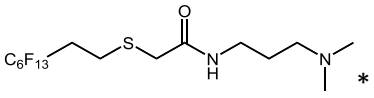	+	522.90>478.06	60	26
		522.90>392.97	60	38
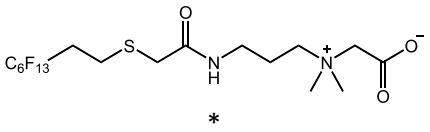	+	580.97>478.07	42	24
		580.97>392.97	42	42
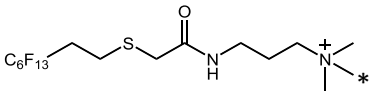	+	537.10>478.08	32	24
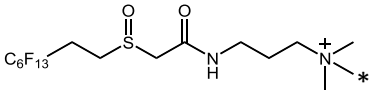	+	552.84>207.10	28	20
		552.84>148.01	28	30
6:2 FTSHA*	+	495.78>393.02	48	36
		495.78>437.03	48	28
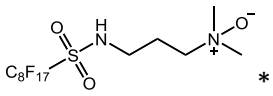	+	600.84>58.10	80	32
		600.84>448.02	80	36

*Transitions for AFFF components optimized with diluted AFFF or in-house synthesized standards

[q] indicates quantifying transitions for compounds with quantitative standards for calibration

[a] indicates that 6:2 FTSAS-SO_2 transition was guessed based on mass spectrum reported by Harding-Marjanovic *et al.*[2] due to insufficient quantity in AFFF extract

Table C3: Recoveries of PFASs from water and sediment matrices (± standard deviation)

Compound	% Recovery from Water	% Recovery from Sediment
PFPeA	96 ± 4	81 ± 11
PFHxA	87 ± 7	84 ± 4
PFHpA	96 ± 12	78 ± 7
PFOA	94 ± 7	82 ± 7
PFBS	93 ± 5	81 ± 8
PFPeS	92 ± 6	80 ± 9
PFHxS	95 ± 7	83 ± 11
PFHpS	93 ± 9	94 ± 5
PFOS	90 ± 8	91 ± 5
4:2 FTSA	86 ± 5	82 ± 4
6:2 FTSA	88 ± 4	89 ± 10
8:2 FTSA	91 ± 7	87 ± 9
EtFOSAA	86 ± 10	83 ± 4
FHxSA	76 ± 6	76 ± 2
FOSA	77 ± 7	77 ± 3
6:2 FTSAm	80 ± 5	80 ± 5
6:2 FTAA	71 ± 12	90 ± 5
6:2 FTAB	88 ± 24	31 ± 2

Table C4: Limit of detection (LOD) and limit of quantitation (LOQ) for PFASs in water and sediment

PFAS	LOD water (ng/L)	LOQ water (ng/L)	LOD sediment (ng/g)	LOQ sediment (ng/g)
PFPeA	0.75	5	0.15	0.5
PFHxA	0.75	2.5	0.06	0.2
PFHpA	0.4	2	0.02	0.1
PFOA	0.25	0.6	0.06	0.2
PFBS	0.05	0.3	0.04	0.15
PFPeS	0.07	0.2	0.06	0.2
PFHxS	0.4	1.2	0.05	0.2
PFHpS	0.2	0.7	0.04	0.2
PFOS	0.05	0.2	0.05	0.2
4:2 FTSA	0.008	0.025	0.03	0.1
6:2 FTSA	0.008	0.025	0.03	0.1
8:2 FTSA	0.015	0.065	0.03	0.1
EtFOSAA	0.05	0.2	0.02	0.09
FHxSA	0.01	0.04	0.02	0.06
FOSA	0.02	0.1	0.03	0.1
6:2 FTSAm	0.2	0.65	0.06	0.2
4:2 FTAB	0.04	0.15	0.03	0.1
6:2 FTAB	0.03	0.2	0.03	0.1
8:2 FTAB	0.03	0.2	0.03	0.1
FTB CH_2 C5	0.09	0.5	0.02	0.1
FTB CHF C5	0.2	0.8	0.05	0.2
FTB CH_2 C7	0.05	0.2	0.02	0.1
FTB CHF C7	0.16	0.45	0.05	0.2
FTB CH_2 C9	0.1	0.3	0.02	0.1
FTB CHF C9	0.1	0.4	0.05	0.2
6:2 FTAA	0.03	0.1	0.025	0.1
6:2 FTSAS-SO2	0.02	0.1	nd	nd
6:2 FTSHA-SO	0.08	0.25	nd	nd
FHxSADA	0.01	0.06	nd	nd
FPeSADA	0.002	0.05	nd	nd
FBSADA	0.002	0.05	nd	nd
FPrSADA	0.01	0.06	nd	nd
FHxSAAA	0.2	0.8	nd	nd
FPeSAAA	0.1	0.5	nd	nd
FBSAAA	0.3	1	nd	nd
FPeSAAA	0.15	0.6	nd	nd
FHxSAB	0.2	0.7	nd	nd
FPeSAB	0.1	0.5	nd	nd
FHxSAAm	nd	nd	0.08	0.3

nd.: These PFASs were not detected with a S/N above 3 in the matrix, LOD and LOQ not determined.

Table C5: Concentrations of PFAAs in water samples in ng/L. (± standard deviation)

Sample	PFPeA	PFHxA	PFHpA	PFOA	PFBS	PFPeS	PFHxS	PFHpS	PFOS
Welland R. 1	153 ± 41	101 ± 16	51 ± 10	52.0 ± 7.0	12.2 ± 1.1	15.0 ± 1.7	150 ± 34	4.67 ± 0.52	151 ± 39
Welland R. 2	106 ± 30	65 ± 6	31.7 ± 6.3	23.6 ± 3.6	10.86 ± 0.95	10.7 ± 1.2	92 ± 21	2.99 ± 0.23	106 ± 18
Welland R. 3	146 ± 22	88 ± 11	41 ± 11	26.6 ± 4.1	11.77 ± 0.93	14.0 ± 0.1	144 ± 19	3.93 ± 0.07	155 ± 24
Welland R. 4	154 ± 30	94 ± 22	35 ± 13	27.3 ± 4.4	12.96 ± 0.59	13.5 ± 1.2	136 ± 21	3.95 ± 0.41	144 ± 18
Welland R. 5	136 ± 27	86 ± 15	29.7 ± 2.1	26.6 ± 3.5	11.8 ± 1.5	11.1 ± 0.9	114 ± 18	2.67 ± 0.21	80 ± 12
Welland R. 6	51 ± 11	34.3 ± 3.2	16.7 ± 1.2	21.6 ± 3.4	4.59 ± 0.28	4.57 ± 0.18	42.7 ± 6.6	2.24 ± 0.01	92 ± 18
Welland R. 7	55 ± 13	37.7 ± 8.4	19.3 ± 3.4	22.3 ± 2.8	4.43 ± 0.46	4.57 ± 0.45	57 ± 10	2.48 ± 0.49	143 ± 28
Welland R. 8	39.7 ± 4.4	27.4 ± 1.7	13.0 ± 3.7	16.6 ± 0.3	3.79 ± 0.48	3.18 ± 0.15	33.9 ± 2.8	1.60 ± 0.20	58.2 ± 4.8
Welland R. 9	36.5 ± 3.1	25.9 ± 2.8	8.6 ± 2.9	16.7 ± 0.7	3.85 ± 0.36	2.46 ±0.23	27.7 ± 1.6	1.04 ± 0.14	64.8 ± 6.5
Welland R. Ref	nd	nd	nd	0.30 ± 0.06*	0.06 ± 0.01*	nd	nd	nd	2.54 ± 0.17
Big Creek 1	6.6 ± 2.2	4.54 ± 0.53	1.97 ± 0.19*	2.59 ± 0.11	1.66 ± 0.23	nd	0.45 ± 0.17*	nd	1.70 ± 0.15
Big Creek 2	4.8 ± 0.6*	2.38 ± 0.45*	0.52 ± 0.09*	1.08 ± 0.14	1.44 ± 0.14	nd	1.26 ± 0.19	nd	1.19 ± 0.04
Etobicoke Crk. Aug	10.9 ± 1.4	15.71 ± 0.38	3.42 ± 0.38	9.00 ± 0.09	4.06 ± 0.34	0.40 ± 0.07	2.18 ± 0.69	0.47 ± 0.07*	10.51 ± 0.03
Etobicoke Crk. Sep	17.8 ± 0.9	15.9 ± 1.5	4.9 ± 1.5	8.01 ± 0.73	4.40 ± 0.15	1.34 ± 0.16	4.66 ± 0.26	0.44 ± 0.07*	15.67 ± 0.15
Don R.	5.01 ± 0.08*	10.07 ± 0.84	3.09 ± 0.53	6.00 ± 0.44	2.49 ± 0.04	nd	0.96 ± 0.05*	0.45 ± 0.06*	7.3 ± 1.2
Humber R	3.87 ± 0.41*	6.69 ± 0.45	3.32 ± 0.14*	3.32 ± 0.42	3.03 ± 0.07	0.13 ± 0.06*	1.72 ± 0.32	0.28 ± 0.13*	7.24 ± 0.36
Grand R.	5.80 ± 0.59	5.44 ± 0.31	1.77 ± 0.55*	3.69 ± 0.05	1.75 ± 0.28	nd	1.22 ± 0.06	nd	2.80 ± 0.13
Thames R.	2.06 ± 0.01*	3.86 ± 0.61	0.71 ± 0.14*	2.66 ± 0.12	1.37 ± 0.11	0.19 ± 0.11*	1.47 ± 0.22	nd	5.7 ± 1.5
Perch Crk	7.3 ± 1.3	10.36 ± 0.72	2.74 ± 0.27	6.36 ± 0.25	3.96 ± 0.10	1.60 ± 0.24	13.40 ± 0.16	0.88 ± 0.12	21.6 ± 1.9
Little Rouge Crk	0.83 ± 0.15*	0.86 ± 0.13*	0.44 ± 0.10*	0.52 ± 0.11*	0.31 ± 0.03	0.07 ± 0.03*	nd	nd	0.05 ± 0.02*
Meretta Lk 2014	76 ± 14	38.0 ± 5.8	21.8 ± 3.2	13.90 ± 0.25	1.93 ± 0.21	1.79 ± 0.18	30.1 ± 4.3	0.80 ± 0.11	45.7 ± 9.9
Resolute Lk 2014	25.3 ± 0.6	16.9 ± 1.6	9.3 ± 1.2	7.73 ± 0.36	0.77 ± 0.11	0.73 ± 0.09	12.6 ± 1.3	0.32 ± 0.10*	24.4 ± 0.2
Resolute Lk 2012	47 ± 11	27.7 ± 2.9	14.1 ± 2.6	9.11 ± 0.30	1.13 ± 0.11	1.23 ± 0.13	20.9 ± 0.8	0.70 ± 0.01	40.6 ± 4.7
Lake of Bays	nd	nd	nd	0.65 ± 0.01	nd	nd	nd	nd	0.36 ± 0.07

nd = not detected above detection limit; * indicates detections that were between LOD and LOQ

Table C6: Concentrations of FTSAs, EtFOSAA, FHxSA, FOSA, and 6:2 FTSAm in water samples in ng/L. (± standard deviation)

Sample	4:2 FTSA	6:2 FTSA	8:2 FTSA	EtFOSAA	FHxSA	FOSA	6:2 FTSAm
Welland R. 1	0.037 ± 0.004[a]	2.53 ± 0.81	0.018 ± 0.016*	nd	18.5 ± 1.6	0.17 ± 0.06	0.84 ± 0.37
Welland R. 2	nd	0.06 ± 0.01[a]	nd	nd	2.53 ± 0.33	0.022 ± 0.017*	nd
Welland R. 3	nd	0.046 ± 0.004[a]	nd	nd	2.53 ± 0.20	0.04 ± 0.02[a]	nd
Welland R. 4	nd	0.036 ± 0.002[a]	nd	nd	2.36 ± 0.11	nd	nd
Welland R. 5	nd	0.07 ± 0.02[a]	nd	0.16 ± 0.08*	4.23 ± 0.15	0.17 ± 0.03*	nd
Welland R. 6	nd	0.11 ± 0.03	nd	0.24 ± 0.13*	3.62 ± 0.41	0.33 ± 0.07	nd
Welland R. 7	nd	0.05 ± 0.01[a]	nd	0.26 ± 0.07	3.14 ± 0.21	0.29 ± 0.03*	nd
Welland R. 8	nd	0.04 ± 0.01[a]	nd	0.48 ± 0.02	1.22 ± 0.06	0.394 ± 0.003	nd
Welland R. 9	nd	0.03 ± 0.01[a]	nd	0.41 ± 0.04	0.99 ± 0.12	0.45 ± 0.05	nd
Welland R. Ref	nd	0.008 ± 0.002*	nd	0.05 ± 0.05*	nd	nd	nd
Big Creek 1	nd	0.025 ± 0.003[a]	nd	0.05 ± 0.01*	0.012 ± 0.011*	0.03 ± 0.01*	nd
Big Creek 2	nd	0.010 ± 0.003*	nd	nd	nd	nd	nd
Etobicoke Crk. Aug	nd	0.18 ± 0.03	0.07 ± 0.01[a]	0.22 ± 0.13*	0.35 ± 0.03	0.91 ± 0.11	0.72 ± 0.06*
Etobicoke Crk. Sept	nd	0.18 ± 0.03	0.04 ± 0.01*	nd	0.53 ± 0.01	0.37 ± 0.03	0.65 ± 0.04*
Don R.	nd	0.13 ± 0.01	0.13 ± 0.02	0.84 ± 0.03	0.12 ± 0.01	1.635 ± 0.001	0.68 ± 0.14
Humber R	nd	0.09 ± 0.01[a]	0.035 ± 0.002*	0.20 ± 0.01	0.32 ± 0.01	0.72 ± 0.05	nd
Grand R.	nd	0.087 ± 0.004[a]	nd	0.09 ± 0.05	0.04 ± 0.01[a]	0.08 ± 0.02	nd
Thames R.	nd	0.047 ± 0.003[a]	nd	0.06 ± 0.01*	0.39 ± 0.05	0.487 ± 0.005	nd
Perch Crk	nd	0.07 ± 0.01[a]	nd	0.18 ± 0.02	0.94 ± 0.04	0.36 ± 0.05	nd
Little Rouge Crk	nd	0.02 ± 0.01*	nd	nd	nd	nd	nd
Meretta Lake 2014	0.09 ± 0.01[a]	0.42 ± 0.01	nd	nd	2.10 ± 0.02	nd	nd
Resolute Lake 2014	nd	0.05 ± 0.01[a]	nd	nd	1.228 ± 0.003	nd	nd
Resolute Lake 2012	nd	0.12 ± 0.03	nd	nd	3.61 ± 0.03	nd	nd
Lake of Bays	nd	nd	nd	0.076 ± 0.006*	nd	nd	nd

nd = not detected above detection limit; * indicates detections that were between LOD and LOQ, [a] indicates concentrations below the lowest calibration level

Table C7: Concentrations of FTABs and approximate concentrations of FTBs in water in ng/L. (± standard deviation)

Averages	4:2 FTAB	6:2 FTAB	8:2 FTAB	FTB CH_2 C5	FTB CHF C5	FTB CH_2 C7	FTB CHF C7	FTB CH_2 C9	FTB CHF C9
Welland R. 1	0.18 ± 0.06	32.7 ± 3.5	nd	12.8 ± 6.7	42 ± 36	9.2 ± 4.7	16 ± 14	nd	nd
Welland R. 2	nd	0.05 ± 0.01*	nd	5.7 ± 2.9	20 ± 17	nd	0.2 ± 0.2*	nd	nd
Welland R. 3	nd	0.225 ± 0.001	nd	9.9 ± 5.4	30 ± 28	3.2 ± 2.7	5.7 ± 5.5	nd	nd
Welland R. 4	nd	0.05 ± 0.01*	nd	5.4 ± 3.0	20 ±18	0.07 ±0.06*	0.5 ± 0.4	nd	nd
Welland R. 5	nd	0.03 ± 0.02*	nd	14.0 ± 7.1	39 ± 34	nd	nd	nd	nd
Welland R. 6	nd	0.07 ± 0.03*	nd	6.6 ± 3.6	19 ±16	nd	nd	nd	nd
Welland R. 7	nd	0.03 ± 0.02*	nd	6.5 ± 3.2	18 ±16	0.08 ± 0.10*	0.2 ± 0.3*	nd	nd
Welland R. 8	nd	0.05 ± 0.02*	nd	1.7 ± 0.9	6.5 ±6.0	nd	nd	nd	nd
Welland R. 9	nd	0.15 ± 0.01*	nd	2.7 ± 1.4	8.1 ±7.0	nd	nd	nd	nd
Welland R. Ref	nd	nd	nd	nd	nd	nd	nd	nd	nd
Big Creek 1	nd	0.20 ± 0.06*	nd	nd	nd	nd	nd	nd	nd
Big Creek 2	nd	0.12 ± 0.01	nd	nd	nd	nd	nd	nd	nd
Etobicoke Crk Aug	nd	21.6 ± 0.7	1.51 ± 0.42	1.9 ± 1.0	6.1 ± 5.6	2.8 ±1.5	7.4 ± 7.0	0.41 ± 0.28	0.42 ± 0.41
Etobicoke Crk Sep	nd	13.1 ± 0.1	1.19 ± 0.32	1.3 ±0.7	3.7 ± 3.4	1.8 ± 1.1	4.8 ± 4.6	0.31 ± 0.25	0.30 ± 0.28*
Don R.	nd	15.5 ± 0.3	4.6 ± 1.2	nd	nd	nd	nd	nd	nd
Humber R	nd	4.46 ± 0.15	1.02 ± 0.30	nd	nd	nd	nd	nd	nd
Grand R.	nd	0.81 ± 0.02	nd	nd	nd	nd	nd	nd	nd
Thames R.	nd	0.06 ± 0.02*	nd	nd	nd	nd	nd	nd	nd
Perch Crk	nd	0.30 ± 0.02	nd	nd	nd	nd	nd	nd	nd
Little Rouge Crk	nd	0.07 ± 0.01*	nd	nd	nd	nd	nd	nd	nd
Meretta Lk. 2014	nd	0.058 ± 0.001*	nd	0.51 ± 0.28	1.4 ± 1.3	nd	nd	nd	nd
Resolute Lk. 2014	nd	nd	nd	0.14 ±0.05*	0.29 ± 0.26*	nd	nd	nd	nd
Resolute Lk. 2012	nd	nd	nd	0.09 ± 0.05*	0.22 ± 0.19*	nd	nd	nd	nd
Lake of Bays	nd	nd	nd	nd	nd	nd	nd	nd	nd

nd = not detected above detection limit; * indicates detections that were between LOD and LOQ; Large standard deviations for FTB concentrations are due to use of average of calibrations using both transitions to reflect uncertainty in the calibration sensitivity for the FTBs.

Table C8: Concentrations of 6:2 FTAA and approx. concentrations of 6:2 FTSAS-SO_2, 6:2 FTSHA-SO, and FASADAs in water in ng/L. (± standard deviation)

Averages	6:2 FTAA	6:2 FTSAS-SO_2	6:2 FTSHA-SO	FHxSADA	FPeSADA	FBSADA	FPrSADA
Welland R. 1	nd	nd	nd	0.36 ± 0.14	0.05 ± 0.03[a]	0.09 ± 0.03*	0.06 ± 0.04*
Welland R. 2	nd	nd	nd	0.10 ± 0.05	0.003 ± 0.008*	nd	nd
Welland R. 3	nd	nd	nd	0.10 ± 0.05	0.004 ± 0.007*	nd	nd
Welland R. 4	nd	nd	nd	0.06 ± 0.03[a]	0.007 ± 0.009*	nd	nd
Welland R. 5	nd	nd	nd	0.029 ± 0.025*	nd	nd	nd
Welland R. 6	nd	nd	nd	0.019 ± 0.016*	nd	nd	nd
Welland R. 7	nd	nd	nd	0.019 ± 0.015*	nd	nd	nd
Welland R. 8	nd	nd	nd	nd	nd	nd	nd
Welland R. 9	nd	nd	nd	0.003 ± 0.005*	nd	nd	nd
Welland R. Ref	nd	nd	nd	nd	nd	nd	nd
Big Crk. 1	nd	nd	nd	nd	nd	nd	nd
Big Crk. 2	nd	nd	nd	nd	nd	nd	nd
Etobicoke Crk. Aug	0.16 ± 0.03	0.83 ± 0.53	0.10 ± 0.04*	nd	nd	nd	nd
Etobicoke Crk. Sept	0.07 ± 0.02*	0.24 ± 0.15	0.29 ± 0.10	nd	nd	nd	nd
Don R.	0.11 ± 0.01	0.04 ± 0.02*	0.19 ± 0.07*	nd	nd	nd	nd
Humber R.	nd	0.08 ± 0.04*	0.13 ± 0.05*	nd	nd	nd	nd
Grand R.	nd	0.04 ± 0.01*	0.10 ± 0.04*	nd	nd	nd	nd
Thames R.	nd	0.02 ± 0.01*	0.09 ± 0.04*	nd	nd	nd	nd
Perch Crk.	nd	nd	nd	nd	nd	nd	nd
Little Rouge Crk.	nd	nd	nd	nd	nd	nd	nd
Meretta Lk. 2014	nd	nd	nd	nd	nd	nd	nd
Resolute Lk. 2014	nd	nd	nd	nd	nd	nd	nd
Resolute Lk. 2012	nd	nd	nd	0.09 ± 0.03*	nd	nd	nd
Lake of Bays	nd	nd	nd	nd	nd	nd	nd

nd = not detected above detection limit; * indicates detections that were between LOD and LOQ; Large standard deviations for 6:2 FTSAS-SO_2, 6:2 FTSHA-SO, and PFASADAs concentrations are due to use of average of calibrations using both transitions to reflect uncertainty in the calibration sensitivity; [a] indicates concentrations below the lowest calibration level

Table C9: Approximate concentrations of perfluoroalkane sulfonamide alkylamine acids (FASAAAs) and perfluoroalkane sulfonamide alkylbetaines (FASABs) in water in ng/L. (± standard deviation)

Sample	FHxSAAA	FPeSAAA	FBSAAA	FPrSAAA	FHxSAB	FPeSAB
Welland R. 1	0.88 ± 0.22	0.37 ± 0.13*	0.61 ± 0.24*	0.22 ± 0.11*	1.42 ± 0.66	0.18 ± 0.08*
Welland R. 2	nd	nd	nd	nd	0.50 ± 0.26*	nd
Welland R. 3	nd	nd	nd	nd	0.49 ± 0.29*	nd
Welland R. 4	nd	nd	nd	nd	0.49 ± 0.24*	nd
Welland R. 5	nd	nd	nd	nd	nd	Nd
Welland R. 6	nd	nd	nd	nd	nd	nd
Welland R. 7	nd	nd	nd	nd	nd	nd
Welland R. 8	nd	nd	nd	nd	nd	nd
Welland R. 9	nd	nd	nd	nd	nd	nd
Welland R. Ref.	nd	nd	nd	nd	nd	nd
Big Crk. 1	nd	nd	nd	nd	nd	nd
Big Crk. 2	nd	nd	nd	nd	nd	nd
Etobicoke Crk. Aug.	nd	nd	nd	nd	nd	nd
Etobicoke Crk. Sept.	nd	nd	nd	nd	nd	nd
Don R.	nd	nd	nd	nd	nd	nd
Humber R.	nd	nd	nd	nd	nd	nd
Grand R.	nd	nd	nd	nd	nd	nd
Thames R.	nd	nd	nd	nd	nd	nd
Perch Crk.	nd	nd	nd	nd	nd	nd
Little Rouge Crk.	nd	nd	nd	nd	nd	nd
Meretta Lk. 2014	nd	nd	0.43 ± 0.22*	nd	0.29 ± 0.11*	nd
Resolute Lk. 2014	nd	nd	0.47 ± 0.16*	nd	0.36 ± 0.16*	nd
Resolute Lk. 2012	nd	nd	nd	nd	0.74 ± 0.33	nd
Lake of Bays	nd	nd	nd	nd	nd	nd

nd = not detected above detection limit; * indicates detections that were between LOD and LOQ

Table C10: Concentrations of PFASs in sediment samples in ng/g (± standard deviation)

PFAS	Welland R. 1	Welland R. 2	Welland R. 5	Welland R. 6	Big Crk. 1
PFPeA	0.22 ± 0.07*	nd	0.18 ± 0.08*	nd	nd
PFHxA	0.20 ± 0.02	nd	0.10 ± 0.04*	0.061 ± 0.021*	nd
PFHpA	0.052 ± 0.029*	nd	nd	nd	nd
PFOA	0.17 ± 0.03*	0.063 ± 0.032*	0.14 ± 0.01*	0.081 ± 0.024*	nd
PFBS	0.041 ± 0.014*	nd	nd	nd	nd
PFPeS	0.068 ± 0.025*	nd	nd	nd	nd
PFHxS	1.14 ± 0.15	0.21 ± 0.03	0.81 ± 0.07	0.24 ± 0.06	nd
PFHpS	0.11 ± 0.03*	0.055 ±0.016*	nd	0.048 ± 0.010*	nd
PFOS	10.00 ± 0.63	8.3 ± 1.1	10.39 ± 0.63	4.17 ± 0.24	0.82 ± 0.11
6:2 FTSA	0.050 ± 0.019*	nd	nd	nd	0.067 ±0.033*
EtFOSAA	nd	nd	0.094 ± 0.014	0.031 ± 0.018*	nd
FHxSA	0.19 ± 0.02	0.039 ± 0.005*	0.089 ± 0.011	0.026 ± 0.002*	nd
FOSA	nd	nd	0.069 ± 0.010*	nd	nd
6:2 FTSAm	0.072 ± 0.033*	nd	nd	nd	nd
6:2 FTAB	0.44 ± 0.05	nd	nd	nd	0.11 ± 0.04
FTB CH_2 C5	0.041 ± 0.027*	nd	0.029 ± 0.024*	nd	nd
FTB CHF C5	0.18 ± 0.17*	nd	0.10 ± 0.09*	nd	nd
FTB CH_2 C7	0.27 ± 0.16	0.040 ± 0.024*	nd	nd	nd
FTB CHF C7	1.01 ± 0.92	0.18 ± 0.17*	0.13 ± 0.13*	nd	nd
FTB CH_2 C9	0.024 ± 0.021*	nd	nd	nd	nd
FTB CHF C9	0.060 ± 0.056*	nd	nd	nd	nd
6:2 FTAA	nd	nd	nd	nd	0.027 ± 0.003*
FHxSAAm	0.090 ± 0.060*	nd	nd	nd	nd

nd = not detected above detection limit; * indicates detections that were between LOD and LOQ; Large standard deviations for FTBs and FHxSAAm concentrations are due to use of average of calibrations using both transitions to reflect uncertainty in the calibration sensitivity.

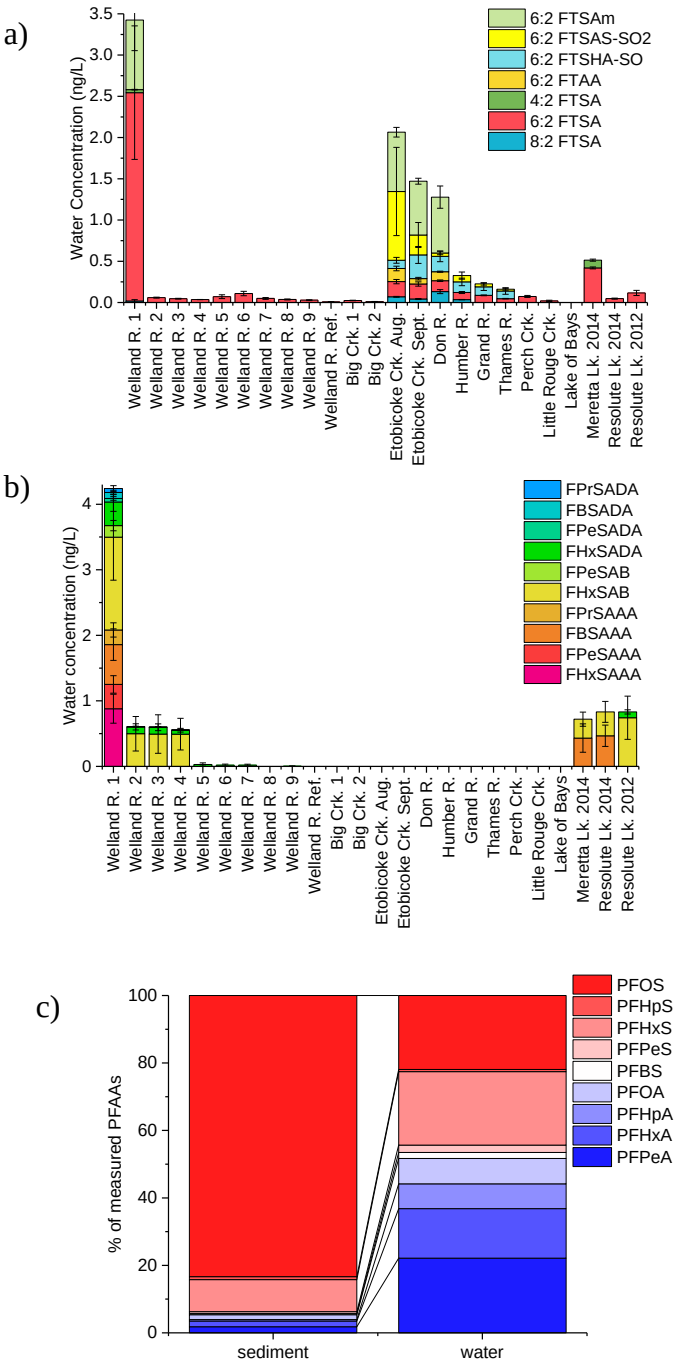

Figure C2: a) Concentrations of fluorotelomer substances other than FTABs and FTBs in surface waters in ng/L with error bars showing standard deviationts. b) Concentrations of fluorotelomer sulfonamido AFFF components in surface waters in ng/L with error bars showing standard deviations. c) Distribution of PFCAs and PFSAs between sediment and water at Welland River 1 sampling site.

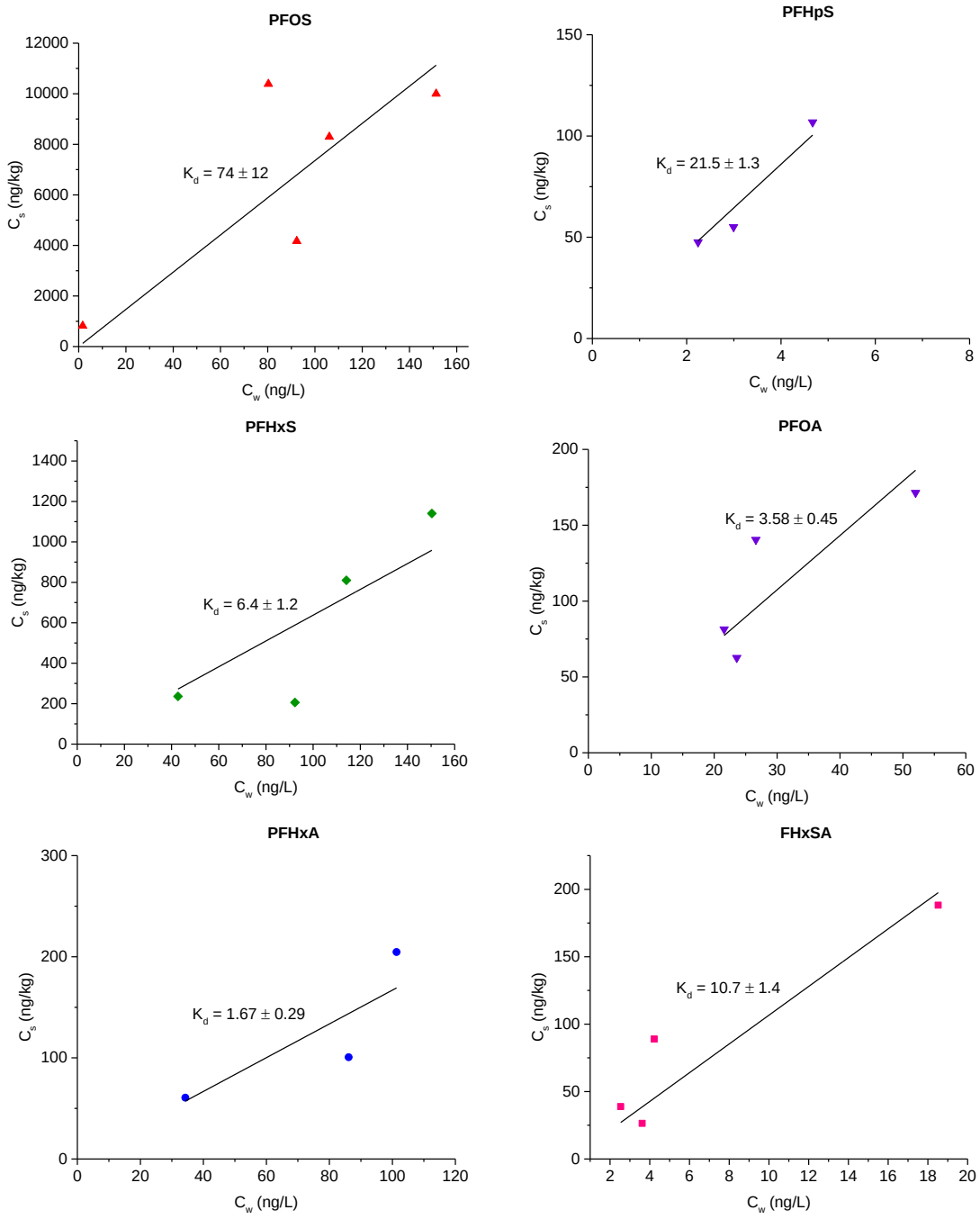

Figure C3: Plots of linear best fit with intercept of zero for concentration in soil versus concentration in water for all PFASs detected in at least three sediment samples and corresponding water samples. The slope determines the K_d and is displayed ± standard error.

Table C11: Sediment water distribution coefficient ($logK_d$) determined from field sediments and waters from the Welland River and Big Creek

PFAS	$logK_d$ (± standard error)
PFHxA	0.22 ± 0.08
PFOA	0.55 ± 0.06
PFHxS	0.80 ± 0.09
PFHpS	1.33 ± 0.03
PFOS	1.87 ± 0.08
FHxSA	1.03 ± 0.06

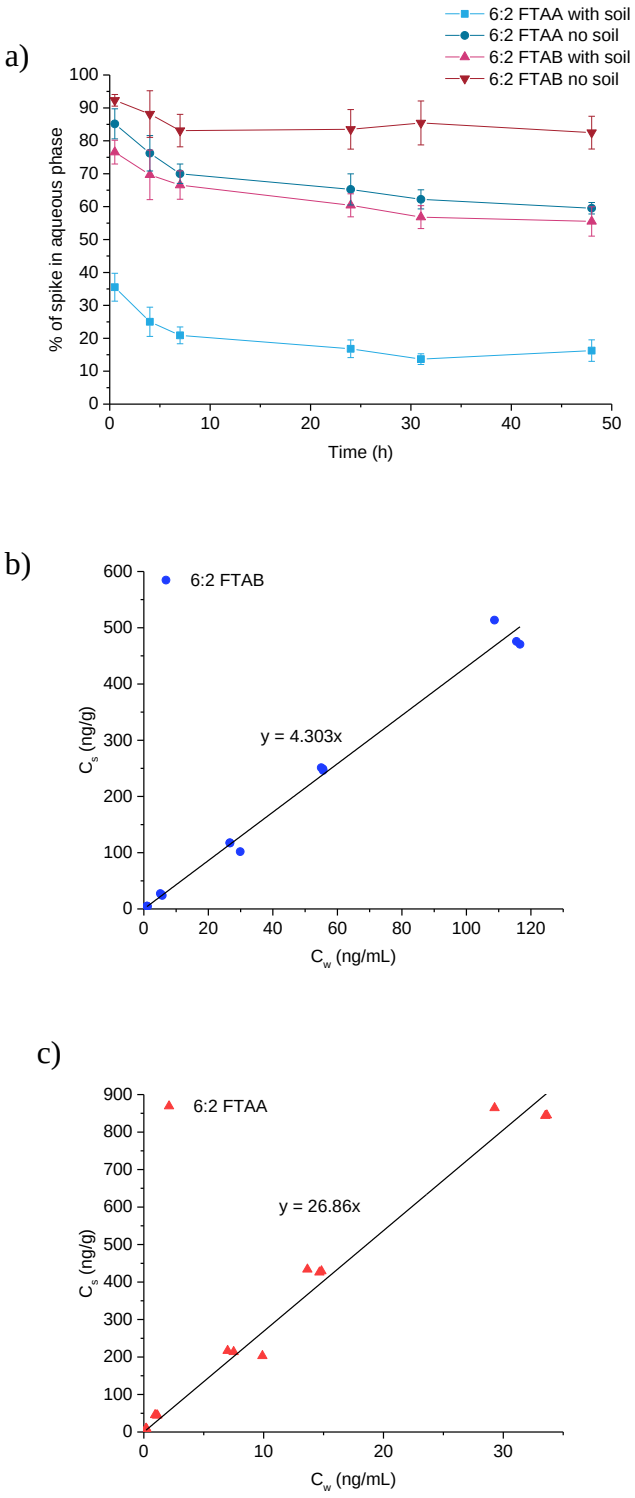

Figure C4: a) Kinetics plot for sorption of 50 ng/mL 6:2 FTAA and 6:2 FTAB in a 1: 5 soil: water system. b) Sorption isotherm for 6:2 FTAB with linear sorption isotherm. c) Sorption isotherm for 6:2 FTAA with linear sorption isotherm.

Table C12: Soil properties for soil used in 6:2 FTAB and 6:2 FTAA batch sorption tests

Sample Location	% organic carbon (OC)	% sand	% silt	% clay	CEC (µmol/g)	Texture	pH
Agricultural field in Northumberland County, ON, Canada	1.9	69	30	1.0	74	sandy loam	5.8

% OC, % sand, % silt, % clay, texture description, and CEC were measured by SGS Agri-Food Laboratories in Guelph, ON

References

(1) D'Agostino, L. A.; Mabury, S. A. Aerobic biodegradation of two fluorotelomer sulfonamide-based aqueous film forming foam components produces perfluoroalkyl carboxylates. *Environ. Toxicol. Chem.* **2017**, DOI: 10.1002/etc.3750

(2) Harding-Marjanovic, K. C.; Houtz, E. F.; Yi, S.; Field, J. A.; Sedlak, D. L.; Alvarez-Cohen, L. Aerobic Biotransformation of Fluorotelomer Thioether Amido Sulfonate (Lodyne) in AFFF-Amended Microcosms. *Environ. Sci. Technol.* **2015**, *49* (13), 7666–7674.